

The Role of Tissue Resident Macrophages During Cryptococcal Infection.

By Sally H. Mohamed



UNIVERSITY OF
BIRMINGHAM

A thesis submitted for the degree of Doctor of Philosophy

March 2023

UNIVERSITY OF
BIRMINGHAM

University of Birmingham Research Archive

e-theses repository

This unpublished thesis/dissertation is copyright of the author and/or third parties. The intellectual property rights of the author or third parties in respect of this work are as defined by The Copyright Designs and Patents Act 1988 or as modified by any successor legislation.

Any use made of information contained in this thesis/dissertation must be in accordance with that legislation and must be properly acknowledged. Further distribution or reproduction in any format is prohibited without the permission of the copyright holder.

Table of Contents

	0
DECLARATION	8
ACKNOWLEDGMENTS	9
ABSTRACT	10
ABBREVIATIONS	12
1	13
INTRODUCTION	13
1.1 Acknowledgment	13
1.2 Human fungal infections	13
1.3 Human exposure to <i>Cryptococcus neoformans</i>	16
1.4 Human diseases caused by <i>Cryptococcus neoformans</i>.	17
1.4.1 Pulmonary Cryptococcosis	18
1.4.2 Cryptococcal meningitis	19
1.4.3 Immune reconstitution inflammatory syndrome	22
1.5 Microbiology of <i>Cryptococcus neoformans</i>	23
1.6 Fungal entry to the CNS	26
1.7 Fungal growth adaptation within the CNS	29
1.7.1 Iron	29
1.7.2 Copper	30
1.8 Host immune responses to <i>Cryptococcus neoformans</i>	32
1.9 Innate immune cell function in controlling <i>Cryptococcus neoformans</i> infection.	35
1.9.1 Dendritic cells	35
1.9.2 Neutrophils	36
1.9.3 Macrophages	37
1.9.4 Monocytes	39
1.10 Adaptive immunity response to <i>Cryptococcus neoformans</i>	40
1.10.1 CD4 T cells	40
1.10.2 B cells	42

1.11 Future perspective	42
2	44
METHODS AND MATERIALS	44
2.1 Mice	44
2.2 Tamoxifen and Diphtheria toxin administration	45
2.3 PLX5622 treatment	45
2.4 <i>C. neoformans</i> growth and mouse infections	46
2.5 <i>C. neoformans</i> growth in PLX5622	47
2.6 Generation of pCTR4 ^{GFP} <i>C. neoformans</i>	47
2.7 Determination of organ fungal burden	47
2.8 Isolation of brain leukocytes	48
2.9 Isolation of meninges leukocytes	48
2.10 Isolation of lung leukocytes	49
2.11 Isolation of peripheral blood leukocytes	49
2.12 Cell isolation from spleen	50
2.13 Cell isolation from bone marrow	50
2.14 Flow cytometry: Surface staining	50
2.15 Flow cytometry: Intracellular staining	51
2.16 Measurement of cytokines	52
2.18 Histology	53
2.19 Imaging	53
2.20 Tissue culture	53
2.21 Gating strategy	54
2.22 Statistics	57
THE ROLE OF BRAIN RESIDENT MACROPHAGES DURING <i>C. NEOFORMANS</i> INFECTION	58
3.1 Author Contributions	58
3.2 Introduction	58

3.2.1 Microglia	59
3.2.2 Perivascular macrophages	62
3.2.3 Meningeal macrophages	63
3.2.4 Choroid Plexus	64
3.2.5 In vivo strategies to manipulate CNS macrophages number and function.	64
3.2.5.1 Chemical manipulation strategies	66
3.2.5.2 Genetic manipulation	67
3.3 Result	70
3.3.1 <i>C. neoformans</i> infects CNS myeloid cells.	70
3.3.2 Brain resident macrophages become infected with <i>C. neoformans</i> .	72
3.3.3 Histology analysis of <i>C. neoformans</i> brain infection.	73
3.3.4 Microglia harbour live <i>C. neoformans</i> intracellularly.	74
3.3.5 Meningeal macrophages become infected with <i>C. neoformans</i> .	75
3.3.7 Depletion of brain-resident macrophages using CX3CR1-iDTR transgenic mice reduces brain fungal burden.	78
3.3.8 Brain resident macrophage depletion with PLX5622 reduces brain fungal burden.	80
3.3.9 Tissue resident macrophage depletion using PLX5622 reduces brain fungal burden only at early time points post-infection.	81
3.3.10 PLX5622 deplete meningeal macrophages in the meninges.	82
3.3.11 Sall ^{CreER} iDTR is not suitable model to deplete microglia.	84
3.3.12 Fungal brain infection is primarily supported by microglia.	85
3.3.13 Intracellular survival within microglia is required for optimal fungal brain infection.	88
3.3.14 <i>C. neoformans</i> is protected from copper starvation within microglia.	90
3.3.15 Copper starvation in other brain myeloid cells	92
3.3.16 IFN γ induces copper restriction in fungal-infected microglia.	93
3.4 Discussion	95
THE EFFECT OF PLX5622 ON SYSTEMIC IMMUNITY DURING PULMONARY FUNGAL INFECTION	102
4.1 Author Contributions	102
4.2 Introduction	102
4.2.1 Immunology of <i>C. neoformans</i> lung infection	103
4.2.2 Alveolar macrophages	105
4.2.3 Interstitial lung macrophages	106
4.3 Result	109
4.3.1 PLX5622 depletes tissue resident macrophages in the CNS.	109
4.3.2 PLX5622 depletes meningeal macrophages during intranasal infection.	111
4.3.3 Depletion of tissue resident macrophages causes reduction in brain fungal burden.	112
4.3.4 Interstitial lung macrophages are depleted by PLX5622.	113
4.3.5 PLX5622 reduces lung fungal burden.	114
4.3.6 PLX5622 has localised effect on fungal burden in the lung and CNS.	115
4.3.9 PLX5622 does not have antifungal properties.	117
4.3.10 Extrapulmonary dissemination to the CNS is reduced by PLX5622 treatment.	118
4.3.11 PLX5622 deplete MHCII ^{hi} interstitial macrophages.	120
4.3.12 <i>C. neoformans</i> localises with interstitial macrophages.	122
4.3.14 Interstitial macrophages expansion is not driven local proliferation.	124
4.3.15 Interstitial macrophages expansion is driven by monocytes.	126
4.3.16 PLX5622 deplete patrolling monocytes (Ly6C ^{low}) in organ-specific manner.	127

4.3.17 Patrolling monocytes (Ly6C ^{low}) play a minor role in extrapulmonary dissemination of <i>C. neoformans</i> .	130
4.3.18 Patrolling monocyte impairment reduce the frequency of MHCII ^{low} IMs.	132
4.3.19 PLX5622 reduces B cells in the brain.	134
4.3.20 CD4 T cell production of IFN γ is reduced in the PLX5622 treated lung.	136
4.3.21 Cytokine production is not changed in PLX5622 treated brain.	138
4.3.22 PLX5622 does not affect fungal burden in <i>Rag1</i> ^{-/-} mice.	139
4.3.23 Interstitial macrophages subset ratio is disrupted in <i>Rag1</i> ^{-/-} mice.	140
4.3.24 PLX5622 causes reduced fungal burden in BALB/c mice.	142
4.4 Discussion	143
5	150
GENERAL DISCUSSION AND FUTURE DIRECTION	150
REFERENCES	156

List of Tables

Table 1. 1: The key PRRs and PAMPs for <i>C. neoformans</i> and their role during infection. ...	35
Table 2. 1: Mouse strain used in this thesis and their strain number, origin and selected reference.....	45
Table 2. 2: <i>C. neoformans</i> strain used in this thesis.....	46
Table 2. 3: list of antibodies used, including clone and fluorophore.	51
Table 3. 1: Resident Macrophages of the CNS: their location, origin and surface markers. .	59
Table 3. 2: Overview of commonly used chemical and genetic microglia depletion models in mice and their approximate timelines, advantages, and disadvantages.	65

List of Figures

Figure 1. 1 <i>C. neoformans</i> cell features:	26
Figure 1. 2 <i>C. neoformans</i> main pattern recognition receptor.	34
Figure 3. 1 Majority of myeloid cells get infected with <i>C. neoformans</i> in vivo	71
Figure 3. 2 Microglia harbour <i>C. neoformans</i> intracellularly.	73
Figure 3. 3 Histology images of <i>C. neoformans</i> infected brain.	74

Figure 3. 4 <i>C. neoformans</i> viability within microglia.....	75
Figure 3. 5 <i>C. neoformans</i> infect meninges immune cells	77
Figure 3. 6 Meningeal macrophages harbour <i>C. neoformans</i> intracellularly.	78
Figure 3. 7 Brain macrophages depletion result in brain burden reduction with no difference in lung.	79
Figure 3. 8 PLX5622 reduces brain fungal burden with no difference in lung.	81
Figure 3. 9 PLX5622 treatment at day 6 post infection.....	82
Figure 3. 10 Meningeal macrophages the only cells depleted with PLX5622 in the meninges.	83
Figure 3. 11 <i>Sall1</i> ^{CreER} is not a suitable model to deplete microglia.	85
Figure 3. 12 <i>Sall1</i> Cre ^{ER} x <i>Csf1</i> ^{flox} specific model to deplete microglia in the CNS.	87
Figure 3. 13 Reduction of fungal brain burden in microglia-depleted mice depends on intracellular growth.....	89
Figure 3. 14 <i>C. neoformans</i> is protected from copper starvation when associated with microglia.	91
Figure 3. 15 <i>C. neoformans</i> is protected from copper starvation when associated with microglia.	92
Figure 3. 16 IFN γ increases fungal copper starvation within microglia.....	94
Figure 4. 1 Pulmonary immunology of <i>C. neoformans</i> infection.....	108
Figure 4. 2 PLX5622 deplete tissue resident macrophages and patrolling monocytes in the CNS.	110
Figure 4. 3 MMs are depleted with PLX5622.....	111
Figure 4. 4 Brain fungal burden is reduced with CSF1R inhibitor treatment at day 14 and 21 post infection.....	112
Figure 4. 5 IMs are depleted with PLX5622.....	114
Figure 4. 6 Lung fungal burden is reduced with CSF1R inhibitor treatment at day 14 and 21 post infection.....	115
Figure 4. 7 PLX5622 deplete spleen macrophages.....	116
Figure 4. 8 Bone marrow macrophages are not affected by PLX5622 treatment.	117
Figure 4. 9 Blood are not affected by PLX5622 treatment.....	117

Figure 4. 10 PLX5622 does not affect fungal growth directly.	118
Figure 4. 11 brain fungal burden is correlated to lung burden.	120
Figure 4. 12 PLX5622 effect lung interstitial macrophages subset.	121
Figure 4. 13 <i>C. neoformans</i> infect tissue resident macrophages in the lung.	123
Figure 4. 14 MHCII ^{hi} IMs are more susceptible to <i>C. neoformans</i> .	123
Figure 4. 15 <i>C. neoformans</i> decrease cell proliferation in interstitial macrophages.	125
Figure 4. 16 Recruited monocytes give rise to IMs expansion during <i>C. neoformans</i> infection.	127
Figure 4. 17 PLX5622 deplete brain patrolling monocytes.	129
Figure 4. 18 Patrolling monocytes play a redundant role in control and dissemination of pulmonary <i>C. neoformans</i> infection.	131
Figure 4. 19 Patrolling monocytes deficiency reduced MHCII ^{low} IMs frequency.	133
Figure 4. 20 PLX5622 deplete brain B cells.	135
Figure 4. 21 IFN γ is reduced in PLX5622 treated lung.	137
Figure 4. 22 PLX5622 does not change brain cytokines production.	139
Figure 4. 23 Fungal burden is not changed between untreated and PLX5622 treated mice in Rag1 ^{-/-} lung and brain.	140
Figure 4. 24 IMs subset ratio changed in <i>Rag1</i> ^{-/-} mice.	141
Figure 4. 25 PLX5622 causes reduced fungal burden in BALB/C mice.	142

Declaration

I hereby declare that this thesis was completed by the author, Sally H. Mohamed, for the degree of PhD, submitted to the University of Birmingham in March 2023. This work has not been presented in any previous application for a degree. All of the work in this thesis was performed by the author, unless otherwise stated in the text. All sources of information have been specifically acknowledged in the text.

Sally H. Mohamed

Acknowledgments

I would first like to thank my supervisor, Dr. Rebecca A. Drummond, for giving me the opportunity to complete my PhD in her lab and for all the support and advice she has giving me over the past 3 years. I would like to thank my co-supervisor, Dr Elizabeth R. Ballou for her advice and support. I have learned a lot from Dr Rebecca Drummond, all her hard working, motivation and ambitious, which I inspire to be and I hope this shown in my work.

I also want to thank the other Birmingham fellows, Dr David bending, Sarah Dimeloe, and Kendle Maslowski for all their advice, support and direction.

I would like to thank biomedical service unit and special thanks for Karen Woodcock for all the training she has giving me over the last few years. I would like to thank all the collaborator I have worked with during my time at Birmingham.

I would like to thank my family, my parents and specifically my husband for all the support me and the encouragement he has giving me during my PhD.

Finally, I thank my funder, the medical research council and the University of Birmingham.

Abstract

Cryptococcus neoformans is a yeast-like fungus that may cause opportunistic infections in vulnerable patients including pulmonary disease and life-threatening meningitis. There is a limited availability of antifungal drugs and the mortality rate of cryptococcal meningitis (CM) remains unacceptably high. Alternative and adjunctive immune-based therapies and vaccines are therefore needed. However, the development of new treatments depends on a comprehensive understanding of the mechanisms mediating antifungal immunity. The specific roles of tissue resident macrophages during *C. neoformans* infection is not well understood, and this is particularly true for central nervous system (CNS) resident macrophages, called microglia. In this thesis, several models of *C. neoformans* infection in microglia-deficient mice was developed and used to elucidate the function of microglia in vivo. Microglia were found to support *C. neoformans* growth by providing a site for the fungus to acquire the important micronutrient copper, thus optimising fungal growth and virulence within the CNS. Stimulation of microglia with IFN γ caused restriction of phagosomal copper to intracellular fungi. In some experiments, microglia were depleted using PLX5622, a small molecular inhibitor of the colony-stimulating factor 1 receptor (CSF1R) that is widely used to deplete macrophages within CNS. In this thesis, the effect of PLX5622 on immune cell populations was assessed at baseline and during *C. neoformans* infection. I found several off-target effects of the drug on lung and spleen macrophages, as well as brain infiltrating patrolling monocytes (Ly6C^{low}). This was important, because PLX5622 treatment significantly reduced lung burden and reduced extrapulmonary dissemination to the CNS (but not to the

spleen and liver) in mice infected via the intranasal route. Fungal lung infection mapped to MHCII^{hi} subset of interstitial lung macrophages, which underwent significant expansion during infection following monocyte replenishment and not local division. Taken together, the data presented in this thesis demonstrate how tissue-resident macrophages can support cryptococcal infection by acting as intracellular infection reservoirs and are an important therapeutic target in the control of *C. neoformans* infection and dissemination.

abbreviations

Central nervous system	CNS
knockout	KO
T helper cells	TH
C-type lectin receptor	CLR
cerebrospinal fluid	CSF
Cryptococcal antigen	CrAg
The World Health Organisation	(WHO
Cryptococcal meningitis	CM
flucytosine	FC
Amphotericin B	AMB
interferon gamma	IFN γ
(Immune reconstitution inflammatory syndrome	IRIS
combination antiretroviral therapy	cART
glucuronoxylomannan	GXM
Glucuroxylomannogalactan	GXMGal
wild type	WT
Dendritic cells	DCs
reactive oxygen species	ROS
tumour necrosis factor- α	TNF- α
interleukin-1b	IL-1b
human brain microvascular endothelial cells	hBMEC
blood brain barrier	BBB
pattern recognition receptors	PRRs
toll like receptor	TLRs
C-type lectin receptor	CLRs
pathogen-associated molecular pattern recognition	
receptors	PAMPs
Human peripheral blood mononuclear cells	PBMCs
neutrophil extracellular traps	NETs
granulocyte-colony stimulating factor	G-CSF
nitric oxide synthase	iNOS
perivascular macrophages	PVM
meningeal macrophages	MM
simian immunodeficiency virus	SIV
colony-stimulating factor 1 receptor	CSF1R
Alveolar macrophages	AMs
Interstitial macrophages	IMs

1

Introduction

1.1 Acknowledgment

Some part of the introduction has been published as a book chapter produced by this thesis author (Mohamed, Nyazika et al. 2022).

1.2 Human fungal infections

Fungal infections have major impact on human health, with the majority of lethal infections cause by *C. neoformans*. In this chapter, I will cover the scope of human fungal infections and detail the microbiology and tissue-specific immunology of cryptococcal diseases.

Fungi cause a wide range of diseases from benign infections of the skin/mucosa to life-threatening invasive fungal infections (Brown, Denning et al. 2012). Invasive fungal infections such as meningitis, pneumonia, fungemia, and complex respiratory conditions are all associated with unacceptably high mortality rates, resulting in more than 1.7 million deaths annually and significant morbidity in over a billion people (Bongomin, Gago et al. 2017). The annual healthcare cost to treat fungal diseases is estimated to be \$15 billion (Richardson and Naglik 2018), causing global economic and societal damage. Despite this, fungal infections remain understudied and underdiagnosed compared to other infectious diseases.

Superficial fungal infections will affect the majority of people at least once in

their lifetime, this is especially true for infections affecting the skin and nails which affect approximately 1.7 billion people worldwide (Havlickova, Czaika et al. 2008). The majority of these infections are caused by the dermatophyte fungi resulting in conditions such as athlete's foot (*T. rubrum* and *T. interdigitale*) which occurs in ~20% of adults, and ringworm (*Trichophyton* and *Microsporum*) that causes 200 million cases each year (Brown, Denning et al. 2012). Furthermore, other common mucosal infections are mucocutaneous candidiasis and vulvovaginal candidiasis, where the former is a major problem in AIDS patients (affecting over 2 million people each year) (Warrier and Sathasivasubramanian 2015), and the latter affecting around 75% of women at least once in their lifetime, with 6% experiencing recurrent episodes (Brown, Denning et al. 2012). These infections are mostly caused by *Candida albicans* and generally easily cured (Gaziano, Sabbatini et al. 2020). Nevertheless, many of these infections are recurrent and cause a lot of distress and poor mental health to affected people who continually suffer from them.

On the other hand, invasive fungal infections are harder to diagnose and treat and are therefore of greater concern. It is estimated that invasive fungal infection causes over 1.5 million death annually (Houšť, Spižek et al. 2020). Most invasive fungal infections are caused by species from the genera of *Candida*, *Cryptococcus*, *Aspergillus*, and *Pneumocystis* (Brown, Denning et al. 2012). These pathogens are associated with high mortality rates ranging from 30 to 90% and successful treatments require early diagnosis and prompt effective antifungal therapy (Valentine, Morrissey et al. 2019). Yet, antifungal drug options are limited to a small number of drug classes, including the polyenes, echinocandins, azoles, and flucytosine (Cowen, Sanglard et al. 2014). Despite the availability of these drugs, survival rates are still low. Moreover, there is a lack of available vaccines to treat

these invasive infections and the emergence of single and multidrug resistance by some of these fungi such as *Aspergillus* species, *Candida glabrata*, and *Candida auris* is alarming (Kuehn 2020). Therefore, there is a need for better diagnostic tools and treatment strategies to preserve drug effectiveness and improve patients' outcomes.

Risk factors that have driven the increase in clinical invasive fungal infections over the last few decades include the increased use of immunosuppressive drugs, the human immunodeficiency virus (HIV)/AIDS pandemic, higher rates of stem cell and solid organ transplantation, oncological therapies, and extensive use of antibiotics (Raman Sharma 2010, Lionakis, Netea et al. 2014, Clark and Drummond 2019). For example, the vast majority of patients with candidiasis are either immunocompromised (neutropenia), on long-term antibiotic treatment, or have experienced major trauma. Furthermore, chronic or severe viral infections predispose to invasive fungal infection for example, patients with severe COVID-19 had greater risk of developing fungal infection, where 30-40% of ventilated patients suffered from aspergillosis and invasive candidiasis (Gangneux, Dannaoui et al. 2022).

Invasive infections by *Candida* species are the fourth most common nosocomial bloodstream infection (Lamoth, Lockhart et al. 2018), with *Candida albicans* being the most common isolated species. Although, there has been a recent change in the distribution of *Candida* species with an increase in the proportion of *Candida glabrata*, *Candida auris*, and *Candida parapsilosis* and these emerging species have higher rates of antifungal drug resistance (Lamoth, Lockhart et al. 2018). *Aspergillus* infections usually affect people with neutropenia, patients on immunosuppressive therapies, obstructive pulmonary diseases, and organ transplant

recipients. The most common *Aspergillus* species that cause invasive infections are *Aspergillus fumigatus*, infecting more than 200,000 people each year with a mortality rate of ~ 50% even when diagnosed and treated and can reach 100% if left untreated (Brown, Denning et al. 2012). Moreover, *Aspergillus fumigatus* can cause nasal and pulmonary allergy affecting millions of people worldwide (Denning, Pleuvry et al. 2013). *Pneumocystis jirovecii* is another opportunistic fungal infection that affects the respiratory system causing pneumonia, which affects more than 400,000 worldwide with 13% to 80% mortality rate (Brown, Denning et al. 2012). Other notable fungal diseases include fungal keratitis, affecting over a million people leading to sight problems and blindness (Srinivasan 2004), and CM, the largest cause of death from a fungal infection in humans (discussed in detail below). Due to the significant impact of fungal infections on global human health, there is an urgent need for more research to understand the mechanism of these infections and their pathogenesis, which will be necessary to find new ways to treat and manage these diseases in the clinic.

1.3 Human exposure to *Cryptococcus neoformans*

Cryptococcus species are the most common cause of fungal meningitis in adults causing over 100,000 deaths a year and are the leading cause of fungal meningitis in AIDS patients (Rajasingham, Govender et al. 2022). Furthermore, *C. neoformans* is the first fungi pathogen that has been placed in the priority pathogen list by World Health Organisation (WHO). *C. neoformans* affects more than million people each year with a mortality rate ranging from 20-70% and is higher in areas where access to the gold standard drugs are limited (Brown, Denning et al. 2012). In addition to *C. neoformans*, another species that cause human infections is *Cryptococcus gattii*

which affects apparently immunocompetent people, compared to *C. neoformans* which primarily affects immunocompromised patients. *C. gattii* is found in tropical regions and in 1999 caused an outbreak in Canada that spread to British Columbia, Washington, and Oregon with fatality reaching up to 30% (Harris, Lockhart et al. 2011). *C. neoformans* is an environmental fungus, found in the soil as well as associated with some plants (e.g. eucalyptus trees) and pigeon guano, with a worldwide distribution (Shourian and Qureshi 2019). *C. neoformans* produces airborne spores that are acquired by inhalation. In healthy people, host defence mechanisms clear these spores from the alveoli in the lung preventing infection. Indeed, a study in New York showed ~70% of samples from children over the age of 5 reacted to *C. neoformans* antigen (Goldman, Khine et al. 2001), suggesting exposure to *C. neoformans* is widespread and occurs during childhood. Furthermore, it's been shown that humans can tolerate viable *Cryptococcus* for years, even decades, after exposure to *C. neoformans* (Garcia-Hermoso, Janbon et al. 1999). However, in immunocompromised patients, the mechanisms that are needed to protect against *C. neoformans* fail, allowing germination and proliferation of *C. neoformans* in the lungs and subsequent dissemination to the other organs including CNS.

1.4 Human diseases caused by *Cryptococcus neoformans*.

Development of CM is strongly associated with defects in T cell immunity, demonstrating the important role of T cell-mediated immunity against *C. neoformans*. Indeed, CM is responsible for 19% of all HIV-related deaths (Rajasingham, Govender et al. 2022). Furthermore, there have been increasing numbers of non-HIV CM being reported. Several of these are also associated with T cell dysfunction

caused by various factors including lymphoma, autoimmune diseases (e.g. lupus, psoriasis, sarcoidosis), immunosuppressive therapy, and idiopathic CD4 lymphocytopenia (Malik, Khan et al. 2012, Williamson, Jarvis et al. 2016). While *C. neoformans* appears capable of invading any organs including the skin, eyes, liver, spleen, and bone/joints, the major affected organs in cryptococcal infection are the lung and CNS, therefore I will only focus here on clinical manifestation most commonly associated with *C. neoformans* (pulmonary cryptococcosis, CM, and Immune Reconstitution Inflammatory Syndrome (IRIS)).

1.4.1 Pulmonary Cryptococcosis

In the lungs, pulmonary cryptococcosis is a common clinical manifestation of *C. neoformans* infection. It can range from pulmonary nodules to more serious life-threatening pneumonia and in severe cases acute respiratory distress syndrome (Liu, Ding et al. 2016). Furthermore, there have been few cases presented with pulmonary cryptococcomas, which is a lung mass that mimics a lung tumour and this mainly presents in immunocompetent patients (Kanjanapradit, Kosjerina et al. 2017, Taniwaki, Yamasaki et al. 2019). Symptoms can range from cough, chest pain, fever, and respiratory failure to asymptomatic. Due to the non-specific symptoms, diagnosis can be missed which could lead to *Cryptococcus* dissemination to other organs (Thornton, Larios et al. 2019). Although pulmonary cryptococcosis mostly affects immunocompromised patients there have been emerging cases seen in immunocompetent patients (Setianingrum, Rautemaa-Richardson et al. 2018). Indeed, a review from China showed 60% of all diagnosed pulmonary cryptococcosis were immunocompetent patients with no known underlying conditions (Kohno, Kakeya et al. 2015, Liu, Ding et al. 2016). However, a study by Hu et al showed that

a polymorphism in the gene encoding Dectin-2 (*CLEC6A*) is associated with susceptibility to pulmonary cryptococcosis (but not disseminated infection) in immunocompetent patients in Chinese population (Hu, Wang et al. 2015). Dectin-2 is a C-type lectin receptor (CLR), which recognises α -mannose within fungal cell walls (see Table 1.1), and is highly expressed by AMs in the human lung (Sun, Xu et al. 2013). Dectin-2 knockout (KO) mice have higher production of T helper 2 (Th2) and IL-4 during experimental *C. neoformans* infection which is associated with disease susceptibility and high fungal burden (Nakamura, Sato et al. 2015). Thus, these studies suggest Dectin-2 may play an important protective role during pulmonary cryptococcosis.

1.4.2 Cryptococcal meningitis

If *C. neoformans* infection is not contained within the lung, the fungus can disseminate via the bloodstream towards distal organs, including the CNS. In the brain, cryptococcosis can present as meningitis, encephalitis, or meningoencephalitis, resulting in increased intracranial pressure or cerebral mass lesions called “cryptococcomas”, which generally present with non-specific symptoms such as headache, fever, memory loss, stiff neck, and vomiting (Gao, Jiao et al. 2017). Indeed, a study showed that 70% of patients with CM were misdiagnosed (Yuanjie, Jianghan et al. 2012), causing a critical delay for treatment and contributing towards low survival rate.

CM can be diagnosed by the identification of encapsulated yeast cells in the cerebrospinal fluid (CSF) using India Ink staining (Abassi, Boulware et al. 2015). However, this method can often return false negatives and is generally insensitive. Currently, tests are based on the antibody-mediated detection of Cryptococcal

antigen (CrAg) are much more sensitive and allow for a rapid and low-cost diagnosis (Vidal and Boulware 2015), which is critical since many cases of CM are localised to countries with limited resources (Borges, Araújo Filho et al. 2019). The CrAg test works by detecting the *Cryptococcus* polysaccharide capsule antigen in the CSF; the latest versions of which are based on a lateral flow assay using an immunochromatographic dipstick. This technique is much faster and simpler than culture and/or microscopy based diagnostic assays, and can be performed at the patients' bedside (Boulware, Rolfes et al. 2014), and is also superior to other CrAg-based detection assays (e.g. latex agglutination assay) that require specialised laboratory equipment and skilled personnel (Binnicker, Jespersen et al. 2012). The WHO recommends CrAg screening is performed in HIV-infected patients with a CD4 count of less than 100-200 cells/ μ l. A study on the effectiveness of CrAg screening in sub-Saharan Africa showed that mortality was significantly decreased when a CrAg screening program was introduced (Deiss, Loreti et al. 2021). Moreover, plasma CrAg titers are correlated with mortality and can lead to early identification of patients at risk of developing severe CM and death, even when symptoms are absent (Rajasingham and Boulware 2020). However, several countries in Africa have limited access to the CrAg test meaning that these effective screening programs are not fully implemented in areas where they would have the greatest benefit. Therefore, improving access to these diagnostic tests is a critical step to help introduce prophylactic antifungal therapy and reduce mortality.

Treatment of CM remains challenging due to the limited selection of antifungal drugs available. Even with treatment, over 70% of patients surviving CM suffer from neurological and sensory impairment, leading to disability and reduced quality of life (Shiri, Loyse et al. 2019). The gold standard drug for CM treatment is the

combination of Amphotericin B (AMB) with flucytosine (5-FC), however a typical course of AMB and 5-FC treatment costs approximately (US)\$800 per patient (Shiri, Loyse et al. 2019), and is usually only available in countries with well-funded healthcare systems. In Africa, only a small number of countries are registered to provide 5-FC, and even when registered there is little evidence it has been prescribed to patients in some areas. Therefore, improving the affordability of 5-FC and enhancing awareness of the drug's effectiveness is a crucial step towards ending CM deaths (Miot, Leong et al. 2021). In addition, the use of liposomal formulations of AMB is hindered by cost. Thus, because the use of AMB-deoxycholate (AMB-d) requires prolonged hospitalization for parenteral administration and is associated with renal and metabolic adverse effects, many resource-limited settings in Africa do not use AMB for the treatment of CM. Currently, the most commonly prescribed antifungal drug for CM in Africa is fluconazole, which has been shown to be inferior to AMB (Boulware, Meya et al. 2014, Jarvis, Bicanic et al. 2014, Ford, Migone et al. 2018, Jarvis, Leeme et al. 2019). There are now several reports of fluconazole resistance developing in *C. neoformans*, associated with chromosomal changes in the fungus (Hope, Stone et al. 2019), making management of CM especially difficult in settings where alternative options are not available. Thus, novel therapeutic approaches are needed. Adjunctive immune-based therapy with interferon gamma (IFN γ) has showed promising results in recent clinical trials (Peter, Bustamante et al. 2004, Jarvis, Meintjes et al. 2012). Treatment with recombinant IFN γ combined with antifungal drugs showed that the addition of recombinant IFN γ resulted in improved clearance of fungi from the CSF compared to patients treated with antifungal drugs alone, although these studies were not large enough to determine if this correlated with improved survival (Peter, Bustamante et al. 2004,

Jarvis, Meintjes et al. 2012). Another experimental treatment that has been suggested is the use of corticosteroids to reduce immunopathology-associated neuroinflammation, such as dexamethasone, which has been shown to reduce mortality in patients with bacterial meningitis (De Gans and Van De Beek 2002). However, dexamethasone treatment for CM in HIV-infected patients actually resulted in a higher mortality rate and disability than in the placebo group, and thus these trials were suspended for safety reasons (Beardsley, Wolbers et al. 2016). We therefore still require better antifungal treatments to improve clinical outcomes in patients with CM, which will depend on a better understanding of the immunology of CM (discussed below).

1.4.3 Immune reconstitution inflammatory syndrome

IRIS is a paradoxical emergence of infection and inflammation observed upon recovery of the immune system, usually seen in HIV-patients after the introduction of combination antiretroviral therapy (cART) whose CD4 T cell numbers begin to increase (Neal, Xing et al. 2017). Indeed, Cryptococcal IRIS has been reported in 8-49% of HIV-infected patients treated with cART (Haddow, Colebunders et al. 2010) with a mortality rate reaching 83% (Shelburne, Darcourt et al. 2005, Haddow, Colebunders et al. 2010). IRIS is thought to be caused by excessive activity of Th1 CD4 T cells. Indeed, patients with IRIS have a dominant Th1 polarisation in the CSF, and depleting CD4 T cells later in infection helps limit mortality and neurological deficits by limiting pathological inflammation in the brain of mice (Neal, Xing et al. 2017). IRIS treatment is usually challenging since the clinical feature is the same as to active cryptococcal infection meaning the wrong treatment could be given which could exacerbate symptoms. This highlights the complexity of the clinical

management of CM and special attention needs to be taken to the underlying immune condition of patients prior to infection to minimise the potential detrimental effect.

1.5 Microbiology of *Cryptococcus neoformans*

C. neoformans is a yeast fungus belonging to the basidiomycetes kingdom. *C. neoformans* have several different morphotypes including spores and yeast. One of the largest contributing factors towards *C. neoformans* virulence is its polysaccharide capsule, located outside the cell wall (Figure 1.1). The capsule is composed of two major constituents, glucuronoxylomannan (GXM) and Glucuroxylomannogalactan (GXMGal), with other minor non-polysaccharide components including mannoprotein and chitin-like structures (Figure 1.1) (Vartivarian, Reyes et al. 1989, Alspaugh 2015). A lot of evidence has suggested that the capsule is fundamental for *C. neoformans* survival inside the host, where capsule defects caused by mutation result in attenuation of *C. neoformans* virulence in mouse infection models and within in vitro systems (Meara and Alspaugh 2012). This is because the capsule renders *C. neoformans* more resistant to phagocyte killing, oxidative stress, and antifungal drugs (Zaragoza, Chrisman et al. 2008, Okagaki, Strain et al. 2010). This shows the importance of understanding the structure and microbiology of *C. neoformans* for understanding its virulence. During infection, *C. neoformans* can undergo drastic morphological changes, modulating the capsule and cell wall to grow in size, reaching up to 100µm in the lung (Feldmesser, Kress et al. 2001). These giant polyploid cells, termed “titan” cells, are more resistant to antifungal drugs and phagocytosis by immune cells, due to their large size (Okagaki, Strain et al. 2010). Moreover, the mechanisms involved that control the formation of titan cells are

poorly understood. In vitro studies have shown environmental factors can stimulate production of titan cells including serum, bacterial peptidoglycan, sodium azide and hypoxia (Dambuza, Drake et al. 2018, Hommel, Mukaremera et al. 2018, Trevijano-Contador, de Oliveira et al. 2018). A recent new study showed that in a phosphate rich environment, *C. neoformans* forms small morphotype cells termed “seed cells” which were critical for extrapulmonary dissemination (Denham, Brammer et al. 2022). Moreover, Gibson et al showed that depending on fungus size, fungus can get stuck in blood vessels leading to blockage and rupture of the vessel leading to the fungus dissemination to surrounding tissues (Gibson, Bojarczuk et al. 2022). These studies shed light on the fungus morphological heterogeneity and the need to understand the mechanisms regulating this heterogeneity. This will help us determine what causes the fungus to disseminate and help us identify strategies to target *C. neoformans* and utilise ways to treat infection and reduce mortality.

Beside capsule, *C. neoformans* have many traits that give it the ability to become virulent within immunosuppressed patients, including encapsulation and melanisation (Warnock 1999). *C. neoformans* can also produce degrading enzymes, such as proteases, lipases, and urease, which contribute to its virulence. These enzymes help *C. neoformans* destroy tissues, proliferate within the host, degrade immune response and disseminate to the CNS (Almeida, Wolf et al. 2015). Urease is another important virulence factor in *C. neoformans* (Figure 1.1). Urease is an enzyme that converts urea into ammonia which is toxic to human cells. Mice infected with a urease-deficient strain had increased survival rate compared to wild-type (WT) (Cox, Mukherjee et al. 2000, Olszewski, Noverr et al. 2004). This was found to be in part related to urease’s function in promoting yeast cell dissemination to the brain (discussed in detail below) (Olszewski, Noverr et al. 2004). Moreover, urease

production by *C. neoformans* was found to be required for the maturation of dendritic cells (DCs) in the lungs (Osterholzer, Surana et al. 2009). These studies highlight the important role of cryptococcal urease in pathogenesis and the potential of utilising them as a drug target.

Lastly, *C. neoformans* has the ability to produce melanin (Figure 1.1), a brown-coloured antioxidant pigment produced by *C. neoformans* in the presence of l-3,4-dihydroxyphenylalanine. Strains lacking in the ability to produce melanin are less virulent in mice (Kwon-Chung and Rhodes 1986), which is thought to be related to the ability of melanin to promote *C. neoformans* survival within hosts, protecting it from phagocytosis by suppressing reactive oxygen species (ROS) (Tajima, Yamanaka et al. 2019). Melanin also mediates increased resistance to antimicrobial peptides [26] and can suppress the production of proinflammatory cytokines such as tumour necrosis factor- α (TNF- α), interleukin-1b (IL-1b), and IL-6 (Wang, Aisen et al. 1995, Lee, Jang et al. 2019, Tajima, Yamanaka et al. 2019). Latest research showed strains isolated from patients that produced faster melanin (measuring *Cryptococcus* colony melanisation) were correlated negatively with patient outcome, suggesting that the kinetic rather than the amount of melanin are more important for *Cryptococcus* virulence (de Sousa, de Oliveira et al. 2022).

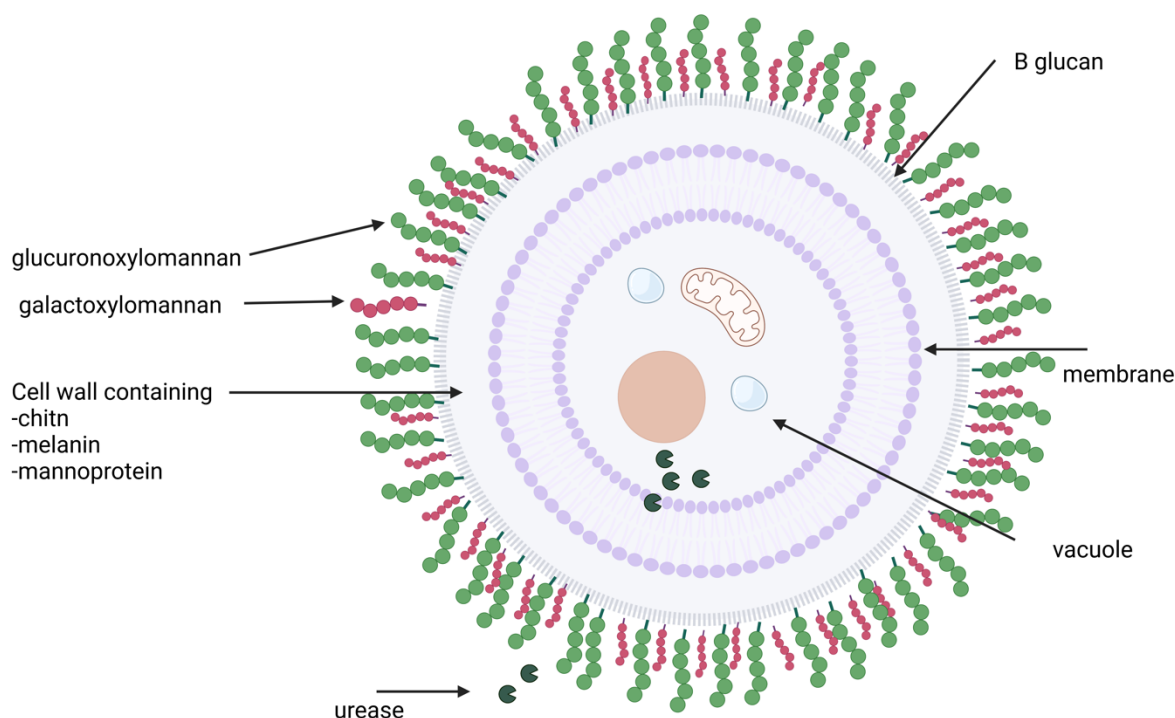


Figure 1. 1 *C. neoformans* cell features: *C. neoformans* cell structure consisting of membrane, cell wall containing chitin, melanin and mannoprotein and capsule. The capsule consisting of GXM and GXMGal.

1.6 Fungal entry to the CNS

The neurotropism of *C. neoformans* is not well understood and neither are the mechanisms involved in CNS invasion. The major pathways that are thought to mediate *C. neoformans* trafficking to the CNS are the Trojan horse method and transcellular migration.

The Trojan horse approach involves *Cryptococcus* yeast getting access to the CNS by transporting inside phagocytic cells, such as macrophages, monocytes, and neutrophils. In support of this hypothesis, a few research studies have shown that depletion of AMs in mice decreased the dissemination of *C. neoformans* to CNS (Kechichian, Shea et al. 2007, Denham and Brown 2018). Another study by the Dromer group compared dissemination to the CNS when mice were infected with bone marrow-derived monocytes previously infected with *C. neoformans* in vitro, or with free yeast. They found that the fungal burden was higher in the brain with

infected bone marrow-derived monocytes compared to free yeast cells, suggesting that infected monocytes were more efficient at brain infection than free yeast (Charlier, Nielsen et al. 2009). Indeed, depleting circulating monocytes at a later stage of infection in mice reduced infection severity and reduced fungal burden by 40% in spleen, lungs, and brain (Charlier, Nielsen et al. 2009), supporting the role of phagocytes in CNS invasion. Moreover, depleting 99% of circulating monocytes in mice before infection abolished the development of CM and cerebral cryptococcomas and reduced fungal burden in the brain by ~90% (Kaufman-Francis, Djordjevic et al. 2018). Neutrophils have also been shown to potentially promote transmission to the brain during *Cryptococcus* infection (Yang, Wang et al. 2019). Using intravital imaging, it was shown that neutrophils can expel *C. neoformans* within the brain vasculature, contributing towards brain infection (Yang, Wang et al. 2019), and depleting circulating neutrophils resulted in a reduced number of yeast cells in the perivascular space and reduced brain fungal burden by ~ 64% (Kaufman-Francis, Djordjevic et al. 2018). Finally, the Trojan horse model has been modelled in vitro, using cryptococcal cells maintained in macrophages to cross human brain microvascular endothelial cells (hBMEC). This model showed a mutant strain of *C. neoformans* deficient in Cps1 (*cps1Δ*) which is a gene involved in hyaluronic acid synthase and important for the fungus binding to Cd44 receptor on hBMEC was less able to cross the blood brain barrier (BBB) in vitro (Santiago-Tirado, Onken et al. 2017).

Another hypothesis for *C. neoformans* entry is the transcellular migration across brain endothelium. Transcellular migration involves the crossing of free yeast directly through the BBB (Chretien, Lortholary et al. 2002, Chang, Stins et al. 2004, Shi, Li et al. 2010). Indeed, using intravital microscopy in mice, it's been shown that free yeast

cells were able to cross the capillary wall and enter the CNS and this migration was urease dependent since using the urease inhibitor fluorofamide reduced transmigration into the brain (Shi, Li et al. 2010). A recent study using NanoString technology revealed a complex signalling process used by *C. neoformans* to cross BBB and found homeobox transcription factor (Hob1) to be a master regulator of *C. neoformans* brain infection, and deleting Hob1 impaired the ability of *C. neoformans* to cross BBB model in vitro (Lee, Hong et al. 2020). Furthermore, the metalloprotease Mpr1 is required for yeasts crossing to the CNS, where it targets brain endothelium specifically (Vu, Tham et al. 2014). Strains lacking Mpr1 failed to cross BBB in vitro and mice infected with this strain showed improved survival and reduced brain fungal burden. Recently, it was demonstrated that internalisation of *C. neoformans* by human brain endothelium depends on EphA2-tyrosine kinase receptors (Aaron, Jamklang et al. 2018), since inhibiting EphA2 prevented transmigration of *C. neoformans* (Aaron, Jamklang et al. 2018). This is seen with other pathogens such as *Chlamydia trachomatis*, Epstein-Barr virus, and malaria parasites (Kaushansky, Douglass et al. 2015, Subbarayal, Karunakaran et al. 2015, Chen, Sathiyamoorthy et al. 2018). Additionally, studies have shown brain endothelium expresses a high level of EphA2, which could alter BBB permeability (Pasquale 2005).

Although there is strong evidence supporting both theories, there is still a lot remained to be answered about these models for example, we still don't know all the genes involved in neurotropism. Furthermore, we still need to understand the complex mechanisms involved between brain-resident phagocytes and *C. neoformans*. Additionally, it is still unknown how HIV infection affects the BBB and how this might affect subsequent *Cryptococcus* infection. Therefore, understanding

other pathogens mechanism of invading CNS and the effect they have of CNS immune cells could help us understand the mechanisms of CNS invasion by *C. neoformans* and help us utilise therapeutic treatments or develop drugs to treat these infections.

1.7 Fungal growth adaptation within the CNS

To survive inside the host, *C. neoformans* must overcome several environmental challenges. These include, temperature, pH, oxygen and nutrient availability, and defence attack by host immune cells (Chun, Liu et al. 2007, Kronstad, Saikia et al. 2012, Ding, Festa et al. 2013, Ost, O'Meara et al. 2015, Bloom, Jin et al. 2019). For this *C. neoformans* must adapt to its restricted environment. The CNS is particularly restricted for several nutrients, and the ability of *C. neoformans* to access these nutrients appears critical for virulence and infection. In this section I will focus on nutrient acquisition of iron and copper by *C. neoformans* within the CNS and how this promotes its infection.

1.7.1 Iron

Iron is an essential metal that involves in many biological processes such as myelin production, oxygen transportation, DNA synthesis and the synthesis of neurotransmitter (Ward, Zucca et al. 2014). Iron level in the CNS needs to be maintained at a homeostasis level, since too much iron can cause neurotoxicity, motor and cognitive defect (Ward, Zucca et al. 2014), as observed in patients with aceruloplasminemia (genetic disorder characterised by iron overload in the CNS) (Marchi, Busti et al. 2019). The restricted level of iron in the CNS is another defence strategy by the host against pathogens, as iron acquisition is important for many

pathogens virulence. Indeed, iron overload in liver transplant recipients has been correlated with enhanced susceptibility to disseminated cryptococcosis (Singh and Sun 2008, Sifri, Sun et al. 2010). Furthermore, iron overload has been shown to exacerbate the outcome of cryptococcal meningoencephalitis in mice (Barluzzi, Saleppico et al. 2002). Research looking at *C. neoformans* transcriptome using gene expression analysis in iron deficient and iron sufficient conditions showed that the lack of iron led to *C. neoformans* remodelling of metabolism of glucose, nitrogen and respiration pathways (Lian, Simmer et al. 2004). Additionally, this study showed iron level affected *C. neoformans* capsule formation, where high iron concentrations resulted in bigger capsule whereas iron limitation reduced capsule production (Lian, Simmer et al. 2004). Moreover, iron has been shown to influence melanin formation which is important for virulence (as discussed above) (Gómez and Nosanchuk 2003) by effecting laccase (enzyme involved in melanin biosynthesis) activity and expression (Gómez and Nosanchuk 2003). *C. neoformans* uses iron transporters to acquire iron where CFT1 plays the major role in iron acquisition (Jung, Sham et al. 2008). Deletion of CFT1 resulted in a reduced virulence in mice and less brain fungal burden. Furthermore, there was reduced dissemination of *C. neoformans* to the brain when mice were infected either intranasally or intravenously with the CFT1-mutant strain. In contrast, lung fungal burden was high compared to brain at the same time suggesting CFT1 is not as important in the lung compared to brain and this might be due to tissue differences in iron level (Jung, Sham et al. 2008).

1.7.2 Copper

Copper is another essential metal for biological process such as biosynthesis of neurotransmitter, energy metabolism, myelin production and immunity. Similar to

iron, there are tissue-specific differences in copper availability, with greater levels detected in lung and low levels in the CNS. In the CNS, copper homeostasis is important for brain development and function, since copper dysregulation has been correlated with neurodegenerative diseases (Opazo, Greenough et al. 2014).

Moreover, copper deficiency leads to brain abnormality and development (Scheiber, Mercer et al. 2014). Indeed, Menkes disease (defect in copper level) result in a severe brain abnormality and mortality by the age of 5 (Tümer and Møller 2010), indicating the essential function of copper. Furthermore, copper plays an essential role in immunity, where copper deficiency leads to bacterial susceptibility in both humans and animals (Jones and Suttle 1983, Crocker, Lee et al. 1992). Research shows copper deficiency has been shown to effect neutrophil and macrophages antibacterial activity (Heresi, Castillo-Durán et al. 1985), thus copper is an essential element of the host defence system (see Chapter 3 for more details).

In term of *C. neoformans*, copper is important for the fungus virulence. Copper is sensed by copper regulator transcription factor (Cuf1), which leads to copper transporter dysregulation CTR4 and CTR2 when copper level is high or induce the expression of CTR2 and CTR4 when copper level is low.(Waterman, Hacham et al. 2007, Chun and Madhani 2010, Jiang, Liu et al. 2011). Deletion of Cuf1 caused growth defect in limited copper condition and infecting mice with this mutant strain led to reduced brain dissemination but no effect on lung infection (Waterman, Hacham et al. 2007), reflecting the low amount of copper in the CNS. During infection *C. neoformans* must overcome the high level of copper available in the lung, therefore, it starts to upregulate copper detoxification gene (CMT1), while in the brain the fungus starts to switch on copper scavenging gene (CTR4) [80]. Indeed, CTR4 expression was increased by *C. neoformans* isolated from the human brain,

and higher CTR4 expression was correlated with CNS dissemination in organ transplant patients (Waterman, Hacham et al. 2007). Additionally, copper plays an important role in melanin production, where it effects laccase activity and Fet3 which is important for iron uptake and for this copper limitation leads to iron limitation (Walton, Idnurm et al. 2005). Furthermore, copper and iron has been shown to interconnect, where some study suggest that copper homeostasis might by regulated by iron (Walton, Idnurm et al. 2005). Indeed, CTR4 transcript has been shown to be altered in different iron level media (Jung, Sham et al. 2006), suggesting an interdependent relationship between copper and iron.

1.8 Host immune repeses to *Cryptococcus neoformans*

Innate immune cells (DCs, monocytes, neutrophils and macrophages) and adaptive immune cells (T cells and B cells) are the line of defence against *C. neoformans*. Control or eradication of *C. neoformans* begins with the recognition of yeast cells via pattern recognition receptors (PRRs), including the CLR and Toll-like receptors (TLRs) (Table 1.1), expressed by these innate immune cells. PRRs bind to pathogen-associated molecular pattern recognition receptors (PAMPs), which are found in the cell wall and capsule of *C. neoformans* (Table 1.1). Indeed, the mannose receptor (MR; CD206) is an important PRR for anti-cryptococcal protection, in part by driving successful CD4 T cell responses against *C. neoformans* (Dan, Kelly et al. 2008) (Figure 1.2). Important PRRs for the recognition of fungi include members of the CLR superfamily (e.g. Dectin-1, Dectin-2, Dectin-3) and TLRs see table 1.1 and figure 1.2. These receptors bind carbohydrate components of the fungal cell wall or surrounding capsule, which leads to the activation of intracellular signalling cascades that can induce activation and differentiation of CD4

helper T cells (Th) via the production of polarising cytokines (Figure 1.2). Their role during *C. neoformans* infection in mice is outlined in table 1.1

CARD9 (caspase recruitment domain-containing protein 9) is a signalling adapter protein expressed by myeloid cells, including neutrophils, DCs, and macrophages, coupled to several CLR family members and essential for activation of CLR-dependent immune responses against fungi (Saijo, Fujikado et al. 2007, Taylor, Tsoni et al. 2007, Saijo, Ikeda et al. 2010, Hardison and Brown 2012) (Figure 1.2). In brief, the CARD9 signalling pathway is activated following CLR ligation by a fungal ligand, leading to the activation of the kinase Syk (spleen tyrosine kinase) and subsequent formation of the CBM signalosome complex, which is made up of CARD9, BCL10 and MALT1. This leads to activation of NF κ B (nuclear factor κ -light-chain-enhancer of activated B cells) and other transcription factors that mediate antifungal immune responses, as well as several other signalling cascades controlling cellular immune responses (e.g. phagocytosis) (Figure 1.2). Due to the central positioning of CARD9 in generating antifungal immune responses, a defect in CARD9 function results in a profound susceptibility to fungal infections in humans and mice. Human peripheral blood mononuclear cells (PBMCs) isolated from CARD9-deficient patients show significant defects in the production of proinflammatory cytokines, such as GM-CSF, IL-1 β , IL-6 and TNF α , specifically in response to fungal stimuli while responses to bacterial stimuli remain intact (Glocker, Hennigs et al. 2009, Drewniak, Gazendam et al. 2013). Indeed, CARD9 deficient-patients do not appear to show enhanced susceptibility to bacterial, viral or parasite infections (Drummond and Lionakis 2016). One of the most striking features of human CARD9 deficiency is the organ-specific localisation of fungal infections observed in these patients, which predominantly involve the oral mucosa, skin and

CNS (Gross, Gewies et al. 2006, Glocker, Hennigs et al. 2009, Lanternier, Pathan et al. 2013, Drummond and Lionakis 2016). Card9-deficient mice are also highly susceptible to systemic fungal infections, including *C. albicans*, *A. fumigatus* and *C. neoformans*, and mimic many of the same immunologic dysfunctions as CARD9-deficient humans (Drummond, Collar et al. 2015). Card9 deficient mice showed increase in Th2 type cytokines and had increased fungal burden when infected with *C. neoformans* compared to Card9 sufficient mice (Campuzano, Castro-Lopez et al. 2020).

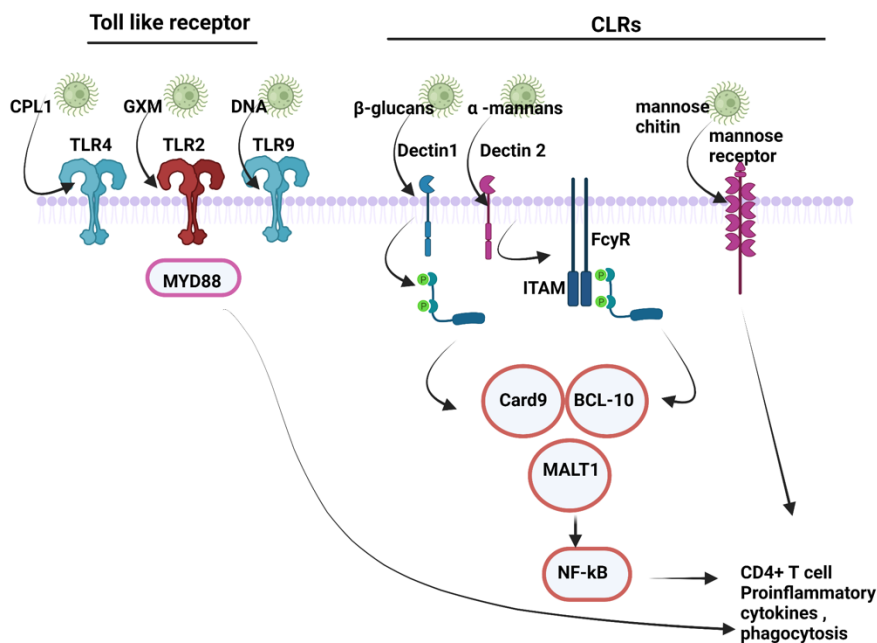


Figure 1. 2C. neoformans main pattern recognition receptor: Selected *C. neoformans* PRRs (Discussed in detail in the 1.7 section) are depicted with their best characterised *C. neoformans* PAMPs and downstream function during *C. neoformans* infection.

Table 1. 1: The key PRRs and PAMPs for *C. neoformans* and their role during infection.

PRR	PAMP	Outcome
TLR2	GXM	TLR2-KO mice had a higher fungal burden than WT and more susceptible to pulmonary <i>Cryptococcus</i> (Yauch, Mansour et al. 2004).
TLR9	<i>Cryptococcus</i> DNA	TLR9-KO mice had higher fungal growth in the lung and had a decreased level of IFN γ and impair DCs accumulation (Qiu, Zeltzer et al. 2012).
TLR4	CPL1	CPL1 activate TLR4 to induce Stat3 cytokines such as arginase 1 and IL-4(Dang, Lei et al. 2022)
Dectin 1 (CLEC7A, CLECSF12, CD369)	β -glucans	Dectin-1 KO mice had phagocytosis reduction by alveolar macrophages compared to WT (Walsh, Wuthrich et al. 2017).
Dectin 2 (CLEC6A, CLEC4N)	α -mannans	Dectin-2 KO mice were more susceptible to pulmonary <i>Cryptococcus</i> and lacked effective Th1 response (Nakamura, Sato et al. 2015).
Dectin 3		Dectin 3 deficient mice show no difference in mice survival or phagocyte <i>cryptococcus</i> compared to WT(Campuzano, Castro-Lopez et al. 2017)
Mannose receptor (CD206)	Mannose and chitin	Mice-deficient in mannose receptors had a higher fungal burden in the lung

1.9 Innate immune cell function in controlling *Cryptococcus neoformans* infection.

1.9.1 Dendritic cells

DCs bridge innate and adaptive immune responses by presenting antigens to naïve T cells. *C. neoformans* Capsule materials can manipulate affect DCs maturation process, where stimulating DCs in vitro with *C. neoformans* did not induce upregulation of MHC I, MHC II or CD83 (markers of DCs maturation) (Vecchiarelli, Pietrella et al. 2003) and thus impacting downstream T cell responses. Targeting

DCs might better the immune response against *C. neoformans*. Indeed, DCs exhibit innate memory-like immune response in vivo when infected with transgenic *C. neoformans* strains that produce mammalian IFN γ (Hole, Wager et al. 2019). DCs isolated from lungs of mice infected with this transgenic strain had a phenotype similar to M1 activated macrophages with increased proinflammatory cytokine production such as IL-2, TNF- α , and IFN γ when challenged with a secondary infection of the lethal WT *C. neoformans* strain following ‘vaccination’ with the transgenic strain (Hole, Wager et al. 2019). These studies reveal an aspect of DCs that can be manipulated or “trained” to induce a memory-like immune response which may be beneficial for future vaccine development against *Cryptococcus* infection.

1.9.2 Neutrophils

Neutrophils are circulating phagocytic cells and their role against *Cryptococcus* is controversial and remains poorly defined. Nonetheless, human neutrophils have been shown to phagocytose *C. neoformans* in vitro (Miller and Mitchell 1991). However, *C. neoformans* appears to be able to interfere with human neutrophils by inhibiting their migration and the formation of neutrophil extracellular traps (NETs) (Richardson, White et al. 1993, Walenkamp, Ellerbroek et al. 2003, Rocha, Nascimento et al. 2015). Treating mice with granulocyte-colony stimulating factor (G-CSF, regulator of neutrophil production and activity) in combination with fluconazole helped reduce the fungal burden in the brain and prolonged survival (Graybill, Bocanegra et al. 1997). On the other hand, neutrophils can have detrimental effect during *C. neoformans* infection, where depleting neutrophils in mice improved mice survival by reducing inflammatory damage in the lungs (Mednick, Feldmesser et al.

2003). Moreover, human studies have indicated that higher neutrophil numbers in the blood are correlated with higher mortality in CM patients (Musubire, Meya et al. 2018). Therefore, the role of neutrophil during *C. neoformans* infection needs further exploration and the mechanisms involved in the detrimental effects need to be investigated.

1.9.3 Macrophages

Macrophages are one of the most abundant populations of myeloid cells and there are different types such as inflammatory monocytes derived and tissue-resident macrophages. In the context of fungal infection majority of studies focuses on inflammatory macrophages, with little done on tissue-specific macrophages (which I will discuss in more detail in Chapters 3 and 4). The ability of macrophages to control cryptococcal infection is associated with two phenotypes; classically activated macrophages (M1) and alternatively activated macrophages (M2) (McQuiston and Williamson 2012). In the context of *C. neoformans* infection, M2 is more permissive for intracellular growth of *C. neoformans* (Leopold Wager and Wormley 2014, Leopold Wager, Hole et al. 2016) while M1 is associated with anti-cryptococcal activity (Arora, Hernandez et al. 2005, Hardison, Ravi et al. 2010, Arora, Olszewski et al. 2011), where they kill fungi by activating iNOS leading to the generation of antifungal nitric oxide (Alspaugh and Granger 1991, Davis, Tsang et al. 2013, Leopold Wager, Hole et al. 2015). During infection, M1/M2 plasticity depends on the cytokine found within the microenvironment, where IFN γ and IL-4 drive the polarisation of M1 and M2 respectively (Davis, Tsang et al. 2013). IFN γ production by Th1 CD4 T cells polarises macrophages to M1 through signal transducer and activator of transcription1 (STAT1) signalling (Leopold Wager, Hole et al. 2015).

STAT1 is critical for M1 polarisation of macrophages and protection against infection, since mice deficient in STAT1 had shifted towards M2 phenotype and an associated higher fungal burden in the lungs compared to WT mice (Leopold Wager, Hole et al. 2015). In addition, using an engineered *C. neoformans* strain that produces murine IFN γ in a pulmonary mouse model showed an elevated level of M1 activation and heightened protection against *C. neoformans* (Hardison, Ravi et al. 2010). Indeed, IFN γ knockout mice have a higher number of M2 macrophages and increased fungal burden in the lungs.

Interestingly, *C. neoformans* can actively skew macrophage polarisation for their benefit. For example, chitin in the *C. neoformans* cell wall is recognised by the host chitinase Chit1, which was found to drive Th2 differentiation and M2 activation in both mice and humans by triggering IL-4 production (Van Dyken, Mohapatra et al. 2014, Wiesner, Specht et al. 2015). Furthermore, *C. neoformans* can also actively inhibit protective macrophage responses, by masking the signal necessary for TNF- α secretion and iNOS induction through their polysaccharide capsule (Naslund, Miller et al. 1995), as well modulating phagosome maturation via urease and other virulence factors (Fu, Coelho et al. 2018).

Although macrophages are important for immunity against *C. neoformans*, there have been debates about whether they also contribute negatively towards the host's outcome. Indeed, higher uptake of *C. neoformans* by macrophages correlated to higher fungal burden in the brain and lower survival rate in patients. Moreover, these patients had an elevated level of IL-4 and M2 activation, suggesting *C. neoformans*-macrophages interaction is important for disease outcome (Hansakon, Mutthakalin et al. 2019). Additionally, macrophages can be a site where *C. neoformans* survives and replicates, thus 'hiding' from the host immune system. Indeed, both in vitro and

in vivo studies showed *C. neoformans* residing inside macrophages (Levitz, Nong et al. 1999, Feldmesser, Kress et al. 2000). Lastly, macrophages have been shown to play part in dissemination of the fungus to the CNS by acting as 'Trojan horses', (as discussed above).

1.9.4 Monocytes

Monocytes can be divided into two main subset classical monocytes and patrolling monocytes, and both have important role in surveillance against pathogens.

Classical monocytes are short lived cells, count for majority of the circulating monocytes and usually recruited to site of infection, where they can differentiate into DCs or macrophages (M1 or M2) (Yona, Kim et al. 2013, Yang, Zhang et al. 2014, Patel, Zhang et al. 2017). Patrolling monocytes are cells that patrol tissue and clear debris and their role during infection is less studied compared to the classical monocytes (Thomas, Tacke et al. 2015). During *C. neoformans* infection, monocytes have been shown to have protective role in controlling infection, where monocytes dysfunction is positively correlate with high fungal burden in the CSF in HIV- patients (Monari, Baldelli et al. 1997, Scriven, Graham et al. 2016). Similarly, mice who are monocytes deficient have higher fungal burden compared to wild-type and are more susceptible to *C. neoformans* infection (Osterholzer, Curtis et al. 2008, Osterholzer, Surana et al. 2009). Furthermore, in vitro studies have shown that monocytes are able to phagocytose *C. neoformans* and act as an antigen presenting cells activating T cells (Vecchiarelli, Retini et al. 2000). Indeed, monocytes-deficient mice had reduced lymphocytes recruitment to the lung including CD4 T cells, CD8 T cells and Natural killer cells (NK) and subsequently reduced IFN γ production (Traynor, Kuziel et al. 2000, Heung and Hohl 2019). Nonetheless, other studies have shown that

monocytes can have determinantal role to the host during infection where monocytes-deficient mice had reduced *C. neoformans* dissemination and improved survival (Heung and Hohl 2019) and as discussed in section 1.6, *C. neoformans* can use monocytes as a trojan horse helps it invading the CNS. Indeed, recent study by Sun et al using intravital microscopy showed that *C. neoformans* uses patrolling monocytes as a carrier to the CNS, where *C. neoformans* moved from the brain vessels to the parenchyma and that patrolling monocytes rather than the classical monocytes are the one that recruited to the brain (Sun, Zhang et al. 2020), highlighting the important role these cells play during infection.

1.10 Adaptive immunity response to *Cryptococcus neoformans*

1.10.1 CD4 T cells

CD4 T cells are adaptive lymphocytes expressing antigen-specific receptors that play a central role in orchestrating immune responses. As outlined above, patients with compromised T cell function are highly susceptible to CM thus indicating the importance of CD4 T cells in mediating immunity against *C. neoformans*. There is growing evidence that T cells are present in the healthy CNS, which have a unique CNS-resident phenotype and are important for CNS homeostasis and animal behaviour (Engelhardt and Ransohoff 2005, Smolders, Remmerswaal et al. 2013, Drummond 2017, Korin, Ben-Shaan et al. 2017). Mice deficient in adaptive immunity (e.g. *Rag1*^{-/-}) have behavioural abnormalities, which was recently linked to their role in promoting microglial maturation in the developing brain (Kipnis, Cohen et al. 2004, Brynskikh, Warren et al. 2008, Derecki, Cardani et al. 2010, Kipnis, Gadani et al. 2012, Filiano, Gadani et al. 2015).

As outlined above, these lymphocytes are thought to be required to activate antifungal killing pathways in myeloid cells. Although, Th1 have shown to be protective against *C. neoformans* in both mice and humans (Peter, Bustamante et al. 2004, Chen, McDonald et al. 2005, Jarvis, Meintjes et al. 2012, Xu, Eastman et al. 2016), depleting CD4 T cells later in infection helps limit mortality and neurological deficits by limiting pathological inflammation in the brain (Neal, Xing et al. 2017). This highlights the need to better understand the role and control of CD4 T cells responding to infection within the CNS. Indeed, the pathological potential of IFN γ in the CNS has been shown in patients with other infections, such as tuberculosis meningitis (Antonelli, Mahnke et al. 2010) and *Toxoplasmosis* (Rb-Silva, Nobrega et al. 2017). However, what causes Th1 to be pathogenic is still unknown and thus it will be important to delineate the exact function and behaviour of these lymphocytes before utilising any therapies that manipulate their function for treatment.

CD4 T cell recruitment to the cryptococcal-infected brain was recently shown to require CXCR3 (Xu, Neal et al. 2020). Both human and murine T cells significantly upregulated CXCR3 in response to *C. neoformans* infection, and this chemokine receptor was required for Th1 polarization. Interestingly, *Cxcr3*^{-/-} mice were protected from infection-associated CNS inflammation and thus had improved survival, but this did not correlate with reduced fungal burden. These studies therefore show that CXCR3⁺ Th1 T cells are not needed to help control fungal infection in the brain, at least in the context of an IRIS-like syndrome (Xu, Neal et al. 2020). Similarly, knockdown of CCR2 in mice was also shown to improve survival independently of fungal control in the CNS, although CCR2 was not involved in the direct recruitment of Th1 T cells to the CNS but acted indirectly by promoting the initial recruitment of inflammatory monocytes (Xu, Ganguly et al. 2021). Collectively, these studies

indicate that T cells have a complex role in CM, both for fungal clearance and mediating immunopathology, which is likely context- and time-dependent.

1.10.2 B cells

B cells have shown to have antifungal role against *C. neoformans* where they produce anti-cryptococcal antibodies that are required for effective opsonisation of the fungus (particularly the capsule) and uptake by phagocytes, including macrophages (Dufaud, Rivera et al. 2018). Patients with X-linked agammaglobulinemia (XLA), an inherited immune-deficiency caused by mutations in the *BTK* gene and characterised by an absence of B cells, have been reported to develop CM (Gupta, Ellis et al. 1987). Furthermore, reduced production of IgM in HIV+ patients has been correlated with a greater risk for developing CM (Subramaniam, Metzger et al. 2009). Treatment with the BTK inhibitor Ibrutinib, a drug used in the treatment of B-cell lymphomas, has been reported to promote CM in a small number of patients, although the exact underlying mechanisms and relative incidence of CM in Ibrutinib-treated patients remain unclear (Chamilos, Lionakis et al. 2018). Mice with B cell and/or antibody deficiencies also have increased susceptibility to *C. neoformans* infection, characterized by higher brain fungal burden (Szymczak, Davis et al. 2013). Thus, B cells provide critical support to phagocytes in the fight against CM and clearance of yeast cells from infected tissues.

1.11 Future perspective

CM are often fatal representing a global problem that is caused by increased in immune suppressed population. Furthermore, there is increase in resistance to limited selection of available antifungal drug. The role of myeloid cells residing within

the CNS during infection with *C. neoformans* is poorly understood. Yet their role would be great new clinical target. Future studies should focus on the role of tissue resident macrophages during *C. neoformans* infection since *C. neoformans* use these cells to reside and proliferate within them. Therefore, by understanding tissue resident macrophages function we might be able to understand why some fungal infections of the brain are common and others are rare. This will help us design new therapeutic targets for this deadly infection. For that, my PhD aim is to understand the role of tissue resident macrophages in an organ specific context and examine whether they are involved in the protection or dissemination of *C. neoformans*.

2

Methods and materials

2.1 Mice

All animals were used at 6-12 weeks of age and maintained in individually ventilated cages (5 mice maximum per cage) at the Biomedical Service Unit (BMSU) at the University of Birmingham. Mice were housed in ventilated cages and provided with food and water ad libitum. All mouse strains used in this thesis are outlined in Table 2.1. The following transgenic mice were originally purchased from Jackson and then bred-in house at BMSU; Cx3cr1^{CreEr}, ROSA26iDTR, Csf1r^{flox}, Cx3cr1^{tmlitt} ccr2^{tm2.1ifc}. Sall1^{CreER} were kindly gifted from Dr Melanie Greter (University of Zurich) and bred in-house at BMSU. Some of these lines were crossed to make new lines (Table 2.1). All animal works are defined by the Animal Scientific Procedure act 1986, regulated by the Home Office and under Project Licence PBE275C33 awarded to Dr Rebecca Drummond. Mice were euthanised at defined time point post-infection (see figure legends) or after humane endpoints had been reached, whichever occurred earlier. Humane endpoints for our studies included 20% weight loss or had a hunched/scruffy appearance for >24 h. All experiments conformed to conditions approved by the Animal Welfare and Ethical Review Board.

Table 2. 1: Mouse strain used in this thesis and their strain number, origin and selected reference.

Mouse strain	Origin/ reference
Wild type (C57BL/6)	Charles River
Csf1rflox	021212 Jackson (Li, Chen et al. 2006)
Cx3cr1 ^{tm1litt} ccr2 ^{tm2.1fc}	032127 Jackson (Li, Wang et al. 2014)
ROSA26iDTR	007900 Jackson (Buch, Heppner et al. 2005)
Cx3cr1 ^{CreEr}	020940 Jackson (Yona, Kim et al. 2013)
Sall1 ^{CreER}	Gift by Melanie Greter (Buttgereit, Lelios et al. 2016)
Sall1 ^{CreEr} x iDTR	Bred in house at BMSU
Sall1 ^{CreER} xCsf1flox	Bred in house at BMSU
Sall1 ^{CreEr} x iDTR	Bred in house at BMSU
Nr4a1 ^{-/-}	Gift from David bending
Rag1 ^{-/-}	Bred in house at BMSU

2.2 Tamoxifen and Diphtheria toxin administration

Tamoxifen was made by dissolving in 100% ethanol (1g/ml) and diluted in corn oil (Sigma) to 100mg/ml. Mice received two doses of tamoxifen by oral gavage (100mg in 100µl) 48 hours apart. These mice were left for either 1 week or 4-6 weeks (see result figure/legend for each model for more details on dose). Diphtheria toxin was injected intraperitoneally 30ng per gram body weight (see result section/legend for dose when used in model).

2.3 PLX5622 treatment

PLX5622 (Plexxikon Inc. Berkley, CA) was formulated in AIN-76A rodent chow by Research Diet Inc. (New Brunswick, NJ) at a concentration of 1200 mg/kg. Mice were provided constant access to either PLX6522 or control diet (AIN-76A without

the drug) for 7 days before infection and where left on diet for the duration of the experiment .

2.4 *C. neoformans* growth and mouse infections

C. neoformans strains used in this study were H99, KN99 α -mCherry, KN99 α -GFP, *rdi1* Δ , *gcs1* Δ , and pCTR4-GFP (Table 2.2). Yeast was routinely grown in YPD broth (2% peptone [Fisher Scientific], 2% glucose [Fisher Scientific], and 1% yeast extract [Sigma]) at 30 °C for 24 hours with shaking at 200rpm. In some experiments, CTR4^{pGFP} *C. neoformans* was grown in copper deficient YNB media (Formedium), supplemented with 2% glucose and copper sulphate (Sigma; see figure legends for specific concentrations). For mouse infections, yeast cells were washed twice in sterile PBS, counted using haemocytometer and 2×10^4 yeast (in 100 μ l) injected intravenously into the lateral tail vein or 2×10^5 yeast cells delivered intranasally (in 20 μ l) pipetted onto the mouse nares under isoflurane anaesthesia.

Table 2. 2: *C. neoformans* strain used in this thesis.

<i>C. neoformans</i> strain	Reference and Details
H99	Wild-type laboratory strain
KN99 α -mCherry	mCherry expression is controlled by the ACT1 promotor (Voelz, Johnston et al. 2010)
KN99 α -GFP	GFP expression is controlled by actin promotor and tryptophan terminator (Voelz, Johnston et al. 2010)
<i>rdi1</i> Δ	<i>Rdi1</i> gene was deleted from H99 strain (Price, Nichols et al. 2008)
<i>gcs1</i> Δ	<i>Gcs1</i> gene was deleted from H99 strain (Rittershaus, Kechichian et al. 2006)
pCTR4-GFP	GFP encoding gene driven by copper deficiency inducible copper importer (CTR4) promotor

2.5 *C. neoformans* growth in PLX5622

In some experiments *C. neoformans* was grown in the presence of PLX5622 for 48 hours. *C. neoformans* was seeded into 96 well plates at 5000 yeast/well, in the presence or absence of PLX5622 (3-12µg /ml) see figure legends for final concentrations. Yeast growth was monitored by serial reading at OD₆₀₀ using a FLUOstar Omega microplate reader. Data was averaged across 3 wells per growth condition.

2.6 Generation of pCTR4^{GFP} *C. neoformans*

The pCTR4-GFP-mCherry strain was generated by transforming the integrative pCTR4-GFP plasmid (Sun, Ju et al. 2014), which has GFP encoding gene driven by copper deficiency inducible copper promotor (CTR4), into KN99α-mCherry. Transformations of *C. neoformans* were completed using biolistic DNA delivery system, as previously described (Toffaletti, Rude et al. 1993). The resulting pCTR4-GFP-mCherry strain was tested through growth on copper-sufficient and copper-deficient media to check correct functioning of the pCTR4 GFP construct.

2.7 Determination of organ fungal burden

For analysis of brain, lung, spleen and liver fungal burdens, animals were euthanised and organs aseptically removed, weighed, homogenised in PBS using a Stuart Handheld homogeniser (Cole Parmer), and serially diluted before plating onto YPD agar supplemented with Penicillin/Streptomycin (Invitrogen). Colonies were counted after incubation at 30°C for 48h and the result expressed as CFU/g tissue.

2.8 Isolation of brain leukocytes

Brains were aseptically removed and collected into ice-cold 7 ml FACS buffer (1X PBS + 0.5% BSA + 0.01% sodium azide) and were gently smashed using a syringe plunger. The suspension was brought to 10mL by adding 3mL of 100% Percoll (GE Healthcare 5 ml 10x PBS and 45 ml Percoll) was added and mixed by inverting gently. The suspension was underlaid with 1.5mL of 70% percoll (diluted in FACS buffer) and then centrifuged at 2450rpm for 30 min at 4 °C with the brake off. The leukocytes at the interphase were collected using a pastette and placed in a 5mL fresh FACS buffer, and then centrifuged at 1500rpm for 5 min at 4 °C. Cell pellets were resuspended in 200µl FACS buffer and filtered through a 100µM filter, then stored on ice prior to staining.

2.9 Isolation of meninges leukocytes

Meninges were collected from euthanised mice by cutting off the top of the skull gently around the edge (over nose, below eye socket and by keeping low around back of the neck and gently peeled back. A curved forceps then used to push the meninges inwards towards the central line. Once all the meninges placed in the central line a forceps used to gently lift up the meninges to release from the skull and place into 1.5mL Eppendorf containing 400µl digest buffer (complete RPMI supplemented with 1mg/ml collagenase [Fisher scientific], 1mg/mL dispase [Sigma] and 40µg/ml DNase [Sigma]). The meninges were digested in a 37 °C water bath for 30 min with intermittent shaking every 5-10 min. The meninges were filtered through a 70µM cell strainer and then centrifuged at 1500rpm for 5 min at 4°C. Cells were resuspended in 200µl FACS buffer and stored on ice prior to staining.

2.10 Isolation of lung leukocytes

Lungs were removed from euthanised mice, minced using scalpel and placed in 4mL digest buffer (RPMI, 10% FBS, 1% Pen/Strep, 1mg/ml collagenase, 1mg/ml dispase and 40µg/ml DNase). The lungs were incubated in a water bath for 40-60 minutes at 37 °C with intermittent shaking every 5-10 min. Lung tissue then was gently smashed using a syringe plunger and filtered through 100µM filter sitting into 6 well plates and washed with 3mL FACS buffer, centrifuge at 1400rpm for 7 min at 4°C. 1mL of 1x BD PharmLyse (BD) was added to each sample and then incubated for 5 min on ice. 5mL of 2mM EDTA/PBS was then added to each sample and the sample passed through 100µM filter into a fresh tube and centrifuged at 1400rpm for 7 min. Cell pellets were resuspended in 200µl FACS buffer, stored on ice, and placed in a FACS tube ready for staining.

2.11 Isolation of peripheral blood leukocytes

Mice were anaesthetised using isoflurane and up to 300µl of blood were obtained via cardiac puncture. Mice were placed in isoflurane chamber until the mouse falls asleep. Mice then placed on isoflurane nose cone. Needle inserted under the sternum into the chest cavity and the syringe plunger was gently pulled back to draw blood. Blood was mixed with 50µl 100mM EDTA solution and stored on ice. 5mL of 1x BD pharmLyse was added to each sample and incubated for 5 min on ice, with gentle inversion after 2.5 min. 8mL of 2mM EDTA in PBS was then added, gently inverted to mix, and samples centrifuged at 1500rpm for 5 min at 4°C. The supernatant was discarded. 5mL FACS was added and gently vortexed, and then centrifuged at 1500rpm for 5 min at 4°C to wash the cells. Cells were resuspended in 200µl FACS buffer, stored on ice and placed in a FACS tube ready for staining.

2.12 Cell isolation from spleen

Spleens were collected and placed in 1 ml PBS stored on ice. Tissues were gently smashed using syringe plunger through a 70 μ M filter. The filter was washed with PBS and samples were centrifuged at 1500rpm for 5 minutes at 4°C. 1ml of 1x BD PharmLyse was added to pellet and incubated for 5 minutes on ice. 5 ml of 2 mM EDTA/PBS was added to each sample and then centrifuged at 1500rpm for 5 minutes at 4°C. Cells were resuspended in 1 ml FACS buffer, stored on ice and 200 μ l placed in a FACS tube ready for staining.

2.13 Cell isolation from bone marrow

Bone marrow was isolated from the right femur leg bone. Bones were flushed with 2mM EDTA/PBS using 25-gauge needle attached to 1 ml syringe. Samples were centrifuged at 1500rpm for 5 minutes at 4°C. Cells were resuspended in 200 μ l FACS buffer filtered using 70 μ M filter, stored on ice and placed in a FACS tube ready for staining.

2.14 Flow cytometry: Surface staining

Cells were washed with 1mL of FACS buffer, centrifuged at 1500rpm for 5 minutes at 4°C. The supernatants were discarded and Fc receptors was blocked with 1 μ l of anti-CD16/32, followed by staining with fluorophore-conjugated antibodies for 15 minutes to 1hour, sitting on ice and in the dark (see Table 2.3 for antibody list). Samples were then washed in FACS buffer then centrifuges at 1500rpm for 5 minutes and suspended in 200-300 μ l FACS buffer. Antibodies were bought from either BioLegend.or BD. Samples were acquired on a BD LSR Fortessa equipped with BD FACSDiva software. Analyses using FlowJo (v10.6.1 TreeStar).

Table 2. 3: list of antibodies used, including clone and fluorophore.

Antigen	Clone	Fluorophore	Company
CD45	30-F11	PE	BioLegend
CD45	30-F11	Buv395	BioLegend
Ly6G	1A8	PerCP/Cy5.5	BioLegend
MHCII	M5/114.15.2	FITC	BioLegend
MHCII	M5/114.15.2	AF700	BioLegend
MHCII	M5/114.15.2	PE-CY7	BioLegend
CD206	C068C2	BV421	BioLegend
F4/80	BM8	APC	BioLegend
CX3CR1	SA011F11	BV605	BioLegend
Ly6C	HK1.4	Alexa-700	BioLegend
CD64	X54-517.1	APC	BioLegend
CD64	X54-517.1	PE	BioLegend
CD64	X54-517.1	PerCP/Cy5.5	BioLegend
SiglecF	S17007L	FITC	BioLegend
SiglecF	S17007L	BV421	BioLegend
CD11b	M1/70	APC-H7	BioLegend
MERTK1	D55MMER	PE-CY7	eBioscience
Arginase	A1exF5	PE	BioLegend
Ki-67	16A8	PerCP/Cy5.5	BioLegend
iNOS	CXNFT	APC	BioLegend
IL-13	eBio13A	PE	BioLegend
IFN- γ	XMG1.2	FITC	BioLegend

2.15 Flow cytometry: Intracellular staining

In some experiments, cells from organs were stimulated using PMA/ionomycin cocktail (BioLegend) diluted in 1:500 and 3 μ g/ml final concentration of brefeldin A (BioLegend) was added. Samples were capped and incubated at 37°C for 4 hours. After stimulation 1 ml of 1x PBS was added to each sample and then centrifuged at 1500rpm for 5 minutes at 4°C. Surface antigens were then stained for as above.

Cells were washed with FACS buffer and 100µl of Fix/Perm buffer (eBioscience) for IFN γ staining was added. BD Fix/Perm (BD Bioscience) for IL-13 and IL-4 staining was added, Tubes were mixed by grating and incubated on ice for at least 30 minutes. Cells were washed using 200µl of 1xPerm wash (eBioscience kit) and centrifuged at 1700rpm for 5 minutes at 4°C. Supernatants were discarded and intracellular antibodies were added (1µl /sample) and samples were left for at least 15 minutes at 4°C. Cells were washed twice with 200µl of 1xPerm wash (eBioscience kit) at 1700rpm for 5 minutes at 4°C and one wash with FACS buffer at 1500rpm for 5 minutes at 4°C. 200µl of FACS buffer was added to each sample prior to acquisition.

2.16 Measurement of cytokines

Lungs and brains were homogenised in 1ml of PBS supplemented with 0.05% Tween20 and 1X protease inhibitor cocktail (Roche). Samples were homogenised and centrifuged at 2000rpm for 5 minutes to remove debris. Samples were centrifuged for second time at 10000rpm for 10 minutes and the supernatant were snap-frozen on dry ice and stored at -80°C prior to analysis. IFN γ , IL-13, IL-4 and IL-10 concentration were determined using DuoSet ELISA (R&D system) following the instructions by manufacture. Briefly, a 96- Maxisorp plated wells were coated with 100µl of the diluted antibody and incubated overnight at room temperature. Wells were washed three times with wash buffer (0.05% Tween20 (sigma) in 1 x PBS) and 300µl of 1 x reagent diluent (bio-technie) was added and incubated at room temperature for 1 hour. Wells were washed as above, 50-100µl of samples or standards were added cover and incubated for 2hr at room temperature then washed as above. 100µl of detection antibody was added to each well and incubated

for 2 hours followed by extensive washing. 100µl of working dilution of Streptavidin-HRP was added and incubated for 20 minutes avoiding direct light. Wells were washed as above and 100µl of substrate solution (BD 1:1 mixture of colour reagent A (H₂O₂) and colour reagent B (Tetramethylbenzidine)) was added and incubated for 20 minutes at room temperature. 50µl of stop solution (2N sulphuric acid) was added to each well then optical density was measured using plate reader set at 450nm.

2.18 Histology

For frozen sections, tissues were placed in OCT filled mould before sectioning. For fixed tissue sections, tissues were placed in 10% formalin for 24 hours before processing and embedding in paraffin wax. Tissue sections were stained using H&E stain or periodic acid-Schiff (PAS) following manufacturer's instructions.

2.19 Imaging

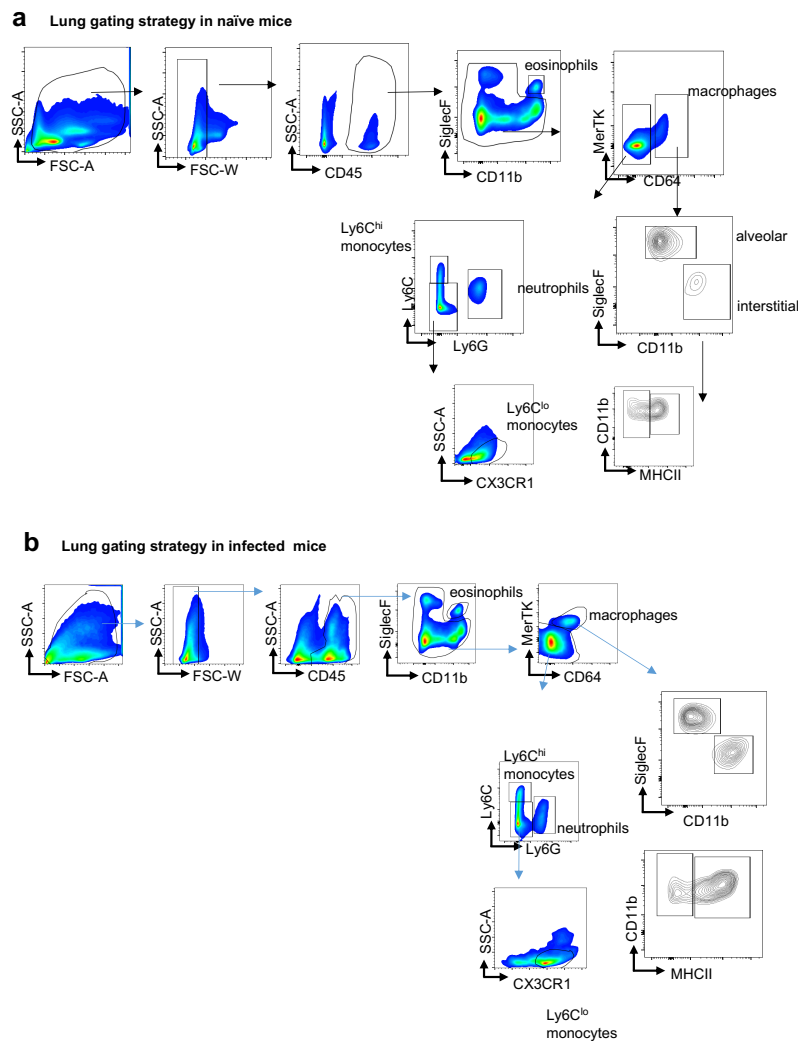
Images were captured using Zeiss Axio Slide Scanner or Zeiss Axio Observer microscope and data analysed using Zen lite blue (version 1.1.2.0).

2.20 Tissue culture

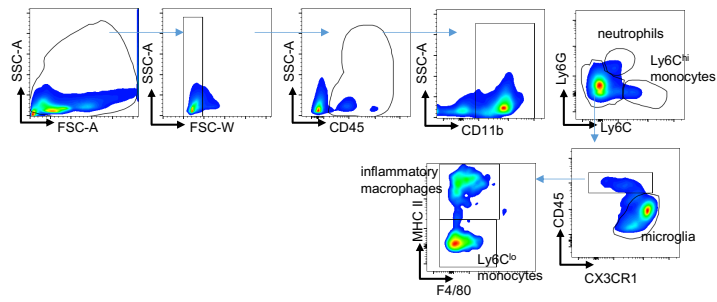
BV2 cells (a kind gift from Dr Michail Lionakis, NIH) were routinely maintained at 37 °C, 5% CO₂ in RPMI (supplemented with GlutaMax and HEPES, Gibco) further supplemented with 10% heat-inactivated foetal bovine serum (Gibco) and 1% Penicillin/Streptomycin (Invitrogen) and were split every 2-3 days after reaching 80-90% confluence. For experiments, BV2 cells were lifted using Trypsin-EDTA (Sigma) and a cell scraper, counted using Trypan blue exclusion and seeded into 12 well plates, at 2x10⁵ cells per well in 1mL media. In some wells, media was further

supplemented with 100ng/mL recombinant mouse IFN γ (BioLegend). After 24 hours, BV2 cells were infected with 1×10^6 *C. neoformans* CTR4^{pGFP} yeast that had been pre-opsionised with 10 μ g/mL anti-glucuronoxylomannan (GXM) antibody (18B7; Millipore) for 15 minutes at room temperature. After 2 hours, plates were placed on ice, media removed and replaced with 1mL ice-cold 2mM EDTA in 1xPBS. BV2 cells were lifted by gentle pipetting on ice and transferred to FACS tubes prior to staining with fluorophore-conjugated antibodies and 5 μ g/mL calcofluor white (Sigma), then acquired immediately on a BDFortessa as above.

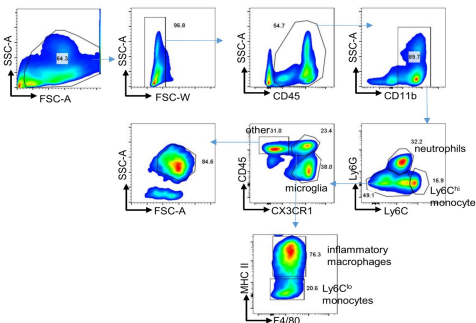
2.21 Gating strategy



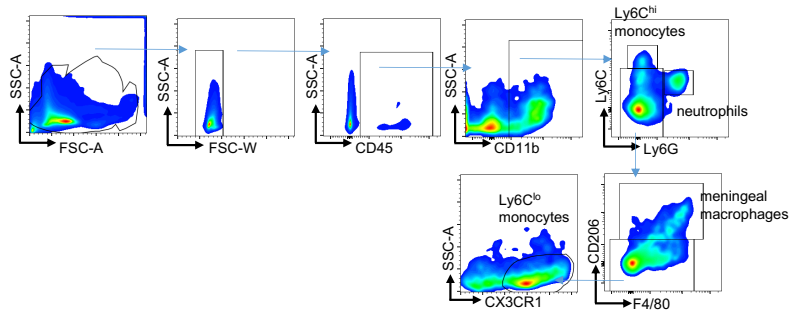
c Brain gating strategy in naïve mice



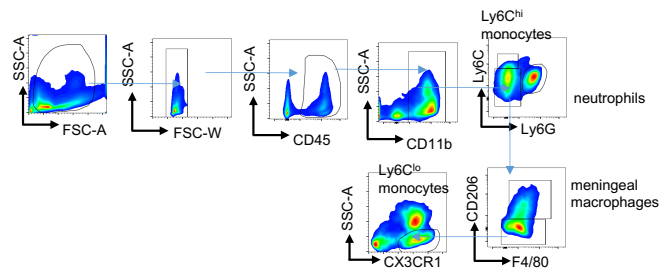
d Brain gating strategy in infected mice



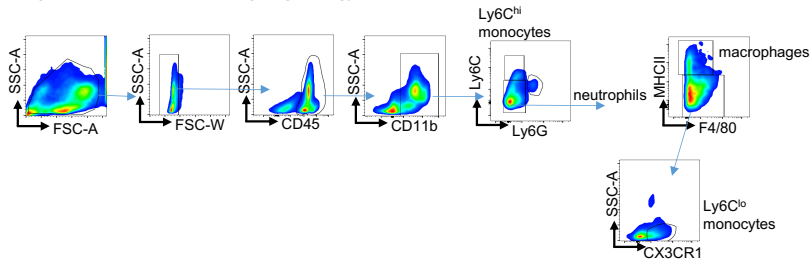
e Meninges gating strategy in naïve mice



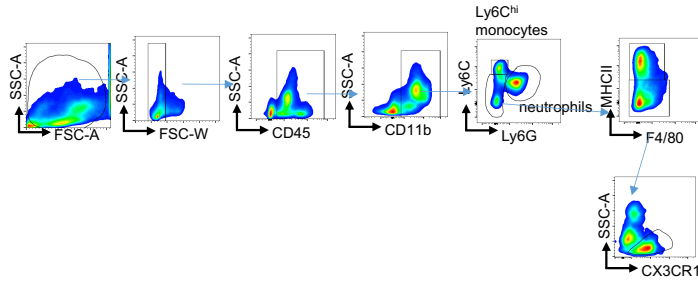
f Meninges gating strategy in infected mice



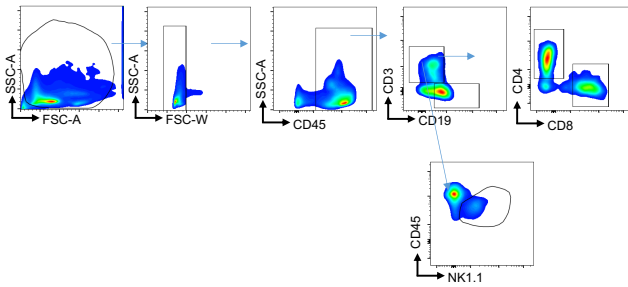
g Bone-marrow/spleen/blood gating strategy in naïve mice



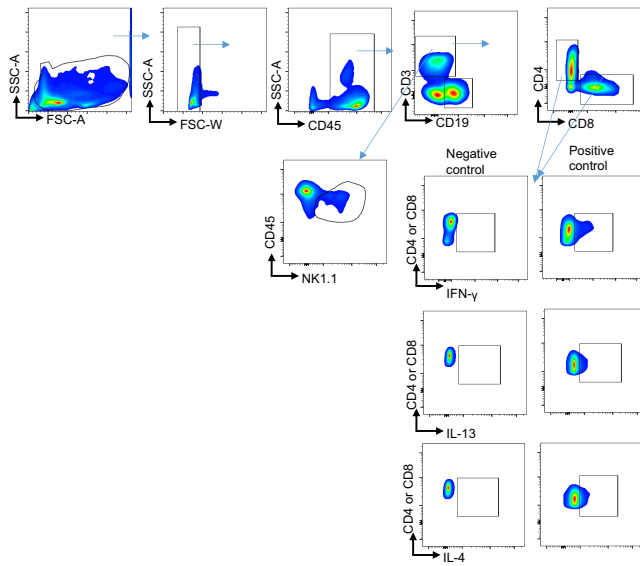
h Bone-marrow/spleen/blood gating strategy in infected mice



i Lung/Brain/Spleen/Blood/Bone marrow lymphocytes gating strategy in naïve mice



j Lung/Brain/Spleen/Blood/Bone marrow lymphocytes gating strategy in infected mice



2.22 Statistics

Statistical analyses were performed using GraphPad Prism 9.0 software. Details of individual tests are included in the figure legends. In general, data was tested for normal distribution by Kolmogorov-Smirnov normality test and analyzed accordingly by unpaired two-tailed *t*-test or Mann Whitney *U*-test. In cases where multiple data sets were analyzed, two-way ANOVA was used with Bonferroni correction. In all cases, *P* values <0.05 were considered significant. We aimed to have n=6 per experiment group, since our power calculations indicated that this sample size would allow for a detection of a 30% difference in the means with a probability of greater than 95%, assuming a standard deviation of around 19% and minimum power 0.8. These calculations are based on years of experience with these models from Dr Rebecca Drummond's lab.

3

The Role of Brain Resident Macrophages During *C. neoformans* infection

3.1 Author Contributions

All the experimental data presented in this chapter was generated by the author of this thesis, except for data shown in Figures, 3.3 and 3.7 and 3.15. Parts of the introduction section within this chapter has been published in a book chapter in which I am the first author (Mohamed, Nyazika et al. 2022). The majority of the Results section has been published online as a preprint (Mohamed, Fu et al. 2022).

3.2 Introduction

Tissue resident macrophages play an essential role in maintaining organ homeostasis and have an important role in immunity against pathogens. Brain resident macrophages are divided into different types including microglia, perivascular macrophages (PVMs), meningeal macrophages (MMs) and choroid plexus macrophages. These are located in specific anatomical locations within the CNS (Table 3.1) and their role in health and disease is recently being elucidated because of the emergence of new technologies. For example, single-cell RNA sequencing has led to better markers for these cells and led to a better understanding of the origin of these cells which can be used to manipulate their function in vivo.

Table 3. 1: Resident Macrophages of the CNS: their location, origin and surface markers.

	Microglia	Perivascular macrophages	Meningeal macrophages	Choroid plexus macrophages
location	parenchyma	Perivascular space	Meninges	Ventricular system of the brain
Origin	Yolk sac	Yolk sac	Yolk sac	Partial turnover from monocytes
Surface marker	CX3CR1, CD11b, CD45 ^{int} , MHCII ^{low}	CX3CR1, CD11b, CD45 ^{hi} , CD206, MHCII ^{hi}	CX3CR1, CD11b, CD206, CD45 ^{hi} MHCII ^{hi} ,	CD45 ^{hi} , CD11b, CX3CR1, MHCII ^{hi}

In this chapter, I will outline the known roles and functions of microglia and other CNS macrophages, particularly in relation to fungal infection, and describe my studies examining how these cells function during experimental *C. neoformans* infection in vivo.

3.2.1 Microglia

Microglia are equipped with important immune weapons that can fight pathogens. Indeed, microglia express multiple PRRs, including CLRs and TLRs. In vitro studies have showed that stimulating microglia using TLR agonists (e.g. Pam₃ CSK₄, LPS, and CpG) drove the production of proinflammatory cytokines such as TNF- α , IL-6, and IL-1, which resulted in enhanced *C. neoformans* phagocytosis and reduced intracellular replication inside microglia (Redlich, Ribes et al. 2013). Immortalised microglia have been shown to phagocytose *C. neoformans* leading to increased iNOS expression which is important for limiting fungal growth (Adami, Sorci et al. 2001, Song 2004). Moreover, microglia are influenced by IFN γ producing CD4 T

cells and provide protection against *C. neoformans* infection. Indeed, IFN γ enhances the anti-cryptococcal activity of microglia in vitro by inducing the expression of iNOS and MHC Class II, potentially allowing their interaction with infiltrating T cells (Blasi 1995, Panek and Benveniste 1995, Aguirre and Miller 2002). A study showed that immunomodulation with CD40 (a T cell co-stimulatory molecule) and the cytokine IL-2 in *C. neoformans*-infected mice reduced the fungal burden in various organs including the brain, which correlated with an IFN γ dependent increase of MHC II expression on microglia (Zhou, Gault et al. 2006). Moreover, IFN γ knockout mice showed the critical role of IFN γ in activating microglia and inducing anti-cryptococcal activity, because mice deficient in IFN γ failed to induce MHCII expression on microglia cells (Zhou, Gault et al. 2007). Thus, CD4 T cells are thought to play an important role in brain antifungal immunity by activating these brain resident macrophages. Nonetheless, studies have shown that microglia may not be sufficient enough to clear yeast cells and they are prone to latent intracellular infection, where *C. neoformans* can survive and replicate inside (Lee, Kress et al. 1995, Lee, Kress et al. 1995). Indeed, post-mortem examinations of human microglia showed *C. neoformans* polysaccharide capsule is engulfed and localised inside of microglia (Lee, Kress et al. 1995). Although microglia can engulf *Cryptococcus* yeast cells, the killing of the yeast cells does not occur in human microglia (from foetal) even when IFN γ is added (Lipovsky, Juliana et al. 1998). Although we can gain limited information using microglia cell lines and in vitro models, in vivo studies are needed to analyse the behaviour of microglia in their natural environment, since microglia from tissues rapidly lose their identity when taken into the culture (Bohlen, Bennett et al. 2017) and cell lines have inherent issues due to their immortalised status. For example, recent studies have shown that microglia cell line differ genetically and

functionally from primary microglia (Das, Kim et al. 2016, Melief, Sneeboer et al. 2016, Gosselin, Skola et al. 2017). In vivo studies analysing antifungal activity of microglia is so far limited. In a murine model of CM-post-infectious inflammatory response syndrome (PIIRIS), full activation of microglia did not occur until 21 days post-infection, which coincided with a significant influx of infiltrating inflammatory myeloid cells and lymphocytes and a decrease in brain fungal burdens (Neal, Xing et al. 2017). A similar observation was made following acute infection with *C. neoformans* in mice, where microglia numbers expanded >1 week post-infection which coincided with an influx of monocytes and T-cells (Kaufman-Francis, Djordjevic et al. 2018). Interestingly, these effects do not occur with *C. gattii*, which demonstrates a reduced capacity for entry into the CNS compared with *C. neoformans*, with *C. gattii*-infected animals typically succumbing to significant lung disease (Kaufman-Francis, Djordjevic et al. 2018). In contrast, recent in vivo studies showed that *C. albicans* CNS infection results in a rapid activation of microglia (within 24h), which quickly initiate protective immunity upon *C. albicans* infection. Microglia highly express CARD9 (Drummond, Collar et al. 2015). Human CARD9 deficiency results in a profound susceptibility to CNS candidiasis, aspergillosis and phaeohyphomycosis but not CM (Lanternier, Barbati et al. 2015, Rieber, Gazendam et al. 2016, Drummond, Franco et al. 2018). It was recently shown that CARD9 expression by microglia is required to sense the fungal toxin Candidalysin which is secreted by *C. albicans* (Drummond, Swamydas et al. 2019). This toxin activated the production of IL-1 β and CXCL1 from microglia, which in turn recruited CXCR2-expressing neutrophils to the brain to clear the fungus (Drummond, Swamydas et al. 2019). CARD9 deficiency does not appear to promote susceptibility to CM in humans, and deficiency in CARD9-coupled CLRs do not promote susceptibility to

CM in experimental mouse models (Campuzano and Wormley 2018, Campuzano, Castro-Lopez et al. 2020). Thus, microglia have an important role in antifungal immunity that is context dependent.

3.2.2 Perivascular macrophages

PVMs in the normal state maintain tight junctions between endothelial cells within the BBB and can phagocytose potential pathogens and stop them from entering the CNS. For example, an early study using a rat model of streptococcal meningitis showed that depleting PVMs using clodronate liposomes correlated with higher bacterial burden, increased illness, and reduced neutrophils recruitment to the CNS (Polfliet, Zwijnenburg et al. 2001). In terms of fungal infections, analysis of human brain autopsy tissue showed that PVMs appear to harbour intracellular *C. neoformans*, indicating that these cells interact with and phagocytose *C. neoformans* (Aguirre and Miller 2002). Indeed, the location of PVMs would ideally position them next to the main site of infection in CM. However, an extensive analysis of cryptococcal brain infection in mice showed that the main myeloid effector cells in the brain following *C. neoformans* infection were monocytes and neutrophils recruited from the blood, and that infection and inflammation were largely confined to the perivascular spaces where CNS-resident macrophages, including PVMs and microglia, were rare (Kaufman-Francis, Djordjevic et al. 2018). Similar to microglia, PVMs may also be detrimental during infection. For example, depleting PVMs during vesicular stomatitis virus-induced encephalitis increased mice survival, through impairing excessive production of proinflammatory cytokines (Steel, Kim et al. 2010). Moreover, it's been shown that PVMs are the primary site for simian immunodeficiency virus (SIV) infection, where the virus can replicate inside affecting

PVMs function and BBB permeability of the CNS (Williams, Corey et al. 2001). This is important in the context of *Cryptococcus* infections because HIV is a major risk factor, and it is still unknown how HIV alters these cells and the subsequent susceptibility to *Cryptococcus* fungi. Thus, PVMs require further exploration within the cryptococcal field to better our understanding of brain-resident macrophages and their influence on pathogenesis.

3.2.3 Meningeal macrophages

The meninges are an overlapping membrane composed of the dura matter, the arachnoid matter, and the pia matter that encloses the entire CNS, providing an additional barrier against pathogens. Several immune cells are found in the meninges including MMs, DCs, mast cells, neutrophils, T cells, and B cells (Weller, Sharp et al. 2018). *C. neoformans* most commonly infects the meninges yet there is little research done to understand the inflammation and fungal clearance within this tissue (Colombo and Rodrigues 2015). Understanding how resident immune cells such as MMs influence infection will be very helpful to the cryptococcal field. Under normal conditions, the MMs are found throughout the meninges, acting as sentinels of their surrounding environment, similar to microglia (Rua, Lee et al. 2019). The MMs are self-renewing and originate from the embryonic yolk sac (Table 3.1). However, during inflammation these macrophages can be repopulated by circulating monocytes (Rua, Lee et al. 2019). This was shown by the McGavern group, where they used an attenuated strain of lymphocytic choriomeningitis virus (LCMV) to cause sublethal meningitis in mice. This infection resulted in depletion of MMs, however, the MMs niche was replenished by monocytes completely by day 30 post-infection (Rua, Lee et al. 2019). The new MMs population had a defect in their

inflammatory cytokine compared to the original MMs, where microbial sensor receptor SIGNR-1 was down-regulated and when challenged with bacteria these cells had a defect in their ability to recruit neutrophils (Rua, Lee et al. 2019). This study highlights the effect of prior infection on CNS macrophages, where the new resident macrophages population had a defect in several genes related to the anti-bacterial immune response. Thus, prior infection affects host immunity to subsequent infections in these types of macrophages, and indeed as mentioned earlier in SIV infection and their effect on PVMs, this could be important in the context of *Cryptococcus* as cryptococcosis usually associated with prior viral infection which is poorly understood and therefore needs further exploring.

3.2.4 Choroid Plexus

Infection of the choroid plexus is rare during CM and for that, it is unlikely involved in anti-cryptococcal immunity (Schwerk, Tenenbaum et al. 2015). However, their role is largely unexplored in the context of invasive fungal infection.

3.2.5 In vivo strategies to manipulate CNS macrophages number and function.

In the last decade, there have been a tremendous effort to develop new tools for manipulating CNS macrophages in vivo. This has been challenging because many of these macrophages share the same markers (Table 3.1). However, significant advances have been made to generate pharmacological and genetic models to either fate-map these cells or knockout different genes to target these cells specifically and examine their role in health and in disease (Table 3.2). In this section I will give an overview of the main strategies that have been used in the last few

years to manipulate and target microglia and other CNS-resident macrophages in vivo.

Table 3. 2: Overview of commonly used chemical and genetic microglia depletion models in mice and their approximate timelines, advantages, and disadvantages.

Depletion model	Timeline for microglia depletion	Advantages	disadvantages	Reference
PLX5622	7 days	Easy to use, adherence to 3Rs principles (no pain to mice) longer depletion with ~90% efficiently	Not microglia specific and affect other brain, lung, liver and spleen macrophages and lymphocytes	(Spangenberg, Severson et al. 2019, Ali, Mansour et al. 2020, Spiteri, Ni et al. 2022)
PLX3397	21 days	Easy to use, Easy to use, adherence to 3Rs principles (no pain to mice) longer depletion with ~70% efficiently	Not microglia specific and affect other CNS macrophages	(Sosna, Philipp et al. 2018, Merry, Brooks et al. 2020)
Cx3cr1 ^{CreER} iDTR	3 day	Quick depletion of microglia with ~90 % efficiently	Repeated dose of tamoxifen and diphtheria, time consuming, effect other CNS macrophages	(Zhao, Alam et al. 2019, Sahasrabudde and Ghosh 2022)
Clodronate liposome	1-5 days	Easy and quick to use with ~80% efficiently	not microglia specific	(Weisser, van Rooijen et al. 2012, Han, Li et al. 2019)
Sall1 ^{creER} xCsf1 ^{flx}	3 day	Microglia specific depletion with ~70-90 % efficiently	Repeated dose of tamoxifen, time consuming, Small percentage of cells in kidney and liver express Sall1	(Buttgereit, Lelios et al. 2016, Eme-Scolan and Dando 2020)
Hexb ^{CreEr} Csf1 ^{flx}	3 day	Microglia specific depletion with ~60 % efficiently,	Repeated dose of tamoxifen, time consuming, Less efficient in depleting microglia.	(Masuda, Amann et al. 2020)

3.2.5.1 Chemical manipulation strategies

One of the main strategies that have been used over the last few years to deplete microglia and brain macrophages is the use of clodronate liposomes. These liposomes are readily phagocytosed by myeloid cells, inhibiting mitochondrial ADP/ATP translocase leading to apoptosis (Lehenkari, Kellinsalmi et al. 2002, Han, Zhu et al. 2019). Clodronate liposomes must be administered using either intravenous or intraperitoneal injection to cross the BBB, and this results in macrophage depletion after 72h (Han, Li et al. 2019). This method is not specific to microglia and can lead to the depletion of other macrophage populations including PVMs and MMs (Table 3.2), as well as circulating monocytes and neutrophils. More recently, depletion of microglia and other brain macrophages has been achieved using small molecular inhibitors of CSF1R. Csf1r signalling is vital for the survival of microglia and other brain macrophages (Elmore, Najafi et al. 2014). CSF1R KO are embryonically lethal because of the pleiotropic role of the receptor and therefore inhibiting the receptor should be carried out at adulthood stage (Ginhoux, Greter et al. 2010, Erblich, Zhu et al. 2011). There have been two main inhibitors of CSF1R developed and used by several research groups, including PLX5622 (Spangenberg, Severson et al. 2019) and PLX3397 (Elmore, Najafi et al. 2014) (Table 3.2). PLX3397 has been shown to have high potency in microglia depletion while PLX5622 has improved BBB penetration compared to PLX3397 (Spangenberg, Severson et al. 2019). Furthermore, PLX5622 has higher specificity for CSF1R whereas PLX3399 can have effects on other related kinases (Liu, Given et al. 2019). These inhibitors can be administered either by oral gavage or in rodent chow and effectively depletes CNS macrophages within 7 days and is reversible with microglia returning to normal numbers within a few days of stopping treatment. Furthermore,

these inhibitors can be given to mice to deplete CNS macrophages for up to 24 weeks, which is not always feasible when using transgenic mice (see below). Recent studies have shown that PLX5622 inhibitors are not specific to CNS macrophages and has some effect on other organs' macrophages such as liver and lung macrophages, and has some effect on lymphocytes (Lei, Cui et al. 2020). However, this has been argued within the field as that study did not provide the dose, the source or the duration of treatment using PLX5622 or showed representative flow cytometry plots for their analysis (Green and Hume 2021). Therefore, PLX5622 effects on haematopoietic cells may be context dependent on dose and duration of the treatment.

3.2.5.2 Genetic manipulation

Over the last few years microglia signature genes have been identified such as *Sall1*, *Hexb*, and *Tmem119* (Buttgereit, Lelios et al. 2016, Kaiser and Feng 2019, Masuda, Amann et al. 2020). *Sall1* and *Tmem119* are microglia specific genes and not expressed by other brain macrophages. Additional gene that is expressed by microglia is *Cx3cr1* which is not microglia specific and other brain macrophages express the gene including PVMs and MMs (Wolf, Yona et al. 2013). The discovery of these genes helped us use their promoters and tag them with either fluorescent reporters and induce expression of Cre recombinase to either fate-map or deplete these macrophages. For example, *Cx3cr1^{GFP}* has been used to identify microglia within tissue where microglia express GFP under the *Cx3cr1* promoter (Parkhurst, Yang et al. 2013, O'Koren, Mathew et al. 2016). Other reporter mice have been developed such as *Sall1^{GFP}* (Takasato, Osafune et al. 2004), *Tmem119^{TdTomato}* (Ruan, Sun et al. 2020) and *Hexb^{TdTomato}* (Masuda, Amann et al. 2020). To deplete

microglia, mice expressing tamoxifen-inducible Cre-recombinase (Cre-ER) under the *Cx3cr1* promoter (Parkhurst, Yang et al. 2013) can be crossed with mice harbouring a *Rosa26-stop-DTR* (Buch, Heppner et al. 2005) allele to generate offspring in which Cre-ER can be activated by tamoxifen to induce expression of diphtheria toxin receptor in microglia. These cells are then sensitive to ablation by diphtheria toxin (Buch, Heppner et al. 2005). To overcome issues of short-lived *Cx3cr1*+ circulating myeloid cells (DCs, monocytes and NK cells), mice have a rest period after tamoxifen treatment for 4-6 weeks allowing replenishment of these short-lived cells from the bone-marrow. Upon diphtheria toxin treatment over 90% of microglia are depleted (Table 3.2). Recent study have shown that diphtheria toxin induced mice model lead to the loss of cervical space fluid/ventricular space by activating IBA1-expressing cells in the choroid plexus and therefore caution is needed when interpreting any phenotype seen after CNS macrophages depletion using this method (Bedolla, Taranov et al. 2022). Recently, we have seen other transgenic mice being used taking advantage of microglia signature genes, for example *Sall1^{CreEr}* mice crossed with *Csf1r^{flx}* (Buttgereit, Lelios et al. 2016), where upon tamoxifen treatment the *Csf1r* is specifically depleted in microglia (Table 3.2). However, small number of cells were shown to express *Sall1* in kidneys and liver (Buttgereit, Lelios et al. 2016, Masuda, Amann et al. 2020). Another stable microglia gene is hexosaminidase subunit beta (*Hexb*), which has been developed to target microglia specifically (Masuda, Amann et al. 2020). *Hexb^{CreEr}* can be used with *Csf1r^{flx}* to deplete *Csf1r* after tamoxifen treatment (Kaiser and Feng 2019). *Hexb^{CreER}* was shown to be more stable during disease compared to *Sall1* and *Tmem119* where they down regulated during pathogenesis. Although these approaches are good, they still have their limitation. For example only ~60 % of microglia (Table 3.2)

are depleted in $\text{Hexb}^{\text{CreEr}} \times \text{Csf1r}^{\text{flx}}$ animals (Kaiser and Feng 2019). Nonetheless, these advances have helped us study microglia leading to the development of new markers to image or use flow cytometry to investigate these cells in vivo. However, further research is needed to investigate other brain resident macrophages and find their signature genes to help us distinguish between brain resident macrophages and how to target each one specifically to investigate their role in health and disease. In this chapter, I will describe my studies examining how brain resident macrophages function during an acute infection model (intravenous route of infection) at early time points with *C. neoformans* infection using different depletion model. One advantage of using acute model is getting a consistent brain infection bypassing lung immune cell. However, you can only use this method for short period of time as mice start to develop meningitis.

3.3 Result

3.3.1 *C. neoformans* infects CNS myeloid cells.

C. neoformans can survive and replicate within macrophage phagosomes, aiding its evasion from the immune system and dissemination to the brain within monocytes (Hole and Wormley 2016). My first approach was to characterise *C. neoformans* infection of myeloid cells within the brain. To examine this, I first examined CNS myeloid cell association with fungi using a green, fluorescent reporter *C. neoformans* strain (GFP- *Cryptococcus*). This allowed me to track fungal uptake by different myeloid cell populations in the brain using flow cytometry (see gating strategy presented in Chapter 2.21). First, I isolated brains from infected mice at day 6, 7 and 8, purified the leukocytes, stained using myeloid markers and processed the cells using flow cytometry. At day 6 the frequency of infected cells in the brain remained low < 1 % (Figure 3.1a, b). At day 7 and 8 the frequency of infected cells increased with some cells Cx3cr1⁺ CD45^{hi} MHCII⁺ (inflammatory macrophages) having frequency of infection at around 30% (Figure 3.1b). I was not able to detect *C. neoformans* infected cells at day 3 or 4 post infection, likely due to very low number of infected cells at that time point which is not detectable by flow cytometry. Since mice were often very ill or reaching their humane endpoints at day 8 post-infection, I decided to focus on day 7 post-infection for the majority of my studies. These experiments revealed that the majority of myeloid cell types get infected with *C. neoformans* reaching peak at day 7. Furthermore, Cx3cr1⁺ CD45^{hi} MHCII⁺ cells had the most infected cells at day 7 and 8, followed by Ly6C^{low} (patrolling monocytes).

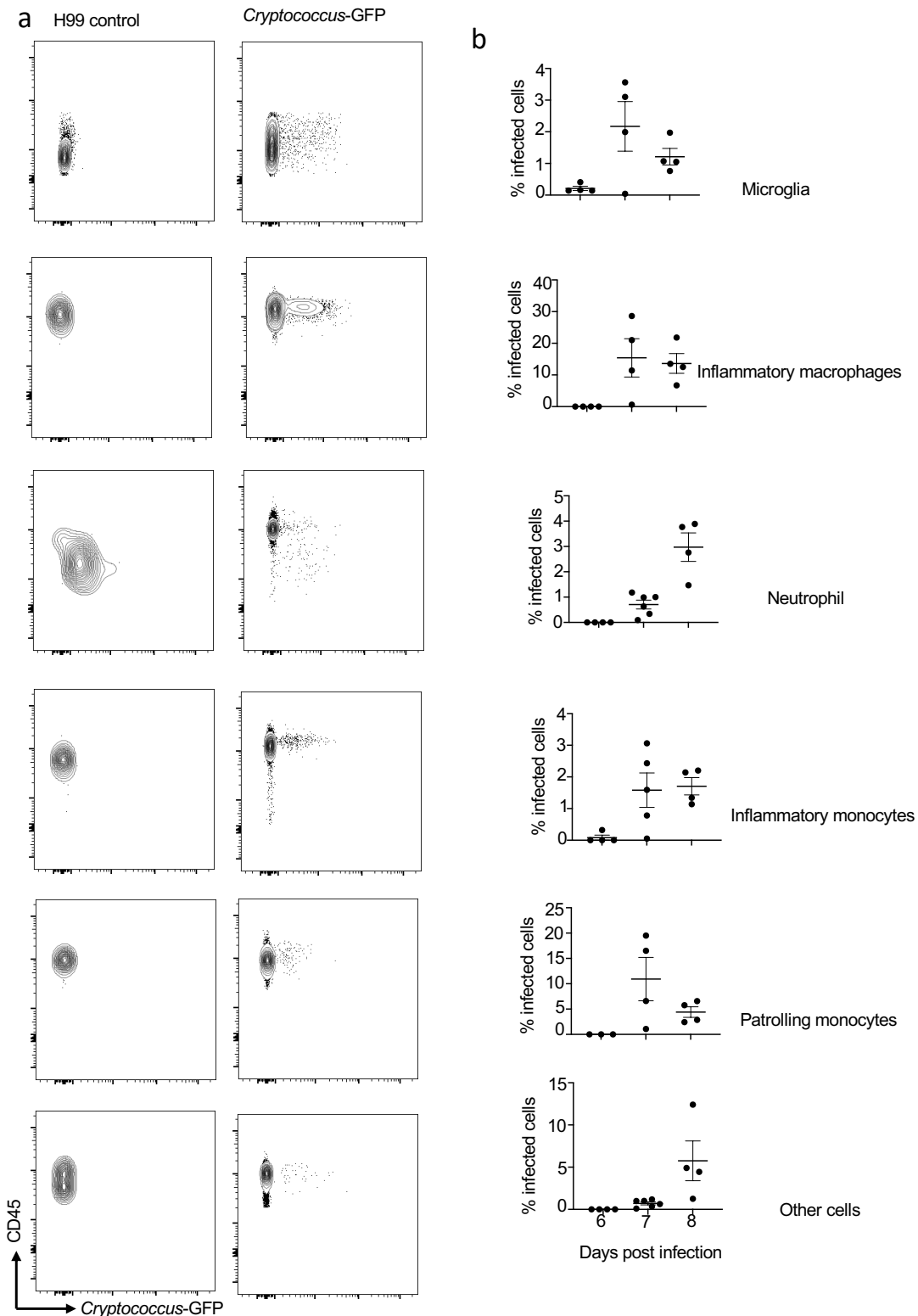


Figure 3.1 Majority of myeloid cell types get infected with *C. neoformans* in vivo. (a) Representative plots gated on myeloid cells in wild-type *C. neoformans* infected mice and GFP-expressing *C. neoformans* infected mice within the brain. (b) The frequency of the indicated infected cell types in the brain at day 6, 7 and 8 post infection. Data present from 1 experiment (n=4 mice) n represent individual mouse.

3.3.2 Brain resident macrophages become infected with *C. neoformans*.

After identifying day 7 post-infection as the peak time point of intracellular infection for most myeloid cells in the brain (Figure 3.1), I next examined this time point in more detail. The result showed that majority of cells had similar intracellular infection rate with Cx3cr1⁺ CD45^{hi} MHCII⁺ and Ly6C^{low} exhibiting the highest level in some animals (Figure 3.2a). For brain-resident microglia, the percentage of total microglia that were infected with *C. neoformans* remained low at ~5% (Figure 3.2a). However, microglia are the most numerous myeloid cells in the brain compared to neutrophil, monocytes and macrophages (Figure 3,2b), and although the percentage of infected microglia remained low this equated to significantly more infected microglia than other cell type in the brain (Figure 3.2c), followed by Cx3cr1⁺ CD45^{hi} MHCII⁺, inflammatory monocytes and neutrophils (Figure 3.2c). Next, I gated on all infected cells by selecting the GFP⁺ population and looked at infected myeloid cells within that (Figure 3.2d). This strategy allowed me to determine the proportion of different myeloid cell types within the infected cells, in comparison to my earlier analysis that focused on frequency of the total myeloid populations. My result showed that over half of all fungal infected cells were microglia (Figure 3.2d), followed by neutrophil, Cx3cr1⁺ CD45^{hi} MHCII⁺, and monocytes. In conclusion, this data shows the rate of infected cells at day 7 is very similar in all myeloid cells. However, the number and the proportion of infected cells were highest in microglia compared to other myeloid cells.

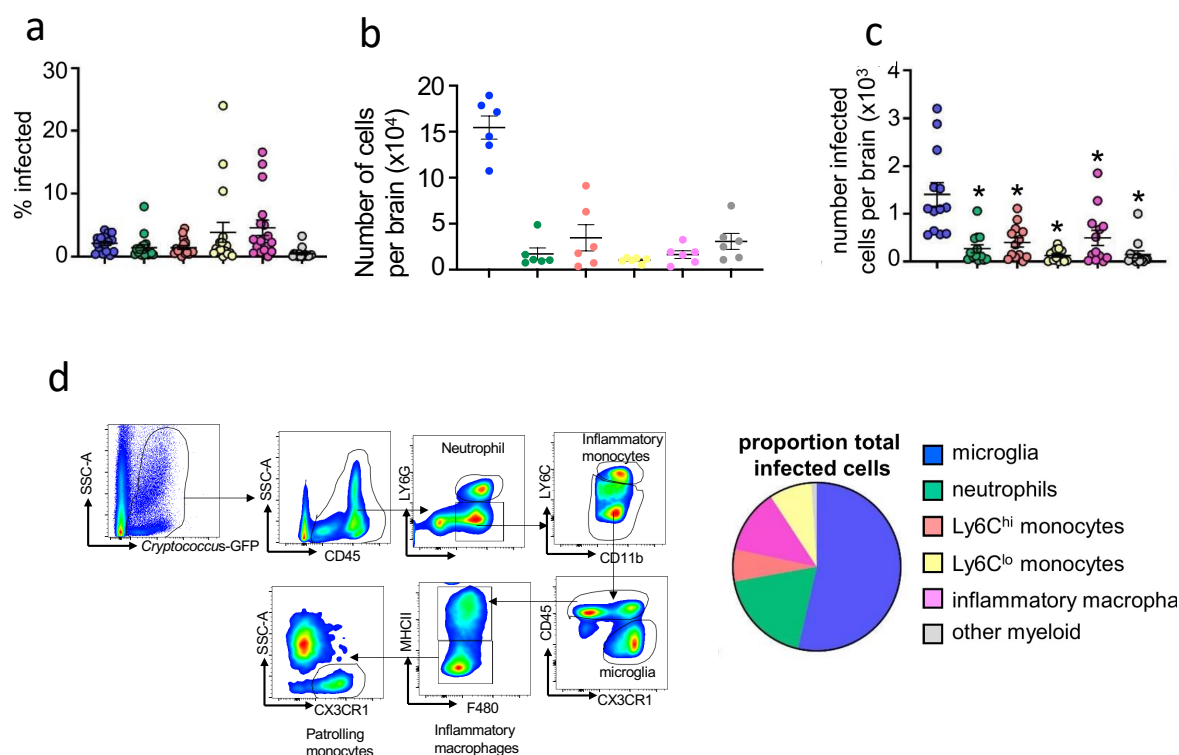


Figure 3.2 Microglia harbour *C. neoformans* intracellularly. (a) Frequency of *C. neoformans* infection within indicated cell types in the brain at day 7 post infection. Data are from 4 independent experiments n= individual mouse (n=17). (b) Total number of myeloid cells in the brain at day 7 post infection (data presented from single experiment). (c). The total number of infected cells infected cell types in the brain at day 7 post-infection. data are from 4 independent experiments (n=14). Data were analysed using one-way ANOVA with Bonferroni. (d) Proportion of total infected cells at day 7 post infection. An average value of 4 independent experiments for each cell type is shown.

3.3.3 Histology analysis of *C. neoformans* brain infection.

Next, I analysed fungal localisation by histology to gain a broader perspective on infection niches within the brain. For that, I isolated mouse brains and froze-fixed using OCT preservative, then sectioned and stained using PAS staining. I found yeast growing in close association with host cells (Figure 3.3a, white arrows) in the brain parenchyma, but also found several areas in the brain where yeasts were growing extracellularly (Figure 3.3a yellow arrows). Next, I wanted to see if similar observation is seen in human. For that I collaborated with a pathologist to look at human brain sample from a patient who died from HIV-associated CM. These

images showed similar pattern where yeasts found residing within immune cells in addition to extensive tissue damage and yeast growing in those areas (figure 3.3b). These experiments revealed that there might be close association between *C. neoformans* and brain cells, but better microscopy images with myeloid cells staining are needed to confirm that.

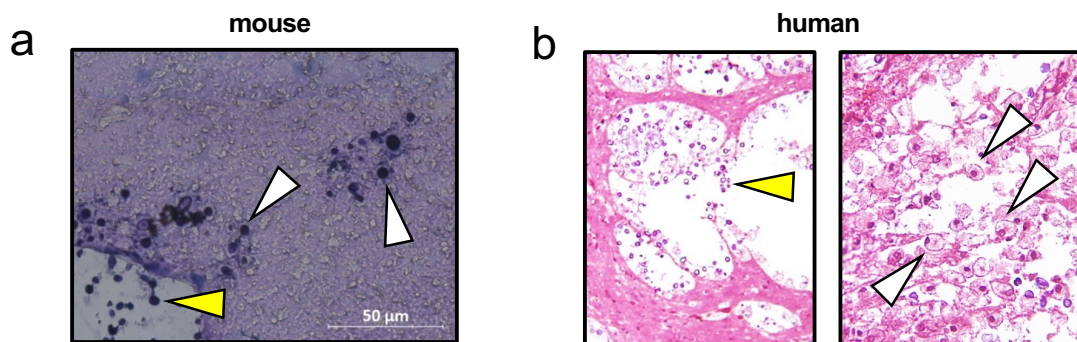


Figure 3. 3 Histology images of *C. neoformans* infected brain. (a) Histology of murine brain section isolated from *C. neoformans* infected mouse at day 7 post-infection, stained with PAS (Periodic acid-Schiff stain). White arrows denote intracellular growing fungus, yellow arrows denote extracellular growing fungus. Samples were fixed using OCT (b) Histology of human brain biopsy isolated post-mortem from a patient with HIV-associated cryptococcal meningitis, formalin-fixed and stained with PAS (done by Robert Lukande, University of Makerere, Uganda). White arrows denote intracellular growing fungus, yellow arrows denote extracellular growing fungus.

3.3.4 Microglia harbour live *C. neoformans* intracellularly.

Since I found that microglia became infected with *C. neoformans*, I next assessed the viability of the *C. neoformans* cells within the microglia population. For that, I sort purified *C. neoformans*-infected microglia (using *Cryptococcus*-GFP strain) and uninfected microglia as control. Next, I did a water wash to lyse microglia and then plated the resulting yeast cells onto fungal growth media to assess fungal viability (Figure 3.4a). This experiment revealed that over 70% of the fungus is viable within microglia (Figure 3.4b), which may indicate that killing capacity of microglia is not

great at phagocytosis the fungus. This data suggest that microglia may act as an intracellular growth niche for *C. neoformans*.

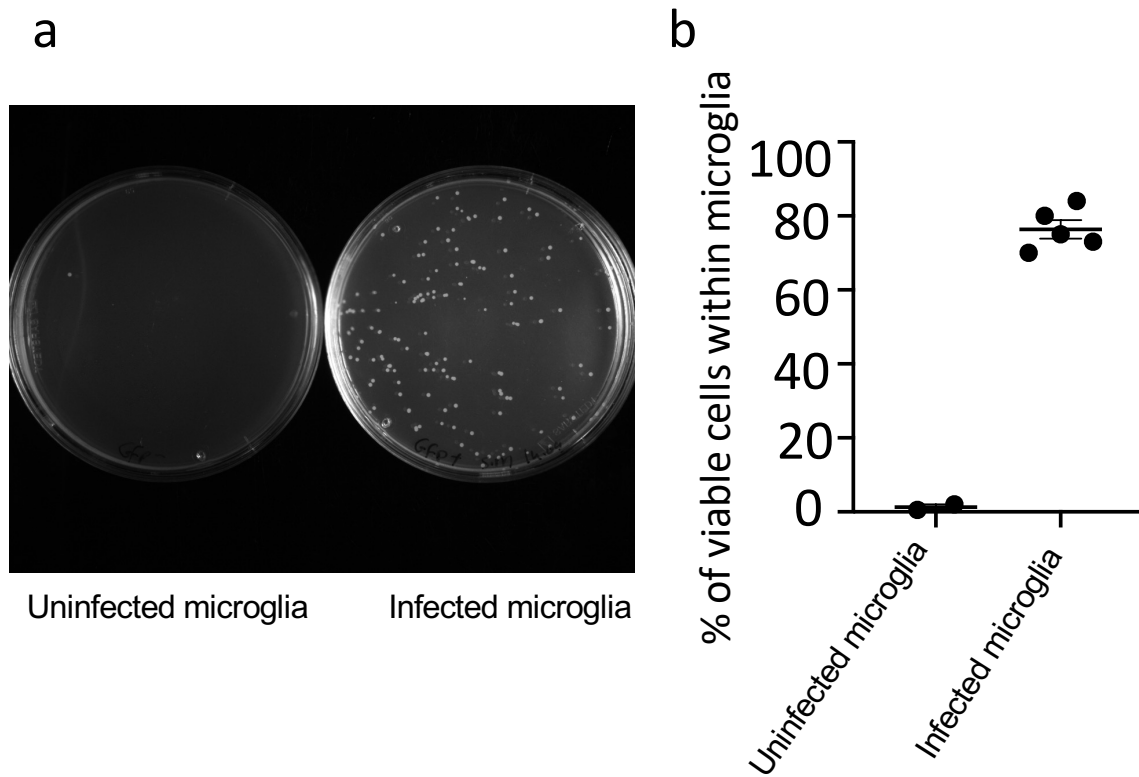


Figure 3. 4 *C. neoformans* viability within microglia. (a) An image of plated uninfected microglia and infected microglia. (b) The percentage of *C. neoformans* viability within microglia. Mice were infected with *Cryptococcus*-GFP intravenously and tissues were collected at day 7 post infection. Point shown technical replicates from one representative experiment.

3.3.5 Meningeal macrophages become infected with *C. neoformans*.

In addition to the brain, the meninges become infected and inflamed during CM, where it is the main site of disease in human (Kambugu, Meya et al. 2008, Abassi, Boulware et al. 2015). To understand the kinetics of which immune cells in the meninges get infected during *C. neoformans* infection, I followed the same experimental model as shown in Figure 3.1 and looked at myeloid cells in the meninges. Similar to brain, I was unable to detect infected myeloid cells at day 3 and 4 post infection (data not shown). Focusing on the later time points, I found that at day 6 post-infection, the percentage of MMs that were infected with *C. neoformans* remained low, averaged ~6% (Figure3.5b). Nonetheless, these tissue-resident

macrophages were the most infected cells followed by inflammatory monocytes and neutrophils (Figure 3.5b). Similarly, at day 8 post-infection, the percentage of infected cells in the meninges were low ~5 % (Figure 3.5b). This data indicate that majority of the fungus is residing extracellularly in the meninges.

Next, I examined the meninges myeloid cells uptake of the fungus focusing on day 7. These experiments revealed that percentage of MMs were highest compared to other myeloid cells (Figure 3.6a). Looking at the total number of infected cells in the meninges, MMs were the most infected cells (Figure 3.6b), followed by other myeloid cells including inflammatory monocytes, neutrophil and Ly6C^{low} (Figure 3.6b). Next, I gated on the total fungal infected cells in the meninges, I found nearly half of all fungal infected cells were in MMs, followed by inflammatory monocytes, neutrophil and Ly6C^{low} (Figure 3.6c). Taken together, this data shows that *C. neoformans* infect meninges myeloid cells and that MMs are the major cell infected in the meninges, indicating a close association between CNS resident macrophages and the fungus.

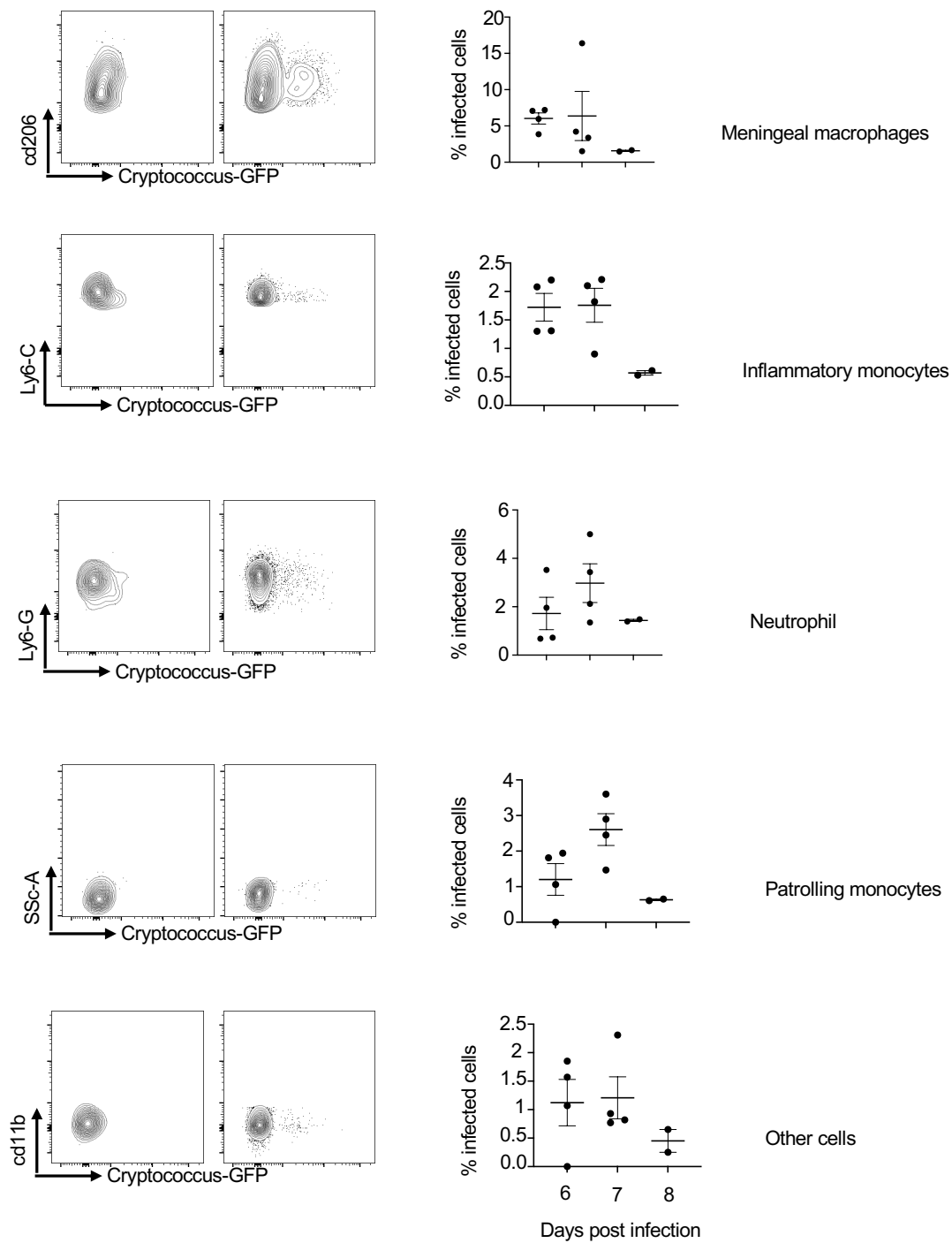


Figure 3.5 *C. neoformans* infect meninges immune cells . (a) Shows representative plots gated on myeloid cells in wild-type *C. neoformans* infected mice and GFP+ *C. neoformans* infected mice in the meninges. (b) The frequency of infected cells in the meninges at day 6, 7 and 8 post infection. Data present from 1 experiment n= individual mouse (n=4 mice).

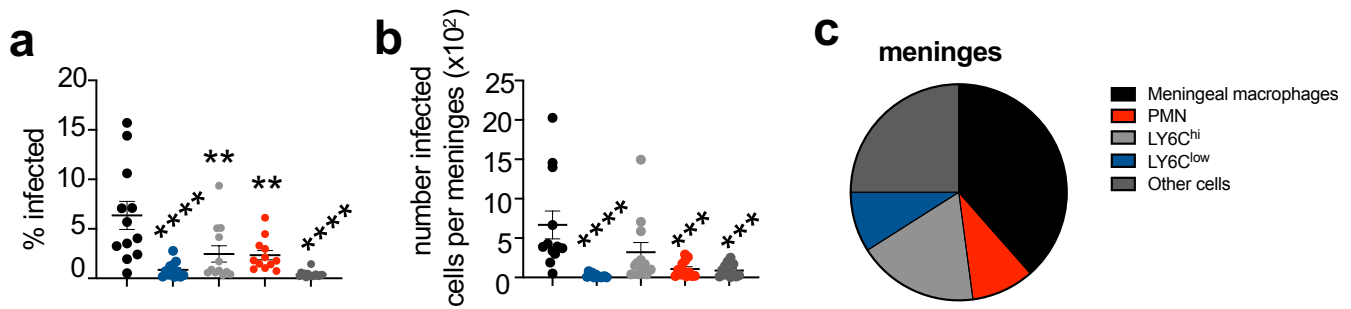


Figure 3.6 Meningeal macrophages harbour *C. neoformans* intracellularly.(a) Frequency of *C. neoformans* infection within indicated cell types in the meninges at day 7 post infection. Data are from 4 independent experiments (n=12). (b) Total number of infected cell types in the meninges at day 7 post-infection. Data are from 4 independent experiments (n=12). Data were analysed using one-way ANOVA (c) Proportion of shown cell types within total infected cells at day 7 post infection. An average value of 4 independent experiments for each cell type is shown. See appendix for gating strategy.

3.3.7 Depletion of brain-resident macrophages using CX3CR1-iDTR transgenic mice reduces brain fungal burden.

Since I found that CNS-resident macrophages harbour the majority of *C. neoformans* intracellularly, I next determined the contribution of CNS-resident myeloid cells in controlling *C. neoformans* infection. For that I used several depletion models to assess brain resident macrophages depletion on brain fungal control. First, my supervisor generated Cx3cr1-Cre^{ER}-iDTR^{fllox} animals in which all long-lived Cx3cr1⁺ cells in the brain are depleted following treatment with diphtheria toxin (Figure 3.7a). In this model, microglia depletion was sustained following intravenous infection with *C. neoformans* (Figure 3.7b). Following microglia depletion, we assessed brain fungal burden and found that depleting microglia reduces brain fungal burden at 3 days post infection but found no difference in lung burden (Figure 3.7c) indicating microglia depletion could have protective effect. Microglia can suppress inflammatory responses in the brain (Fu et al., 2020; Sariol et al., 2020). For that I examined whether microglia depletion led to change in inflammatory myeloid cells recruitment including neutrophil inflammatory monocytes and Ly6C^{low} in microglia depleted and their WT littermate, which were heterozygous for the Cx3cr1-CreER allele. We

found that microglia depletion did not affect inflammatory recruitment myeloid cells to the brain (Figure 3.7d). Taken together this data shows that depleting CNS resident macrophages reduce brain fungal burden specifically with no difference in the lung.

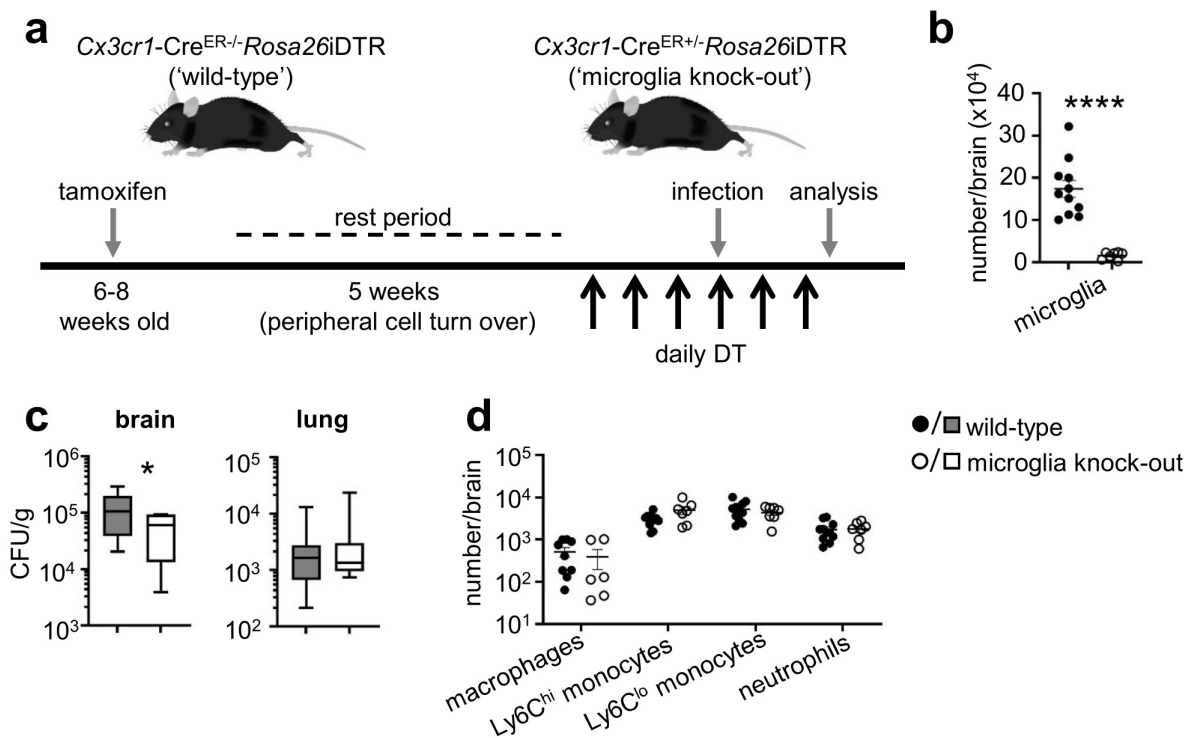


Figure 3. 7 Brain macrophages depletion result in brain burden reduction with no difference in lung. Schematic of diphtheria toxin-based depletion of brain-resident macrophages. *Cx3cr1-Cre^{ER}* mice were crossed with *iDTR* mice. Resulting wild-type and Cre-expressing ('microglia knock-out') littermates are treated with tamoxifen to induce Cre expression and left to rest for 5 weeks to enable turn-over of monocyte-derived macrophages prior to daily treatment with diphtheria toxin to initiate cell depletion before and during intravenous *C. neoformans* H99 infection. (b) Total number of microglia in wild-type (n=11) and microglia knock-out (n=7) brains at day 3 post-infection. Data are pooled from 2 independent experiments and analysed by unpaired two-tailed t-test. ****P<0.0001. (c) Fungal burdens in the brain and lung of wild-type (n=11) and microglia knockout out (n=7) at day 3 post infection. Data are pooled from 2 independent experiment and analysed by Mann Whitney U-test. *P<0.05. (d) Total number of indicated inflammatory cells in the brains of wild-type (n=11) and knockout mice (n=6) at day 3 post infection. Data are pooled form 2 independent experiments. Data generated by Rebecca Drummond.

3.3.8 Brain resident macrophage depletion with PLX5622 reduces brain fungal burden.

An alternative model to depleting brain-resident macrophages that does not rely on transgenic animals is the drug PLX5622 (Rice, Spangenberg et al. 2015). This drug is a CSF1R inhibitor that allows for elimination of microglia and other CNS macrophages (Spangenberg, Severson et al. 2019), as discussed in detail in section 3.2.4. C57BL/6 mice were given either PLX5622 or control diet for 7 days, prior to intravenous infection with *C. neoformans* and remained on diet for the duration of infection and data analysed at day 3 post infection (Figure 3.8a). I found that PLX5622 treated mice had significantly reduced microglia number compared to untreated group (Figure 3.8b). Similar to the $Cx3cr1^{CreER}$ model presented in Figure 3.7, I found that microglia-depleted mice (treated with PLX5622) had reduced brain fungal burden (Figure 3.8c) with no difference in lung burden (Figure 3.8c). Next, I measured the recruitment of inflammatory myeloid cells including neutrophils, inflammatory monocytes and $Ly6C^{low}$ in PLX5622 treated mice and their controlled group. I found minor but significant difference in macrophages, $Ly6C^{low}$ and neutrophil recruitment cells to the brain in PLX5622 treated mice compared to untreated mice (Figure 3.8d). Taken together this data shows that depleting CNS resident macrophages with PLX5622 reduces brain fungal burden.

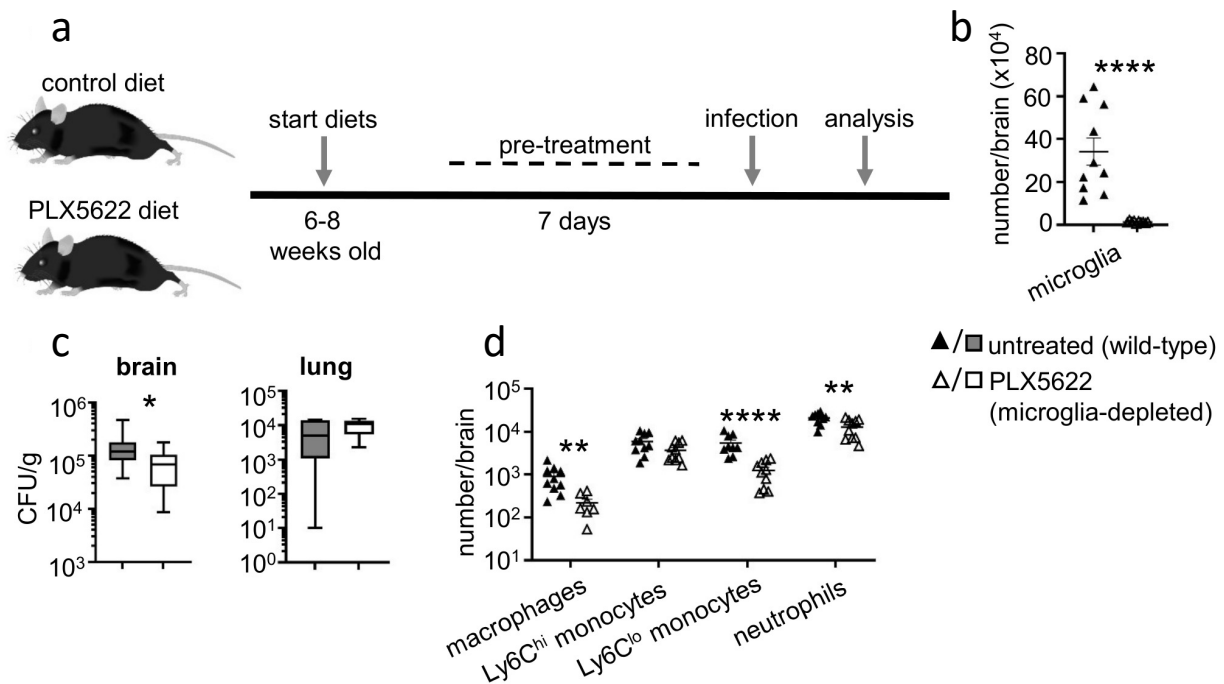


Figure 3. 8 PLX5622 reduces brain fungal burden with no difference in lung. (a) Schematic of PLX5622 treatment. Wild-type C57BL/6 mice were fed either control or PLX5622 diets for 7 days and were continued throughout infection. Mice infected with h99 intravenously (b) Total number of microglia in untreated (n=10) and PLX5622-treated (n=10) brains at day 3 post-infection. Data are pooled from 2 independent experiments and analysed by unpaired two-tailed t-test. ****P<0.0001. (c) Fungal burdens in the brain and lung of untreated (n=14) and PLX5622 treated (n=14) at day 3 post infection. data are pooled from 3 independent experiments and analysed by Mann Whitney U-test. *p<0.05. (d) Total number of indicated inflammatory cells in the brains of untreated (n=10) and PLX5622 treated (n=10) at day 3 post infection. Data are pooled from 2 independent experiments.

3.3.9 Tissue resident macrophage depletion using PLX5622 reduces brain fungal burden only at early time points post-infection.

Next, I examined the effect of tissue resident macrophages depletion on brain fungal burden at day 6 post infection to determine the longer-term impact of microglia depletion on control of *C. neoformans* infection. At day 6 post infection I found PLX5622 treated mice had sustained microglia depletion compared to untreated group (Figure 3.9a). Similar to day 3 post infection, I found significant reductions in the number of Ly6C^{low} and macrophages in the brain with no difference in neutrophil and inflammatory monocytes (Figure 3.9b). Next, I wanted to assess the fungal

burden at day 6 post infection, I saw no difference in either brain or lung between PLX5622 treated mice and untreated mice (Figure 3.9c). Taken together this data shows that microglia play a minimal role in controlling brain infection at late time point post-infection.

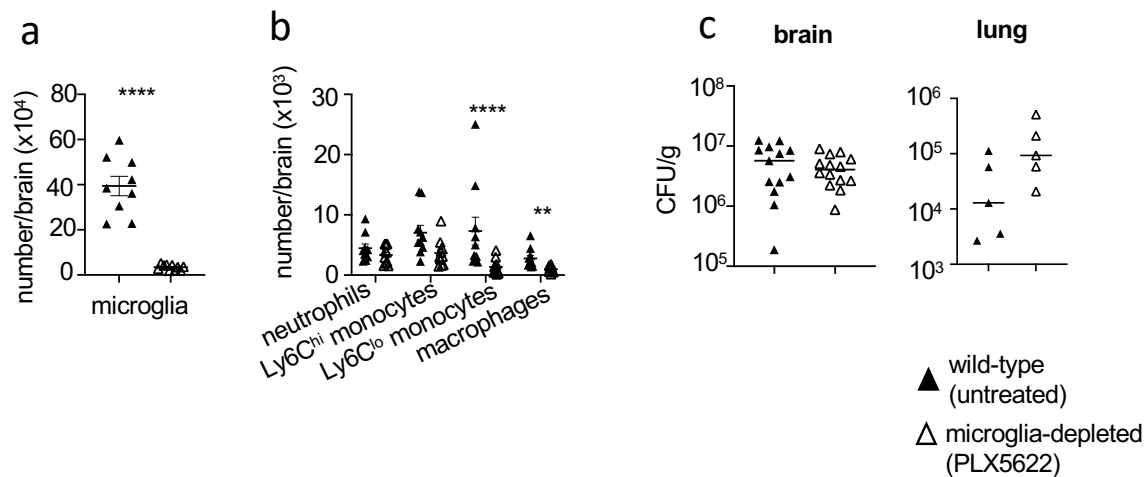


Figure 3. 9 PLX5622 treatment at day 6 post infection. (a) Total number of microglia in untreated (n=9) and PLX5622-treated (n=10) brains at day 6 post infection. Data are pooled from 2 independent experiments and analysed by unpaired two-tailed t-test. ****P<0.0001. (b) Total number of indicated inflammatory cells in the brains of untreated (n=10) and PLX5622 treated (n=10) at day 6 post infection. Data are pooled from 2 independent experiments. (c) Fungal burdens in the brain and lung of untreated (n=10) and PLX5622 treated (n=10) at day 6 post infection. data are pooled from 2 independent experiments and analysed by Mann Whitney U-test. **P<0.01

3.3.10 PLX5622 deplete meningeal macrophages in the meninges.

PLX5622 treatment can also deplete other CNS-resident macrophages, including MMs (Wheeler, Sariol et al. 2018, Lei, Cui et al. 2020). I confirmed that PLX5622 treatment depleted macrophages (Figure 3.8d) and appears to have some effect on the Ly6C^{low} population in the brain (Figure 3.8d). I wanted to confirm if PLX5622 treatment causes changes in meningeal myeloid cells. Following the same PLX5622 treatment regime as before, I measured the total number of myeloid cells in the meninges. I found the only cells to be affected by PLX5622 treatment in the meninges are the MMs (Figure 3.10a), and no effect on inflammatory monocytes or

neutrophil requirement to the meninges at day 3 post infection (Figure 3.10b) and similarly at day 6 post infection (Figure 3.10 c,d). Furthermore, I saw no difference in Ly6C^{low} in the meninges either at day 3 or 6 post infection, suggesting that PLX5622 might have effect on Ly6C^{low} cells in organ specific manner. This data confirms that PLX5622 deplete MMs in the meninges with no difference in other myeloid cells.

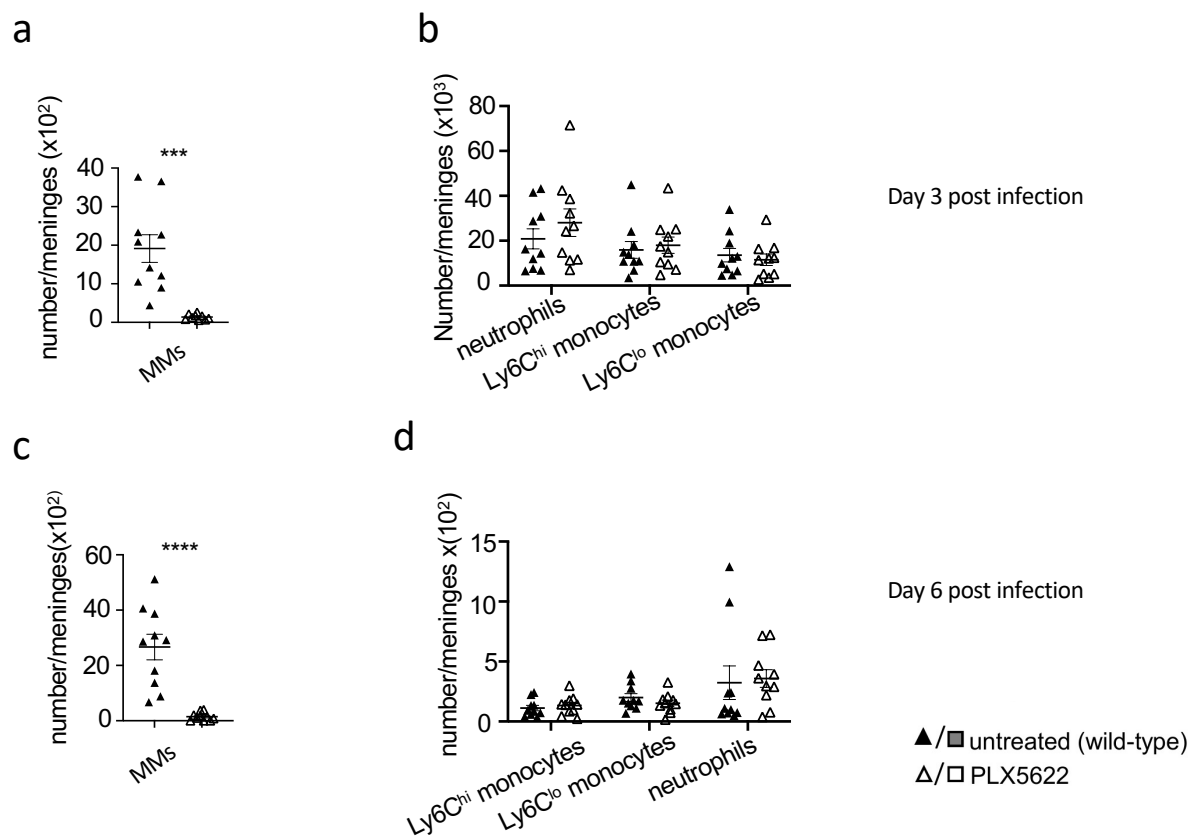


Figure 3. 10 Meningeal macrophages the only cells depleted with PLX5622 in the meninges. (a) Total number of MMs in untreated (n=10) and PLX5622-treated (n=10) brains at day 3 post-infection. Data are pooled from 2 independent experiments and analysed by unpaired two-tailed t-test. ****P<0.0001. (b) Total number of indicated inflammatory cells in the meninges of untreated (n=10) and PLX5622 treated (n=10) at day 3 post infection. Data are pooled from 2 independent experiments. (c) Total number of meningeal macrophages in untreated (n=10) and PLX5622-treated (n=10) brains at day 6 post-infection. Data are pooled from 2 independent experiments and analysed by unpaired two-tailed t-test. ****P<0.0001. (d) Total number of indicated inflammatory cells in the meninges of untreated (n=10) and PLX5622 treated (n=10) at day 6 post infection. Data are pooled from 2 independent experiments.

3.3.11 *Sall1*^{CreER}iDTR is not suitable model to deplete microglia.

PLX5622 treatment depletes other CNS-resident macrophages, including inflammatory macrophages and meningeal macrophages (Figure 3.4d & 3.5b). Moreover, the *Cx3cr1*-Cre^{ER} line has been shown to additionally target non-microglia populations in certain contexts (Zhao, Alam et al. 2019, Masuda, Amann et al. 2022). Therefore, I sought to generate a mouse model to enable specific depletion of microglia while leaving other CNS-resident and inflammatory macrophages intact, to determine whether the reduction in brain fungal burdens I observed was due to loss of microglia and/or other CNS-resident macrophages. *Sall1* is microglia signature gene that is specifically expressed by microglia and not other CNS-resident macrophages (Buttgereit, Lelios et al. 2016). I therefore, generated *Sall1*-Cre^{ER}-iDTR^{flox} mice. Where the Cre recombinase expression is driven by the *Sall1* promoter and Cre-mediated excision of STOP cassette render cells sensitive to diphtheria toxin. Mice are then left for 4-6 weeks after tamoxifen treatment so any short-lived cells expressing *Sall1* will be replaced by new one that do not express Cre recombinase while long lived cell such as microglia will continue to express Cre. I then injected diphtheria toxin which will bind to diphtheria toxin receptor and causes cell death in any cell that express the Cre. Mice were bred to be heterozygous for the iDTR flox allele, and wild-type littermate which is heterozygous for the *Sall1*-Cre^{ER} allele. all animals being treated with tamoxifen and DT (regardless of genotype). In pilot experiments, the first dose of diphtheria toxin had no effect on the mice which appeared normal and healthy. However, Cre-expressing mice started to lose weight within the first 24h (Figure 3.11a). After the second dose of diphtheria toxin, Cre-expressing mice became non-responsive and were moribund, while WT mice appeared healthy. I tried a second pilot lowering the dose of diphtheria toxin but

Cre⁺ mice continued to die. These experiments were therefore terminated. Upon autopsy inspection, I found the kidneys of Cre-expressing mice were very pale, and the liver had a mottled appearance compared to the control mice who had healthy-looking kidneys and liver (data not shown). This data suggests there might be some long lived Sall1-expressing cells in liver and/or kidney were responding to diphtheria toxin and were vital for viability.

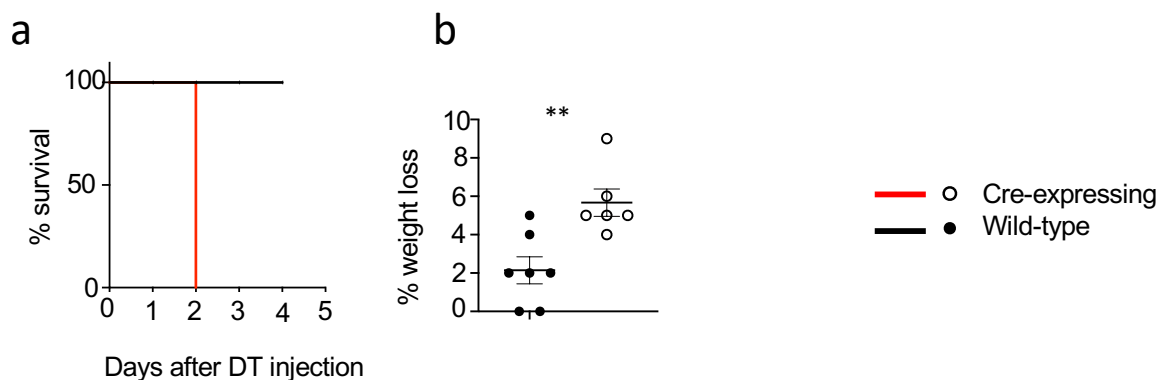


Figure 3.11 Sall1^{CreER} is not a suitable model to deplete microglia. (a) Survival graph showing the % of mice survival after DT dose. Red line is Cre-expressing and black line is WT. (b). Graph showing the % weight loss of mice before DT injection and after. Data are pooled from two independent experiments and analysed accordingly by two-tailed unpaired t-tests or two-tailed Mann Whitney U-test * $P < 0.05$. n= individual mice Cre- (n=7) Cre+ (n=6).

3.3.12 Fungal brain infection is primarily supported by microglia.

After confirming that Sall1-Cre^{ER}-iDTR model is not suitable, I generated new mouse model to enable specific depletion of microglia while leaving other CNS-resident macrophages intact. I generated another transgenic model by crossing Sall1^{CreER} animals with Csf1r^{flx} (Figure 3.12a) mice to deplete Csf1r specifically in microglia as these cells significantly depended on CSF1R signalling (as described in section 3.3.8) and this should not affect non-myeloid tissues as Csf1r is predominantly expressed by macrophages.

Following tamoxifen treatment, I found Cre-expressing mice had significant reduction in microglia number compared to their WT litter mate (Figure 3.12b). This depletion was specific to microglia, since I found no difference in other myeloid cells, including

Cx3cr1⁺ CD45^{hi} MHCII⁺ population, monocytes, and neutrophils (Figure 3.12c). Furthermore, there was no difference in MMs in Cre-expressing mice compared to WT control (Figure 3.12d) and no difference seen in any other meningeal myeloid cells (Figure 3.12e). I further confirmed there was no off-target effect on lung immune cells (Figure 3.12f), indicating specific depletion of microglia. Importantly, these microglia-specific depleted mice had significantly reduced brain fungal burden and no effect on lung fungal burden (Figure 3.12fg). These data indicate that the reduction in fungal infection in the other models (see section 3.3.7 and 3.3.8) is primarily due to the loss of microglia, and that targeted depletion of these cells has a protective effect leading to reduced fungal brain infection.

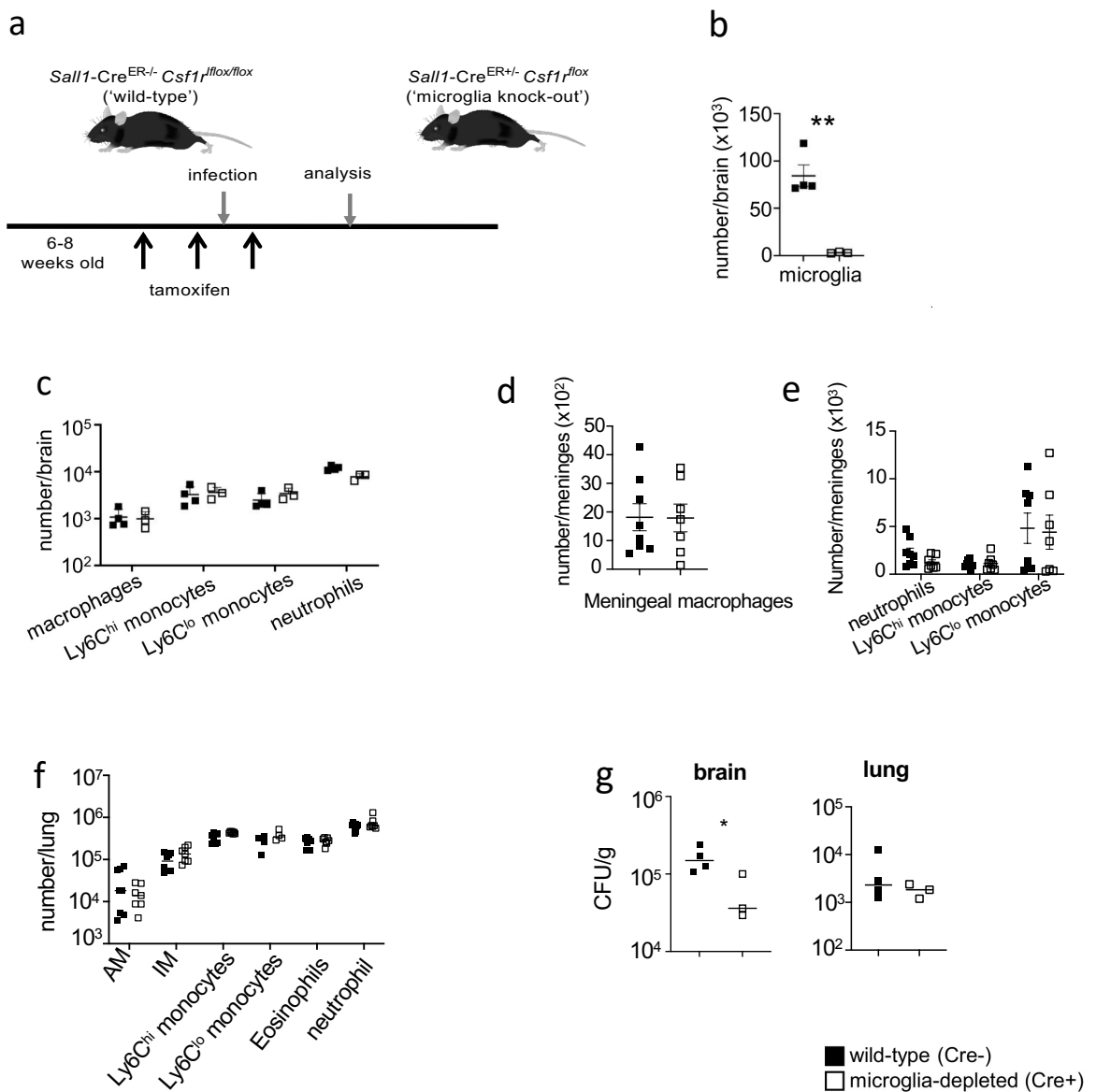


Figure 3. 12 *Sall1Cre^{ER}xCsf1^{fl/fl}* specific model to deplete microglia in the CNS.

(a) Schematic of *Sall1Cre* depletion of brain-resident macrophages. *Sall1-Cre^{ER}* mice were crossed with *Csf1^{fl/fl}* mice. Resulting wild-type and Cre-expressing ('microglia knock-out') littermates are treated with tamoxifen to initiate cell depletion before and after intravenous *C. neoformans* H99 infection. (b) Total number of microglia in wild-type (n=4) and microglia-depleted (n=3) brains at day 3 post-infection. Data are representative of 1 independent experiment and analysed by unpaired two-tailed t-test. **P<0.05. (c) Total number of indicated inflammatory cells in the brains of wild-type (n=4) and microglia-depleted (n=3) brains at day 3 post-infection. (d) Total number of meningeal macrophages in wild-type (n=8) and microglia-depleted mice (n=7). (e) Total number of myeloid cells in the meninges wild-type (n=8) and microglia-depleted mice (n=7). (f) Total number of myeloid cells in the lung wild-type (n=8) and microglia-depleted mice (n=7). (g) Fungal burdens in the brain and lung of wild-type (n=4) and microglia-depleted (n=3) brains at day 3 post-infection. Data are represented from 1 independent experiment and analysed by Mann Whitney U-test. *p<0.05.

3.3.13 Intracellular survival within microglia is required for optimal fungal brain infection.

Since I found that microglia hosted intracellular fungi (Figure 3.1d) and the fungi was viable (Figure 3.4b), I next examined the relevance of this intracellular growth to the supportive role of microglia in infection revealed by my depletion experiments (Figures 3.7, 3.8 and 3.12). For that, I searched the literature for fungal mutants that either have dependency or inability for survival within macrophage phagosomes. I chose the strains $\Delta rdi1$ *C. neoformans*, a mutant strain that is unable to survive within macrophages but has normal growth rate in rich media and susceptibility to ROS/NOs as WT strain (Price, Nichols et al. 2008) and $\Delta gcs1$ *C. neoformans*, a mutant strain that is unable to survive extracellularly as it needs a neutral/alkaline pH to grow (Kechichian, Shea et al. 2007). First, I infected WT mice with these mutants to assess their virulence and suitability for my models. I found that $\Delta gcs1$ *C. neoformans* was avirulent in an intravenous infection model and did not result in sufficient fungal burden to determine meaningful differences in downstream experiments (Figure 3.13a). This strain was therefore excluded from further study and instead I focused on $\Delta rdi1$ mutant strain, which could infect the brain in my chosen infection model. I first performed histological examination on brain samples of mice infected with $\Delta rdi1$ and the parental strain control (H99) and observed that most yeast was growing 'extracellular' in areas of tissue damage at 3 days post-infection, whereas wild-type *C. neoformans* yeasts were mostly intracellular at 3 days post-infection (Figure 3.13b). This confirmed the mutant can only grow extracellularly and therefore can be used to test how relevant is the intracellular growth within microglia. Next, I infected mice that were either microglia-sufficient (Control diet) or microglia-depleted (PLX5622 diet) with WT or $\Delta rdi1$ *C. neoformans*

and measured brain fungal burden. Compared to wild-type *C. neoformans* brain fungal burden was significantly reduced in mice infected with the $\Delta rdi1$ mutant strain (Figure 3.8c). Importantly, while microglia depletion caused a significant reduction in brain infection when using wild-type strain, this did not reach a significant difference with $\Delta rdi1$ mutant (Figure 3.8c). I found no difference in the lung in microglia-sufficient (Control) or microglia-depleted (PLX5622) with either WT *C. neoformans* or $\Delta rdi1$ (Figure 3.8d). Taken together this data indicates that the reduced brain fungal burden I have with microglia depletion is at least partially dependent on the ability of the fungus to survive intracellularly.

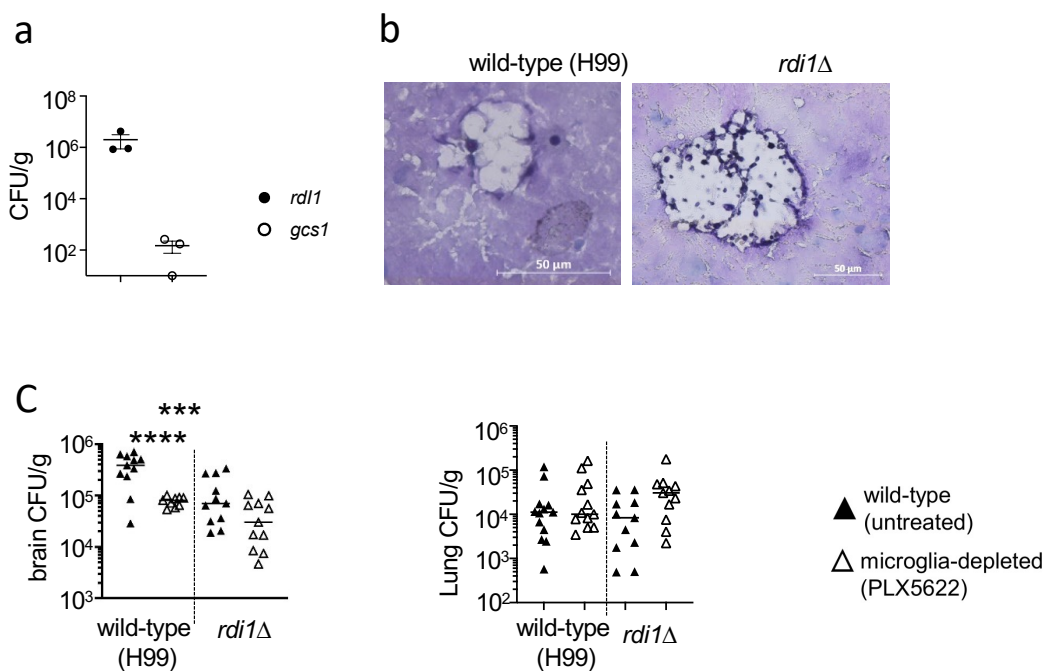


Figure 3.13 Reduction of fungal brain burden in microglia-depleted mice depends on intracellular growth. (a) Fungal burden of mutant strain $\Delta rdi1$ and $\Delta gcs1$. (b) Representative histology from brain of mice infected with wild-type *C. neoformans* H99 or $\Delta rdi1$ *C. neoformans* at day 3 post-infection, stained with PAS. (c) Brain fungal burdens in untreated or PLX5622-treated mice at day 3 post-infection, infected with either wild-type *C. neoformans* H99 (n=11 wild-type, n=9 microglia-depleted) or $\Delta rdi1$ *C. neoformans* (n=11 wild-type, n=11 microglia-depleted). Data are pooled from 2 independent experiments and analysed by one-way ANOVA with Bonferroni correction. (d) Lung fungal burdens in untreated or PLX5622-treated mice at day 3 post-infection, infected with either wild-type *C. neoformans* H99 (n=13 wild-type, n=12 microglia-depleted) or $\Delta rdi1$ *C. neoformans* (n=11 wild-type, n=11 microglia-depleted). Data are pooled from 2 independent experiments.

3.3.14 *C. neoformans* is protected from copper starvation within microglia.

Although *C. neoformans* burden went down with microglia depletion, it was not clear what would the reason be since *C. neoformans* could still grow extracellularly, which suggest that there must be an advantage being inside microglia compared to extracellular. This led me to think about the micronutrients difference in the extracellular compartment within the brain and inside microglia. In the brain, micronutrients are restricted and this is particularly true for copper and iron. These metals are usually found at higher intracellular concentration within cells, including microglia, than extracellularly (Gaier, Eipper et al. 2013). I hypothesis that microglia may protect *C. neoformans* from nutrient starvation in the brain and provide a site for nutrient acquisition for intracellular fungi. To test this hypothesis, I focused on copper acquisition since the genetic network regulating copper starvation is well characterised in *C. neoformans* (Ding, Festa et al. 2013). *C. neoformans* upregulates copper importer CTR4 in copper restricted environment (Ding, Festa et al. 2013). For that, we generated CTR4 reporter strain in which the expression of GFP transgene under the control of the CTR4 promotor (*C. neoformans* CTR4^{pGFP}) into a constitutively expressing mCherry background strain. To start with a master student in our lab (Alanoud Alselami) compared the expression of CTR4 by yeast in either copper-deficient media or where copper was added to the media. At 10 μ M copper, there was no detection of CTR4^{pGFP} expression (Figure 3.13a) and in copper-deficient media the GFP transgene expression increased ~90 % indicating copper starve condition (Figure 3.13a). I next used this reporter strain as a tool to compare the expression of CTR4 by yeast cells inside microglia with extracellular yeast in the brain by measuring the expression of GFP in mice (Figure3.13b). I found that extracellular yeast upregulated CTR4^{pGFP} expression and this has been

previously shown within the CNS [42] (Figure 3.9b). In contrast, yeast within microglia had significantly reduced CTR4^{pGFP} expression (Figure 3.9b), indicating that copper concentration inside microglia is adequate for fungal growth. To check that these results were not an artefact of different fluorescent properties of yeast inside host cells versus free yeast, I normalised CTR4^{pGFP} expression to a constitutively expressed mCherry housekeeper. Similar result was found in normalised CTR4^{pGFP} expression (Figure 3.13). So far, this data shows that *C. neoformans* uses microglia as a site to protect itself from copper starvation inside CNS.

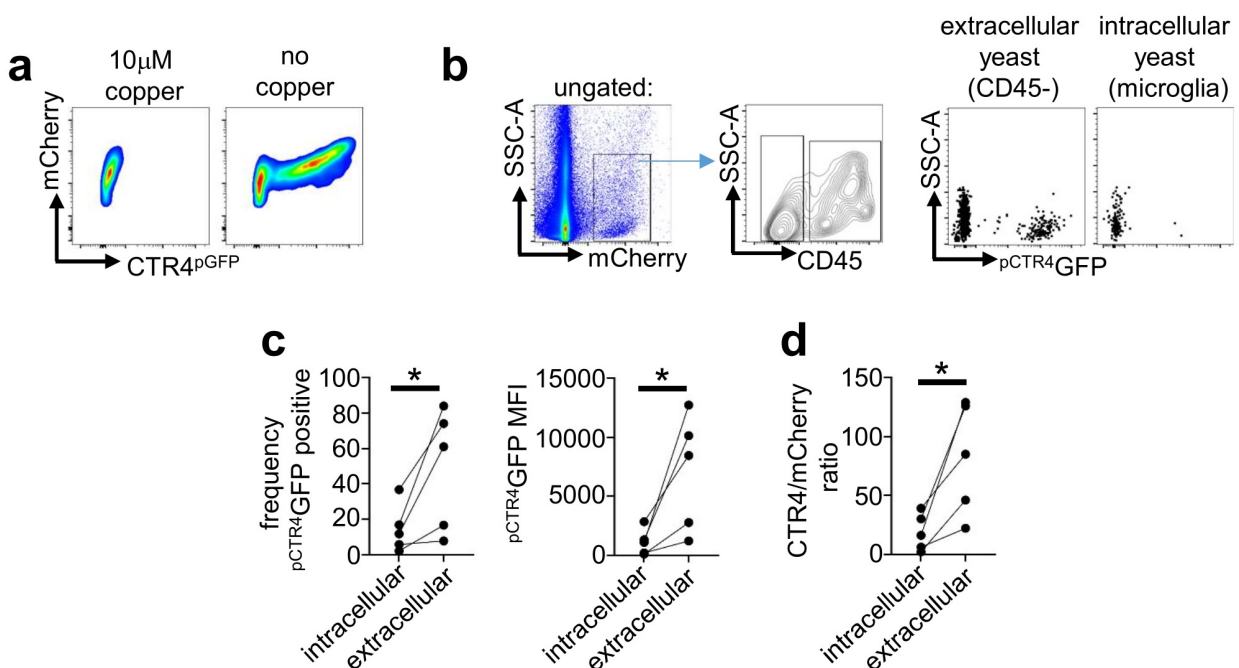


Figure 3. 14 *C. neoformans* is protected from copper starvation when associated with microglia. (a) Example flow cytometry plots of pCTR4 GFP *C. neoformans* grown in copper deficient YNB media with and without copper supplementation for 18 hours. mCherry is under the control of ACT1 promoter and acts as a housekeeper, GFP expression is controlled by the CTR4 promoter. (b) Gating strategy for analysing pCTR4-GFP yeast cells in the brains of mice at day 7 post-infection. Yeast were first gated on using the mCherry marker, then split into extracellular and intracellular (cd45+) groups. Intracellular yeast were further gated to specifically analyse microglia (Ly6G⁻, Ly6C⁻, CD45^{int} cx3cr1⁺). (c) Frequency of GFP⁺ cells and median fluorescent intensity (MFI) of pCTR4 GFP in yeast cells that were extracellular or intracellular within microglia. Each point represent an individual mouse. Data are pooled from two independent experiments and analysed by two-tailed t-test *P<0.01. (d) Ratio between GFP and mCherry in yeast cells that were extracellular or intracellular within microglia. Each point represent individual mouse. Data are pooled from two different experiments and analysed by paired two-tailed t-test.

3.3.15 Copper starvation in other brain myeloid cells

Previous data have shown that infecting murine macrophages cell line in vitro shows upregulation of CTR4 suggesting that these cells have low amount of copper (Waterman, Hacham et al. 2007, Waterman, Park et al. 2012). For that, I took an advantage of the CTR4^{pGFP} strain and I examined the GFP expression in other brain myeloid cells to assess if copper restriction or access was different between different cell types in the brain during infection. I found a trend of higher percentage of GFP + yeasts inside inflammatory macrophages (Cx3cr1⁺ CD45^{hi} MHCII⁺) (Figure 3.15 a,b), indicating that macrophages might be inducing copper starvation compared to microglia. Next, I compared GFP expression in neutrophils, inflammatory monocytes and patrolling monocytes and found no difference in any of these myeloid cells compared to microglia (Figure 3.15b), although some mice had induced copper starvation in patrolling monocytes .

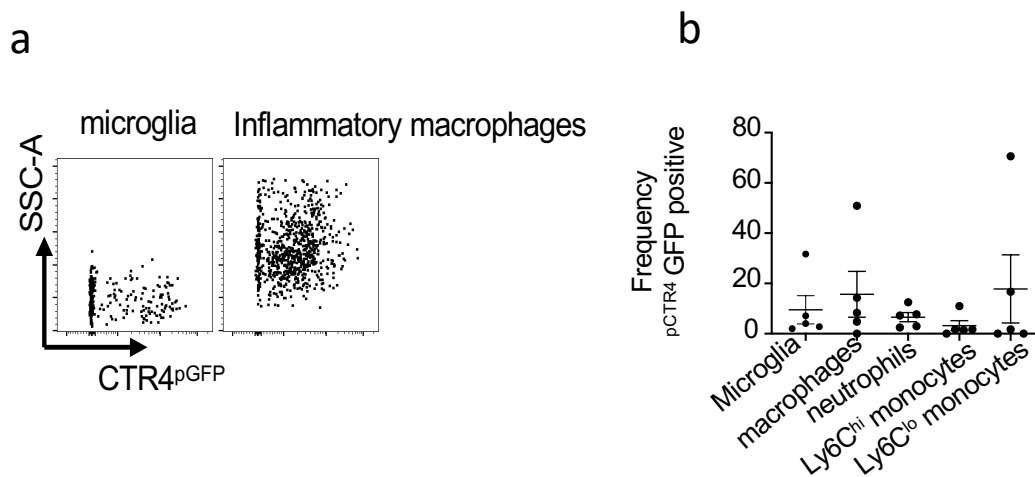


Figure 3. 15 *C. neoformans* is protected from copper starvation when associated with microglia. (a) Example flow cytometry plots of pCTR4^{GFP} *C.neoformans* in microglia and inflammatory macrophages. (b) Frequency of GFP+ cells of pCTR4^{GFP} in yeast cells that were intracellular within indicated immune cells. Each point represent an individual mouse (n=5). Data are pooled from two independent experiments.

3.3.16 IFN γ induces copper restriction in fungal-infected microglia.

IFN γ is an important cytokine that has been shown to have protective immunity against *C. neoformans* (Williamson, Jarvis et al. 2017). IFN γ has also been shown to activate macrophages to increase NO and fungal killing (Leopold Wager, Hole et al. 2015). Furthermore, IFN γ has been shown to modulate copper concentration in macrophages to by inducing starvation in order to control pathogen replication (Shen, Beucler et al. 2018) or increasing copper to induce toxicity (Djoko, Ong et al. 2015). For example, treating *H. capsulatum* infected BMDMs with IFN γ reduced copper concentration within macrophages (Shen, Beucler et al. 2018). Whether this protective effect happens during *C. neoformans* infection has not been explored. For that, we wanted to test if IFN γ modulates copper concentration within microglia to induce nutritional immunity. We infected murine microglia cell line BV2 with CTR4^{pGFP} and compared GFP expression in untreated microglia or IFN γ treated microglia (Figure 3.15a). We found IFN γ treated microglia had significantly higher yeast expression GFP compared to untreated microglia (Figure 3.15b). We normalised CTR4^{pGFP} expression to a constitutively expressed mCherry housekeeper. Similar result was found in normalised CTR4^{pGFP} expression (Figure 3.15c). This suggest that IFN γ induces copper restriction within microglia phagosomes resulting in an increased fungal copper starvation effect.

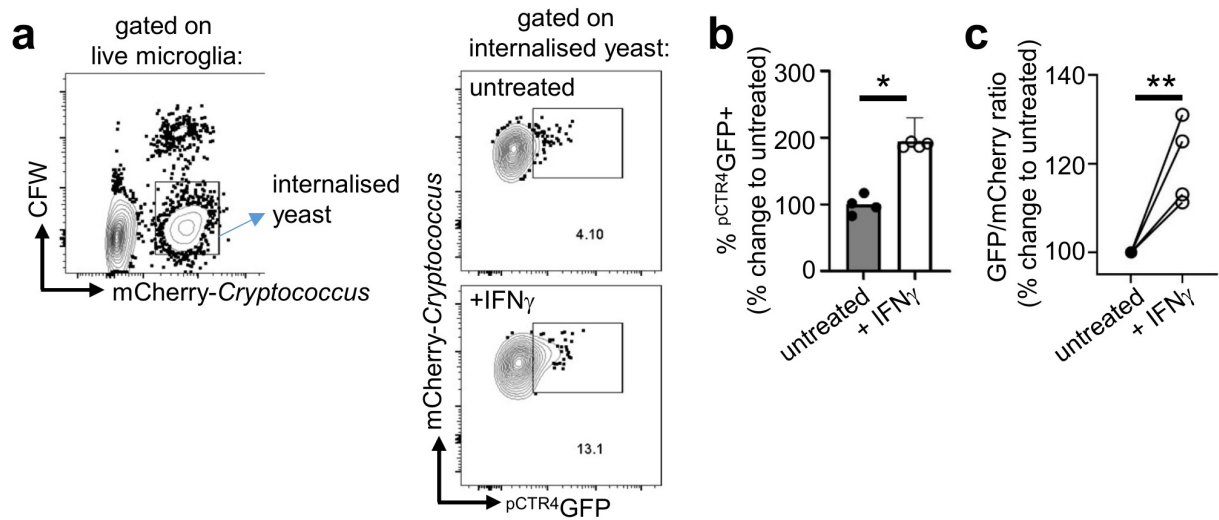


Figure 3.16 IFN γ increases fungal copper starvation within microglia. (a) Gating strategy used to compare pCTR4 GFP expression by intracellular yeast within untreated or IFN γ treated microglia. Cells were first gated to exclude free yeast, doublets, and dead cells. Yeast bound to surface of microglia but not internalised were removed from analysis using a calcofluor white (CFW) counter stain for the fungal cell wall. (b) Frequency of intracellular pCTR4 GFP+ yeast in untreated and IFN γ treated microglia after 2 hours of infection. bars represent mean. Data are from 4 independent experiments, point shown technical replicates from one representative experiment. Data are analysed by unpaired two-tailed t-test. (c) Ratio between mCherry and pCTR4 GFP expression by intracellular yeast in untreated and IFN γ treated microglia after 2 hours of infection. Each point represents mean value from technical replicates from 4 independent experiments. Data are analysed by unpaired two tailed t-test **P<0.01. Data generated by Alanoud Alselami.

3.4 Discussion

This chapter aimed to further understand the role of tissue resident macrophages in the CNS during *C. neoformans* infection at early time points post infection, using an acute infection model (intravenous infection). I found that microglia support early fungal growth of *C. neoformans* in the brain. Using three different depletion strategies I found depleting microglia resulted in a reduced fungal burden.

Furthermore, I found that intracellular residence inside microglia has advantage for the fungus. Using a fungal reporter strain to track copper starvation response I found *C. neoformans* is protected from copper starvation within microglia, promoting CNS infection.

CNS infections with *C. neoformans* is often lethal and hard to treat, and the mechanisms responsible for host antifungal immunity and the role played by brain-resident myeloid cells during infection are not well understood. Examining the association between CNS innate myeloid cells and *C. neoformans*, I found myeloid cells become infected with the fungus and by analysing the total number of infected cells I found intimate relationship between tissue resident macrophages and *C. neoformans* in CNS. Similarly, histology of *C. neoformans* infected human brain showed similar pattern where the fungus resides within innate immune cells. Indeed, human microglia has been shown to host *C. neoformans* intracellularly in vitro (C. Lee, Kress et al. 1995). Furthermore, *C. neoformans* are able to manipulate macrophages to its advantage, for example *C. neoformans* able to change the phagosome maturation by inducing early removal of Rad5 and Rad11 (maturation markers). Moreover, *C. neoformans* alter the phagosome acidification and calcium influx (Smith, Dixon et al. 2015), making them inadequate in killing the fungus and suitable site for replication (Mansour, Reedy et al. 2014, Smith, Dixon et al. 2015).

Microglia have been shown to have important role in CNS immunity against bacteria, viruses and *C. albicans* fungal infection (Wheeler, Sariol et al. 2018, Drummond, Swamydas et al. 2019, Batista, Still et al. 2020). However, in my work depleting microglia have a therapeutic effect by reducing brain fungal burden during *C. neoformans* infection. Microglia has been shown to be the major producer of neutrophil chemoattractants to the brain during *C. albicans* infection by IL-1 β and CXCL1 production (Drummond, Swamydas et al. 2019). Moreover, microglia can cause monocytes infiltration helping the clearance of viral infection (Spiteri, Wishart et al. 2022) and inflammatory T cells infiltration during *T. gondii* parasite infection (Batista, Still et al. 2020). However, my work showed little evidence for microglia role in monocytes or neutrophil recruitment to the brain during *C. neoformans* infection, as I do not see any changes in these myeloid cells in any of my depleting models compared to microglia deficient mice. This might be because *C. neoformans* has a thick capsule shielding it from microglia recognition and therefore activation in early point of infection. Indeed, during PIIRIS model, microglia did not become fully activated until day 21 post infection despite high brain fungal burden (Neal, Xing et al. 2017). Furthermore, *C. neoformans* capsule GXM has been shown to induce IL-8 in microglia cell line (but not astrocytes) which lead to neutrophil migration inhibition towards IL-8 and this has been seen in CSF in patients with CM (Lipovsky, Gekker et al. 1998). Moreover GXM has been shown to be potent inhibitors of monocytes, neutrophils and lymphocytes (Dong and Murphy 1995) and down regulate the production of macrophage inflammatory protein α (MIP1 α) and MIP1 β in human microglia cell line (Goldman, Song et al. 2001). In addition, *C. neoformans* secretes a mannose-rich capsule which shields the fungal cell wall from recognition by CARD9-coupled receptors, such as Dectin-1 (Walsh, Wuthrich et al. 2017). Indeed,

patients with deficiencies in Dectin1/Card9 do not appear to be more susceptible to CM (Drummond, Franco et al. 2018), suggesting these pathways might not be useful for recognising and initiating immunity against *C. neoformans*. The innate receptors that elicit *C. neoformans* recognition by brain macrophages is still not known, but potentially happens by cross talk with IFN γ producing CD4 T cells. Some of microglia depletion method that I have used have been shown to have off target effect on non-microglia macrophages in the CNS including PVMs including the PLX5622 inhibitor (Kerkhofs, van Hagen et al. 2020, Spiteri, Ni et al. 2022). The role of non-microglia macrophages during infection and whether they are involved in dissemination/prevention of *C. neoformans* crossing the BBB is not fully understood. Since perivascular space can act as an entry route for infected-phagocytes into the CNS in mice (Kaufman-Francis, Djordjevic et al. 2018). Furthermore, PVMs have been shown to be heavily infected with *C. neoformans* and seen in the PVS during infection (Kaufman-Francis, Djordjevic et al. 2018)[20]. Thus, it is possible that PVMs may be involved in the initial control of brain infection, and it is possible by using PLX5622 or Cx3cr1^{CreERT} x iDTR depletion model disrupted fungal invasion strategies and contributing to the reduced fungal burden. To eliminate that I tried using more specific model to deplete microglia, one approach I tried is using Sall1^{CreERT} x iDTR, in this model all long-lived Sall1+ cells are depleted following treatment with diphtheria toxin. However, Cre-expressing mice became very ill after receiving the second dose of diphtheria toxin and developed unusual kidney pathology that I noted post-mortem. Although *Sall1* is expressed highly in microglia, it is also expressed in other tissues including liver and heart in the development stage (Abedin, Imai et al. 2011). Furthermore, *Sall1* is involved in kidney development and has a critical role in nephrogenesis, since *Sall1* mutation is embryonically lethal due to kidney

dysgenesis (Nishinakamura, Matsumoto et al. 2001). Moreover, human mutation of *SALL1* results in Townes-Brocks syndrome, which is associated with kidney disease and can progress to kidney failure in childhood. These patients also have CNS problems, linked with *Sall1* expression in microglia (Faguer, Pillet et al. 2008). One study found rare *Sall1*-expressing cells in adult mouse kidney which proliferated following acute kidney injury (Abedin, Imai et al. 2011). The illness seen in these mice was surprising because *Sall1* is not thought to control adult kidney function, and since I left mice for 4-6 weeks after tamoxifen short lived cells should have been replaced by new cells that do not express Cre recombinase, but my data suggests *Sall1* expressing cells are present in adult mice kidney that must be long lived cells and they are vital for mice survival. For that reason, I instead generated *Sall1^{CreER}Csf1r^{fllox}* animals. In those mice, only microglia were depleted, and kidneys were unaffected. This is likely because I target CSF1R which is mainly expressed by macrophages. Similar to the previous depletion models (i.e., PLX5622), I saw a reduction in brain fungal burden in microglia depleted mice, indicating the microglia are the main macrophages in the CNS promoting fungal growth.

Future studies are needed to examine the role on non-microglia macrophages during *C. neoformans* and examine whether they have a role in protection or dissemination during CM. Indeed, recent study has shown that MMs have protective role during lymphocytic choriomeningitis virus (LCMV) and by developing transcranial delivery approach to deliver PLX5622 in the meninges, MMs can be depleted specifically (Rebejac, Eme-Scolan et al. 2022). This study highlights the important role of MMs during infection where by depleting them the meninges become heavily infected with the virus which lead to the spread to the CNS and fatal meningitis in mice (Rebejac, Eme-Scolan et al. 2022). Similarly, it would be important to understand MMs role

during CM since it is the main site of disease in human (Kambugu, Meya et al. 2008, Abassi, Boulware et al. 2015).

The microenvironment of the CNS has a significant influence on *C. neoformans* growth and virulence (Watkins, King et al. 2017). *C. neoformans* has evolved a range of nutrient acquisition mechanisms that support host infection (Silva, Schrank et al. 2011). One metal that is important for the fungus is copper which is critical for mitochondrial respiration and other biochemical processes (Desai and Kaler 2008). Majority of copper in the CNS found within immune cells and it exceed extracellular copper by 1000-fold (Gaier, Eipper et al. 2013) as copper can be toxic to neuron. Furthermore, microglia have been shown to express high copper transport in Alzheimer plaque (Lovell, Robertson et al. 1998). Since copper is restricted in the CNS *C. neoformans* have been shown to upregulate copper transporter (CTR4) in the brain and mutation in *CTR4* gene results in an avirulent phenotype specifically within the brain (Ding, Festa et al. 2013, Sun, Ju et al. 2014, Sun, Ju et al. 2014). Whether microglia involved in fungal adaptation by providing access to copper is not known. For that I wanted to test whether microglia provide access to copper to the fungus promoting growth within the CNS. For that I tracked *C. neoformans* copper sensing using a *CTR4*^{pGFP} strain, similar to previous publish data I found *C. neoformans* highly expressing CTR4 in the brain, suggesting copper limited environment in the brain (Ding, Festa et al. 2013, Sun, Ju et al. 2014). Interestingly, there was significant reduction in *CTR4*^{pGFP} expression with microglia compared to extracellular yeast, indicating adequate level of copper inside these cells. Similar observation is seen with *Histoplasma capsulatum* (intracellular yeast), where Ctr3 copper transporter is upregulated in copper limited environment and this was important for the fungus to grow in copper inside macrophages (Shen, Beucler et al.

2018). In addition to microglia, I looked at CTR4 expression in other brain myeloid cells including macrophages, neutrophil, inflammatory monocytes and patrolling monocytes (Ly6C^{low}). Compared to microglia macrophages was trending to higher expression of CTR4 which might indicate that macrophages induce copper starvation although more repeat is needed to have a confirmed conclusion. This has been seen in murine macrophage cell lines (J774.1 or RAW264.7) infected with *C. neoformans*, where the expression of CTR4 yeast was increased intracellularly indicating these cells have low amount of copper (Waterman, Hacham et al. 2007, Waterman, Park et al. 2012) and similarly this is seen with *Histoplasma capsulatum* (Shen, Beucler et al. 2018). Examining neutrophil and monocytes showed no difference in CTR4 expression to microglia, suggesting these cells might have adequate amount of copper.

IFN γ has been shown to activate copper starvation response in macrophages during *H. capsulatum* marked by increased CTR3 expression (Shen, Beucler et al. 2018), indicating protective immunity by IFN γ . Furthermore, IFN γ treatment in patients have shown to reduce fungal burden in CSF and increase survival rate however, what cause this protective effect is not known. I therefore, wanted to examine the role of IFN γ on microglia copper response during *C. neoformans* and whether similar mechanism to *H. capsulatum* is seen here. Indeed, my data showed that IFN γ treatment appeared to stimulate microglia limiting copper concentration inside these cells limiting fungal intracellular growth in the CNS. Moreover, *C. neoformans* have shown to decrease ATP7A (mammalian phagosome copper transporter) at 14 days post infection consistent with IFN γ production in AMs (Ding, Festa et al. 2013) which potentially could explain how IFN γ induce copper starvation and immunity. Moreover, IFN γ treatment in microglia cell line (BV2) has been shown to alter copper trafficking

by re-distributing ATP7A from Golgi vesicles to the cytoplasmic space, indicating a potential mechanism for how IFN γ can change copper concentration (Zheng, White et al. 2010). Future study needs to look at whether IFN γ treatment in vivo have similar effect on microglia CTR4 expression during *C. neoformans* and how conditionally depletion of CTR4 in microglia effect the phenotype I see in microglia depleted mice.

In conclusion this chapter shows microglia as an important host for intracellular fungal infection at early time point, protecting the fungus from copper starvation in the brain and treating microglia with IFN γ can help in increasing nutritional immunity in these tissue resident macrophages to limit their supporting role in brain infection.

4 The effect of PLX5622 on systemic Immunity during pulmonary fungal infection

4.1 Author Contributions

All the experimental data presented in this chapter was generated by the author of this thesis, except for data shown in Figure 4.6a, 4.13 a&c. The majority of the Results section has been published online as a preprint (Mohamed, Vanhoffelen et al. 2022).

4.2 Introduction

Tissue resident macrophages are one of the most abundant populations of myeloid cells and are integral to the pathogenesis of *C. neoformans*. *C. neoformans* can cause lung infection, where pulmonary cryptococcosis is the most common manifestation of the disease (Setianingrum, Rautemaa-Richardson et al. 2019). Tissue resident macrophages have also been shown to act as a reservoir for *C. neoformans* in both brain and lung. Recent studies have shown that *C. neoformans* produce secreted peptide CPL-1 inducing arginase expression within lung interstitial macrophages (IMs) promoting intracellular growth (Dang, Lei et al. 2021), as increased expression of arginase result in less iNOS utilising, reducing NO which result in less killing of the fungus. We still do not know if arginase drives fungal survival in other ways.

The ability of the fungus to access and infect tissue resident macrophages is therefore critical for the infection.

Tissue resident macrophages highly express CSF1R and different subset have varying levels of sensitivity to the growth factor CSF1, which correlate with their survival dependency of CSF1R. CSF1R inhibitor (PLX5622) is therefore an effective tool in depleting macrophages where signalling survival is dependent on the receptor (see chapter 3 for details) (Spangenberg, Severson et al. 2019). As mentioned in chapter 3, there is a controversy over the specificity of PLX5622, however to study chronic and long-term infections, PLX5622 is a readily available method that can be given to mice for up to 6 weeks with little adverse effects, and enable study of macrophage depletion for these longer time frames (Spangenberg, Severson et al. 2019).

In this chapter I used PLX5622 in a model of chronic *C. neoformans* infection and discovered several unanticipated effects that led to new discoveries on the role of lung-tissue resident macrophages in pathogenesis of *Cryptococcus* infection.

4.2.1 Immunology of *C. neoformans* lung infection

Innate and adaptive immunity are involved in the lung immune response to *C. neoformans*. Lung macrophages (AMs) are one of the first cells to encounter *C. neoformans* and initiated response (Nelson, Hawkins et al. 2020). The function of lung macrophages of whether they are protective or involved in the dissemination of *C. neoformans* is not very clear (discussed in detail below). During infection inflammatory monocytes have been shown to be recruited to the lung and mediate

fungal trafficking to lung draining lymph node (Heung and Hohl 2019). Interestingly, depleting inflammatory monocytes improved mice survival and reduce fungal dissemination (Heung and Hohl 2019). Eosinophils are another cell type that has been shown to play a role in *C. neoformans* infection, where they have been found to be in close association with the fungus in vivo (Feldmesser, Casadevall et al. 1997). Furthermore, eosinophils have been shown to be act as a APCs in rats, triggering Th1 response (Garro, Chiapello et al. 2011). Indeed, eosinophilia have been shown in blood and lung of recovered patients, suggesting that eosinophils may have protective role during *C. neoformans* infection (Yokoyama, Kadowaki et al. 2018). On the other hand, eosinophils have also been shown to drive Th2 response in some patients (Pfeffer, Sen et al. 2010). In the mouse lung, eosinophils have also been shown to contribute to IL-4 production (Piehler, Stenzel et al. 2011). Recent research has shown that CD200R1 is responsible for regulating eosinophilia during *C. neoformans* infection but altering lung eosinophils number had no effect on fungal burden (Salek-Ardakani, Bell et al. 2019).

Lung DCs have been shown to play protective roles during *C. neoformans* infection, where they mediated the adaptive immune system by presenting *C. neoformans* derived antigens to T cells (Wozniak, Vyas et al. 2006, Nelson, Hawkins et al. 2020). Moreover, recruited DCs to the lung correlated with protection in mice (Wozniak, Vyas et al. 2006). Once adaptive immune response is initiated, CD4 T cells is crucial part of immunity, where they drive recruitment of macrophages, neutrophils and eosinophils (Huffnagle, Lipscomb et al. 1994). CD8 T cell are another important component of the adaptive immune system, since they can mediate *C. neoformans* killing (Ma, Spurrell et al. 2002), and depleting these cells resulted in reduced survival rate in mice (Mody, Chen et al. 1994). B cells have important role in the

protection against *C. neoformans*, where depleting them caused higher rate of dissemination from lung to brain in mice (Dufaud, Rivera et al. 2018). Moreover, treating AMs with IgM sera increased phagocytosis, suggesting IgM might be initiator of early immunity in the lung (Dufaud, Rivera et al. 2018).

4.2.2 Alveolar macrophages

AMs are one of the first line of defence against inhaled pathogens. AMs originate from the embryonic yolk sac and are maintained by self-renewal, with their survival and differentiation depending on GM-CSF (Gomez Perdiguero, Klapproth et al. 2015, Hoeffel, Chen et al. 2015) (Figure 4.1). Recent studies have shown that there are two populations of AMs with different ontogeny. In addition to the resident, self-maintained AMs population, there was a second population derived from monocytes which appeared during infection (Lafuse, Rajaram et al. 2019, Kulikauskaite and Wack 2020). Resident AM have the ability to engulf pathogen and release protective cytokines such as IFN γ and repair tissue by removing apoptotic cells (Herold, Mayer et al. 2011, Wynn and Vannella 2016). Monocyte-derived AMs have proinflammatory response and in some cases can stimulate a cytokine storm which exacerbates tissue injury (Lin, Suzuki et al. 2008, Hou, Xiao et al. 2021). However, monocyte-derived AMs gave mice better protection against *Streptococcus pneumoniae* when re-infected and released protective IL-6 cytokines (Aegerter, Kulikauskaite et al. 2020). Furthermore, monocytes derived AMs have been shown to be important for tissue repair and homeostatic functioning of lung following injury and the differentiation of monocytes-derived AMs is dependent on the transcription factor EGR2 (McCowan, Fercoq et al. 2021).

In terms of *Cryptococcus* infection, AMs are one of the first cell type to initiate anti-cryptococcal immune responses in the lung. AMs have been shown to have the ability to clear *Cryptococcus* yeast cells (Feldmesser, Kress et al. 2000). Indeed, culturing human AMs with *C. neoformans* inhibits yeast cell replication (Weinberg, Becker et al. 1987). In addition, depleting AMs before infecting mice with *C. neoformans* resulted in exacerbated symptoms and increased death rate (Osterholzer, Milam et al. 2009). However, *C. neoformans* have been shown to reside and replicate inside AMs under conditions that are not yet fully defined (Figure 4.1) and thus, the anti-cryptococcal activity of alveolar macrophages may determine whether infection is contained or latent infection is established (McQuiston and Williamson 2012).

4.2.3 Interstitial lung macrophages

IMs are another type of tissue-resident macrophage in the lung, although their function and origin are less understood than AMs. Recent research has showed that lung IMs consist of different subpopulation that localise differently in the lung (Figure 4.1). Most studies agree that there are two main subset of lung IMs defined as MHCII^{hi}Lyve1^{low}IMs and MHCII^{low}Lyve1^{hi} IMs (Schyns, Bai et al. 2019). MHCII^{hi} IMs are found surrounding nerve bundles and are associated with immunoregulatory gene expression and antigen presentation capacity (Schyns, Bai et al. 2019, Ural, Yeung et al. 2020). In contrast, MHCII^{low} Lyve1^{hi} IMs are associated with blood vessels and their function is to control cell infiltration into lung and wound healing processes (Schyns, Bai et al. 2019, Ural, Yeung et al. 2020). During *Mycobacterium tuberculosis* infection, IM have been showing to have protective role since depleting them using intravenous injection of clodronate liposomes increased bacterial burden,

whereas depleting AMs reduced bacterial burden demonstrating divergent responses for these two lung macrophage subsets (Huang, Nazarova et al. 2018). Furthermore, during *M. tuberculosis* infection there was a robust increase in IM numbers in the lung, and monocyte transfer experiments showed that this increase was primarily monocyte derived although local proliferation of IMs was also found to be a contributing factor (Huang, Nazarova et al. 2018) (Figure 4.1).

During influenza infection MHCII⁺IMs have been shown to robustly increase by proliferating and regulate inflammatory response by producing inflammatory cytokines (Ural, Yeung et al. 2020). Moreover, this study showed MHCII⁺ IMs originate from embryonic precursors and their survival depended on CSF1R signalling with little contribution from monocytes (Ural, Yeung et al. 2020). In contrast, a study by Chakrov et al (Chakarov, Lim et al. 2019), identified the same population but in their case, monocytes did contribute to the MHCII⁺ IMs subset. This difference in studies shows how complex lung tissue is, and whether different stimuli such as inflammatory condition or microbiota contribute to macrophages origin and maintenance is still not known. Therefore, future studies need to investigate the origin of macrophages sub population and how different stimuli affect their development and functions.

In the context of fungal infection, IMs studies have been neglected and few studies have examined their role during *C. neoformans* compared to AMs. Recently, one study showed *C. neoformans* is mostly associated with IMs rather than AMs, and during infection IMs are the major cell type that express arginase-1 which polarize IMs to an M2 phenotype (Dang, Lei et al. 2021) (Figure 4.1), which creates a preferable environment for the fungus to proliferate. Future studies are urgently needed to look at the role of IM during fungal infection especially since these cells

appear to harbour the fungus and promote infection. In this chapter, I will describe my studies examining Lung interstitial macrophages characterisation and their function during chronic infection (intranasal route of infection) model with *C. neoformans* infection. Intranasal route of infection was chosen as it's a more physiological relevant, where yeasts first infect lungs then disseminate to other organs mimicking real life infection route and you can study infection progressing for longer period. However, infection with intranasal route is more variable.

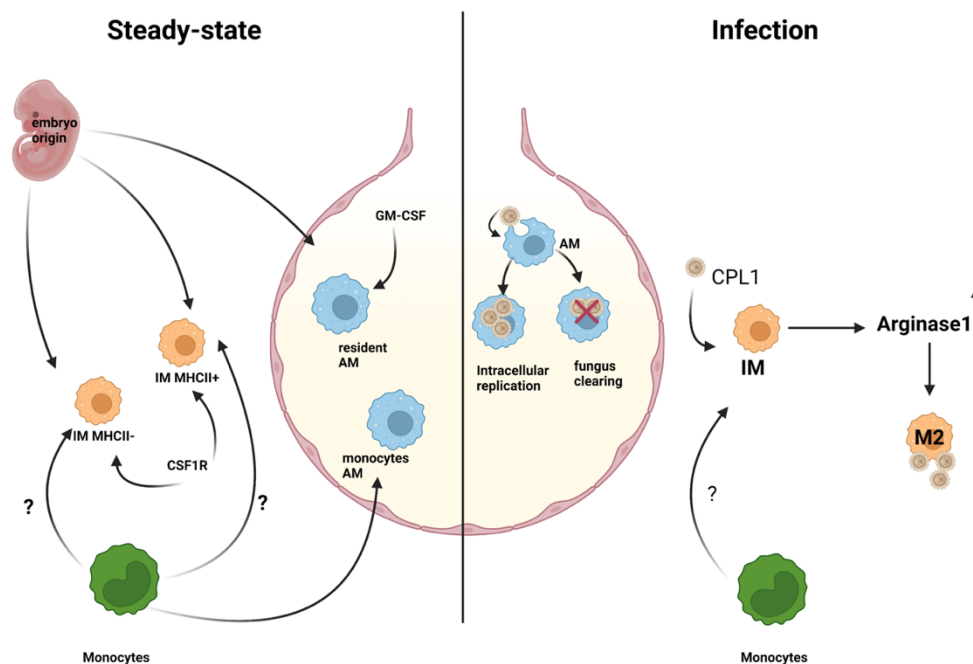


Figure 4. 1 Pulmonary immunology of *C. neoformans* infection. (Left panel) In steady state resident alveolar macrophages originate from embryo circulate the lung and some monocytes alveolar macrophages might be present. Interstitial macrophages have two subset, MHCII+ and MHCII- and their origin from embryo and there is a still debate whether monocytes contribute to their turnover. (Right panel) During *Cryptococcus* infection, alveolar macrophages first encounter the fungus and can either clear the infection or the fungus uses alveolar to replicate. *C. neoformans* produce CPL1 inducing arginase in IMs promoting M2 phenotype.

4.3 Result

4.3.1 PLX5622 depletes tissue resident macrophages in the CNS.

In the previous chapter (Figure 3.8), I have shown that PLX5622 can deplete tissue resident macrophages in the CNS including microglia, MMs and inflammatory macrophages (Cx3cr1⁺ CD45^{hi} MHCII⁺) during acute intravenous infection. Next, I wanted to assess the effect of PLX5622 on control of fungal infection by tissue resident macrophages during intranasal infection, which mimics the natural infection route in humans. For that, C57BL/6 mice were given either PLX5622 or control diet for 7 days, prior to intranasal infection with *C. neoformans* and remained on diet for the duration of infection and data analysed at day 0, 7, 14 and 21 post infection (Figure 4.1a). I found that PLX5622 treated mice had ~90% reduction in microglia number compared to untreated mice and that depletion was sustained during infection for up to 3 weeks (Figure 4.2b). Next, I measured the recruitment of inflammatory myeloid cells including neutrophils, inflammatory monocytes and inflammatory macrophages (Cx3cr1⁺ CD45^{hi} MHCII⁺) in the PLX5622 treated brain and the untreated mice. I found no difference in inflammatory monocytes and neutrophil number in the PLX5622-treated mice (Figure 4.2 c, d). However, there was significant difference in inflammatory macrophages (Cx3cr1⁺ CD45^{hi} MHCII⁺) (Figure 4.2e), similar to my observations made in Chapter 3. Furthermore, no increase in inflammatory myeloid cell recruitment was observed during infection even at 3 weeks post infection. In contrast, I saw a significant reduction in microglia number between uninfected mice and day 7 post-infection in untreated group ($p=0.0152$) and macrophages number between uninfected mice and day 7 ($p=0.0119$) and 14 ($p=0.0247$) (Figure 4.2 b and e), which may reflect the previously published observation of infection-driven death in these cell types.

Taken together this data shows that PLX5622 deplete tissue resident macrophages in the CNS and that depletion is sustained for 3 weeks post infection with *C. neoformans*.

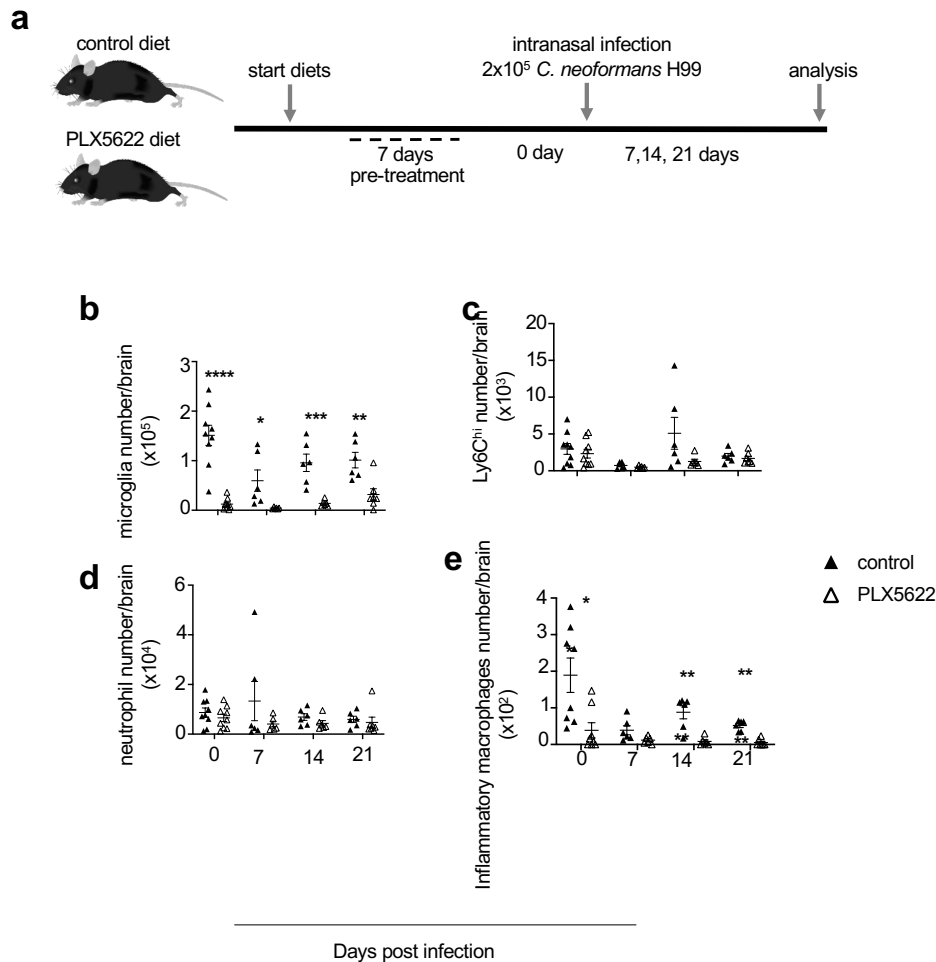


Figure 4. 2 PLX5622 deplete tissue resident macrophages and patrolling monocytes in the CNS. (a) Schematic of PLX5622 treatment. Wild-type C57BL/6 mice were fed either control or PLX5622 diets for 7 days and continued the diet for the duration of the infection. Mice infected with *C. neoformans* H99 intranasally (b) Total number of microglia in untreated and PLX5622-treated brains at day 0, 7, 14 and 21 post infection. (c) Total number of indicated inflammatory cells in the brains of untreated and PLX5622 treated brains at day 0, 7, 14 and 21 post infection. (d) Total number of indicated inflammatory cells in the brains of untreated PLX5622 treated brains at day 0, 7, 14 and 21 post infection. (e) Total number of indicated inflammatory cells in the brains of untreated and PLX5622 treated brains at day 0, 7, 14 and 21 post infection. Data are pooled from 2 independent experiments and analysed by unpaired two-tailed t-test * $P < 0.05$, ** $P < 0.01$, *** $P < 0.001$, **** $P < 0.0001$. Total number of mice at day 0 untreated (n=10), PLX5622 treated (10), untreated (n=6) and PLX5622 treated (n=6) at day 7, 14 and 21 post infection. Untreated group= black solid triangle, PLX5622 treatment open triangle.

4.3.2 PLX5622 depletes meningeal macrophages during intranasal infection.

To assess the effect of PLX5622 on MMs, I followed the same PLX5622 treatment regime as before (Figure 4.2a). I measured the total number of myeloid cells in the meninges. I found the only cells to be affected by PLX5622 treatment in the meninges are the MMs (Figure 4.3a), and no effect on inflammatory monocytes or neutrophil recruitment to the meninges at all days measured (Figure 4.3b, c), similar to my observations in Chapter 3. Additionally, I found MMs the only cells to have total significant increase in number during infection when comparing day 0 to 21 in the meninges, but no increase in other inflammatory cells recruitment (Figure 4.3a). This data confirms that PLX5622 maintains depletion of MMs during chronic fungal infection within the meninges with no difference in other myeloid cells.

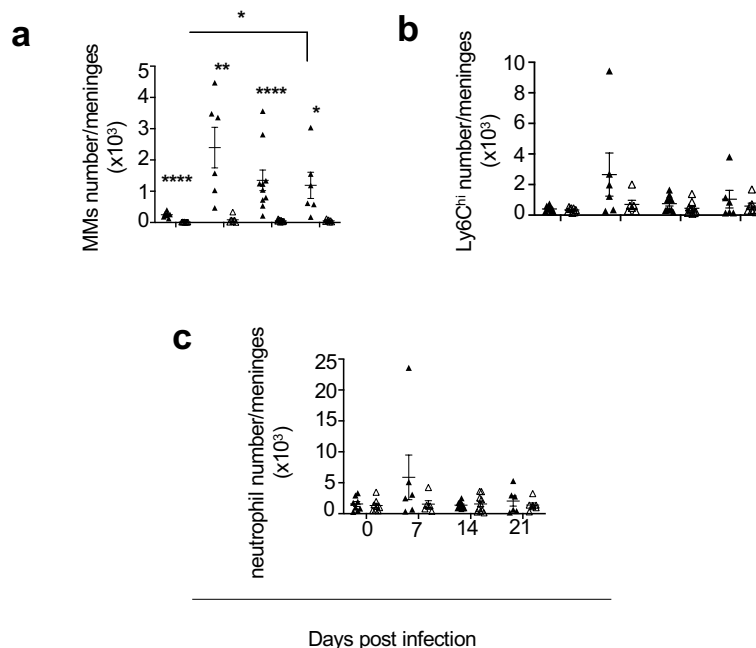


Figure 4. 3 MMs are depleted with PLX5622. (a) Total number of MMs in untreated (Black triangle) and PLX5622-treated (Open triangle) brains at day 0, 7,14 and 21 post infection. (b) Total number of indicated inflammatory cells in the meninges of untreated and PLX5622 treated brains at day 0, 7,14 and 21 post infection. (c) Total number of indicated inflammatory cells in the meninges of untreated PLX5622 treated brains at day 0, 7,14 and 21 post infection. Data are pooled from 2 independent experiments and analysed by unpaired two-tailed t-test *P<0.05, **P<0.01, ***P<0.001, ****P<0.0001. Total number of mice at day 0 untreated (n=10), PLX5622 treated (10), untreated (n=6) and PLX5622 treated (n=6) at day 7,14 and 21 post infection.

4.3.3 Depletion of tissue resident macrophages causes reduction in brain fungal burden.

After confirming that PLX5622 deplete tissue resident macrophages in the CNS, I wanted to assess this effect on brain fungal burden using the intranasal route of infection. In chapter 3 (Figure 3.8) I showed that depleting CNS resident macrophages caused a reduction in fungal infection within the PLX5622 treated brain compared to untreated brain at day 3 post infection. Next, I examined the effect of depleting tissue resident macrophages in the CNS using the intranasal route at day 7, 14 and 21 post infection. Interestingly, I found that depleting tissue resident macrophages had no effect on brain fungal burden at day 7 post infection (Figure 4.4a). However, a significant reduction in fungal burden was observed at day 14 and 21 post infection (Figure 4.4a). This data shows that depleting tissue resident macrophages in the CNS has therapeutic effect during *C. neoformans* infection and this effect is seen at a later time point of infection when infecting mice intranasally.

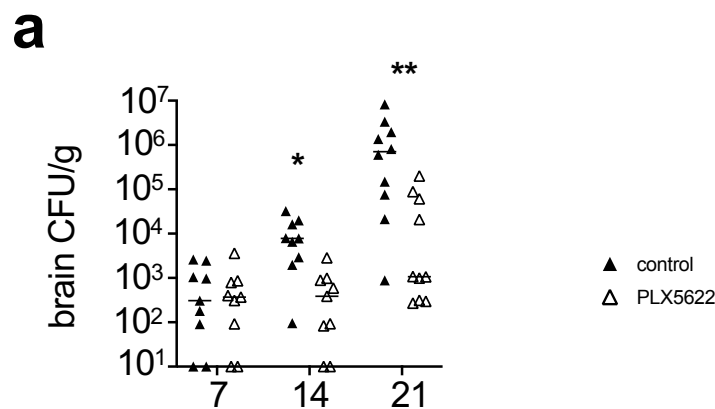


Figure 4. 4 Brain fungal burden is reduced with CSF1R inhibitor treatment at day 14 and 21 post infection. (a) Fungal burden in the brain of mice infected with intranasal infection at day 7, 14 and 21 post infection. Each point represents individual mouse. Data are pooled from 2 independent experiments analysed by unpaired two-tailed t-test *P<0.05, **P<0.01

4.3.4 Interstitial lung macrophages are depleted by PLX5622.

There have been a few recent reports which have suggested that PLX5622 has effects on non CNS macrophages where CSF1R is critical for survival (Lei, Cui et al. 2020), this effect was particularly seen in spleen, bone marrow and lung. I next wanted to assess the effect of PLX5622 treatment on lung macrophages during *C. neoformans* infection, since the lung is the initial site of infection with the intranasal route (Setianingrum, Rautemaa-Richardson et al. 2019). I measured the total number of lung myeloid cells from mice given either control diet or PLX5622 diet for 1 week, using flow cytometry (see chapter 2.21 for gating strategy). I found at steady state, PLX5622 treatment specifically depleted IMs, whereas AMs numbers were unaffected (Figure 4.5a). Next, I measured the total number of inflammatory myeloid cells including inflammatory monocytes and neutrophils and saw no difference between PLX5622 treated lung compared to control (Figure 4.5 b,c). Previous studies have shown that eosinophils contribute to *C. neoformans* pathogenesis, where higher eosinophils in the lung correlated to more susceptibility to *C. neoformans* infection (Huffnagle, Boyd et al. 1998, Holmer, Evans et al. 2014). For that I wanted to assess if PLX5622 influenced eosinophil recruitment to the lung. I saw no difference in the total number of eosinophils in PLX5622 treated lung compared to control at steady state (Figure 4.5d). Next, I measured the total number of myeloid cells at different time post infection and saw no difference in AMs, inflammatory monocytes, neutrophil and eosinophil (Figure 4.5 a,b,c & d respectively). Measuring the total number of IMs I saw PLX5622 significantly reduced IMs numbers compared to control at day 21 post infection (Figure 4.5a). Furthermore, in contrast to the brain I saw a significant increase in inflammatory myeloid cells in the lung at day 21 post infection compared to day 0 and PLX5622

did not affect that (Figure 4.5 b,c,d). Taken together this data shows that PLX5622 deplete lung IMs at steady state and during infection.

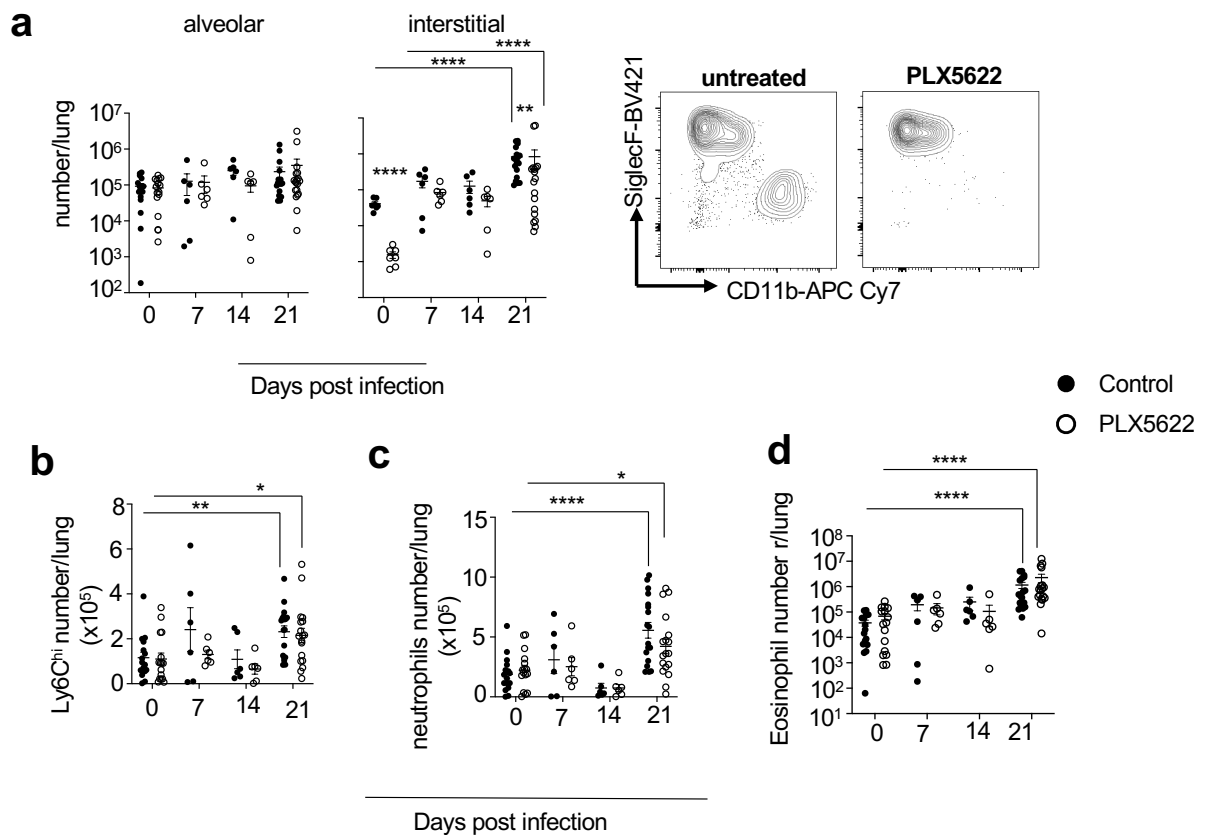


Figure 4. 5 IMs are depleted with PLX5622. (a) Total number of AMs and IMs in untreated and PLX5622-treated lung at different time post infection with example plot showing PLX5622 effect on IMs (b) Total number of Ly6C^{hi} in the lung of untreated and PLX5622 treated lung at different time post infection. Data are pooled from 2-4 independent experiments and analysed by unpaired two-tailed t-test. (c) Total number of neutrophils in untreated and PLX5622 treated lung at different time post infection. (d) Total number of eosinophils in the lung of untreated PLX5622 treated lung at different time post infection. Data are pooled from 2-4 independent experiments and analysed by unpaired two-tailed t-test *P<0.01, **P<0.01, ****P<0.0001. Total number of mice at day 7 untreated (n=6), PLX5622 treated (n=6), total number of mice at day 14 untreated (n=6), PLX5622 treated (n=6) and total number of mice at day 21 untreated (n=18), PLX5622 treated (n=19).

4.3.5 PLX5622 reduces lung fungal burden.

Recently lung IMs has been shown to be a *C. neoformans* reservoir of intracellular infection (Dang, Lei et al. 2021). I therefore wanted to assess how depleting IMs using PLX5622 affected lung fungal burden following intranasal infection, particularly as I had found reduced brain fungal burdens with this treatment in this infection model. I treated mice with PLX5622 for 1 week before intranasal infection with *C.*

neoformans and measured lung fungal burden at day 7, 14 and 21 post infection. Interestingly, I saw depleting IMs reduced fungal burden at day 14 and 21 post infection with no difference seen at day 7 post infection (Figure 4.6a). This data shows that depleting lung IMs has therapeutic effect by reducing fungal burden during *C. neoformans* infection.

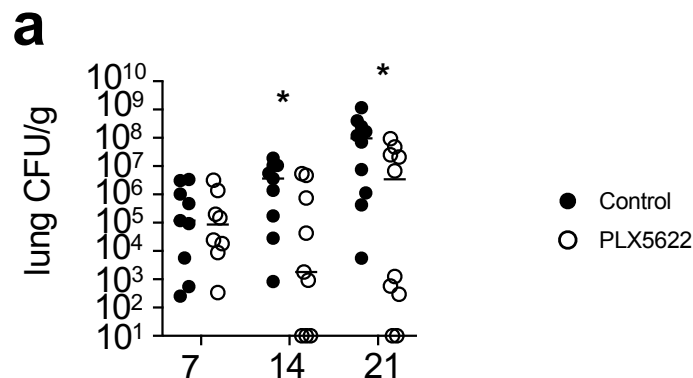


Figure 4. 6 Lung fungal burden is reduced with CSF1R inhibitor treatment at day 14 and 21 post infection. (a) Fungal burden in the lung of mice infected with intranasal infection at day 7, 14 and 21 post infection. Each point represents individual mouse. Data are pooled from 2 independent experiments analysed by unpaired two-tailed t-test *P<0.05.

4.3.6 PLX5622 has localised effect on fungal burden in the lung and CNS.

Next, I wanted to examine the effect of PLX5622 on other organs (See chapter 2.21 for gating). First, I measured the total number of myeloid cells in the spleen and found that PLX5622 depleted spleen macrophages at steady state (Figure 4.7a). I also measured the total number of inflammatory monocytes and neutrophils and saw no changes between untreated spleen and PLX5622 treated spleen (Figure 4.7 b,c). As I had found that spleen macrophages were affected by PLX5622, I also checked myeloid cell numbers in the bone marrow and blood but found no significant alterations in these tissues (Figure 4.8a, b,c and Figure 4.9 a,b respectively). Since lung fungal burden was reduced in PLX5622 treated lung (Figure 4.6a), I wanted to

assess this in other organs such as spleen since I had significant reduction in spleen macrophages. I measured spleen fungal burden at day 21 post infection and saw no difference in fungal burden between untreated spleen and PLX5622 treated spleen (Figure 4.7d). Previous study has shown that liver macrophages have protective role during *C. neoformans* infection (Sun, Zhang et al. 2020). In addition, PLX5622 may affect liver macrophages in some contexts (Lei, Cui et al. 2020). I assessed liver fungal burden at day 21 post infection but found that PLX5622 has no effect on liver fungal burden, although PLX5622 treated liver was trending to have higher fungal burden (Figure 4.7d). Taken together this data shows that PLX5622 reduces fungal burden which is localised to lung and CNS. This can be profound since *C. neoformans* mainly target lung and CNS.

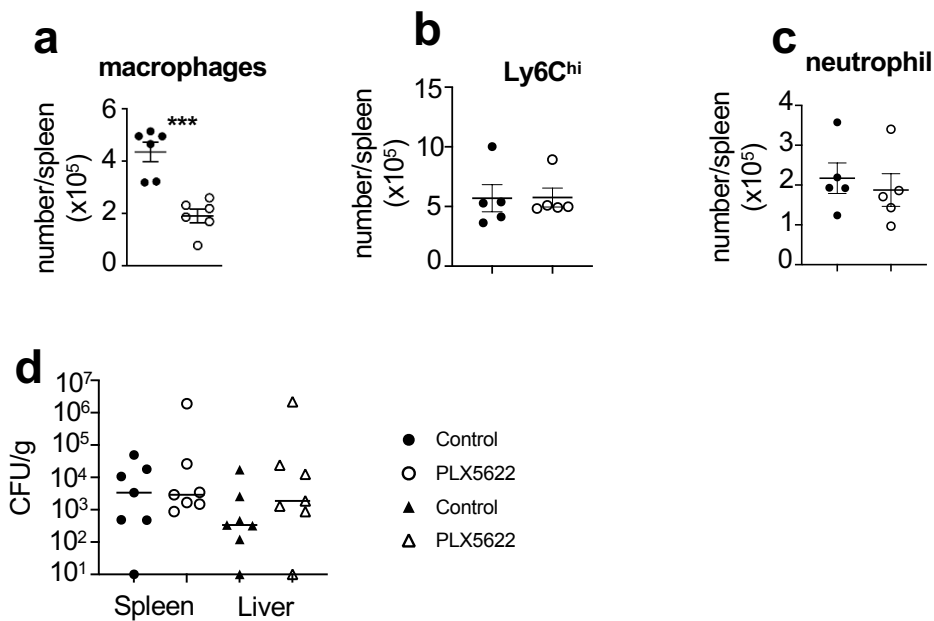


Figure 4. 7 PLX5622 deplete spleen macrophages. (a) The total number of Spleen macrophages at steady state. (n=6 untreated mice) and (n=6 PLX5622 treated mice). Data are pooled from 2 independent experiment and analysed by unpaired two-tailed t-test * **P<0.01 (b) the total number of Ly6C^{hi} at steady state. Data generated from single experiment. (c)The total number of neutrophils at steady state. Data generated from single experiment (n=5 mice per group). (d). fungal burden of spleen and liver at day 21 post infection of mice infected intranasally with h99. Data are pooled from 2 independent experiments (n=7 mice per group).

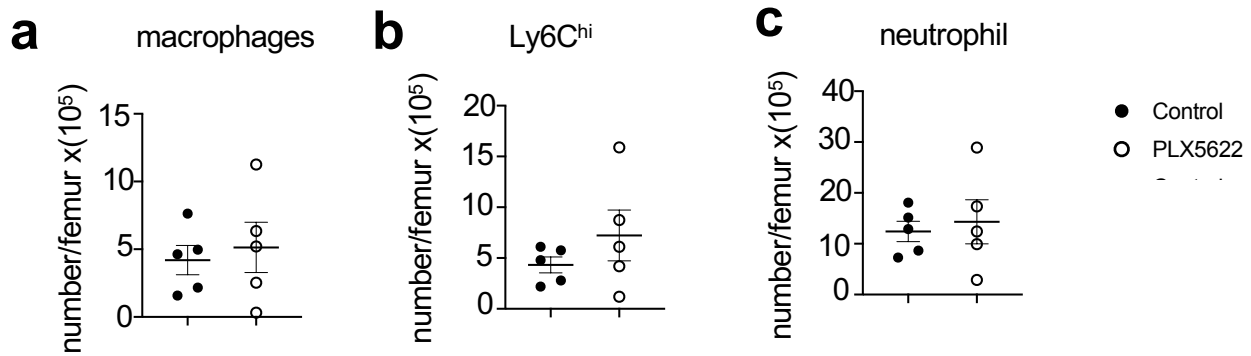


Figure 4. 8 Bone marrow macrophages are not affected by PLX5622 treatment. (a) The total number of bone marrow macrophages at steady state. (b) The total number of bone marrow Ly6C^{hi} monocytes at steady state. (c) The Total number of bone marrow neutrophil at steady state. Data are generated from single experiments (n=5 mice per group).

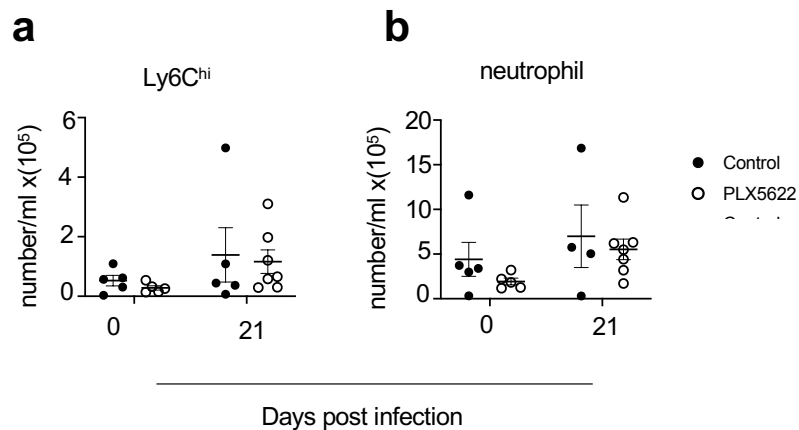


Figure 4. 9 Blood is not affected by PLX5622 treatment. (a)The total number blood monocytes at steady state (n=5 mice per group) and at day 21 post infection in untreated (n=5 mice) and PLX5622 treated (n=7 mice). Data are generated from 1-2 experiments. (b) The Total number of blood neutrophil at steady state (n=5 mice per group) and at day 21 post infection in untreated (n=5 mice) and PLX5622 treated (n=7 mice). Data are generated from 1-2 experiments.

4.3.9 PLX5622 does not have antifungal properties.

Since I saw reduced fungal burden in both brain and lung (Figure 4.4, 4.6), I wanted to rule out a direct effect of PLX5622 on the fungus. To test this, I grew *C. neoformans* in YPD media (untreated culture) and YPD media with added PLX5622 (Treated culture) at various concentrations. The concentration I chose to test was

based on previous study that have measured PLX5622 concentration in brain and serum of PLX5622-treated mice (Elmore, Hohnsfield et al. 2018). I found no difference in *C. neoformans* growth in treated culture at different concentration with PLX5622 compared to untreated culture (Figure 4.10a). Taken together this data shows the reduction in fungal burden in brain and lung is not caused by direct effect of PLX5622 treatment on fungal growth.

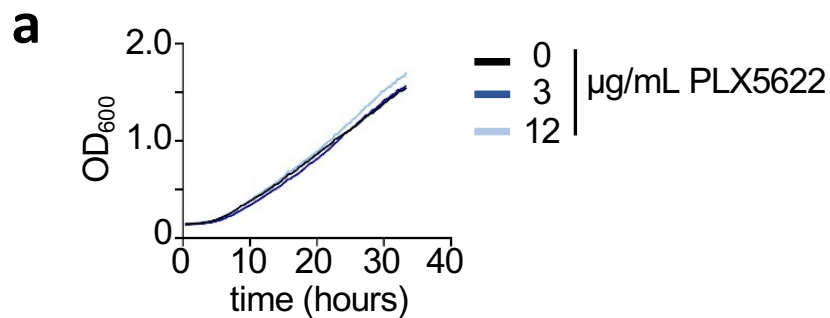


Figure 4. 10 PLX5622 does not affect fungal growth directly. (a) Growth curve of *C. neoformans* grown in YPD media (untreated) or YPD media and added different concentration of PLX5622 (3,12 µg/mL). Data represented of 2 independent experiments.

4.3.10 Extrapulmonary dissemination to the CNS is reduced by PLX5622 treatment.

Previously it has been shown that the rate of lung infection can determine the kinetic of extrapulmonary dissemination to the CNS (Vanherp, Ristani et al. 2019). In chapter 3 I showed that microglia support *C. neoformans* brain infection by acting as a reservoir during acute intravenous infection. The loss of microglia in PLX5622 treated mice (intranasal route) may cause reduction in brain fungal burden by removing this growth niche. However, the fungal burden difference I observe in PLX5622 treated brain (intranasal route) is much larger than PLX5622 treated brain (intravenous route). This larger difference may be caused by additive effects of microglia loss and a reduced extrapulmonary dissemination from lung, especially since the reduction is more pronounced at day 14 and 21 in both organs. To explore

this, I correlated lung and brain fungal burdens in the same mice to determine whether higher lung burdens predicted greater brain infection (and thus increased extrapulmonary dissemination). Indeed, I found mice with higher lung infection had greater brain infection (p 0.008, R^2 0.8 and R 0.9), and PLX5622 treatment did not disrupt this relationship at day 21 post infection (p 0.003, R^2 0.7 and R 0.8)(Figure 4.11a), although I cannot rule out additional independent effect of microglia loss on control of brain infection. To examine this further I depleted macrophages after infection to test whether the reduction of fungal growth I observed in the brain was because of microglia loss or reduced dissemination from lung. I infected mice with *C. neoformans* intranasally, waited for 7 days then started mice on either control diet or PLX5622 treatment before analysis of lung and brain fungal burdens 7 days of starting the diet (14 days post infection) (Figure 4.11b). In this model, I found no difference in the lung fungal burden between untreated and PLX5622 treated group (Figure 4.11c). In contrast, PLX5622 treated brain had significantly higher fungal burden compared to untreated brain when microglia were depleted after infection was established (Figure 4.11c). Furthermore, correlation analysis showed that lung and brain fungal burden are correlated in untreated mice (p 0.008, R^2 0.6 and R 0.8) and PLX5622 treated mice (p 0.016, R^2 0.5 and R 0.7) (Figure 4.11d), as observed in the previous model. This suggest that the reduced brain fungal burden I have in PLX5622 treated mice is due to the reduced lung burden. In conclusion, PLX5622 treatment causes a reduction in extrapulmonary dissemination to the CNS.

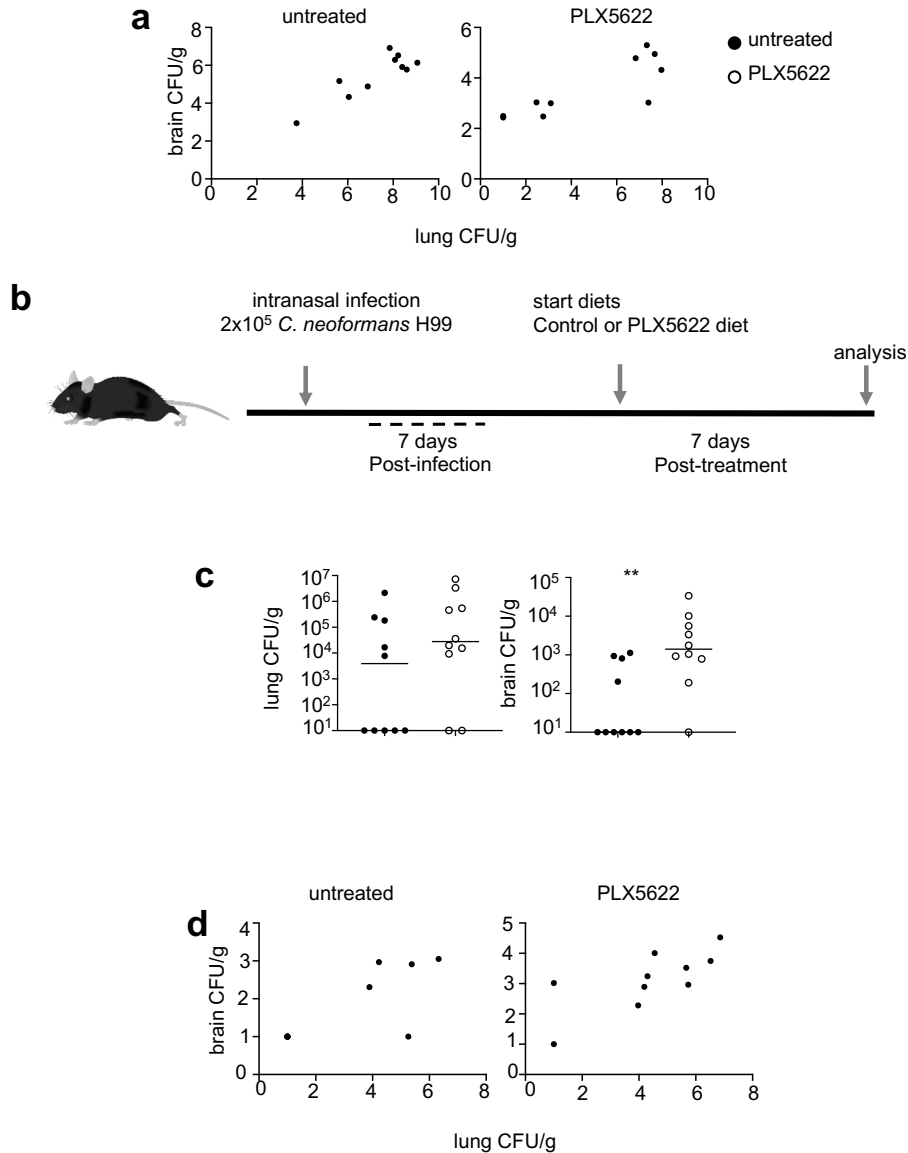


Figure 4. 11 brain fungal burden is correlated to lung burden. (a) Correlation between fungal burdens in the lung and brain of the same mice that were either untreated (n=10) or PLX5622-treated (n=10) at day 21 post infection. Data are pooled from 2 independent experiments. (b) Cartoon model starting PLX5622 or control diet after 7 days post- infection and analysing data at day 14 post-infection with *C. neoformans*. (c) Fungal burden of lung and brain in PLX5622 depleted macrophages after intranasal infection. Data generated at 14 days post infection from 2 independent experiments and analysed by unpaired t test **P<0.001. untreated (n=10) and PLX5622 treated (n=10 mice). (d). Correlation between fungal burdens in the lung and brain of the same mice that were either untreated (n=10) or PLX5622-treated (n=10) at day 14 post infection

4.3.11 PLX5622 deplete MHCII^{hi} interstitial macrophages.

Since PLX5622 specifically depleted IMs in the lung, and this correlated with a reduction in lung infection and dissemination to the CNS, I further characterised

these cells in response to *C. neoformans* infection focusing on day 0 and 21 post infection. Lung IMs comprise a heterogenous population of different functional subsets, as outlined in the introduction of this chapter (Schyns, Bai et al. 2019, Ural, Yeung et al. 2020). Most studies agree on the existence of two subpopulations of interstitial macrophages, subdivided by MHCII expression. I therefore used MHCII to subdivide IMs into two subsets (Figure 4.12a) and assessed their response their dynamics and interaction with *C. neoformans*. First, I looked at the total number of these subsets at steady state and day 21 post infection. I found that MHCII^{hi} IM were found in a higher ratio both at day 0 and day 21 post infection compared to MHCII^{low} IMs (Figure 4.12b). Since I saw that IMs expanded at day 21 post infection, I examined whether one subset was responsible for that. I found both populations expanded during infection (Figure 4.12b). Next, I wanted to examine the effect of PLX5622 treatment on these subsets. I found PLX5622 treatment significantly abolished MHCII^{hi} IMs and had less of an impact on the less numerous MHCII^{low} IM (Figure 4.12b). This data showed *C. neoformans* causes expansion of MHCII^{hi} IMs during infection and these cells are removed by PLX5622 treatment.

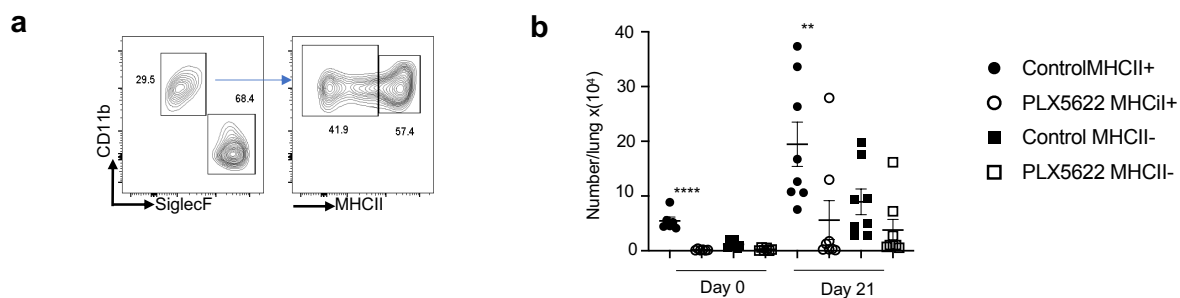


Figure 4. 12 PLX5622 effect lung interstitial macrophages subset. (a) Example flow cytometry of IMs gating strategy used in this study. (b) Total number of IMs subsets in the lung of uninfected and infected mice that were either untreated (n=6) or PLX5622 treated (n=8). Data are pooled from 2 independent experiments and analysed by two-way ANOVA. ****p<0.0001, **p<0.01.

4.3.12 *C. neoformans* localises with interstitial macrophages.

Next, I wanted to assess the relationship between lung IMs and *C. neoformans* following infection. I infected mice intranasally with mCherry-expressing *C. neoformans* to track the fungus localisation to different myeloid cell populations in the lung using flow cytometry (Figure 4.13a). These experiments revealed when fungal burden was higher (>0.05% of total lung events), *C. neoformans* primarily localised in the IMs compared to AMs (Figure 4.13b). In contrast, when fungal burden was lower (<0.05% of total lung events), *C. neoformans* had greater proportion uptake by AMs compared to IMs (Figure 4.13b). This data indicates that IMs might be more susceptible to intracellular infection, promoting a greater level of infection.

Intracellular infection by *C. neoformans* requires expression of arginase by the macrophage to support fungal growth in the phagosome and prevent killing. I therefore tested arginase expression and compared IMs to AMs within the infected lung using intracellular flow cytometry. I found arginase expression was dramatically increased in IMs following infection compared to AMs (Figure 4.14a). My data supports recent work (published as I was developing this data) which showed IMs were primarily susceptible to intracellular fungal infection via arginase induction (Dang, Lei et al. 2021). Lastly, I wanted to assess which subset of IMs are more associated with *C. neoformans* and arginase expression. Following infection, I found that MHCII^{hi} IMs were the predominant subset interacting with *C. neoformans*, regardless of the total frequency of infected cells (Figure 4.14b). Next, I measured the expression of arginase in these subsets and in line with MHCII^{hi} harbouring more fungus and were expressing higher level of arginase (Figure 4.14c). Taken together

this data shows that MHCII^{hi} IMs are susceptible to intracellular infection with *C. neoformans*.

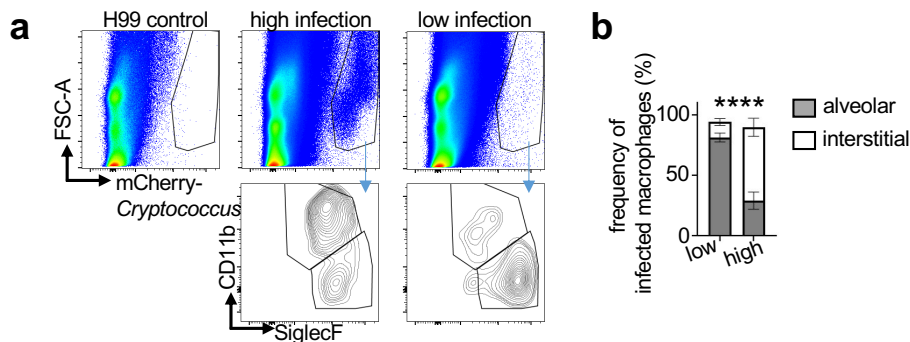


Figure 4.13 *C. neoformans* infect tissue resident macrophages in the lung. (a) Example flow cytometry showing ungated lung sample from mice infected with non-fluorescent *C. neoformans* (h99 gating control), and mice infected with mCherry-*C. neoformans* that were grouped as having 'high infection' or 'low infection'. Yeasts were further gated as CD45+CD64+MerTK+ to isolated infected macrophages which were further split into AMs and IMs populations (bottom row). (b) Frequency of infected AMs and IMs (within total infected macrophages gate, Cd45+Cd64+MerTK+) in mice (n=9) with high (n=3) or low (n=6) infection of the lung. Data are pooled from 2 independent experiments and analysed by two-way ANOVA. ****P<0.001.

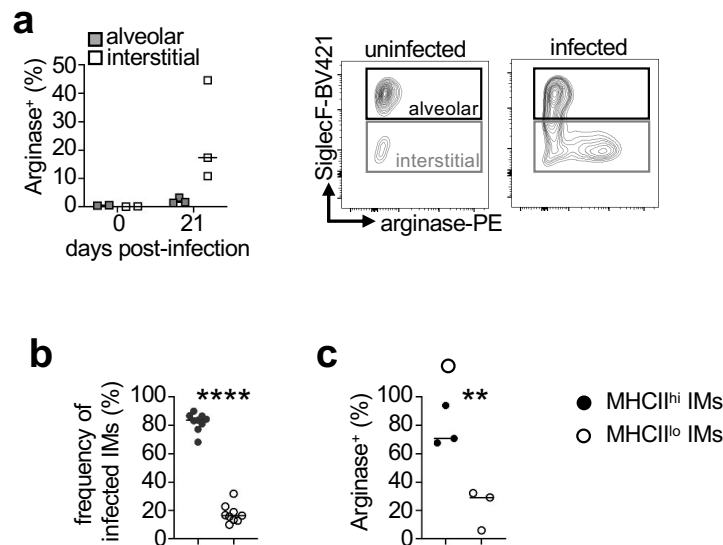


Figure 4.14 MHCII^{hi} IMs are more susceptible to *C. neoformans*. (a) Frequency of arginase expression within AMs and IMs in uninfected (n=2 mice per group) and infected (n=3 mice per group). Example plot are gated on CD64+MerTK+ macrophages. Data are from single experiment. (b) frequency of *C. neoformans* infection within MHCII^{hi} IMs and MHCII^{lo} IMs (within total infected IMs). Data are pooled from 2 independent experiments (n=9 total mice) and analysed by unpaired t-test. ****P<0.001. (c) frequency of arginase expression in MHCII^{hi} IMs and MHCII^{lo} IMs in the *C. neoformans* infected lung. Data are from single experiment (n=3 mice per group).

4.3.14 Interstitial macrophages expansion is not driven local proliferation.

Previous studies have shown that inflammation or infection can cause either loss or expansion of lung macrophages (Sabatel, Radermecker et al. 2017, Bain and MacDonald 2022). As can be seen from my data presented in Figure 4.5, I noticed that my IM population appeared to be expanding with infection. I therefore wanted to explore this further. Type-2 cytokines such as IL-4 can cause macrophages proliferation (Jenkins, Ruckerl et al. 2011) and a key feature of *C. neoformans* lung infection is inducing type -2 response. Furthermore, eosinophils have been shown to contribute to IL-4 production during *C. neoformans* (Piehler, Stenzel et al. 2011). Since I observed significant increase in eosinophil during infection (Figure 4.5d), I wanted to measure the level of IL-4 and IL-13 in the lung during infection. I found increased IL-4 and IL-13 concentration in infected lung (Figure 4.15a,b) although did not reach significant. Next, I examined whether PLX5622 treatment change Type-2 response. I found no difference in IL-4 and IL-13 in homogenised lung (Figure 4.15a, b) or in eosinophils recruitment (Figure 4.5d). Next, I examined macrophage proliferation using Ki67 staining and flow cytometry. This was important to check and examine since *C. neoformans* has been shown to block cell cycle in macrophages (Ben-Abdallah, Sturny-Leclère et al. 2012). In uninfected mice I found little proliferation happening in AMs and eosinophils, with a greater proportion of IMs staining positive for KI-67 (Figure 4.15c). During infection, there was a significant decrease in proliferation level in eosinophils and IMs cells (Figure 4.15c). Next, I measured IMs subset for Ki-67 and found no significant difference between MHCII^{hi} IMs and MHCII^{low} IMs (Figure 4.15d). In conclusion, this data shows that IMs

expansion is not driven by local proliferation, and instead *C. neoformans* causes proliferation rates to decrease in these cells.

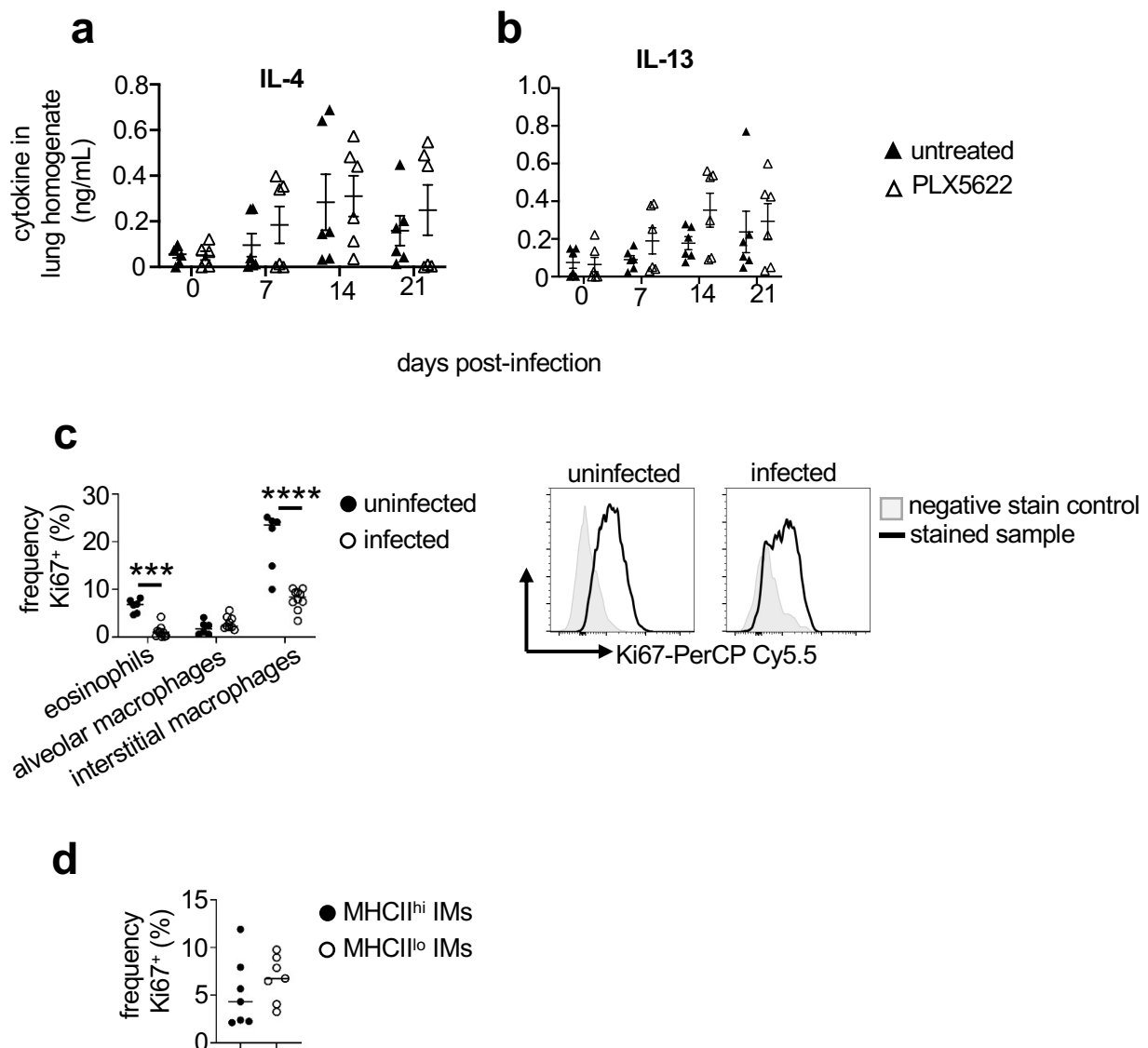


Figure 4.15 *C. neoformans* decrease cell proliferation in interstitial macrophages. (a) The concentration of IL-4 in total lung homogenates at day 0,7,14 and 21 post infection. (b)The concentration of IL-13 in total lung homogenates at day 0,7,14 and 21 post infection untreated (n=6) and PLX5622 treated (n=6). Data are pooled from 2 independent experiment and each point represent an individual mouse. (c)Frequency of Ki67 in eosinophils, AMs and IMs in the lung of uninfected (n=6) and at day 21 post infection (n=9) mice. Example histograms are gated on IMs for infected lung stained with Ki67(black line) or fluorescence minus one control (grey filled histogram). Data are pooled from 2 independent experiments and analysed by two-way ANOVA. ****P<0.001.(d) the frequency of Ki67+ in MHCII^{hi} IMs and MHCII^{lo} IMs. Data are pooled from 2 independent experiment (n=7).

4.3.15 Interstitial macrophages expansion is driven by monocytes.

Previous study has shown that monocytes fuel IMs expansion during *Mycobacterium tuberculosis* infection (Huang, Nazarova et al. 2018). Since IMs expansion I see during fungal infection is not driven by local proliferation, I wanted to examine if monocytes differentiate into IMs causing my observed increase in the IMs population. For that, I used a dual reporter mouse expressing red fluorescent protein in CCR2 and green fluorescent protein CX3CR1, where CX3CR1 and CCR2 are both knockin alleles (Saederup, Cardona et al. 2010). The Cx3cr1-GFP-Ccr2-RFP reporter mice enable me to track expression of tissue resident (CX3CR1) and monocyte (Ccr2) markers in IMs during *C. neoformans* infection. First, I assessed this at base line and found that MHCII^{hi} IMs mostly consist of CX3Cr1+CCr2- (tissue-resident), with a small population of CX3CR1+CCR2+ monocyte-derived cells (Figure 4.16a). In contrast, MHCII^{low} lacked CCR2+ population, indicating that monocytes do not contribute to this population (Figure 4.16a). During infection, I found a population of CX3CR1^{low} CCR2+ emerged in both IMs subsets, possibly representing immature monocyte-derived cells contributing to lung IMs following infection (Figure 4.16a). Next, I examined eosinophils and AMs and could not detect any CX3CR1 or CCR2 expression in these cells (Figure 4.16b). Taken together, this data shows that IMs population dynamically changes in response to fungal infection and monocytes drive IMs expansion which might be driven by the decreased capacity to proliferate caused by *C. neoformans*.

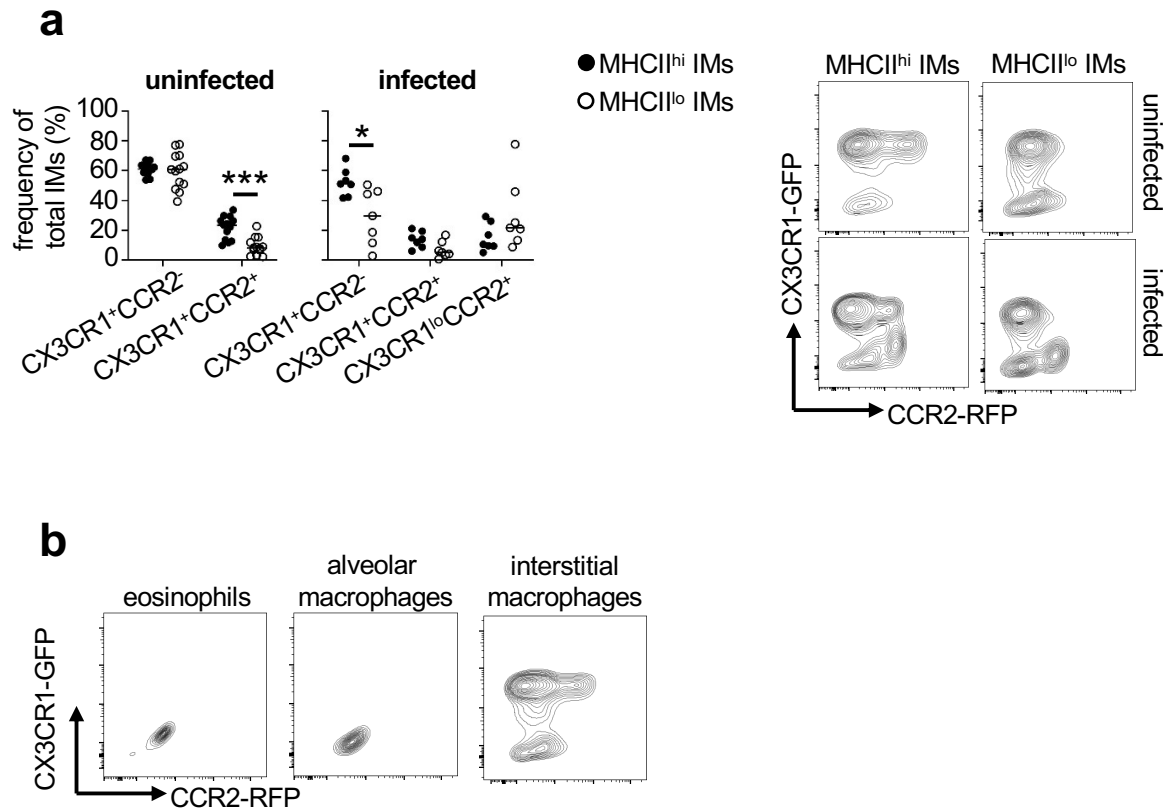


Figure 4. 16 Recruited monocytes give rise to IMs expansion during *C. neoformans* infection. (a) Frequency of IMs positive for Cx3Cr1 and CCR2 expression in uninfected (n=13) and day 21 post infection (n=7). Example plots are gated on the indicated IMs sub-populations. Data are pooled from 2-3 independent experiments and analysed by two-way ANOVA. *P<0.05, ***P<0.005. (b) Example plot showing background expression levels of CX3CR1 and CCR2 in the indicated cell types within the infected lung.

4.3.16 PLX5622 deplete patrolling monocytes (Ly6C^{low}) in organ-specific manner.

Monocytes are a heterogeneous group of circulating myeloid cells. The two major functional classes of these are classical inflammatory monocytes (Ly6C^{hi} in mice) or non-classical patrolling monocytes (Ly6C^{low}) [23]. Some studies have indicated that PLX5622 induces depletion of both or one of these monocyte subsets [10, 13, 14], while others have observed no effect on either subset [15, 16]. In this study I saw no change in Ly6C^{hi} in PLX5622 treated organs compared to control (Figure 4.2c, 4.3b, 4.5b, 4.7b, 4.8b, 4.9a). To determine whether PLX5622 causes loss of Ly6C^{low} at steady state and day 21 post infection, I quantified the number of Ly6C^{low} in the blood, lung, spleen, bone marrow and CNS. I found no difference in Ly6C^{low} number

in untreated group and PLX5622 treated at day 0 or day 21 post-infection in the blood, spleen or bone marrow (Figure 4.17a-c). Next, I examine the total number of Ly6C^{low} in the lung and found no difference between untreated and PLX5622 treated lung at steady state and day 21 post infection (Figure 4.17d). Additionally, I saw a significant increase in Ly6C^{low} at day 21 post infection compared to day 0 in the untreated lung (Figure 4.17d), following similar trend to other myeloid cells recruitment in the lung (Figure 4.5a,b,c,d). Finally, I measured the total number of Ly6C^{low} in both meninges and brain. Interestingly, I saw a significant decrease in Ly6C^{low} in the brain both at day 0 and day 21 post infection in PLX5622 treated brain compared to untreated brain (Figure 4.17e). Infection did not significantly change the number of Ly6C^{low} in these tissues. Taken together, this data suggests that PLX5622 depletes Ly6C^{low} population in an organ dependent manner and in this study, we see PLX5622 deplete Ly6C^{low} in the brain only with no change seen in other tested organs.

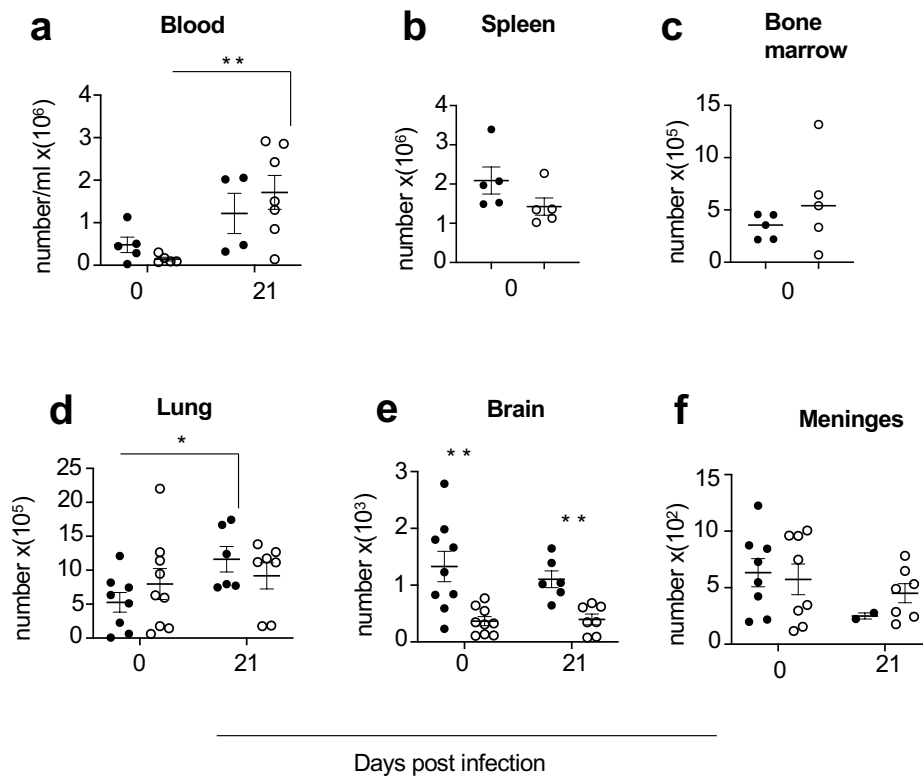


Figure 4. 17 PLX5622 deplete brain patrolling monocytes. (a)The total number of bloods Ly6C^{low} monocytes at day 0 untreated (n=5 mice) and PLX5622 treated (n=5 mice) data generated from single experiment and day 21 post infection untreated (n=4mice) and PLX5622 (n=7 mice). (b) The total number spleen Ly6C^{low} monocytes at day 0 untreated (n=5 mice) and PLX5622 treated (n=5 mice per group). (c) The total number of bone marrow Ly6C^{low} monocytes at day 0 untreated (n=5 mice) and PLX5622 treated (n=8 mice). (d)The total number of lungs Ly6C^{low} monocytes at day 0 untreated (n=8 mice) and PLX5622 treated (n=9 mice) data generated from 2 experiment and day 21 post infection untreated (n=6 mice) and PLX5622 (n=7 mice). Data are generated from 2 independent experiment and analysed by unpaired two-tailed t-test *P<0.05. (e)The total number of brains Ly6C^{low} monocytes at day 0 untreated (n=9 mice) and PLX5622 treated (n=9 mice) data generated from 2 experiment and day 21 post infection untreated (n=6 mice) and PLX5622 (n=7 mice). Data are generated from 2 independent experiment and analysed by unpaired two-tailed t-test **P<0.01. (f)The total number of meninges Ly6C^{low} monocytes at day 0 untreated (n=8 mice) and PLX5622 treated (n=8 mice) data generated from 2 experiment and day 21 post infection untreated (n=2 mice) and PLX5622 (n=7 mice). Data are generated from 2 independent.

4.3.17 Patrolling monocytes (Ly6C^{low}) play a minor role in extrapulmonary dissemination of *C. neoformans*.

Recent study has shown that Ly6C^{low} cells act as a Trojan Horses and drive dissemination of *C. neoformans* into the CNS (Sun, Zhang et al. 2020). These experiments were performed using the intravenous route of infection and therefore the role of these monocytes in extrapulmonary dissemination is not understood. Since I found depletion of Ly6C^{low} cells with the brain using PLX5622 (Figure 4.17e), I wanted to test whether the brain reduction I observed (Figure 4.4a) was due to the reduction in Trojan Horse related dissemination within these cells. To examine this, I first measured the recruitment of Ly6C^{low} to the CNS after intranasal infection. I saw no significant increase in the number of Ly6C^{low} cells in the brain or meninges at day 7, 14 and 21 post intranasal infection (Figure 4.18a). Next, I used transgenic mice that are deficient in circulating Ly6C^{low} cells to determine the role of these cells in anti-cryptococcal immunity following pulmonary infection. Nr4a1 is a transcription factor has role in regulating the differentiation and survival of Ly6C^{low} cells (Hanna, Carlin et al. 2011). To confirm that *Nr4a1*^{-/-} mice have deficiency in Ly6C^{low} cells I measured the frequency of Ly6C^{low} cells and inflammatory monocytes in blood, bone marrow, spleen, lung and brain. I found *Nr4a1*^{-/-} mice had significantly reduced Ly6C^{low} cells frequency compared to WT in all organs (Figure 4.18b). In addition, inflammatory monocytes were not changed in bone marrow, blood and lung (Figure 4.18b). However, I observed some significant increase in inflammatory monocytes in the brain and a significant decrease in inflammatory monocytes in the spleen (Figure 4.18b). Next, I used *Nr4a1*^{-/-} and I infected these mice intranasally with *C. neoformans* and assessed fungal burden at day 21 post infection. I found no significant difference between *Nr4a1*^{-/-} and WT control in lung and brain (Figure

4.18c). In conclusion, this data shows that Ly6C^{low} cells play a redundant role in dissemination and control of *C. neoformans* infection following intranasal infection.

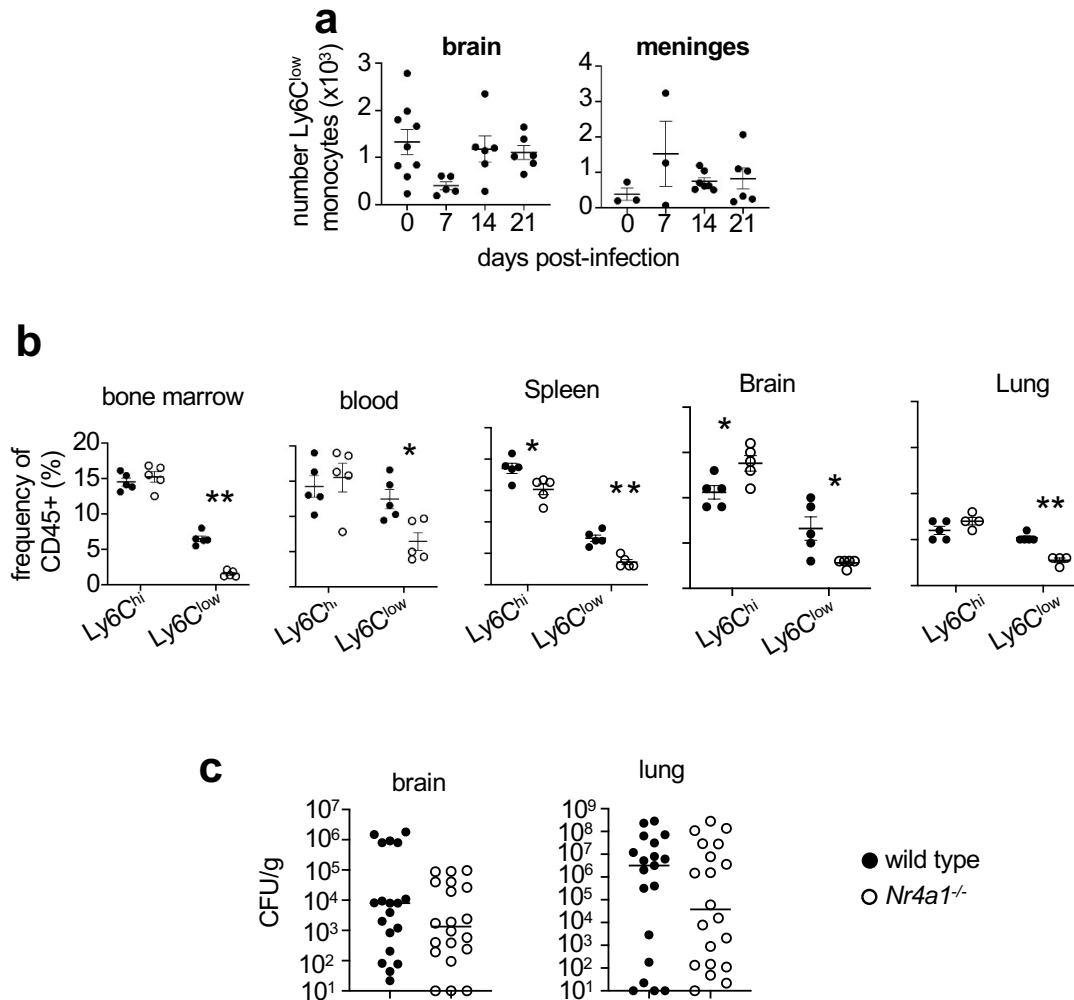


Figure 4. 18 Patrolling monocytes play a redundant role in control and dissemination of pulmonary *C. neoformans* infection. (a) The total number of brain and meninges Ly6C^{low} monocytes of wild-type C57BL/6 mice at indicated time point post infection. Each point represents a single animal. Data are pooled from 1 (meninges) or 2 (brain) independent experiments. (b). frequency of Ly6C^{hi} and Ly6C^{low} monocytes in the bone marrow, peripheral blood, spleen, lung, and brain of uninfected *Nr4a1*^{-/-} (n=5 mice) and wild-type controls (n=5 mice). Data is generated from single experiment and analysed by unpaired t-test *P<0.05, **P<0.01. (c) Fungal burdens in the brain and lung at day 21 post infection in wild-type (n=19 mice) and *Nr4a1*^{-/-} (n=20 mice). Data are pooled from 3 independent experiments.

4.3.18 Patrolling monocyte impairment reduce the frequency of MHCII^{low} IMs.

Recent study has shown that Ly6C^{low} cells give rise to lung interstitial macrophages subset (Schyns, Bai et al. 2019). Indeed, my own data suggested that monocytes were important drivers of IM expansion during pulmonary lung infection. I therefore took advantage of my *Nr4a1*^{-/-} mice and assessed whether loss of Ly6C^{low} cells affected my lung interstitial macrophages subsets. After confirming that *Nr4a1*^{-/-} mice are impaired in Ly6C^{low} cells in the blood and lung (Figure 4.18b), I measured the frequency and total number of IMs at day 0 and day 21. I found no difference in bulk IMs frequency and total number between wild-type and *Nr4a1*^{-/-} mice at both day 0 and day 21 (Figure 4.19a), confirming previous findings (Schyns, Bai et al. 2019). However, at the steady state the frequency of MHCII^{hi} IMs was higher in *Nr4a1*^{-/-} mice compared to wild-type (Figure 4.19b). In contrast I found MHCII^{low} IMs significantly lower in *Nr4a1*^{-/-} mice compared to wild type (Figure 4.19b). Next, I measured the total number of both subsets and found the total number is not changed for either MHCII^{hi} IMs and MHCII^{low} IMs in *Nr4a1*^{-/-} compared to wild-type (Figure 4.19b). Moreover, I measured the frequency and total number of these two populations at day 21 post intranasal infection with *C. neoformans*. Similar to steady state, I found the frequency of MHCII^{hi} IMs to be increased in *Nr4a1*^{-/-} mice compared to wild type and significant decrease in MHCII^{low} IMs (Figure 4.19c). Next, I measured the total number of these two populations but found no difference between these two populations in *Nr4a1*^{-/-} mice compared to wild-type (Figure 4.19c). During *C. neoformans* infection, IMs sub populations expanded at day 21 post infection (Figure 4.5a). Therefore, I wanted to assess whether I could still see this expansion in *Nr4a1*^{-/-} mice. Indeed, I saw MHCII^{hi} IMs significantly increase at day 21 post infection in both wild-type and *Nr4a1*^{-/-} mice (Figure 4.19d). In contrast there was no

difference in MHCII^{low} IMs in wild-type and *Nr4a1*^{-/-} mice between day 0 and day 21 (Figure 4.19d). Taken together this data shows that frequency of MHCII^{low} IMs might be dependent on Ly6C^{low} cells.

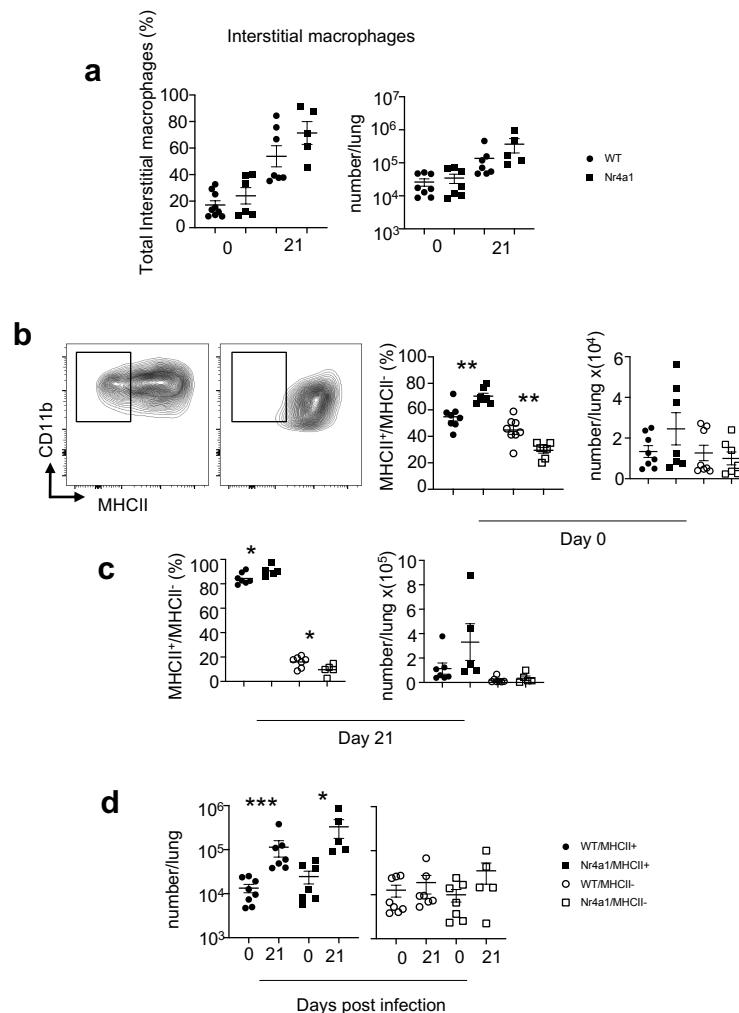


Figure 4. 19 Patrolling monocytes deficiency reduced MHCII^{low} IMs frequency. (a) The frequency and the total number of IMs in wild-type (n= 9 mice) and *Nr4a1*^{-/-} mice (n=6) at steady state and day 21 post intranasal infection with *C. neoformans* wild-type (n= 7 mice) and *Nr4a1*^{-/-} mice (n=5 mice). Data are pooled from 2 independent experiments. (b) Example plot showing IMs subset gating, the frequency and total number of MHCII^{hi} IMs and MHCII^{low} IMs at steady state wild type (n=8) and *Nr4a1*^{-/-} mice (n=7 mice). Data are pooled from 2 independent experiments and analysed by unpaired t test **P<0.01. (c) the frequency and total number of MHCII^{hi} IMs and MHCII^{low} at day 21 post infection wild type (n=7) and *Nr4a1*^{-/-} mice (n=5 mice). Data are pooled from 2 independent experiment and analysed by unpaired t test *P<0.05. (d) the total number of analysed by unpaired t test ***P<0.01. (d). The total number of MHCII^{hi} IMs and MHCII^{low} comparing day 0 to 21 post infection in wild-type and *Nr4a1*^{-/-} mice. Data are pooled from 2 independent experiment and analysed by unpaired t test *P<0.05, **P<0.01.

4.3.19 PLX5622 reduces B cells in the brain.

T cells mediate protective immunity against *Cryptococcus* infection in both humans and mice, since CD4 T cell deficiency is major risk factor for cryptococcal infection (Jo, Kim et al. 2002, Ma, Spurrell et al. 2002, Zheng, Ma et al. 2007, Sharma, Lal et al. 2010, Mukaremera and Nielsen 2017). PLX5622 has been shown in some context to cause dysfunction of circulating lymphocytes (Lei, Cui et al. 2020). Since I only saw reduction in fungal burden at day 14 and 21 and no difference at day 7 between untreated mice and PLX5622 treated mice in both brain and lung (Figure 4.4 and 4.6), it raised the question of whether adaptive immunity have a role in the phenotype observed in PLX5622 treated mice. For that, I hypothesise an expansion of some adaptive immune cell populations in PLX5622 treated mice given a protective effect against *C. neoformans* in this group. I therefore examined the effect of PLX5622 on lymphocytes (CD4 T cells, CD8 T cells, B cells and NK cells) in lung, brain, spleen, bone marrow and blood at steady state and day 21 post intranasal infection with *C. neoformans*. I found no difference in the lung, blood or spleen lymphocytes at both day 0 and day 21 post infection (Figure 4.20a, c, e). In the brain, PLX5622 caused a significant reduction in B cells both at steady state and day 21 post infection, with no changes seen in other lymphocytes (Figure 4.20b). Furthermore, I assessed bone marrow lymphocytes at day 0 and day 21 post infection. Previous study have shown that PLX5622 causes CD4 and CD8 suppression and upregulation of B cells (Lei, Cui et al. 2020). Indeed, I saw B cells to be significantly upregulated in the bone marrow of PLX5622 treated mice compared to untreated group (Figure 4.20d). Although I did not see suppression in CD4 and CD8 at steady state, during infection these two populations significantly reduced in both untreated and PLX5622 treated mice (Figure 4.20d).

In conclusion, this data shows that PLX5622 treatment reduces B cell numbers in the brain yet boosts their numbers in the bone marrow.

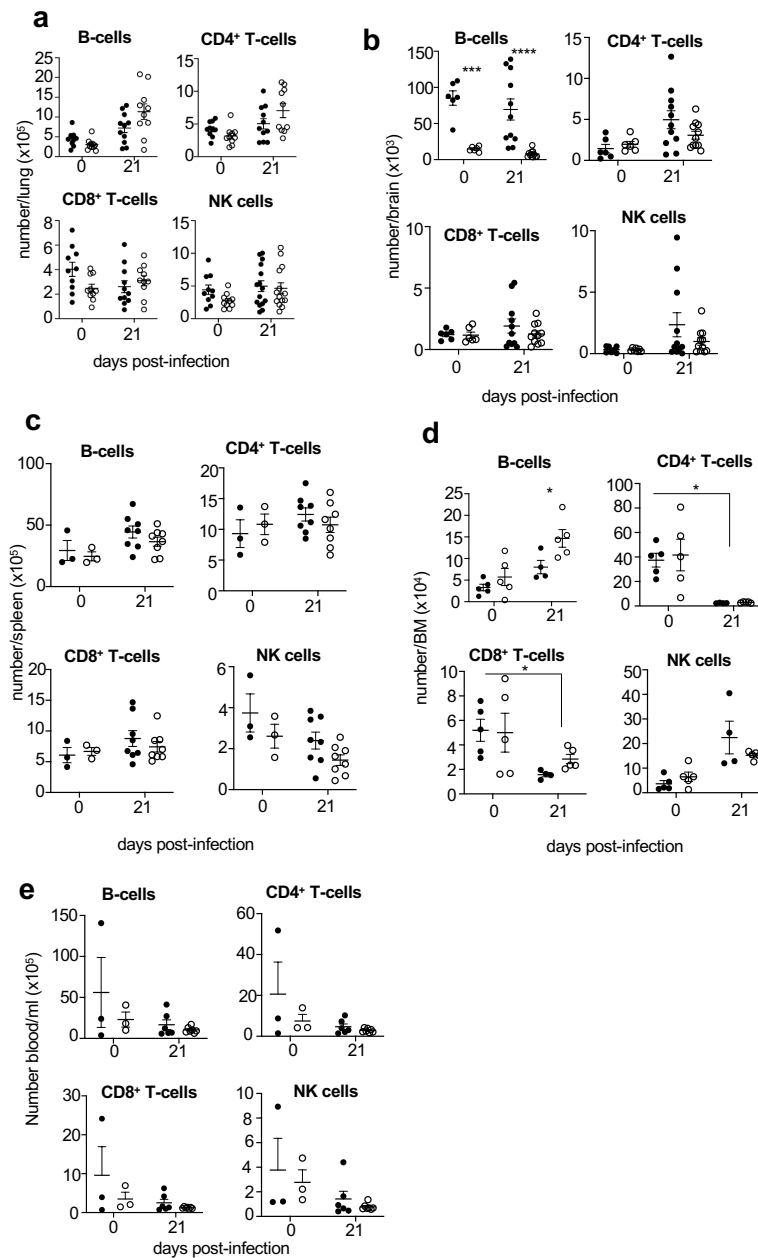


Figure 4. 20 PLX5622 deplete brain B cells. (a) The total number of lung lymphocytes (Cd19, CD4, CD8, NK) at day 0 untreated (n=10 mice) and PLX5622 treated (n=10 mice) and at day 21 post infection untreated (n=11 mice) and PIX5622 treated (n=10). Data are pooled from 2 independent experiments. (b) The total number of brain lymphocytes (Cd19, CD4, CD8, NK) at day 0 untreated (n=6 mice) and PLX5622 treated (n=6 mice) and at day 21 post infection untreated (n=11 mice) and PIX5622 treated (n=11). Data are pooled from 2 independent experiments and analysed by two-way ANOVA ***P<0.001 and ****P< 0.0001. (c) The total number of spleen lymphocytes (Cd19, CD4, CD8, NK) at day 0 untreated (n=3 mice) and PLX5622 treated (n=3 mice) and at day 21 post infection untreated (n=8 mice) and PIX5622 treated (n=8). Data are generated from 1 experiment at day 0 and 2 independent experiments at day 21. (d) The total number of bone marrow lymphocytes (Cd19, CD4, CD8, NK) at day 0 untreated (n=5 mice) and PLX5622 treated (n=5 mice) and at day 21 post infection untreated

(n=4 mice) and PLX5622 treated (n=5). Data are generated from single experiment and analysed by two-way ANOVA *P<0.05. (e) The total number of blood lymphocytes (Cd19, CD4, CD8, NK) at day 0 untreated (n=3 mice) and PLX5622 treated (n=3 mice) and at day 21 post infection untreated (n=6 mice) and PLX5622 treated (n=7). Data are generated from 1 experiment at day 0 and 2 independent experiments at day 21 post infection.

4.3.20 CD4 T cell production of IFN γ is reduced in the PLX5622 treated lung.

Although there was no difference in the number of lymphocytes between untreated and treated mice (Figure 4.20), this doesn't account for a potential functional difference. I therefore measured cytokine production from lymphocytes including IFN γ , IL-4 and IL-13. First, I assessed the frequency of CD4, CD8 and NK cells producing IFN γ in the lung of untreated mice and PLX5622 treated mice at day 21 post infection. I observed a significant decrease in CD4 T cells producing IFN γ in the PLX5622 treated lung compared to untreated (Figure 4.21a). I next measured the total number of T cells producing IFN γ but found no difference in the total number (Figure 4.21a). Next, I measured total IFN γ concentration in homogenised whole lung at day 0 and day 21 post infection. I found no difference in IFN γ at day 0 between untreated and PLX5622 treated (Figure 4.21b). In contrast, at day 21 post infection, IFN γ was reduced in PLX5622 lung (Figure 4.21b), confirming the intracellular staining result (Figure 4.21a). Moreover, I measured the frequency of IL-13 and IL-4 and found IL-13 trending to be lower in PLX5622 compared to control while no obvious trend seen in IL-4. Analysing homogenised lung showed no difference in IL-13 and IL-14 measured by ELISA, between untreated and PLX5622 treated lung (Figure 4.15a, b). Finally, Tregs cells have been shown to expand during pulmonary infection with *C. neoformans*, causing Th2 cytokines suppression mediating better fungal control (Schulze, Piehler et al. 2014). I found no difference in frequency or number of CD4 Tregs cells between untreated mice and PLX5622 treated mice at day 21 post infection (Figure 4.21d). Furthermore, I found no

difference in total IL-10 concentration within whole lung in untreated and PLX5622 treated lung at either day 0 or day 21 post infection (Figure 4.21e). Taken together, this data shows that CD4 T cell producing IFN γ is reduced in PLX5622 treated lung.

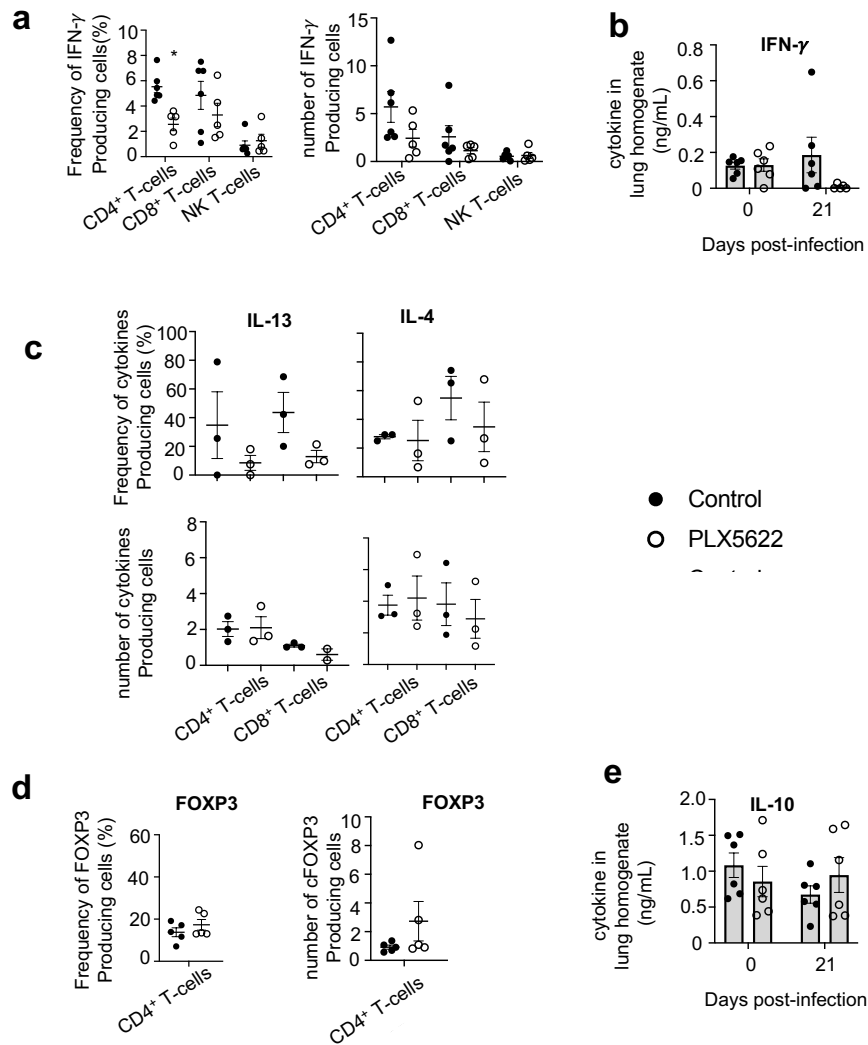


Figure 4. 21 IFN γ is reduced in PLX5622 treated lung. (a) The frequency and total number of CD4, CD8 and NK cells producing IFN- γ at day 21 post infection in untreated (n=6 mice) and PLX5622 treated (n=5). Data are pooled from 2 independent experiment and analysed by two-way ANOVA *P<0.05. (b) The concentration of IFN- γ in total lung homogenates at day 0 and 21 post infection, untreated (n=6) and PLX5622 treated (n=6). Data are pooled from 2 independent experiment and each point represent an individual mouse. (c) Frequency and total number CD4 and CD8 producing IL-13 and IL-4 in untreated (n=3 mice) and PLX5622 treated (n=3 mice) at day 21 post infection. Data are generated from a single experiment. (d) The Frequency and total number CD4 and CD8 producing FOXP3 in untreated (n=5 mice) and PLX5622 treated (n=5 mice) Data are generated from single experiment. (e) The concentration of IL-10 in total lung homogenates at day 0 and 21 post infection, untreated (n=6) and PLX5622 treated (n=6). Data are pooled from 2 independent experiment and each point represent an individual mouse.

4.3.21 Cytokine production is not changed in PLX5622 treated brain.

Next, I wanted to assess the cytokine production and functional capacity of lymphocytes within the brain. For that, I measured different cells producing cytokines such as IFN γ , IL-4 and IL-13. First, I assessed the frequency and number of CD4 and CD8 T cells producing IFN γ in the brain of untreated mice and PLX5622 treated mice at day 21 post infection. I found no significant difference in IFN γ production between untreated and PLX5622 treated brain, nonetheless there was a trend of IFN γ increase by CD4 T cells in PLX5622 treated brain (Figure 4.22a). Next, I measured the frequency and total number of CD4 and CD8 T cells producing IL-4 and I saw no difference between untreated and PLX5622 treated brain (Figure 4.22a). However, there was a trend of decrease in IL-4 in PLX5622 treated brain. Lastly, I measured the measure the frequency and total number of CD4 and CD8 T cells producing IL-13. I saw no obvious difference between the untreated and PLX5622 treated brain, a trend of decreased IL-13 in PLX5622 treated brain was observed (Figure 4.22c). In addition, I measured IFN γ , IL-4 and IL-13 using ELISA in homogenised whole brain, however none of these cytokines were detectable in the brain at the day 21 post infection (data not shown). In conclusion, this data shows that there is little effect of PLX5622 on cytokine production within the brain, although more experiments are needed to assess whether the trends observed are consistent.

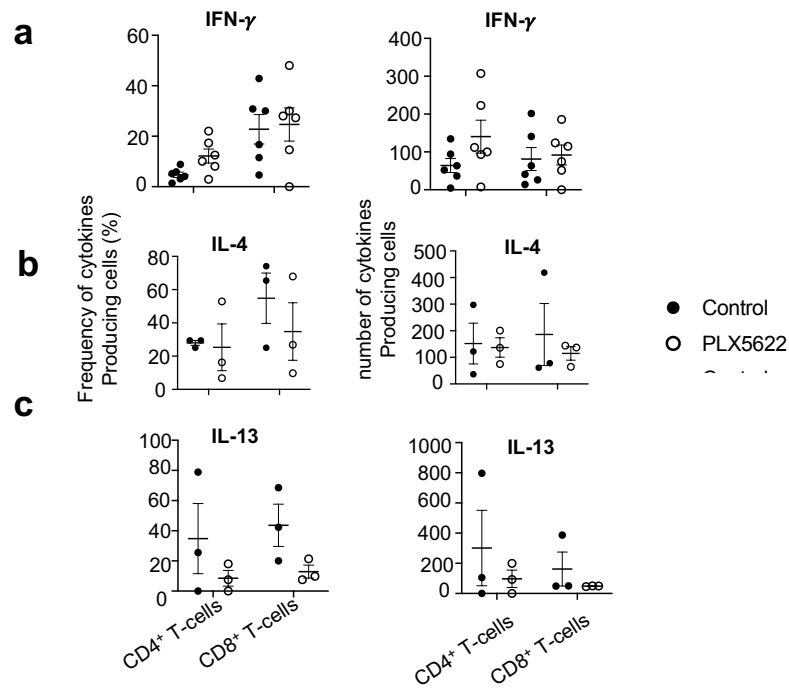


Figure 4.22 PLX5622 does not change brain cytokines production. (a) The frequency and total number of CD4 and CD8 cells producing IFN γ at day 21 post infection in untreated (n=6 mice) and PLX5622 treated (n=6). Data are pooled from 2 independent experiment (b) The frequency and total number of CD4 and CD8 cells producing IL-4 at day 21 post infection in untreated (n=3 mice) and PLX5622 treated (n=3). Data are generated from single experiment. (c) The frequency and total number of CD4 and CD8 cells producing IL-13 at day 21 post infection in untreated (n=3 mice) and PLX5622 treated (n=3). Data are generated from single experiment.

4.3.22 PLX5622 does not affect fungal burden in *Rag1*^{-/-} mice.

Since I observed some defect in functional responses of CD4 T cells in PLX5622 treated mice, I wanted to determine fungal burden after intranasal infection in *Rag1*^{-/-} mice. *Rag1*^{-/-} mice lack mature T cells and B cells and can be used to assess whether adaptive immunity plays a role in the PLX5622 effects. Previous study has shown that *C. neoformans* burden is similar between WT and *Rag1*^{-/-} mice at day 14 post infection in brain and lung (Dufaud, Rivera et al. 2018). For this, day 14 post infection was a good time point to choose as the two strains burden are equivalent and my PLX5622 effects begins to show. I found no difference between untreated group and PLX5622 treated mice at day 14 post infection (Figure 4.23a).

Furthermore, I found no difference in *Rag1*^{-/-} mice between untreated and PLX5622 treated mice at day 21 post infection (Figure 4.23a), suggesting adaptive immunity might be playing a role in the effects seen in PLX5622 treated mice.

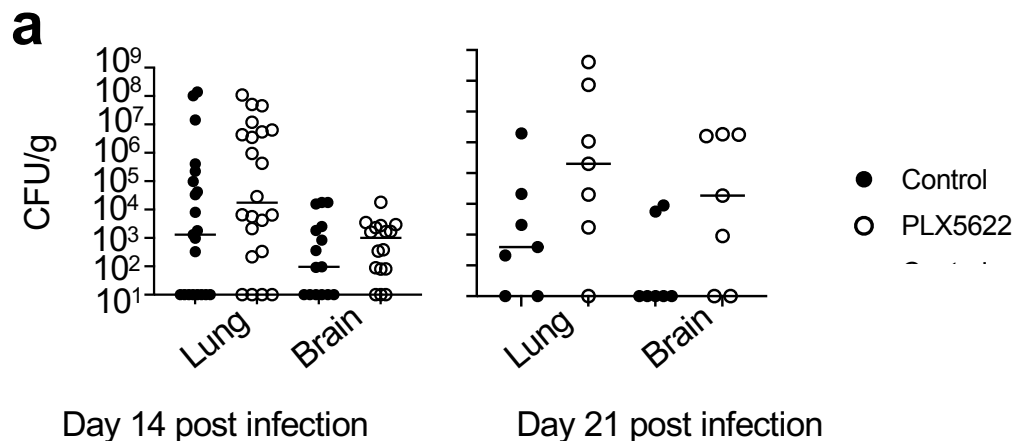


Figure 4. 23 Fungal burden is not changed between untreated and PLX5622 treated mice in *Rag1*^{-/-} lung and brain. (a) Fungal burden in the lung and brain of mice infected with intranasal infection at day 14 or 21 post infection in *Rag1*^{-/-} mice. Each point represents individual mouse. Data are pooled from 4-6 independent experiments.

4.3.23 Interstitial macrophages subset ratio is disrupted in *Rag1*^{-/-} mice.

Since the difference in adaptive immune responses were minor (Figure 4.20), this could not explain the no difference in fungal burdens between untreated and PLX5622 treated *Rag1*^{-/-} mice. Recent study has shown in the absence of CD4 T cells microglia has abnormal behaviour and defect in synaptic pruning (Pasciuto, Burton et al. 2020). For this, I hypothesised that the loss of phenotype in Rag mice is due to myeloid cells. For that, I first examined brain myeloid cells at steady state and day 21 post-infection. I found no clear difference in the total number of microglia, neutrophils or inflammatory monocytes in this tissue (Figure 4.24a). Next, I looked at the total number of lung myeloid cells and I saw no difference between *Rag1*^{-/-} and WT mice at day 0 and day 21 post infection (Figure 4.24b). However, there was a

significant difference in inflammatory monocytes at day 0 which disappeared during infection (Figure 4.24b). Furthermore, I investigated lung interstitial macrophages and found a significant difference in the ratio between MHCII^{hi} IMs and MHCII^{low} IMs. There was a trend showing an increase of MHCII^{low} IMs in *Rag1*^{-/-} compared to WT (Figure 4.24c). Whether there is a functional difference in these macrophages will need further investigating. In conclusion, this data shows that the ratio of MHCII^{hi} IMs and MHCII^{low} IMs in *Rag1*^{-/-} mice is different compared to WT mice and since IMs effects lung fungal burden and dissemination. Thus, this difference in IMs ratio potentially the cause of no difference in fungal burden seen in *Rag1*^{-/-} mice.

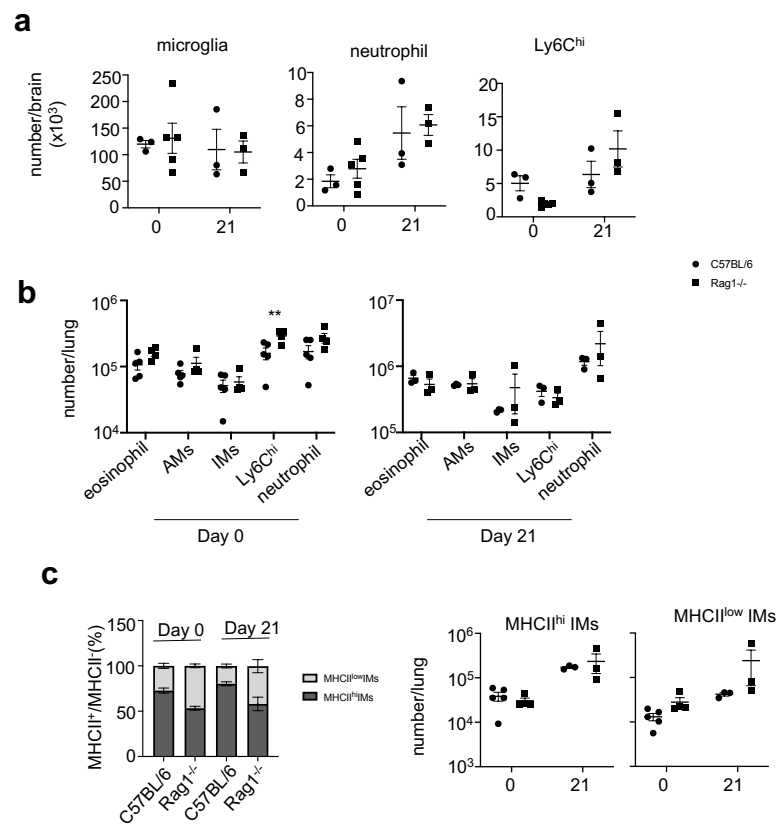


Figure 4. 24 IMs subset ratio changed in *Rag1*^{-/-} mice. (a) The total number of brain myeloid in wild-type at day 0 (n=3 mice), *Rag1*^{-/-} (n=5 mice) and at day 21 post infection wild-type at day 0 (n=3 mice), *Rag1*^{-/-} (n=3 mice). Data generated from single experiment. (b) The total number of lung myeloid in wild-type at day 0 (n=5 mice), *Rag1*^{-/-} (n=5 mice) and 21 post infection wild-type at day 0 (n=3 mice), *Rag1*^{-/-} (n=3 mice). Data generated from single experiment and analysed by two-way ANOVA **P<0.001 (c) Stacked bar showing the proportion of MHCII^{hi} IMs and MHCII^{low} IMs in wild-type and *Rag1*^{-/-} mice at day 0 and day 21 post infection.

4.3.24 PLX5622 causes reduced fungal burden in BALB/c mice.

Previous study has shown that different laboratory mice strains have different susceptibility to *Cryptococcus*, where BALB/c mice have been shown to be more resistant to *C. neoformans* than other mice strains (Zaragoza, Alvarez et al. 2007). Recently, it has been shown that C57BL/c and BALB/c have different macrophages response during nematode infection, where monocytes expansion only occurring in C57BL/c and implementation program of monocytes-to-macrophages conversion failed in BALB/c (Finlay, Parkinson et al. 2023). Therefore, I wanted to test PLX5622 treatment in BALB/c mice to test whether I observe reduced fungal burden with treatment similar to the C57BL/6 strain. I followed the same protocol as before, where BALB/c mice were fed with either control diet or PLX5622 diet for 7 days before infecting them with *C. neoformans* intranasally. Lung and brain tissues were analysed at day 14 post infection. I found PLX5622 caused similar phenotype in BALB/c mice since the PLX5622 treated lung had significantly reduced fungal burden compared to the untreated group (Figure 4,25a). Next, I examined brain fungal burden and I found a similar trend where PLX5622 treated brain had lower fungal burden than untreated brain (Figure 4.25a). Taken together, PLX5622 causes a reduced lung and brain fungal burden independent of mouse strain.

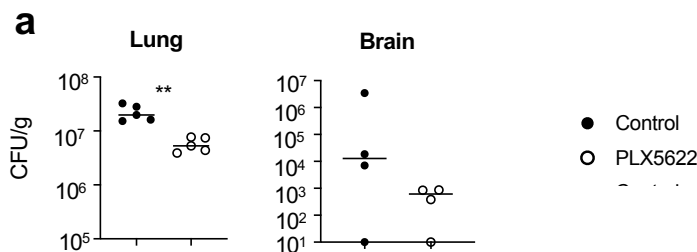


Figure 4. 25 PLX5622 causes reduced fungal burden in BALB/C mice. (a) Fungal burden in the lung and brain of mice infected with intranasal infection at day 14, post infection. Each point represents individual mouse. Data are pooled single experiment and analysed by unpaired t test. **P<0.001 untreated (n=5 mice) and PLX5622 treated (n=5 mice).

4.4 Discussion

In this chapter I examined the effect of PLX5622 treatment on the immune system and control of extrapulmonary dissemination during *C. neoformans* infection. I found that PLX5622 depleted tissue resident macrophages including microglia, MMs, spleen macrophages, and lung IMs. I also found reducing lung IMs caused a reduction in lung fungal burden and extrapulmonary dissemination to the brain. PLX5622 limited fungal infection within MHCII^{hi} IMs which expanded during *C. neoformans* infection, following monocyte replenishment.

PLX5622 is a CSF1R inhibitor which has been used extensively to deplete CNS macrophages (microglia) (Spangenberg, Severson et al. 2019). Mice lacking in CSF1R lack brain macrophages (Pridans, Raper et al. 2018). Furthermore, human mutation in this receptor causes loss of microglia and patients develop brain abnormalities (Oosterhof, Chang et al. 2019). Recent reports have showed that PLX5622 can be unspecific and affect other non-CNS macrophages and lymphocytes (Lei, Cui et al. 2020). Indeed, PLX5622 depleted splenic macrophages, and lung IMs. In chapter 3, I showed that depleting microglia reduced brain fungal burden using an intravenous route of infection. In this chapter, I used PLX5622 treatment during *C. neoformans* infection using the intranasal route. Similar to the intravenous route, I saw depleting brain macrophages caused reduced fungal burden in the brain at day 14 and 21 post infection. The lung is believed to be the initial site of infection following *C. neoformans* exposure in humans (Setianingrum, Rautemaa-Richardson et al. 2019). Previous study showed that mice with a higher fungal burden in the lung developed brain infection more rapidly in an intranasal infection model, suggesting lung fungal burden influences brain dissemination (Vanherp, Ristani et al. 2019). Moreover, a recent study by Walsh et al showed immune cells in

the lungs move *C. neoformans* spores from the lung-draining lymph node where they then can disseminate to the brain (Walsh, Botts et al. 2019). In contrast, others challenge the idea that the initial site with intranasal infection is the lung and suggest no correlation between lung and brain burden. Instead, intranasal route of infection results in a nasal colonisation by *C. neoformans*, and there is some evidence that yeasts enter the brain within 3 hours of infection using this inoculation route (Coelho, Camacho et al. 2019). Interestingly, I found a similar reduction in lung fungal burden in the PLX5622 treated mice, which may have exaggerated the reduced fungal brain burden by reducing the rate of extrapulmonary dissemination. Indeed, I found a strong correlation between lung and brain burden in my infection model, in line with other reports (Vanherp, Ristani et al. 2019). In contrast, I saw no difference in spleen and liver burden between untreated and PLX5622 treated, suggesting the extrapulmonary dissemination to these organs is not affected by infection load in the lung. Furthermore, extrapulmonary dissemination is influenced by *C. neoformans* cell morphology. In the lung, *C. neoformans* forms titan cells that are unable to be phagocytosed (Dambuza, Drake et al. 2018, Zhou and Ballou 2018). Once infection progressed, *C. neoformans* forms small seeding cells that are more able to disseminate to CNS, liver and spleen, and have higher survival rate in the CNS (Denham, Brammer et al. 2022). Whether PLX5622 had any effect on *C. neoformans* morphology will need to be examined, although I found no change in *C. neoformans* growth within different PLX5622 concentrations in vitro.

Circulating monocytes have been shown to further influence *C. neoformans* dissemination. Indeed, infecting mice with *C. neoformans*-infected monocytes resulted in higher dissemination to the brain than mice infected with free yeast

(Charlier, Nielsen et al. 2009). Furthermore, patrolling monocytes have been shown to carry *C. neoformans* to the brain during intravenous infection (Sun, Zhang et al. 2020). I found PLX5622 affected these cells specifically in the brain, similar to other studies that reported PLX5622 mediated depletion of monocytes within the CNS (Feng, Valdearcos et al. 2017, Paschalis, Lei et al. 2018). However, we found PLX5622 does not affect circulating monocytes in the blood, in line with other studies that have shown similar result (Paschalis, Lei et al. 2018, Lei, Cui et al. 2020). This suggests that PLX5622 does not directly affect monocytes, but it could be the result of brain macrophages depletion leading to recruitment defect. Since I saw a reduction in brain patrolling monocytes, I explored their role further using intranasal infection with *C. neoformans* and mice lacking patrolling monocytes, Nr4a1 deficient mice (Hanna, Carlin et al. 2011). I found no difference in fungal burden between mice lacking patrolling monocytes and WT mice indicating that these cells might not have an important role during intranasal infection and their role might be infection route dependent. Inflammatory monocytes have also been shown to be detrimental to host immune response, where they get recruited to lung during *C. neoformans* infection and depleting them caused improved survival by reducing lung burden and dissemination (Heung and Hohl 2019). The specific mechanism by which inflammatory monocytes promote *C. neoformans* infection is not clear and did not depend on adaptive immunity, eosinophils, or arginase expression (Heung and Hohl 2019). One explanation could be that by targeting monocytes, the replenishment and expansion of lung tissue macrophages might be changed in these studies, which may influence fungal burden. Indeed, total macrophages number was reduced in the lung of monocyte depleted mice (Heung and Hohl 2019). I found IMs, particularly the MHCII^{hi} IMs subset, significantly expanded during infection, which was driven by

monocytes, since local proliferation of IMs was reduced during infection. Our understanding of the ontogeny of IM is still evolving, but does appear to be influenced by monocytes that increase during age and inflammation (Bain and MacDonald 2022). Indeed, IMs have been shown to expand during *Mycobacterium tuberculosis* and this expansion is driven by monocytes, and depleting blood monocytes abolished IMs expansion suggesting blood monocytes are responsible for that expansion (Huang, Nazarova et al. 2018). Furthermore, recent study have shown that patrolling monocytes give rise to IMs subset (Schyns, Bai et al. 2019). Indeed, I saw increased number in both lung inflammatory monocytes and patrolling monocytes during *C. neoformans* infection. However, using *Nr4a1*^{-/-} mice did not abolish IMs expansion. Nonetheless, I saw a significant decrease in MHCII^{low} IMs frequency. Future experiments would need to confirm the origin of IMs expansion, potentially by performing a monocyte adoptive transfer experiment or through detailed analysis of *Ccr2*^{-/-} (inflammatory monocytes deficient) mice.

Recent reports have described two subsets of IMs that exist within lung and largely agree on MHCII^{hi} and MHCII^{low} IM (Chakarov, Lim et al. 2019, Schyns, Bai et al. 2019, Ural, Yeung et al. 2020). MHCII^{hi} IMs are associated with nerves (Ural, Yeung et al. 2020), although there some variation on their location (Schyns, Bai et al. 2019) and may act as antigen presenting cells. MHCII^{low} IM co-express Lyve1 and CD206 and they are associated with blood vessels and involved in wound healing and regulation of inflammation (Chakarov, Lim et al. 2019). In my study, I found MHCII^{hi} IMs are susceptible to *C. neoformans* infection which correlated with significant upregulation of arginase. My data independently validates a recent study where they show *C. neoformans* secretes CPL-1 peptide, which induced arginase expression

and M2 polarisation within IMs (Dang, Lei et al. 2021). Future studies should image these two subsets and look at their localisation in the lung and their interaction with the fungus, and whether PLX5622 influences these parameters. Interestingly, using PLX5622 in the intravenous model I saw no difference in lung fungal burden despite IMs depletion. Whether this was solely because of the route of infection used or the timing of infection will need further examination. Furthermore, using intravenous route of infection, the fungus will encounter IMs first while during intranasal infection the fungus will encounter AMs first. Whether the interplay between these two macrophage subsets would affect this will need to be investigated. Additionally, since MHCII^{low} subset localises near to blood vessel this may mean they encounter the fungus first and hence more protective than MHCII^{hi}, but this will need to be further assessed, potentially by depleting one subset and looking fungal burden, however there is no tools to study this yet.

In this study, using high dose of PLX5622 caused a specific depletion of IMs particularly MHCII^{hi} IMs with no difference seen in AMs. Previous study have reported similar finding where PLX5622 caused a depletion in IMs, although characterisation of specific subsets was not examined in this study (Lei, Cui et al. 2020). In contrast, other studies have reported that mice lacking CSF1R do not have significant changes in lung macrophages (Pridans, Raper et al. 2018, Rojo, Raper et al. 2019). This suggests that the depletion I see in IMs is due to the high dose of PLX5622 and combination of direct effect on IMs and indirect effect on replenishment monocytes. Although, I see no evidence of PLX5622 affecting monocytes in the blood and lung. The expression level of CSF1 by IMs and AMs is the same. However, IMs have been shown to uptake CSF1 more compared to AMs,

with greater dependence on the CSF1R for their survival and signaling (Hawley, Rojo et al. 2018). Although the ontogeny of IMs is shown to be self-maintained, studies have reported these cells do require monocytes for their maintenance and turnover (Chakarov, Lim et al. 2019, Schyns, Bai et al. 2019). Whether PLX5622 affects monocyte-differentiation into the IMs pool during infection will need further study. The factors that influence tissue resident macrophages replenishment by monocytes during infection will be an important future area to explore.

Lymphocytes have an important role during *C. neoformans* infection, where they have been shown to be protective. IFN γ producing CD4 T cells are associated with protective Th1 response and mice deficient in IFN γ are more susceptible to *Cryptococcus* infection (Huffnagle, Yates et al. 1991, Campuzano and Wormley 2018). IFN γ is also needed to prevent intracellular replication within macrophages, as shown/discussed in chapter 3. Moreover, B cells have also shown to be protective by producing antibody against *C. neoformans* enabling opsonisation and efficient phagocytosis, since mice lacking B cells or antibody have shown to be more susceptible and have quicker dissemination from lung to brain (Dufaud, Rivera et al. 2018, Rohatgi, Nakouzi et al. 2018). Some studies have shown that PLX5622 may have off target effects on lymphocytes including T cells and B cells (Lei, Cui et al. 2020). This have been argued within the field to whether this effect is widespread or dependent on dose and timing of PLX5622 treatment. For that I extensively characterized lymphocyte numbers in multiple tissues at steady state and during infection. I saw no clear effect of PLX5622 on the lymphoid population in any of the tissues examined. However, I did see reduction in B cell in the brain but whether this a direct effect of PLX5622 or indirect effect of macrophages depletion will need

further investigation. Furthermore, no clear difference in cytokine production was found, although I did see a reduction in IFN γ CD4 T cell production in the lung at day 21 post infection, but this was probably due to the reduced fungal burden in PLX5622 treated lung rather than a direct effect, since I found no difference in homogenised lung at steady state. Lung and brain CFU were comparable in *Rag1*^{-/-} between control and PLX5622 treatment and PLX5622 did not cause a reduction in fungal burden, suggesting potential role of lymphocytes in the reduced fungal burden seen in C57BL/6 mice. However, the ratio of IMs subset was disrupted in *Rag1*^{-/-} lung compared to wild-type mice, where MHCII^{hi} IMs population were lower. This potentially caused the phenotype to disappear as the population affected by PLX5622 is not as prominent. Furthermore, *Rag1*^{-/-} lack T cells and antibody making them inefficient in phagocytosis and killing the fungus, hence keeping the fungal burden high.

In summary, this chapter shows that high dose of PLX5622 treatment has a therapeutic effect for *C. neoformans* infection by removing intracellular growth niche in the lung and brain. Furthermore, I show PLX5622 can be useful strategy to deplete lung IMs, showing their important role in *C. neoformans* pathogenesis and extrapulmonary dissemination.

5

General Discussion and Future Direction

The research presented in this thesis aimed to further understand the role of tissue resident macrophages during *C. neoformans* infection. It was shown that brain resident macrophages (microglia) provide a site for the fungus to acquire restricted nutrients (such as copper) that are limited in the brain (chapter 3). In the lung, IMs (particularly MHCII^{hi} IMs) were found to play an important role in controlling fungal infection in the lung and extrapulmonary dissemination to the brain. Taken together, these results show the important role of tissue resident macrophages in controlling *C. neoformans* infection in an organ specific manner. Additionally, they highlight previously unappreciated roles of tissue resident macrophages in promoting fungal infection and demonstrate how targeting these populations may have therapeutic benefit.

The main CNS resident macrophages are microglia. The role of microglia during *C. neoformans* infection was not yet conclusively described and no in vivo study has definitively examined their function. I addressed this gap in the literature in my research. In my thesis, I have described a new function for this macrophage population in controlling brain infection by *C. neoformans* using microglia-deficient animals. However, the phenotype of these mice was most readily observed at early time points post-infection following intravenous challenge with the fungus. At later time points, the specific role of microglia was not clear. This could be because at

later time points the fungal burden is too high to distinguish a difference and may reflect a limitation of the animal model used. Additionally, adaptive immunity might have a role to play at a later time point which complicates data interpretation. For example, IFN γ production has been shown to influence the fungal burden (Chen, McDonald et al. 2005, Wormley, Perfect et al. 2007), but the protective mechanisms of anti-cryptococcal immunity mediated by IFN γ is not fully resolved. There is a potential interplay between microglia and IFN γ , whereby IFN γ activates microglia to initiate protective responses hence removing microglia might remove the protective immune response when IFN γ is around. Priming microglia with IFN γ have been shown to activate inflammatory responses, induce proliferation and drive upregulation of iNOS in microglia (Ta, Dikmen et al. 2019). In Chapter 3, I showed that microglia stimulation with IFN γ restricted phagosomal copper from *C. neoformans*. Therefore, administration of IFN γ may benefit patients by modulating fungal access to copper and modulation of tissue-resident macrophage responses in the CNS. Indeed, adjunctive IFN γ immunotherapy in HIV patients with CM has been shown to increase the rate of fungal clearance in CSF (Jarvis, Meintjes et al. 2012). Whether the fungal clearance observed in this early clinical trial was due to IFN γ mediated restriction of copper in microglia would need further exploration. Future studies could aim to examine whether manipulating copper levels in patients affect fungal burden and/or antifungal immune responses in the CNS. Serum copper levels are higher in HIV patients compared to control subjects (Moreno, Artacho et al. 1998), but whether this enhances susceptibility to *Cryptococcus* infection is unknown. Brain copper level has been shown to increase with age (Fu, Jiang et al. 2015). In addition, older mice have been shown to have higher brain and liver burden than young mice (Aguirre, Gibson et al. 1998). Interestingly, older mice died quicker

than young mice, and this was not dependent on T cells as T cells response was the same in old and young mice (Aguirre, Gibson et al. 1998). This raises the question of whether copper level has a role to play in this phenotype. Manipulating brain copper level has been done with other diseases such as Alzheimer's by using oral zinc acetate and through restrictive copper diet (Harris, Gray et al. 2020). Therefore, it is interesting to speculate that manipulating copper concentration could be a new strategy for HIV patients at risk of disseminated *Cryptococcus* infection.

In Chapter 4, I found that lung IMs have an important role during *C. neoformans* infection and depleting them reduced lung fungal burden. Previous studies have published controversial results about the correlation between brain and lung fungal burden. I showed that CNS and lung fungal burden were correlated in my models, and by reducing lung fungal burden we could further reduce brain burden. The next question to ask is how the brain gets seeded with fungal cells from the lung. A recent study has shown that *C. neoformans* forms a small morphotype called "seed cells" which have higher rate of extrapulmonary entry to other organs (Denham, Brammer et al. 2022). Nonetheless, the size of the yeast was not the only factor that influenced extrapulmonary dissemination, but a fungal specific factor is also needed which this study could not identify. Identifying seeding cells early might have diagnostic value in identifying individuals with potential cryptococcal dissemination. Further research is needed to focus on how seed cells disseminate to other organs. For example, it is not yet clear whether there is continuous seeding from blood into the brain, or whether fungi may first invade into the lymphatics and draining lymph nodes. Indeed, a study by Walsh et al showed immune cells, particularly AMs, in the lungs move *C. neoformans* spores into the lung-draining lymph node where they

then disseminated to the brain (Walsh, Botts et al. 2019). Therefore, identifying the fungus in lymph node in patients might be used as an early sign of dissemination to the CNS. In addition, we need to examine how spores escape from the lung and whether IMs play a role in this. *Cryptococcus* infection of human cervical lymph node have been reported (Philip, Kaur et al. 2012, Gilles, Arbefeville et al. 2018) , indicating this tissue might be a site of intermediate infection between lung and other organs. One limitation of the work presented in my thesis is that examination of lymph nodes and the morphology of *C. neoformans* was not performed. Whether PLX5622 affected *C. neoformans* morphology (e.g., by inhibiting seed cell formation) or expression of virulence factors was not tested but is an important area for consideration in future studies going forward.

Only a few studies have looked at IMs in the context of fungi. One study showed IMs can be a site for *Cryptococcus* to proliferate in vivo and transferring infected lung IMs led to CNS dissemination (Santangelo, Zoellner et al. 2004). A recent study by the Madhani lab showed that *C. neoformans* particularly polarised IMs into M2 phenotype by inducing arginase expression within IMs (Dang, Lei et al. 2022). In chapter 4, I replicated some of these findings. I showed MHCII^{hi} IMs are more susceptible to *C. neoformans* infection which correlated with a significant upregulation of arginase. As in the Madhani study, arginase was limited to the IM population and not the AM population. Taken together, these studies highlight the important role of IMs during cryptococcal infection and future work should examine the localisation and position of these cells during infection. Future investigation should aim to determine the location of IMs and their interaction with the fungus and how their location and interaction with the fungus changes as infection progress.

This will help us determine IMs subset function and whether they help the fungus escape the lymph node to disseminate to the brain. One limitation in my studies is the lack of microscopy and spatial analysis of IMs subset location and position, and whether PLX5622 disrupts their location and hence their interaction with the fungus. This would be important for future work going forward. In order to further understand how IMs promote infection and their function during *C. neoformans* infection, better tools are required. Therefore, generating transgenic mice whereby IMs could be depleted would be advantageous, particularly depleting one subset and not the other is needed to specifically target the cells that promote infection, and this may hold therapeutic value for future studies. However, one complication is that IMs can be replenished by monocytes from the blood. How these monocyte-derived IMs differ from tissue-resident IMs, particularly during cryptococcal dissemination, is an exciting area for future investigation and will be critical for our understanding of IMs ontogeny and their function during disease.

My work has laid the groundwork for future translational studies, in which the therapeutic potential of the research could be exploited to improve patients' survival. This is important, since fungal infections are on the increase as the size of immunocompromised populations is continuing to expand, resulting in emerging serious fungal infections and complex clinical cases exacerbated by hard-to-treat fungal diseases. For example, during the COVID19 pandemic there was a significant increase in the number of cases of mucormycosis cases in India, caused by pre-existing diseases such as diabetes, increase use of steroid and weakened immune systems. Treatment of mucormycosis is challenging and we saw over 49% mortality in mucormycosis with Covid-19 (Hoenigl, Seidel et al. 2022). There is an unmet

clinical need and it is urgent that we increase our efforts in studying fungal infections and finding new ways to treat and diagnose them. The WHO has initiated the first global effort to prioritise fungal pathogens and the need for more research and development in the area. In 2022, they published the first fungal pathogen priority list, where *C. neoformans* was the top pathogen in the critical priority group. Furthermore, in 2021 a global campaign was launched by Global Action for Fungal Infection (GAFFI) to end CM deaths by 2030. This goal will only be achieved with the help of more research, with a particular focus on understanding why this fungus has tropism toward the CNS and how macrophages help establish infection and promote extrapulmonary dissemination.

References

- Aaron, P. A., M. Jamklang, J. P. Uhrig and A. Gelli (2018). "The blood-brain barrier internalises *Cryptococcus neoformans* via the EphA2-tyrosine kinase receptor." *Cellular microbiology* **20**(3): 10.1111/cmi.12811.
- Abassi, M., D. R. Boulware and J. Rhein (2015). "Cryptococcal Meningitis: Diagnosis and Management Update." *Current Tropical Medicine Reports* **2**(2): 90-99.
- Abassi, M., D. R. Boulware and J. Rhein (2015). "Cryptococcal Meningitis: Diagnosis and Management Update." *Curr Trop Med Rep* **2**(2): 90-99.
- Abedin, M. J., N. Imai, M. E. Rosenberg and S. Gupta (2011). "Identification and Characterization of Sall1-Expressing Cells Present in the Adult Mouse Kidney." *119*(4): e75-e82.
- Adami, C., G. Sorci, E. Blasi, A. L. Agneletti, F. Bistoni and R. Donato (2001). "S100B expression in and effects on microglia." *Glia* **33**(2): 131-142.
- Aegerter, H., J. Kulikauskaite, S. Crotta, H. Patel, G. Kelly, E. M. Hessel, M. Mack, S. Beinke and A. Wack (2020). "Influenza-induced monocyte-derived alveolar macrophages confer prolonged antibacterial protection." *Nat Immunol* **21**(2): 145-157.
- Aguirre, K. and S. Miller (2002). "MHC class II-positive perivascular microglial cells mediate resistance to *Cryptococcus neoformans* brain infection." *Glia* **39**(2): 184-188.
- Aguirre, K. M., G. W. Gibson and L. L. Johnson (1998). "Decreased resistance to primary intravenous *Cryptococcus neoformans* infection in aged mice despite adequate resistance to intravenous rechallenge." *Infect Immun* **66**(9): 4018-4024.
- Almeida, F., J. M. Wolf and A. Casadevall (2015). "Virulence-Associated Enzymes of *Cryptococcus neoformans*." *Eukaryotic cell* **14**(12): 1173-1185.
- Alspaugh, J. A. (2015). "Virulence mechanisms and *Cryptococcus neoformans* pathogenesis." *Fungal Genetics and Biology* **78**: 55-58.
- Alspaugh, J. A. and D. L. Granger (1991). "Inhibition of *Cryptococcus neoformans* replication by nitrogen oxides supports the role of these molecules as effectors of macrophage-mediated cytostasis." *Infection and immunity* **59**(7): 2291-2296.
- Antonelli, L. R., Y. Mahnke, J. N. Hodge, B. O. Porter, D. L. Barber, R. DerSimonian, J. H. Greenwald, G. Roby, J. Mican, A. Sher, M. Roederer and I. Sereti (2010). "Elevated frequencies of highly activated CD4+ T cells in HIV+ patients developing immune reconstitution inflammatory syndrome." *Blood* **116**(19): 3818-3827.
- Arora, S., Y. Hernandez, J. R. Erb-Downward, R. A. McDonald, G. B. Toews and G. B. Huffnagle (2005). "Role of IFN- γ in Regulating T2 Immunity and the Development of Alternatively Activated Macrophages during Allergic Bronchopulmonary Mycosis." *The Journal of Immunology* **174**(10): 6346.
- Arora, S., M. A. Olszewski, T. M. Tsang, R. A. McDonald, G. B. Toews and G. B. Huffnagle (2011). "Effect of Cytokine Interplay on Macrophage Polarization during Chronic Pulmonary Infection with *Cryptococcus neoformans*." *Infection and Immunity* **79**(5): 1915-1926.
- Bain, C. C. and A. S. MacDonald (2022). "The impact of the lung environment on macrophage development, activation and function: diversity in the face of adversity." *Mucosal Immunol* **15**(2): 223-234.
- Barluzzi, R., S. Saleppico, A. Nocentini, J. R. Boelaert, R. Neglia, F. Bistoni and E. Blasi (2002). "Iron overload exacerbates experimental meningoencephalitis by *Cryptococcus neoformans*." *J Neuroimmunol* **132**(1-2): 140-146.
- Batista, S. J., K. M. Still, D. Johanson, J. A. Thompson, C. A. O'Brien, J. R. Lukens and T. H. Harris (2020). "Gasdermin-D-dependent IL-1 α release from microglia promotes protective immunity during chronic *Toxoplasma gondii* infection." *Nature Communications* **11**(1): 3687.
- Beardsley, J., M. Wolbers, F. M. Kibengo, A.-B. M. Ggayi, A. Kamali, N. T. K. Cuc, T. Q. Binh, N. V. V. Chau, J. Farrar, L. Merson, L. Phuong, G. Thwaites, N. Van Kinh, P. T. Thuy, W. Chierakul, S. Siriboon, E. Thiansukhon, S. Onsanit, W. Supphamongkolchaikul, A. K. Chan, R. Heyderman, E. Mwinjiwa, J. J. Van Oosterhout, D. Imran, H. Basri, M. Mayxay, D. Dance, P. Phimmasone, S. Rattanavong, D. G. Lalloo and J. N. Day (2016). "Adjunctive Dexamethasone in HIV-Associated Cryptococcal Meningitis." *New England Journal of Medicine* **374**(6): 542-554.
- Bedolla, A., A. Taranov, F. Luo, J. Wang, F. Turcato, E. M. Fugate, N. H. Greig, D. M. Lindquist, S. A. Crone, J. Goto and Y. Luo (2022). "Diphtheria toxin induced but not CSF1R inhibitor mediated microglia ablation model leads to the loss of CSF/ventricular spaces in vivo that is independent of cytokine upregulation." *Journal of Neuroinflammation* **19**(1).

Ben-Abdallah, M., A. Sturny-Leclère, P. Avé, A. Louise, F. Moyrand, F. Weih, G. Janbon and S. Mémet (2012). "Fungal-induced cell cycle impairment, chromosome instability and apoptosis via differential activation of NF- κ B." *PLoS Pathog* **8**(3): e1002555.

Binnicker, M. J., D. J. Jespersen, J. E. Bestrom and L. O. Rollins (2012). "Comparison of Four Assays for the Detection of Cryptococcal Antigen." *Clinical and Vaccine Immunology* **19**(12): 1988-1990.

Blasi, E. (1995). "Role of nitric oxide and melanogenesis in the accomplishment of anticryptococcal activity by the BV-2 microglial cell line." *Journal of Neuroimmunology* **58**(1): 111-116.

Bloom, A. L. M., R. M. Jin, J. Leipheimer, J. E. Bard, D. Yergeau, E. A. Wohlfert and J. C. Panepinto (2019). "Thermotolerance in the pathogen *Cryptococcus neoformans* is linked to antigen masking via mRNA decay-dependent reprogramming." *Nat Commun* **10**(1): 4950.

Bohlen, C. J., F. C. Bennett, A. F. Tucker, H. Y. Collins, S. B. Mulinyawe and B. A. Barres (2017). "Diverse Requirements for Microglial Survival, Specification, and Function Revealed by Defined-Medium Cultures." *Neuron* **94**(4): 759-773.e758.

Bongomin, F., S. Gago, R. O. Oladele and D. W. Denning (2017). "Global and Multi-National Prevalence of Fungal Diseases-Estimate Precision." *Journal of fungi (Basel, Switzerland)* **3**(4): 57.

Borges, M. A. S. B., J. A. D. Araújo Filho, R. D. B. A. Soares, J. E. Vidal and M. D. Turchi (2019). "False-negative result of serum cryptococcal antigen lateral flow assay in an HIV-infected patient with culture-proven cryptococcaemia." *Medical Mycology Case Reports* **26**: 64-66.

Boulware, D. R., D. B. Meya, C. Muzoora, M. A. Rolfes, K. Huppler Hullsiek, A. Musubire, K. Taseera, H. W. Nabeta, C. Schutz, D. A. Williams, R. Rajasingham, J. Rhein, F. Thienemann, M. W. Lo, K. Nielsen, T. L. Bergemann, A. Kambugu, Y. C. Manabe, E. N. Janoff, P. R. Bohjanen, G. Meintjes and C. T. Team (2014). "Timing of antiretroviral therapy after diagnosis of cryptococcal meningitis." *The New England journal of medicine* **370**(26): 2487-2498.

Boulware, D. R., M. A. Rolfes, R. Rajasingham, M. Von Hohenberg, Z. Qin, K. Taseera, C. Schutz, R. Kwizera, E. K. Butler, G. Meintjes, C. Muzoora, J. C. Bischof and D. B. Meya (2014). "Multisite Validation of Cryptococcal Antigen Lateral Flow Assay and Quantification by Laser Thermal Contrast." *20*(1): 45-53.

Brown, G. D., D. W. Denning, N. A. R. Gow, S. M. Levitz, M. G. Netea and T. C. White (2012). "Hidden Killers: Human Fungal Infections." *Science Translational Medicine* **4**(165): 165rv113-165rv113.

Brynskikh, A., T. Warren, J. Zhu and J. Kipnis (2008). "Adaptive immunity affects learning behavior in mice." *Brain Behav Immun* **22**(6): 861-869.

Buch, T., F. L. Heppner, C. Tertilt, T. J. Heinen, M. Kremer, F. T. Wunderlich, S. Jung and A. Waisman (2005). "A Cre-inducible diphtheria toxin receptor mediates cell lineage ablation after toxin administration." *Nat Methods* **2**(6): 419-426.

Buttgereit, A., I. Lelios, X. Yu, M. Vrohings, N. R. Krakoski, E. L. Gautier, R. Nishinakamura, B. Becher and M. Greter (2016). "Sall1 is a transcriptional regulator defining microglia identity and function." *Nat Immunol* **17**(12): 1397-1406.

Buttgereit, A., I. Lelios, X. Yu, M. Vrohings, N. R. Krakoski, E. L. Gautier, R. Nishinakamura, B. Becher and M. Greter (2016). "Sall1 is a transcriptional regulator defining microglia identity and function." *Nat Immunol* **17**: 1397.

C. Lee, S., Y. Kress, D. W. Dickson and A. Casadevall (1995). "Human microglia mediate anti-*Cryptococcus neoformans* activity in the presence of specific antibody." *Journal of Neuroimmunology* **62**(1): 43-52.

Campuzano, A., N. Castro-Lopez, A. J. Martinez, M. A. Olszewski, A. Ganguly, C. Leopold Wager, C.-Y. Hung and F. L. Wormley, Jr. (2020). "CARD9 Is Required for Classical Macrophage Activation and the Induction of Protective Immunity against Pulmonary Cryptococcosis." *mBio* **11**(1): e03005-03019.

Campuzano, A., N. Castro-Lopez, A. J. Martinez, M. A. Olszewski, A. Ganguly, C. Leopold Wager, C. Y. Hung and F. L. Wormley, Jr. (2020). "CARD9 Is Required for Classical Macrophage Activation and the Induction of Protective Immunity against Pulmonary Cryptococcosis." *mBio* **11**(1).

Campuzano, A. and F. Wormley (2018). "Innate Immunity against *Cryptococcus*, from Recognition to Elimination." *Journal of Fungi* **4**(1): 33.

Campuzano, A. and F. L. Wormley (2018). "Innate Immunity against *Cryptococcus*, from Recognition to Elimination." *J Fungi (Basel)* **4**(1).

Chakarov, S., H. Y. Lim, L. Tan, S. Y. Lim, P. See, J. Lum, X. M. Zhang, S. Foo, S. Nakamizo, K. Duan, W. T. Kong, R. Gentek, A. Balachander, D. Carbajo, C. Bleriot, B. Malleret, J. K. C. Tam, S. Baig, M. Shabeer, S. E. S. Toh, A. Schlitzer, A. Larbi, T. Marichal, B. Malissen, J. Chen, M. Poidinger, K. Kabashima, M. Bajenoff, L. G. Ng, V. Angeli and F. Ginhoux (2019). "Two distinct interstitial macrophage populations coexist across tissues in specific subtissular niches." *Science* **363**(6432).

Chamilos, G., M. S. Lionakis and D. P. Kontoyiannis (2018). "Call for Action: Invasive Fungal Infections Associated With Ibrutinib and Other Small Molecule Kinase Inhibitors Targeting Immune Signaling Pathways." *Clin Infect Dis* **66**(1): 140-148.

Chang, Y. C., M. F. Stins, M. J. McCaffery, G. F. Miller, D. R. Pare, T. Dam, M. Paul-Satyaseela, K. S. Kim and K. J. Kwon-Chung (2004). "Cryptococcal yeast cells invade the central nervous system via transcellular penetration of the blood-brain barrier." *Infection and immunity* **72**(9): 4985-4995.

Charlier, C., K. Nielsen, S. Daou, M. Brigitte, F. Chretien and F. Dromer (2009). "Evidence of a role for monocytes in dissemination and brain invasion by *Cryptococcus neoformans*." *Infect Immun* **77**(1): 120-127.

Charlier, C., K. Nielsen, S. Daou, M. Brigitte, F. Chretien and F. Dromer (2009). "Evidence of a Role for Monocytes in Dissemination and Brain Invasion by *Cryptococcus neoformans*." **77**(1): 120-127.

Chen, G.-H., R. A. McDonald, J. C. Wells, G. B. Huffnagle, N. W. Lukacs and G. B. Toews (2005). "The Gamma Interferon Receptor Is Required for the Protective Pulmonary Inflammatory Response to *Cryptococcus neoformans*." *Infection and Immunity* **73**(3): 1788.

Chen, G. H., R. A. McDonald, J. C. Wells, G. B. Huffnagle, N. W. Lukacs and G. B. Toews (2005). "The gamma interferon receptor is required for the protective pulmonary inflammatory response to *Cryptococcus neoformans*." *Infect Immun* **73**(3): 1788-1796.

Chen, J., K. Sathiyamoorthy, X. Zhang, S. Schaller, B. E. Perez White, T. S. Jardetzky and R. Longnecker (2018). "Ephrin receptor A2 is a functional entry receptor for Epstein-Barr virus." *Nature microbiology* **3**(2): 172-180.

Chretien, F., O. Lortholary, I. Kansau, S. Neuville, F. Gray and F. Dromer (2002). "Pathogenesis of cerebral *Cryptococcus neoformans* infection after fungemia." *J Infect Dis* **186**(4): 522-530.

Chun, C. D., O. W. Liu and H. D. Madhani (2007). "A Link between Virulence and Homeostatic Responses to Hypoxia during Infection by the Human Fungal Pathogen *Cryptococcus neoformans*." *PLoS Pathogens* **3**(2): e22.

Chun, C. D. and H. D. Madhani (2010). "Ctr2 links copper homeostasis to polysaccharide capsule formation and phagocytosis inhibition in the human fungal pathogen *Cryptococcus neoformans*." *PLoS One* **5**(9).

Clark, C. and R. A. Drummond (2019). "The Hidden Cost of Modern Medical Interventions: How Medical Advances Have Shaped the Prevalence of Human Fungal Disease." *Pathogens (Basel, Switzerland)* **8**(2): 45.

Coelho, C., E. Camacho, A. Salas, A. Alanio and A. Casadevall (2019). "Intranasal Inoculation of *Cryptococcus neoformans* in Mice Produces Nasal Infection with Rapid Brain Dissemination." *mSphere* **4**(4).

Colombo, A. C. and M. L. Rodrigues (2015). "Fungal colonization of the brain: anatomopathological aspects of neurological cryptococcosis." *Anais da Academia Brasileira de Ciências* **87**(2 suppl): 1293-1309.

Cowen, L. E., D. Sanglard, S. J. Howard, P. D. Rogers and D. S. Perlin (2014). "Mechanisms of Antifungal Drug Resistance." *Cold Spring Harbor perspectives in medicine* **5**(7): a019752-a019752.

Cox, G. M., J. Mukherjee, G. T. Cole, A. Casadevall and J. R. Perfect (2000). "Urease as a virulence factor in experimental cryptococcosis." *Infection and immunity* **68**(2): 443-448.

Crocker, A., C. Lee, G. Aboko-Cole and C. Durham (1992). "Interaction of nutrition and infection: effect of copper deficiency on resistance to *Trypanosoma lewisi*." *J Natl Med Assoc* **84**(8): 697-706.

Dambuza, I. M., T. Drake, A. Chapuis, X. Zhou, J. Correia, L. Taylor-Smith, N. LeGrave, T. Rasmussen, M. C. Fisher, T. Bicanic, T. S. Harrison, M. Jaspars, R. C. May, G. D. Brown, R. Yuecel, D. M. MacCallum and E. R. Ballou (2018). "The *Cryptococcus neoformans* Titan cell is an inducible and regulated morphotype underlying pathogenesis." *PLoS Pathogens* **14**(5): e1006978.

Dambuza, I. M., T. Drake, A. Chapuis, X. Zhou, J. Correia, L. Taylor-Smith, N. LeGrave, T. Rasmussen, M. C. Fisher, T. Bicanic, T. S. Harrison, M. Jaspars, R. C. May, G. D. Brown, R. Yuecel, D. M. MacCallum and E. R. Ballou (2018). "The *Cryptococcus neoformans* Titan cell is an inducible and regulated morphotype underlying pathogenesis." *PLoS Pathog* **14**(5): e1006978.

Dan, J. M., R. M. Kelly, C. K. Lee and S. M. Levitz (2008). "Role of the Mannose Receptor in a Murine Model of *Cryptococcus neoformans* Infection." **76**(6): 2362-2367.

Dang, E. V., S. Lei, A. Radkov and H. D. Madhani (2021). "Mechanism of innate immune reprogramming by a fungal meningitis pathogen." *bioRxiv*: 2021.2009.2002.458767.

Dang, E. V., S. Lei, A. Radkov, R. F. Volk, B. W. Zaro and H. D. Madhani (2022). "Secreted fungal virulence effector triggers allergic inflammation via TLR4." *Nature* **608**(7921): 161-167.

Das, A., S. H. Kim, S. Arifuzzaman, T. Yoon, J. C. Chai, Y. S. Lee, K. S. Park, K. H. Jung and Y. G. Chai (2016). "Transcriptome sequencing reveals that LPS-triggered transcriptional responses in established microglia BV2 cell lines are poorly representative of primary microglia." *J Neuroinflammation* **13**(1): 182.

Davis, M. J., T. M. Tsang, Y. Qiu, J. K. Dayrit, J. B. Freij, G. B. Huffnagle and M. A. Olszewski (2013). "Macrophage M1/M2 Polarization Dynamically Adapts to Changes in Cytokine Microenvironments in *Cryptococcus neoformans* Infection." *mBio* **4**(3): e00264-00213-e00264.

De Gans, J. and D. Van De Beek (2002). "Dexamethasone in Adults with Bacterial Meningitis." New England Journal of Medicine **347**(20): 1549-1556.

de Sousa, H. R., G. P. de Oliveira, Jr., S. O. Frazão, K. C. M. Gorgonha, C. P. Rosa, E. M. Garcez, J. Lucas, Jr., A. F. Correia, W. F. de Freitas, H. M. Borges, L. G. Brito Alves, H. C. Paes, L. Trilles, M. D. S. Lazera, M. M. Teixeira, V. L. Pinto, Jr., M. S. S. Felipe, A. Casadevall, I. Silva-Pereira, P. Albuquerque and A. M. Nicola (2022). "Faster Cryptococcus Melanization Increases Virulence in Experimental and Human Cryptococcosis." J Fungi (Basel) **8**(4).

Deiss, R., C. V. Loreti, A. G. Gutierrez, E. Filipe, M. Tatia, S. Issufo, I. Ciglenecki, A. Loarec, H. Vivaldo, C. Barra, C. Siufi, L. Molfino and N. Tamayo Antabak (2021). "High burden of cryptococcal antigenemia and meningitis among patients presenting at an emergency department in Maputo, Mozambique." PLOS ONE **16**(4): e0250195.

Denham, S. T., B. Brammer, K. Y. Chung, M. A. Wambaugh, J. M. Bednarek, L. Guo, C. T. Moreau and J. C. S. Brown (2022). "A dissemination-prone morphotype enhances extrapulmonary organ entry by *Cryptococcus neoformans*." Cell Host Microbe **30**(10): 1382-1400.e1388.

Denham, S. T. and J. C. S. Brown (2018). "Mechanisms of Pulmonary Escape and Dissemination by *Cryptococcus neoformans*." J Fungi (Basel) **4**(1).

Denning, D. W., A. Pleuvry and D. C. Cole (2013). "Global burden of allergic bronchopulmonary aspergillosis with asthma and its complication chronic pulmonary aspergillosis in adults." Med Mycol **51**(4): 361-370.

Derecki, N. C., A. N. Cardani, C. H. Yang, K. M. Quinnes, A. Carihfield, K. R. Lynch and J. Kipnis (2010). "Regulation of learning and memory by meningeal immunity: a key role for IL-4." The Journal of experimental medicine **207**(5): 1067-1080.

Desai, V. and S. G. Kaler (2008). "Role of copper in human neurological disorders." The American Journal of Clinical Nutrition **88**(3): 855S-858S.

Ding, C., Richard A. Festa, Y.-L. Chen, A. Espart, Ò. Palacios, J. Espín, M. Capdevila, S. Atrian, J. Heitman and Dennis J. Thiele (2013). "Cryptococcus neoformans Copper Detoxification Machinery Is Critical for Fungal Virulence." Cell Host & Microbe **13**(3): 265-276.

Djoko, K. Y., C.-I. Y. Ong, M. J. Walker and A. G. McEwan (2015). "The Role of Copper and Zinc Toxicity in Innate Immune Defense against Bacterial Pathogens*." Journal of Biological Chemistry **290**(31): 18954-18961.

Dong, Z. M. and J. W. Murphy (1995). "Intravascular cryptococcal culture filtrate (CneF) and its major component, glucuronoxylomannan, are potent inhibitors of leukocyte accumulation." Infect Immun **63**(3): 770-778.

Drewniak, A., R. P. Gazendam, A. T. Tool, M. van Houdt, M. H. Jansen, J. L. van Hamme, E. M. van Leeuwen, D. Roos, E. Scalais, C. de Beaufort, H. Janssen, T. K. van den Berg and T. W. Kuijpers (2013). "Invasive fungal infection and impaired neutrophil killing in human CARD9 deficiency." Blood **121**(13): 2385-2392.

Drummond, R. (2017). "Neuro-Immune Mechanisms of Anti-Cryptococcal Protection." Journal of Fungi **4**(1): 4.

Drummond, R. A., A. L. Collar, M. Swamydas, C. A. Rodriguez, J. K. Lim, L. M. Mendez, D. L. Fink, A. P. Hsu, B. Zhai, H. Karauzum, C. M. Mikelis, S. R. Rose, E. M. N. Ferre, L. Yockey, K. Lemberg, H. S. Kuehn, S. D. Rosenzweig, X. Lin, P. Chittiboina, S. K. Datta, T. H. Belhorn, E. T. Weimer, M. L. Hernandez, T. M. Hohl, D. B. Kuhns and M. S. Lionakis (2015). "CARD9-Dependent Neutrophil Recruitment Protects against Fungal Invasion of the Central Nervous System." PLOS Pathogens **11**(12): e1005293.

Drummond, R. A., L. M. Franco and M. S. Lionakis (2018). "Human CARD9: A Critical Molecule of Fungal Immune Surveillance." Front Immunol **9**: 1836.

Drummond, R. A. and M. S. Lionakis (2016). "Mechanistic Insights into the Role of C-Type Lectin Receptor/CARD9 Signaling in Human Antifungal Immunity." Frontiers in Cellular and Infection Microbiology **6**.

Drummond, R. A., M. Swamydas, V. Oikonomou, B. Zhai, I. M. Dambuza, B. C. Schaefer, A. C. Bohrer, K. D. Mayer-Barber, S. A. Lira, Y. Iwakura, S. G. Filler, G. D. Brown, B. Hube, J. R. Naglik, T. M. Hohl and M. S. Lionakis (2019). "CARD9+ microglia promote antifungal immunity via IL-1 β - and CXCL1-mediated neutrophil recruitment." Nat Immunol **20**(5): 559-570.

Drummond, R. A., M. Swamydas, V. Oikonomou, B. Zhai, I. M. Dambuza, B. C. Schaefer, A. C. Bohrer, K. D. Mayer-Barber, S. A. Lira, Y. Iwakura, S. G. Filler, G. D. Brown, B. Hube, J. R. Naglik, T. M. Hohl and M. S. Lionakis (2019). "CARD9+ microglia promote antifungal immunity via IL-1 β - and CXCL1-mediated neutrophil recruitment." Nature Immunology **20**(5): 559-570.

Dufaud, C., J. Rivera, S. Rohatgi and L. A. Pirofski (2018). "Naïve B cells reduce fungal dissemination in *Cryptococcus neoformans* infected Rag1(-/-) mice." Virulence **9**(1): 173-184.

Elmore, M. R., A. R. Najafi, M. A. Koike, N. N. Dagher, E. E. Spangenberg, R. A. Rice, M. Kitazawa, B. Matusow, H. Nguyen, B. L. West and K. N. Green (2014). "Colony-stimulating factor 1 receptor signaling is necessary for microglia viability, unmasking a microglia progenitor cell in the adult brain." Neuron **82**(2): 380-397.

Elmore, M. R. P., L. A. Hohsfield, E. A. Kramár, L. Soreq, R. J. Lee, S. T. Pham, A. R. Najafi, E. E. Spangenberg, M. A. Wood, B. L. West and K. N. Green (2018). "Replacement of microglia in the aged brain reverses cognitive, synaptic, and neuronal deficits in mice." *Aging Cell* **17**(6): e12832.

Engelhardt, B. and R. M. Ransohoff (2005). "The ins and outs of T-lymphocyte trafficking to the CNS: anatomical sites and molecular mechanisms." *Trends in Immunology* **26**(9): 485-495.

Erblich, B., L. Zhu, A. M. Etgen, K. Dobrenis and J. W. Pollard (2011). "Absence of colony stimulation factor-1 receptor results in loss of microglia, disrupted brain development and olfactory deficits." *PLoS One* **6**(10): e26317.

Faguer, S., A. Pillet, N. Chassaing, M. Merhenberger, P. Bernadet-Monrozies, J. Guitard and D. Chauveau (2008). "Nephropathy in Townes-Brocks syndrome (SALL1 mutation): imaging and pathological findings in adulthood." *PLoS One* **24**(4): 1341-1345.

Feldmesser, M., A. Casadevall, Y. Kress, G. Spira and A. Orlofsky (1997). "Eosinophil-Cryptococcus neoformans interactions in vivo and in vitro." *Infect Immun* **65**(5): 1899-1907.

Feldmesser, M., Y. Kress and A. Casadevall (2001). "Dynamic changes in the morphology of Cryptococcus neoformans during murine pulmonary infection." *Microbiology* **147**(Pt 8): 2355-2365.

Feldmesser, M., Y. Kress, P. Novikoff and A. Casadevall (2000). "Cryptococcus neoformans is a facultative intracellular pathogen in murine pulmonary infection." *Infect Immun* **68**(7): 4225-4237.

Feldmesser, M., Y. Kress, P. Novikoff and A. Casadevall (2000). "Cryptococcus neoformans is a facultative intracellular pathogen in murine pulmonary infection." *Infection and immunity* **68**(7): 4225-4237.

Feng, X., M. Valdearcos, Y. Uchida, D. Lutrin, M. Maze and S. K. Koliwad (2017). "Microglia mediate postoperative hippocampal inflammation and cognitive decline in mice." *JCI Insight* **2**(7): e91229.

Filiano, A. J., S. P. Gadani and J. Kipnis (2015). "Interactions of innate and adaptive immunity in brain development and function." *Brain research* **1617**: 18-27.

Finlay, C. M., J. E. Parkinson, L. Zhang, B. H. K. Chan, J. Ajendra, A. Chenery, A. Morrison, I. Kaymak, E. L. Houlder, S. Murtuza Baker, B. R. Dickie, L. Boon, J. E. Konkel, M. R. Hepworth, A. S. MacDonald, G. J. Randolph, D. Rückerl and J. E. Allen (2023). "T helper 2 cells control monocyte to tissue-resident macrophage differentiation during nematode infection of the pleural cavity." *Immunity* **56**(5): 1064-1081.e1010.

Ford, N., C. Migone, A. Calmy, B. Kerschberger, S. Kanters, S. Nsanzimana, E. J. Mills, G. Meintjes, M. Vitoria, M. Doherty and Z. Shubber (2018). "Benefits and risks of rapid initiation of antiretroviral therapy." *AIDS (London, England)* **32**(1): 17-23.

Fu, M. S., C. Coelho, C. M. De Leon-Rodriguez, D. C. P. Rossi, E. Camacho, E. H. Jung, M. Kulkarni and A. Casadevall (2018). "Cryptococcus neoformans urease affects the outcome of intracellular pathogenesis by modulating phagolysosomal pH." *PLOS Pathogens* **14**(6): e1007144.

Fu, S., W. Jiang and W. Zheng (2015). "Age-dependent increase of brain copper levels and expressions of copper regulatory proteins in the subventricular zone and choroid plexus." *Front Mol Neurosci* **8**: 22.

Gaier, E. D., B. A. Eipper and R. E. Mains (2013). "Copper signaling in the mammalian nervous system: synaptic effects." *J Neurosci Res* **91**(1): 2-19.

Gangneux, J. P., E. Dannaoui, A. Fekkar, C. E. Luyt, F. Botterel, N. De Prost, J. M. Tadié, F. Reizine, S. Houzé, J. F. Timsit, X. Iriart, B. Riu-Poulenc, B. Sendid, S. Nseir, F. Persat, F. Wallet, P. Le Pape, E. Canet, A. Novara, M. Manai, E. Cateau, A. W. Thille, S. Brun, Y. Cohen, A. Alanio, B. Mégarbane, M. Cornet, N. Terzi, L. Lamhaut, E. Sabourin, G. Desoubeaux, S. Ehrmann, C. Hennequin, G. Voiriot, G. Nevez, C. Aubron, V. Letscher-Bru, F. Meziani, M. Blaize, J. Mayaux, A. Monsel, F. Boquel, F. Robert-Gangneux, Y. Le Tulzo, P. Seguin, H. Guegan, B. Autier, M. Lesouhaitier, R. Pelletier, S. Belaz, C. Bonnal, A. Berry, J. Leroy, N. François, J. C. Richard, S. Paulus, L. Argaud, D. Dupont, J. Menotti, F. Morio, M. Soulié, C. Schwebel, C. Garnaud, J. Guitard, S. Le Gal, D. Quinio, J. Morcet, B. Laviolle, J. R. Zahar and M. E. Bougnoux (2022). "Fungal infections in mechanically ventilated patients with COVID-19 during the first wave: the French multicentre MYCOVID study." *Lancet Respir Med* **10**(2): 180-190.

Gao, L.-W., A.-X. Jiao, X.-R. Wu, S.-Y. Zhao, Y. Ma, G. Liu, J. Yin, B.-P. Xu and K.-L. Shen (2017). "Clinical characteristics of disseminated cryptococcosis in previously healthy children in China." *BMC Infectious Diseases* **17**(1).

Garcia-Hermoso, D., G. Janbon and F. Dromer (1999). "Epidemiological evidence for dormant Cryptococcus neoformans infection." *Journal of clinical microbiology* **37**(10): 3204-3209.

Garro, A. P., L. S. Chiapello, J. L. Baronetti and D. T. Masih (2011). "Eosinophils elicit proliferation of naive and fungal-specific cells in vivo so enhancing a T helper type 1 cytokine profile in favour of a protective immune response against Cryptococcus neoformans infection." *Immunology* **134**(2): 198-213.

Gaziano, R., S. Sabbatini, E. Roselletti, S. Perito and C. Monari (2020). "Saccharomyces cerevisiae-Based Probiotics as Novel Antimicrobial Agents to Prevent and Treat Vaginal Infections." *Frontiers in Microbiology* **11**.

Gibson, J. F., A. Bojarczuk, R. J. Evans, A. A. Kamuyango, R. Hotham, A. K. Lagendijk, B. M. Hogan, P. W. Ingham, S. A. Renshaw and S. A. Johnston (2022). "Blood vessel occlusion by *Cryptococcus neoformans* is a mechanism for haemorrhagic dissemination of infection." *PLoS Pathog* **18**(4): e1010389.

Gilles, S. R., S. S. Arbefeville, P. Ferrieri and E. L. Courville (2018). "Lymph Node With Extensive Involvement by *Cryptococcus* Shortly Following Liver Transplantation." *Lab Med* **49**(3): e78-e81.

Ginhoux, F., M. Greter, M. Leboeuf, S. Nandi, P. See, S. Gokhan, M. F. Mehler, S. J. Conway, L. G. Ng, E. R. Stanley, I. M. Samokhvalov and M. Merad (2010). "Fate mapping analysis reveals that adult microglia derive from primitive macrophages." *Science* **330**(6005): 841-845.

Glocker, E.-O., A. Hennigs, M. Nabavi, A. A. Schäffer, C. Woellner, U. Salzer, D. Pfeifer, H. Veelken, K. Warnatz, F. Tahami, S. Jamal, A. Manguiat, N. Rezaei, A. A. Amirzargar, A. Plebani, N. Hanneschläger, O. Gross, J. Ruland and B. Grimbacher (2009). "A homozygous CARD9 mutation in a family with susceptibility to fungal infections." *The New England journal of medicine* **361**(18): 1727-1735.

Goldman, D., X. Song, R. Kitai, A. Casadevall, M. L. Zhao and S. C. Lee (2001). "*Cryptococcus neoformans* induces macrophage inflammatory protein 1alpha (MIP-1alpha) and MIP-1beta in human microglia: role of specific antibody and soluble capsular polysaccharide." *Infect Immun* **69**(3): 1808-1815.

Goldman, D. L., H. Khine, J. Abadi, D. J. Lindenberg, L.-a. Pirofski, R. Niang and A. Casadevall (2001). "Serologic Evidence for *Cryptococcus neoformans* Infection in Early Childhood." *Pediatrics* **107**(5): e66.

Gómez, B. L. and J. D. Nosanchuk (2003). "Melanin and fungi." *Curr Opin Infect Dis* **16**(2): 91-96.

Gomez Perdiguero, E., K. Klapproth, C. Schulz, K. Busch, E. Azzoni, L. Crozet, H. Garner, C. Trouillet, M. F. de Bruijn, F. Geissmann and H. R. Rodewald (2015). "Tissue-resident macrophages originate from yolk-sac-derived erythro-myeloid progenitors." *Nature* **518**(7540): 547-551.

Gosselin, D., D. Skola, N. G. Coufal, I. R. Holtman, J. C. M. Schlachetzki, E. Sajti, B. N. Jaeger, C. O'Connor, C. Fitzpatrick, M. P. Pasillas, M. Pena, A. Adair, D. D. Gonda, M. L. Levy, R. M. Ransohoff, F. H. Gage and C. K. Glass (2017). "An environment-dependent transcriptional network specifies human microglia identity." *Science* **356**(6344).

Graybill, J. R., R. Bocanegra, C. Lambros and M. F. Luther (1997). "Granulocyte colony stimulating factor therapy of experimental cryptococcal meningitis." *35*(4): 243-247.

Green, K. N. and D. A. Hume (2021). "On the utility of CSF1R inhibitors." *Proc Natl Acad Sci U S A* **118**(4).

Gross, O., A. Gewies, K. Finger, M. Schäfer, T. Sparwasser, C. Peschel, I. Förster and J. Ruland (2006). "Card9 controls a non-TLR signalling pathway for innate anti-fungal immunity." *Nature* **442**(7103): 651-656.

Gupta, S., M. Ellis, T. Cesario, M. Ruhling and B. Vayuvegula (1987). "Disseminated cryptococcal infection in a patient with hypogammaglobulinemia and normal T cell functions." *Am J Med* **82**(1): 129-131.

Haddow, L. J., R. Colebunders, G. Meintjes, S. D. Lawn, J. H. Elliott, Y. C. Manabe, P. R. Bohjanen, S. Sungkanuparph, P. J. Easterbrook, M. A. French, D. R. Boulware and H. I. V. a. I. International Network for the Study of (2010). "Cryptococcal immune reconstitution inflammatory syndrome in HIV-1-infected individuals: proposed clinical case definitions." *The Lancet. Infectious diseases* **10**(11): 791-802.

Han, J., K. Zhu, X. M. Zhang and R. A. Harris (2019). "Enforced microglial depletion and repopulation as a promising strategy for the treatment of neurological disorders." *Glia* **67**(2): 217-231.

Han, X., Q. Li, X. Lan, L. El-Mufti, H. Ren and J. Wang (2019). "Microglial Depletion with Clodronate Liposomes Increases Proinflammatory Cytokine Levels, Induces Astrocyte Activation, and Damages Blood Vessel Integrity." *Mol Neurobiol* **56**(9): 6184-6196.

Hanna, R. N., L. M. Carlin, H. G. Hubbeling, D. Nackiewicz, A. M. Green, J. A. Punt, F. Geissmann and C. C. Hedrick (2011). "The transcription factor NR4A1 (Nur77) controls bone marrow differentiation and the survival of Ly6C- monocytes." *Nat Immunol* **12**(8): 778-785.

Hansakon, A., P. Mutthakalin, P. Ngamskulrungronj, M. Chayakulkeeree and P. Angkasekwina (2019). "*Cryptococcus neoformans* and *Cryptococcus gattii* clinical isolates from Thailand display diverse phenotypic interactions with macrophages." *Virulence* **10**(1): 26-36.

Hardison, S. E. and G. D. Brown (2012). "C-type lectin receptors orchestrate antifungal immunity." *Nature immunology* **13**(9): 817-822.

Hardison, S. E., S. Ravi, K. L. Wozniak, M. L. Young, M. A. Olszewski and F. L. Wormley (2010). "Pulmonary Infection with an Interferon- γ -Producing *Cryptococcus neoformans* Strain Results in Classical Macrophage Activation and Protection." **176**(2): 774-785.

Harris, C. J., N. E. Gray, M. Caruso, M. Hunter, M. Ralle and J. F. Quinn (2020). "Copper Modulation and Memory Impairment due to Hippocampal Tau Pathology." *J Alzheimers Dis* **78**(1): 49-60.

Harris, J. R., S. R. Lockhart, E. Debess, N. Marsden-Haug, M. Goldoft, R. Wohrle, S. Lee, C. Smelser, B. Park and T. Chiller (2011). "Cryptococcus gattii in the United States: clinical aspects of infection with an emerging pathogen." *Clin Infect Dis* **53**(12): 1188-1195.

Havliczkova, B., V. A. Czaika and M. Friedrich (2008). "Epidemiological trends in skin mycoses worldwide." *Mycoses* **51 Suppl 4**: 2-15.

Hawley, C. A., R. Rojo, A. Raper, K. A. Sauter, Z. M. Lisowski, K. Grabert, C. C. Bain, G. M. Davis, P. A. Louwe, M. C. Ostrowski, D. A. Hume, C. Pridans and S. J. Jenkins (2018). "Csf1r-mApple Transgene Expression and Ligand Binding In Vivo Reveal Dynamics of CSF1R Expression within the Mononuclear Phagocyte System." *J Immunol* **200**(6): 2209-2223.

Heresi, G., C. Castillo-Durán, C. Muñoz, M. Arévalo and L. Schlesinger (1985). "Phagocytosis and immunoglobulin levels in hypocupremic infants." *Nutrition Research* **5**(12): 1327-1334.

Herold, S., K. Mayer and J. Lohmeyer (2011). "Acute lung injury: how macrophages orchestrate resolution of inflammation and tissue repair." *Front Immunol* **2**: 65.

Heung, L. J. and T. M. Hohl (2019). "Inflammatory monocytes are detrimental to the host immune response during acute infection with Cryptococcus neoformans." *PLoS Pathog* **15**(3): e1007627.

Hoeffel, G., J. Chen, Y. Lavin, D. Low, F. F. Almeida, P. See, A. E. Beaudin, J. Lum, I. Low, E. C. Forsberg, M. Poidinger, F. Zolezzi, A. Larbi, L. G. Ng, J. K. Chan, M. Greter, B. Becher, I. M. Samokhvalov, M. Merad and F. Ginhoux (2015). "C-Myb(+) erythro-myeloid progenitor-derived fetal monocytes give rise to adult tissue-resident macrophages." *Immunity* **42**(4): 665-678.

Hoenigl, M., D. Seidel, A. Carvalho, S. M. Rudramurthy, A. Arastehfar, J. P. Gangneux, N. Nasir, A. Bonifaz, J. Araiza, N. Klimko, A. Serris, K. Lagrou, J. F. Meis, O. A. Cornely, J. R. Perfect, P. L. White and A. Chakrabarti (2022). "The emergence of COVID-19 associated mucormycosis: a review of cases from 18 countries." *Lancet Microbe* **3**(7): e543-e552.

Hole, C. and F. L. Wormley, Jr. (2016). "Innate host defenses against Cryptococcus neoformans." *J Microbiol* **54**(3): 202-211.

Hole, C. R., C. M. L. Wager, N. Castro-Lopez, A. Campuzano, H. Cai, K. L. Wozniak, Y. Wang and F. L. Wormley (2019). "Induction of memory-like dendritic cell responses in vivo." *Nature Communications* **10**(1).

Holmer, S. M., K. S. Evans, Y. G. Asfaw, D. Saini, W. A. Schell, J. G. Ledford, R. Frothingham, J. R. Wright, G. D. Sempowski and J. R. Perfect (2014). "Impact of surfactant protein D, interleukin-5, and eosinophilia on Cryptococcosis." *Infect Immun* **82**(2): 683-693.

Hommel, B., L. Mukaremera, R. J. B. Cordero, C. Coelho, C. A. Desjardins, A. Sturny-Leclère, G. Janbon, J. R. Perfect, J. A. Fraser, A. Casadevall, C. A. Cuomo, F. Dromer, K. Nielsen and A. Alanio (2018). "Titan cells formation in Cryptococcus neoformans is finely tuned by environmental conditions and modulated by positive and negative genetic regulators." *PLoS pathogens* **14**(5): e1006982-e1006982.

Hope, W., N. R. H. Stone, A. Johnson, L. McEntee, N. Farrington, A. Santoro-Castelazo, X. Liu, A. Lucaci, M. Hughes, J. D. Oliver, C. Giamberardino, S. Mfinanga, T. S. Harrison, J. R. Perfect and T. Bicanic (2019). "Fluconazole Monotherapy Is a Suboptimal Option for Initial Treatment of Cryptococcal Meningitis Because of Emergence of Resistance." *mBio* **10**(6): e02575-02519.

Hou, F., K. Xiao, L. Tang and L. Xie (2021). "Diversity of Macrophages in Lung Homeostasis and Diseases." *Front Immunol* **12**: 753940.

Houšť, J., J. Spižek and V. Havlíček (2020). "Antifungal Drugs." *Metabolites* **10**(3).

Hu, X.-P., R.-Y. Wang, X. Wang, Y.-H. Cao, Y.-Q. Chen, H.-Z. Zhao, J.-Q. Wu, X.-H. Weng, X.-H. Gao, R.-H. Sun and L.-P. Zhu (2015). "Dectin-2 polymorphism associated with pulmonary cryptococcosis in HIV-uninfected Chinese patients." **53**(8): 810-816.

Huang, L., E. V. Nazarova, S. Tan, Y. Liu and D. G. Russell (2018). "Growth of Mycobacterium tuberculosis in vivo segregates with host macrophage metabolism and ontogeny." *J Exp Med* **215**(4): 1135-1152.

Huffnagle, G. B., M. B. Boyd, N. E. Street and M. F. Lipscomb (1998). "IL-5 is required for eosinophil recruitment, crystal deposition, and mononuclear cell recruitment during a pulmonary Cryptococcus neoformans infection in genetically susceptible mice (C57BL/6)." *J Immunol* **160**(5): 2393-2400.

Huffnagle, G. B., M. F. Lipscomb, J. A. Lovchik, K. A. Hoag and N. E. Street (1994). "The role of CD4+ and CD8+ T cells in the protective inflammatory response to a pulmonary cryptococcal infection." *J Leukoc Biol* **55**(1): 35-42.

Huffnagle, G. B., J. L. Yates and M. F. Lipscomb (1991). "Immunity to a pulmonary Cryptococcus neoformans infection requires both CD4+ and CD8+ T cells." *J Exp Med* **173**(4): 793-800.

Jarvis, J. N., T. Bicanic, A. Loyse, D. Namarika, A. Jackson, J. C. Nussbaum, N. Longley, C. Muzoora, J. Phulusa, K. Taseera, C. Kanyembe, D. Wilson, M. C. Hosseinipour, A. E. Brouwer, D. Limmathurotsakul, N. White, C. van der Horst, R. Wood, G. Meintjes, J. Bradley, S. Jaffar and T. Harrison (2014). "Determinants of mortality in a

combined cohort of 501 patients with HIV-associated Cryptococcal meningitis: implications for improving outcomes." Clinical infectious diseases : an official publication of the Infectious Diseases Society of America **58**(5): 736-745.

Jarvis, J. N., T. B. Leeme, M. Molefi, A. A. Chofle, G. Bidwell, K. Tsholo, N. Tlhako, N. Mawoko, R. K. K. Patel, M. W. Tenforde, C. Muthoga, G. P. Bisson, J. Kidola, J. Changalucha, D. Lawrence, S. Jaffar, W. Hope, S. L. F. Molloy and T. S. Harrison (2019). "Short-course High-dose Liposomal Amphotericin B for Human Immunodeficiency Virus-associated Cryptococcal Meningitis: A Phase 2 Randomized Controlled Trial." Clinical Infectious Diseases **68**(3): 393-401.

Jarvis, J. N., G. Meintjes, K. Rebe, G. N. Williams, T. Bicanic, A. Williams, C. Schutz, L.-G. Bekker, R. Wood and T. S. Harrison (2012). "Adjunctive interferon- γ immunotherapy for the treatment of HIV-associated cryptococcal meningitis." **26**(9): 1105-1113.

Jarvis, J. N., G. Meintjes, K. Rebe, G. N. Williams, T. Bicanic, A. Williams, C. Schutz, L.-G. Bekker, R. Wood and T. S. Harrison (2012). "Adjunctive interferon- γ immunotherapy for the treatment of HIV-associated cryptococcal meningitis: a randomized controlled trial." AIDS (London, England) **26**(9): 1105-1113.

Jarvis, J. N., G. Meintjes, K. Rebe, G. N. Williams, T. Bicanic, A. Williams, C. Schutz, L. G. Bekker, R. Wood and T. S. Harrison (2012). "Adjunctive interferon- γ immunotherapy for the treatment of HIV-associated cryptococcal meningitis: a randomized controlled trial." Aids **26**(9): 1105-1113.

Jenkins, S. J., D. Ruckerl, P. C. Cook, L. H. Jones, F. D. Finkelman, N. van Rooijen, A. S. MacDonald and J. E. Allen (2011). "Local macrophage proliferation, rather than recruitment from the blood, is a signature of TH2 inflammation." Science **332**(6035): 1284-1288.

Jiang, N., X. Liu, J. Yang, Z. Li, J. Pan and X. Zhu (2011). "Regulation of copper homeostasis by Cuf1 associates with its subcellular localization in the pathogenic yeast *Cryptococcus neoformans* H99." FEMS Yeast Res **11**(5): 440-448.

Jo, E. K., H. S. Kim, M. Y. Lee, M. Iseki, J. H. Lee, C. H. Song, J. K. Park, T. J. Hwang and H. Kook (2002). "X-linked hyper-IgM syndrome associated with *Cryptosporidium parvum* and *Cryptococcus neoformans* infections: the first case with molecular diagnosis in Korea." J Korean Med Sci **17**(1): 116-120.

Jones, D. G. and N. F. Suttle (1983). "The effect of copper deficiency on the resistance of mice to infection with *Pasteurella haemolytica*." J Comp Pathol **93**(1): 143-149.

Jung, W. H., A. Sham, T. Lian, A. Singh, D. J. Kosman and J. W. Kronstad (2008). "Iron source preference and regulation of iron uptake in *Cryptococcus neoformans*." PLoS Pathog **4**(2): e45.

Jung, W. H., A. Sham, R. White and J. W. Kronstad (2006). "Iron regulation of the major virulence factors in the AIDS-associated pathogen *Cryptococcus neoformans*." PLoS Biol **4**(12): e410.

Kaiser, T. and G. Feng (2019). "Tmem119-EGFP and Tmem119-CreERT2 Transgenic Mice for Labeling and Manipulating Microglia." eNeuro **6**(4).

Kambugu, A., D. B. Meya, J. Rhein, M. O'Brien, E. N. Janoff, A. R. Ronald, M. R. Kanya, H. Mayanja-Kizza, M. A. Sande, P. R. Bohjanen and D. R. Boulware (2008). "Outcomes of cryptococcal meningitis in Uganda before and after the availability of highly active antiretroviral therapy." Clin Infect Dis **46**(11): 1694-1701.

Kanjanapradit, K., Z. Kosjerina, W. Tanomkiat, W. Keeratichananont and S. Panthuwong (2017). "Pulmonary Cryptococcosis Presenting With Lung Mass: Report of 7 Cases and Review of Literature." Clinical medicine insights. Pathology **10**: 1179555717722962-1179555717722962.

Kaufman-Francis, K., J. T. Djordjevic, P.-G. Juillard, S. Lev, D. Desmarini, G. E. R. Grau and T. C. Sorrell (2018). "The Early Innate Immune Response to, and Phagocyte-Dependent Entry of, *Cryptococcus neoformans* Map to the Perivascular Space of Cortical Post-Capillary Venules in Neurocryptococcosis." The American Journal of Pathology **188**(7): 1653-1665.

Kaufman-Francis, K., J. T. Djordjevic, P. G. Juillard, S. Lev, D. Desmarini, G. E. R. Grau and T. C. Sorrell (2018). "The Early Innate Immune Response to, and Phagocyte-Dependent Entry of, *Cryptococcus neoformans* Map to the Perivascular Space of Cortical Post-Capillary Venules in Neurocryptococcosis." Am J Pathol **188**(7): 1653-1665.

Kaushansky, A., A. N. Douglass, N. Arang, V. Vigdorovich, N. Dambrauskas, H. S. Kain, L. S. Austin, D. N. Sather and S. H. Kappe (2015). "Malaria parasites target the hepatocyte receptor EphA2 for successful host infection." Science **350**(6264): 1089-1092.

Kechichian, T. B., J. Shea and M. Del Poeta (2007). "Depletion of alveolar macrophages decreases the dissemination of a glucosylceramide-deficient mutant of *Cryptococcus neoformans* in immunodeficient mice." Infect Immun **75**(10): 4792-4798.

Kerkhofs, D., B. T. van Hagen, I. V. Milanova, K. J. Schell, H. van Essen, E. Wijnands, P. Goossens, W. M. Blankesteyn, T. Unger, J. Prickaerts, E. A. Biessen, R. J. van Oostenbrugge and S. Foulquier (2020).

"Pharmacological depletion of microglia and perivascular macrophages prevents Vascular Cognitive Impairment in Ang II-induced hypertension." *Theranostics* **10**(21): 9512-9527.

Kipnis, J., H. Cohen, M. Cardon, Y. Ziv and M. Schwartz (2004). "T cell deficiency leads to cognitive dysfunction: implications for therapeutic vaccination for schizophrenia and other psychiatric conditions." *Proceedings of the National Academy of Sciences of the United States of America* **101**(21): 8180-8185.

Kipnis, J., S. Gadani and N. C. Derecki (2012). "Pro-cognitive properties of T cells." *Nature reviews. Immunology* **12**(9): 663-669.

Kohn, S., H. Kakeya, K. Izumikawa, T. Miyazaki, Y. Yamamoto, K. Yanagihara, K. Mitsutake, Y. Miyazaki, S. Maesaki, A. Yasuoka, T. Tashiro, M. Mine, M. Uetani and K. Ashizawa (2015). "Clinical features of pulmonary cryptococcosis in non-HIV patients in Japan." *J Infect Chemother* **21**(1): 23-30.

Korin, B., T. L. Ben-Shaanan, M. Schiller, T. Dubovik, H. Azulay-Debby, N. T. Boshnak, T. Koren and A. Rolls (2017). "High-dimensional, single-cell characterization of the brain's immune compartment." *Nature Neuroscience* **20**(9): 1300-1309.

Kronstad, J., S. Saikia, E. D. Nielson, M. Kretschmer, W. Jung, G. Hu, J. M. Geddes, E. J. Griffiths, J. Choi, B. Cadieux, M. Caza and R. Attarian (2012). "Adaptation of *Cryptococcus neoformans* to mammalian hosts: integrated regulation of metabolism and virulence." *Eukaryot Cell* **11**(2): 109-118.

Kuehn, B. M. (2020). "Multidrug-Resistant *Candida auris* Concern Stems From New York Cases." *JAMA* **323**(8): 702.

Kulikauskaitė, J. and A. Wack (2020). "Teaching Old Dogs New Tricks? The Plasticity of Lung Alveolar Macrophage Subsets." *Trends Immunol* **41**(10): 864-877.

Kwon-Chung, K. J. and J. C. Rhodes (1986). "Encapsulation and melanin formation as indicators of virulence in *Cryptococcus neoformans*." *Infection and immunity* **51**(1): 218-223.

Lafuse, W. P., M. V. S. Rajaram, Q. Wu, J. I. Moliva, J. B. Torrelles, J. Turner and L. S. Schlesinger (2019). "Identification of an Increased Alveolar Macrophage Subpopulation in Old Mice That Displays Unique Inflammatory Characteristics and Is Permissive to *Mycobacterium tuberculosis* Infection." *The Journal of Immunology* **203**(8): 2252.

Lamoth, F., S. R. Lockhart, E. L. Berkow and T. Calandra (2018). "Changes in the epidemiological landscape of invasive candidiasis." *Journal of Antimicrobial Chemotherapy* **73**(suppl_1): i4-i13.

Lanternier, F., E. Barbati, U. Meinzer, L. Liu, V. Pedergrana, M. Migaud, S. Héritier, M. Chomton, M.-L. Frémond, E. Gonzales, C. Galeotti, S. Romana, E. Jacquemin, A. Angoulvant, V. Bidault, D. Canioni, J. Lachenaud, D. Mansouri, S. A. Mahdavian, P. Adimi, N. Mansouri, M. Jamshidi, M.-E. Bournoux, L. Abel, O. Lortholary, S. Blanche, J.-L. Casanova, C. Picard and A. Puel (2015). "Inherited CARD9 deficiency in 2 unrelated patients with invasive *Exophiala* infection." *The Journal of infectious diseases* **211**(8): 1241-1250.

Lanternier, F., S. Pathan, Q. B. Vincent, L. Liu, S. Cypowyj, C. Prando, M. Migaud, L. Taibi, A. Ammar-Khodja, O. Boudghene Stambouli, B. Guellil, F. Jacobs, J.-C. Goffard, K. Schepers, V. Del Marmol, L. Boussofara, M. Denguezli, M. Larif, H. Bachelez, L. Michel, G. Lefranc, R. Hay, G. Jouvion, F. Chretien, S. Fraitag, M.-E. Bournoux, M. Boudia, L. Abel, O. Lortholary, J.-L. Casanova, C. Picard, B. Grimbacher and A. Puel (2013). "Deep Dermatophytosis and Inherited CARD9 Deficiency." *New England Journal of Medicine* **369**(18): 1704-1714.

Lee, D., E.-H. Jang, M. Lee, S.-W. Kim, Y. Lee, K.-T. Lee and Y.-S. Bahn (2019). "Unraveling Melanin Biosynthesis and Signaling Networks in *Cryptococcus neoformans*." *mBio* **10**(5): e02267-02219.

Lee, K.-T., J. Hong, D.-G. Lee, M. Lee, S. Cha, Y.-G. Lim, K.-W. Jung, A. Hwangbo, Y. Lee, S.-J. Yu, Y.-L. Chen, J.-S. Lee, E. Cheong and Y.-S. Bahn (2020). "Fungal kinases and transcription factors regulating brain infection in *Cryptococcus neoformans*." *Nature Communications* **11**(1).

Lee, S. C., Y. Kress, D. W. Dickson and A. Casadevall (1995). "Human microglia mediate anti-*Cryptococcus neoformans* activity in the presence of specific antibody." *J Neuroimmunol* **62**(1): 43-52.

Lee, S. C., Y. Kress, M. L. Zhao, D. W. Dickson and A. Casadevall (1995). "*Cryptococcus neoformans* survive and replicate in human microglia." *Lab Invest* **73**(6): 871-879.

Lehenkari, P. P., M. Kellinsalmi, J. P. Näpänkangas, K. V. Ylitalo, J. Mönkkönen, M. J. Rogers, A. Azhayev, H. K. Väänänen and I. E. Hassinen (2002). "Further insight into mechanism of action of clodronate: inhibition of mitochondrial ADP/ATP translocase by a nonhydrolyzable, adenine-containing metabolite." *Mol Pharmacol* **61**(5): 1255-1262.

Lei, F., N. Cui, C. Zhou, J. Chodosh, G. Vavvas Demetrios and I. Paschalis Eleftherios (2020). "CSF1R inhibition by a small-molecule inhibitor is not microglia specific; affecting hematopoiesis and the function of macrophages." *Proceedings of the National Academy of Sciences* **117**(38): 23336-23338.

Lei, F., N. Cui, C. Zhou, J. Chodosh, D. G. Vavvas and E. I. Paschalis (2020). "CSF1R inhibition by a small-molecule inhibitor is not microglia specific; affecting hematopoiesis and the function of macrophages." Proceedings of the National Academy of Sciences **117**(38): 23336.

Lei, F., N. Cui, C. Zhou, J. Chodosh, D. G. Vavvas and E. I. Paschalis (2020). "CSF1R inhibition by a small-molecule inhibitor is not microglia specific; affecting hematopoiesis and the function of macrophages." Proc Natl Acad Sci U S A **117**(38): 23336-23338.

Leopold Wager, C. M., C. R. Hole, K. L. Wozniak, M. A. Olszewski, M. Mueller and F. L. Wormley (2015). "STAT1 Signaling within Macrophages Is Required for Antifungal Activity against *Cryptococcus neoformans*." Infect Immun **83**(12): 4513-4527.

Leopold Wager, C. M., C. R. Hole, K. L. Wozniak, M. A. Olszewski, M. Mueller and F. L. Wormley, Jr. (2015). "STAT1 signaling within macrophages is required for antifungal activity against *Cryptococcus neoformans*." Infection and immunity **83**(12): 4513-4527.

Leopold Wager, C. M., C. R. Hole, K. L. Wozniak and F. L. Wormley (2016). "Cryptococcus and Phagocytes: Complex Interactions that Influence Disease Outcome." Frontiers in Microbiology **7**.

Leopold Wager, C. M. and F. L. Wormley (2014). "Classical versus alternative macrophage activation: the Ying and the Yang in host defense against pulmonary fungal infections." Mucosal Immunology **7**(5): 1023-1035.

Levitz, S. M., S. H. Nong, K. F. Seetoo, T. S. Harrison, R. A. Speizer and E. R. Simons (1999). "Cryptococcus neoformans resides in an acidic phagolysosome of human macrophages." Infection and immunity **67**(2): 885-890.

Lian, T., M. I. Simmer, C. A. D'Souza, B. R. Steen, S. D. Zuyderduyn, S. J. M. Jones, M. A. Marra and J. W. Kronstad (2004). "Iron-regulated transcription and capsule formation in the fungal pathogen *Cryptococcus neoformans*." Molecular Microbiology **55**(5): 1452-1472.

Lin, K. L., Y. Suzuki, H. Nakano, E. Ramsburg and M. D. Gunn (2008). "CCR2+ monocyte-derived dendritic cells and exudate macrophages produce influenza-induced pulmonary immune pathology and mortality." J Immunol **180**(4): 2562-2572.

Lionakis, M. S., M. G. Netea and S. M. Holland (2014). "Mendelian Genetics of Human Susceptibility to Fungal Infection." Cold Spring Harbor Perspectives in Medicine **4**(6): a019638-a019638.

Lipovsky, M. M., G. Gekker, S. Hu, L. C. Ehrlich, A. I. Hoepelman and P. K. Peterson (1998). "Cryptococcal glucuronoxylomannan induces interleukin (IL)-8 production by human microglia but inhibits neutrophil migration toward IL-8." J Infect Dis **177**(1): 260-263.

Lipovsky, M. M., A. E. Juliana, G. Gekker, S. Hu, A. I. M. Hoepelman and P. K. Peterson (1998). "Effect of Cytokines on Anticryptococcal Activity of Human Microglial Cells." Clinical and Diagnostic Laboratory Immunology **5**(3): 410.

Liu, K., H. Ding, B. Xu, R. You, Z. Xing, J. Chen, Q. Lin and J. Qu (2016). "Clinical analysis of non-AIDS patients pathologically diagnosed with pulmonary cryptococcosis." Journal of thoracic disease **8**(10): 2813-2821.

Liu, Y., K. S. Given, E. L. Dickson, G. P. Owens, W. B. Macklin and J. L. Bennett (2019). "Concentration-dependent effects of CSF1R inhibitors on oligodendrocyte progenitor cells ex vivo and in vivo." Exp Neurol **318**: 32-41.

Lovell, M. A., J. D. Robertson, W. J. Teesdale, J. L. Campbell and W. R. Markesbery (1998). "Copper, iron and zinc in Alzheimer's disease senile plaques." J Neurol Sci **158**(1): 47-52.

Ma, L. L., J. C. Spurrell, J. F. Wang, G. G. Neely, S. Eelman, A. M. Krensky and C. H. Mody (2002). "CD8 T cell-mediated killing of *Cryptococcus neoformans* requires granulysin and is dependent on CD4 T cells and IL-15." J Immunol **169**(10): 5787-5795.

Malik, A., P. A. Khan, F. Shujatullah, N. Fatima, M. Shameem and A. Siddiqui (2012). "Rapid development of IRIS in the form of cryptococcal meningitis after beginning ART." **1**(1): 56-58.

Mansour, M. K., J. L. Reedy, J. M. Tam and J. M. Vyas (2014). "Macrophage *Cryptococcus* interactions: an update." Curr Fungal Infect Rep **8**(1): 109-115.

Marchi, G., F. Busti, A. Lira Zidanes, A. Castagna and D. Girelli (2019). "Aceruloplasminemia: A Severe Neurodegenerative Disorder Deserving an Early Diagnosis." Front Neurosci **13**: 325.

Masuda, T., L. Amann, G. Monaco, R. Sankowski, O. Staszewski, M. Krueger, F. Del Gaudio, L. He, N. Paterson, E. Nent, F. Fernández-Klett, A. Yamasaki, M. Frosch, M. Fliegau, L. F. P. Bosch, H. Ulupinar, N. Hagemeyer, D. Schreiner, C. Dorrier, M. Tsuda, C. Grothe, A. Joutel, R. Daneman, C. Betsholtz, U. Lendahl, K.-P. Knobeloch, T. Lämmermann, J. Priller, K. Kierdorf and M. Prinz (2022). "Specification of CNS macrophage subsets occurs postnatally in defined niches." Nature **604**(7907): 740-748.

Masuda, T., L. Amann, R. Sankowski, O. Staszewski, M. Lenz, P. d'Errico, N. Snaidero, M. J. Costa Jordão, C. Böttcher, K. Kierdorf, S. Jung, J. Priller, T. Misgeld, A. Vlachos, M. Meyer-Luehmann, K.-P. Knobeloch and M. Prinz (2020). "Novel Hexb-based tools for studying microglia in the CNS." Nature Immunology **21**(7): 802-815.

McCowan, J., F. Fercoq, P. M. Kirkwood, W. T'Jonck, L. M. Hegarty, C. M. Mawer, R. Cunningham, A. S. Mirchandani, A. Hoy, D. C. Humphries, G. R. Jones, C. G. Hansen, N. Hirani, S. J. Jenkins, S. Henri, B. Malissen, S. R. Walmsley, D. H. Dockrell, P. T. K. Saunders, L. M. Carlin and C. C. Bain (2021). "The transcription factor EGR2 is indispensable for tissue-specific imprinting of alveolar macrophages in health and tissue repair." *Sci Immunol* **6**(65): eabj2132.

McQuiston, T. J. and P. R. Williamson (2012). "Paradoxical roles of alveolar macrophages in the host response to *Cryptococcus neoformans*." *Infection and Immunity* **18**(1): 1-9.

Meara, T. R. and J. A. Alspaugh (2012). "The *Cryptococcus neoformans* Capsule: a Sword and a Shield." *Clinical Microbiology Reviews* **25**(3): 387.

Mednick, A. J., M. Feldmesser, J. Rivera and A. Casadevall (2003). "Neutropenia alters lung cytokine production in mice and reduces their susceptibility to pulmonary cryptococcosis." *Infection and Immunity* **33**(6): 1744-1753.

Melief, J., M. A. Sneebouer, M. Litjens, P. R. Ormel, S. J. Palmem, I. Huitinga, R. S. Kahn, E. M. Hol and L. D. de Witte (2016). "Characterizing primary human microglia: A comparative study with myeloid subsets and culture models." *Glia* **64**(11): 1857-1868.

Miller, M. F. and T. G. Mitchell (1991). "Killing of *Cryptococcus neoformans* strains by human neutrophils and monocytes." *Infection and Immunity* **59**(1): 24-28.

Miot, J., T. Leong, S. Takuva, A. Parrish and H. Dawood (2021). "Cost-effectiveness analysis of flucytosine as induction therapy in the treatment of cryptococcal meningitis in HIV-infected adults in South Africa." *BMC Health Services Research* **21**(1).

Mody, C. H., G. H. Chen, C. Jackson, J. L. Curtis and G. B. Toews (1994). "In vivo depletion of murine CD8 positive T cells impairs survival during infection with a highly virulent strain of *Cryptococcus neoformans*." *Mycopathologia* **125**(1): 7-17.

Mohamed, S. H., M. S. Fu, S. Hain, A. Alselami, E. Vanhoffelen, Y. Li, E. Bojang, R. Lukande, E. R. Ballou, R. C. May, C. Ding, G. V. Velde and R. A. Drummond (2022). "Microglia protect fungi against copper starvation and promote brain infection." *bioRxiv*: 2022.2009.2007.506901.

Mohamed, S. H., T. K. Nyazika, K. Ssebambulidde, M. S. Lionakis, D. B. Meya and R. A. Drummond (2022). "Fungal CNS Infections in Africa: The Neuroimmunology of Cryptococcal Meningitis." *Front Immunol* **13**: 804674.

Mohamed, S. H., E. Vanhoffelen, M. S. Fu, E. Cosway, G. Anderson, G. V. Velde and R. A. Drummond (2022). CSF1R inhibition by PLX5622 reduces pulmonary fungal infection by depleting MHCII^{hi} interstitial lung macrophages, Cold Spring Harbor Laboratory.

Monari, C., F. Baldelli, D. Pietrella, C. Retini, C. Tascini, D. Francisci, F. Bistoni and A. Vecchiarelli (1997). "Monocyte dysfunction in patients with acquired immunodeficiency syndrome (AIDS) versus *Cryptococcus neoformans*." *J Infect* **35**(3): 257-263.

Moreno, T., R. Artacho, M. Navarro, A. Pérez and M. D. Ruiz-López (1998). "Serum copper concentration in HIV-infection patients and relationships with other biochemical indices." *Sci Total Environ* **217**(1-2): 21-26.

Mukaremera, L. and K. Nielsen (2017). "Adaptive Immunity to *Cryptococcus neoformans* Infections." *J Fungi (Basel)* **3**(4).

Musubire, A. K., D. B. Meya, J. Rhein, G. Meintjes, P. R. Bohjanen, E. Nuwagira, C. Muzoora, D. R. Boulware, K. H. Hullsiek, Coat and A. t. teams (2018). "Blood neutrophil counts in HIV-infected patients with cryptococcal meningitis: Association with mortality." *PloS one* **13**(12): e0209337-e0209337.

Nakamura, Y., K. Sato, H. Yamamoto, K. Matsumura, I. Matsumoto, T. Nomura, T. Miyasaka, K. Ishii, E. Kanno, M. Tachi, S. Yamasaki, S. Saijo, Y. Iwakura and K. Kawakami (2015). "Dectin-2 Deficiency Promotes Th2 Response and Mucin Production in the Lungs after Pulmonary Infection with *Cryptococcus neoformans*." *Infection and Immunity* **83**(2): 671.

Naslund, P. K., W. C. Miller and D. L. Granger (1995). "*Cryptococcus neoformans* fails to induce nitric oxide synthase in primed murine macrophage-like cells." *Infection and Immunity* **63**(4): 1298.

Neal, L. M., E. Xing, J. Xu, J. L. Kolbe, J. J. Osterholzer, B. M. Segal, P. R. Williamson and M. A. Olszewski (2017). "CD4⁺ T Cells Orchestrate Lethal Immune Pathology despite Fungal Clearance during *Cryptococcus neoformans* Meningoencephalitis." *mBio* **8**(6): e01415-01417.

Nelson, B. N., A. N. Hawkins and K. L. Wozniak (2020). "Pulmonary Macrophage and Dendritic Cell Responses to *Cryptococcus neoformans*." *Frontiers in Cellular and Infection Microbiology* **10**(37).

Nishinakamura, R., Y. Matsumoto, K. Nakao, K. Nakamura, A. Sato, N. G. Copeland, D. J. Gilbert, N. A. Jenkins, S. Scully, D. L. Lacey, M. Katsuki, M. Asashima and T. Yokota (2001). "Murine homolog of SALL1 is essential for ureteric bud invasion in kidney development." *Development* **128**(16): 3105-3115.

O'Koren, E. G., R. Mathew and D. R. Saban (2016). "Fate mapping reveals that microglia and recruited monocyte-derived macrophages are definitively distinguishable by phenotype in the retina." *Sci Rep* **6**: 20636.

Okagaki, L. H., A. K. Strain, J. N. Nielsen, C. Charlier, N. J. Baltes, F. Chrétien, J. Heitman, F. Dromer and K. Nielsen (2010). "Cryptococcal Cell Morphology Affects Host Cell Interactions and Pathogenicity." *PLoS Pathogens* **6**(6): e1000953.

Olszewski, M. A., M. C. Noverr, G.-H. Chen, G. B. Toews, G. M. Cox, J. R. Perfect and G. B. Huffnagle (2004). "Urease expression by *Cryptococcus neoformans* promotes microvascular sequestration, thereby enhancing central nervous system invasion." *The American journal of pathology* **164**(5): 1761-1771.

Oosterhof, N., I. J. Chang, E. G. Karimiani, L. E. Kuil, D. M. Jensen, R. Daza, E. Young, L. Astle, H. C. van der Linde, G. M. Shivaram, J. Demmers, C. S. Latimer, C. D. Keene, E. Loter, R. Maroofian, T. J. van Ham, R. F. Hevner and J. T. Bennett (2019). "Homozygous Mutations in CSF1R Cause a Pediatric-Onset Leukoencephalopathy and Can Result in Congenital Absence of Microglia." *Am J Hum Genet* **104**(5): 936-947.

Opazo, C. M., M. A. Greenough and A. I. Bush (2014). "Copper: from neurotransmission to neuroproteostasis." *Front Aging Neurosci* **6**: 143.

Ost, K. S., T. R. O'Meara, N. Huda, S. K. Esher and J. A. Alspaugh (2015). "The *Cryptococcus neoformans* alkaline response pathway: identification of a novel rim pathway activator." *PLoS Genet* **11**(4): e1005159.

Osterholzer, J. J., J. L. Curtis, T. Polak, T. Ames, G. H. Chen, R. McDonald, G. B. Huffnagle and G. B. Toews (2008). "CCR2 mediates conventional dendritic cell recruitment and the formation of bronchovascular mononuclear cell infiltrates in the lungs of mice infected with *Cryptococcus neoformans*." *J Immunol* **181**(1): 610-620.

Osterholzer, J. J., J. E. Milam, G.-H. Chen, G. B. Toews, G. B. Huffnagle and M. A. Olszewski (2009). "Role of dendritic cells and alveolar macrophages in regulating early host defense against pulmonary infection with *Cryptococcus neoformans*." *Infection and immunity* **77**(9): 3749-3758.

Osterholzer, J. J., R. Surana, J. E. Milam, G. T. Montano, G.-H. Chen, J. Sonstein, J. L. Curtis, G. B. Huffnagle, G. B. Toews and M. A. Olszewski (2009). "Cryptococcal urease promotes the accumulation of immature dendritic cells and a non-protective T2 immune response within the lung." *The American journal of pathology* **174**(3): 932-943.

Osterholzer, J. J., R. Surana, J. E. Milam, G. T. Montano, G. H. Chen, J. Sonstein, J. L. Curtis, G. B. Huffnagle, G. B. Toews and M. A. Olszewski (2009). "Cryptococcal urease promotes the accumulation of immature dendritic cells and a non-protective T2 immune response within the lung." *Am J Pathol* **174**(3): 932-943.

Panek, R. B. and E. N. Benveniste (1995). "Class II MHC gene expression in microglia. Regulation by the cytokines IFN-gamma, TNF-alpha, and TGF-beta." *The Journal of Immunology* **154**(6): 2846.

Parkhurst, C. N., G. Yang, I. Ninan, J. N. Savas, J. R. Yates, 3rd, J. J. Lafaille, B. L. Hempstead, D. R. Littman and W. B. Gan (2013). "Microglia promote learning-dependent synapse formation through brain-derived neurotrophic factor." *Cell* **155**(7): 1596-1609.

Paschalis, E. I., F. Lei, C. Zhou, V. Kapoulea, R. Dana, J. Chodosh, D. G. Vavvas and C. H. Dohlman (2018). "Permanent neuroglial remodeling of the retina following infiltration of CSF1R inhibition-resistant peripheral monocytes." *Proc Natl Acad Sci U S A* **115**(48): E11359-e11368.

Pasciuto, E., O. T. Burton, C. P. Roca, V. Lagou, W. D. Rajan, T. Theys, R. Mancuso, R. Y. Tito, L. Kouser, Z. Callaerts-Vegh, A. G. de la Fuente, T. Prezzemolo, L. G. Mascali, A. Brajic, C. E. Whyte, L. Yshii, A. Martinez-Muriana, M. Naughton, A. Young, A. Moudra, P. Lemaitre, S. Poovathingal, J. Raes, B. De Strooper, D. C. Fitzgerald, J. Dooley and A. Liston (2020). "Microglia Require CD4 T Cells to Complete the Fetal-to-Adult Transition." *Cell* **182**(3): 625-640.e624.

Pasquale, E. B. (2005). "Eph receptor signalling casts a wide net on cell behaviour." *Nature Reviews Molecular Cell Biology* **6**(6): 462-475.

Patel, A. A., Y. Zhang, J. N. Fullerton, L. Boelen, A. Rongvaux, A. A. Maini, V. Bigley, R. A. Flavell, D. W. Gilroy, B. Asquith, D. Macallan and S. Yona (2017). "The fate and lifespan of human monocyte subsets in steady state and systemic inflammation." *J Exp Med* **214**(7): 1913-1923.

Peter, B. Bustamante, E. Ticona, Richard, Philip, A. Reboli, J. Aberg, R. Hasbun and Henry (2004). "Recombinant Interferon-γ1b as Adjunctive Therapy for AIDS-Related Acute Cryptococcal Meningitis." *The Journal of Infectious Diseases* **189**(12): 2185-2191.

Pfeffer, P. E., A. Sen, S. Das, M. Sheaff, A. Sivaramkrishnan, D. E. Simcock and B. Turner (2010). "Eosinophilia, meningitis and pulmonary nodules in a young woman." *Thorax* **65**(12): 1066, 1085.

Philip, K. J., R. Kaur, M. Sangeetha, K. Masih, N. Singh and A. Mani (2012). "Disseminated cryptococcosis presenting with generalized lymphadenopathy." *J Cytol* **29**(3): 200-202.

Piehler, D., W. Stenzel, A. Grahner, J. Held, L. Richter, G. Köhler, T. Richter, M. Eschke, G. Alber and U. Müller (2011). "Eosinophils contribute to IL-4 production and shape the T-helper cytokine profile and inflammatory response in pulmonary cryptococcosis." *Am J Pathol* **179**(2): 733-744.

Polfliet, M. M. J., P. J. G. Zwijnenburg, A. M. Van Furth, T. Van Der Poll, E. A. Dopp, C. Renardel De Lavalette, E. M. L. Van Kesteren-Hendriks, N. Van Rooijen, C. D. Dijkstra and T. K. Van Den Berg (2001). "Meningeal and Perivascular Macrophages of the Central Nervous System Play a Protective Role During Bacterial Meningitis." *167*(8): 4644-4650.

Price, M. S., C. B. Nichols and J. A. Alspaugh (2008). "The Cryptococcus neoformans Rho-GDP dissociation inhibitor mediates intracellular survival and virulence." *Infect Immun* **76**(12): 5729-5737.

Pridans, C., A. Raper, G. M. Davis, J. Alves, K. A. Sauter, L. Lefevre, T. Regan, S. Meek, L. Sutherland, A. J. Thomson, S. Clohisey, S. J. Bush, R. Rojo, Z. M. Lisowski, R. Wallace, K. Grabert, K. R. Upton, Y. T. Tsai, D. Brown, L. B. Smith, K. M. Summers, N. A. Mabbott, P. Piccardo, M. T. Cheeseman, T. Burdon and D. A. Hume (2018). "Pleiotropic Impacts of Macrophage and Microglial Deficiency on Development in Rats with Targeted Mutation of the Csf1r Locus." *J Immunol* **201**(9): 2683-2699.

Rajasingham, R. and D. R. Boulware (2020). "Cryptococcal Antigen Screening and Preemptive Treatment—How Can We Improve Survival?" *Clinical Infectious Diseases* **70**(8): 1691-1694.

Rajasingham, R., N. P. Govender, A. Jordan, A. Loyse, A. Shroufi, D. W. Denning, D. B. Meya, T. M. Chiller and D. R. Boulware (2022). "The global burden of HIV-associated cryptococcal infection in adults in 2020: a modelling analysis." *The Lancet Infectious Diseases* **22**(12): 1748-1755.

Raman Sharma, R. (2010). "Fungal infections of the nervous system: Current perspective and controversies in management." *International Journal of Surgery* **8**(8): 591-601.

Rb-Silva, R., C. Nobrega, E. Reiriz, S. Almeida, R. Sarmiento-Castro, M. Correia-Neves and A. Horta (2017). "Toxoplasmosis-associated IRIS involving the CNS: a case report with longitudinal analysis of T cell subsets." *BMC infectious diseases* **17**(1): 66-66.

Rebejac, J., E. Eme-Scolan, L. Arnaud Paroutaud, S. Kharbouche, M. Teleman, L. Spinelli, E. Gallo, A. Roussel-Queval, A. Zarubica, A. Sansoni, Q. Bardin, P. Hoest, M. C. Michallet, C. Brousse, K. Crozat, M. Manghani, Z. Liu, F. Ginhoux, D. B. McGavern, M. Dalod, B. Malissen, T. Lawrence and R. Rua (2022). "Meningeal macrophages protect against viral neuroinfection." *Immunity* **55**(11): 2103-2117.e2110.

Redlich, S., S. Ribes, S. Schütze, H. Eiffert and R. Nau (2013). "Toll-like receptor stimulation increases phagocytosis of Cryptococcus neoformans by microglial cells." **10**(1): 71.

Rice, R. A., E. E. Spangenberg, H. Yamate-Morgan, R. J. Lee, R. P. S. Arora, M. X. Hernandez, A. J. Tenner, B. L. West and K. N. Green (2015). "Elimination of Microglia Improves Functional Outcomes Following Extensive Neuronal Loss in the Hippocampus." *Journal of Neuroscience* **35**(27): 9977-9989.

Richardson, J. and J. Naglik (2018). "Special Issue: Mucosal Fungal Infections." *Journal of Fungi* **4**(2): 43.

Richardson, M. D., L. J. White, I. C. McKay and G. S. Shankland (1993). "Differential binding of acapsulate and encapsulated strains of Cryptococcus neoformans to human neutrophils." *J Med Vet Mycol* **31**(3): 189-199.

Rieber, N., R. P. Gazendam, A. F. Freeman, A. P. Hsu, A. L. Collar, J. A. Sugui, R. A. Drummond, C. Rongkavilit, K. Hoffman, C. Henderson, L. Clark, M. Mezger, M. Swamydas, M. Engholm, R. Schüle, B. Neumayer, F. Ebel, C. M. Mikelis, S. Pittaluga, V. K. Prasad, A. Singh, J. D. Milner, K. W. Williams, J. K. Lim, K. J. Kwon-Chung, S. M. Holland, D. Hartl, T. W. Kuijpers and M. S. Lionakis (2016). "Extrapulmonary Aspergillus infection in patients with CARD9 deficiency." **1**(17).

Rocha, J. D., M. T. Nascimento, D. Decote-Ricardo, S. Corte-Real, A. Morrot, N. Heise, M. P. Nunes, J. O. Previato, L. Mendonca-Previato, G. A. DosReis, E. M. Saraiva and C. G. Freire-de-Lima (2015). "Capsular polysaccharides from Cryptococcus neoformans modulate production of neutrophil extracellular traps (NETs) by human neutrophils." *Sci Rep* **5**: 8008.

Rohatgi, S., A. Nakouzi, L. J. Carreño, M. Slosar-Cheah, M. H. Kuniholm, T. Wang, P. G. Pappas and L. A. Pirofski (2018). "Antibody and B Cell Subset Perturbations in Human Immunodeficiency Virus-Uninfected Patients With Cryptococcosis." *Open Forum Infect Dis* **5**(1): ofx255.

Rojo, R., A. Raper, D. D. Ozdemir, L. Lefevre, K. Grabert, E. Wollscheid-Lengeling, B. Bradford, M. Caruso, I. Gazova, A. Sánchez, Z. M. Lisowski, J. Alves, I. Molina-Gonzalez, H. Davtyan, R. J. Lodge, J. D. Glover, R. Wallace, D. A. D. Munro, E. David, I. Amit, V. E. Miron, J. Priller, S. J. Jenkins, G. E. Hardingham, M. Blurton-Jones, N. A. Mabbott, K. M. Summers, P. Hohenstein, D. A. Hume and C. Pridans (2019). "Deletion of a Csf1r enhancer selectively impacts CSF1R expression and development of tissue macrophage populations." *Nat Commun* **10**(1): 3215.

Rua, R., J. Y. Lee, A. B. Silva, I. S. Swafford, D. Maric, K. R. Johnson and D. B. McGavern (2019). "Infection drives meningeal engraftment by inflammatory monocytes that impairs CNS immunity." *Nature Immunology* **20**(4): 407-419.

Ruan, C., L. Sun, A. Kroshilina, L. Beckers, P. De Jager, E. M. Bradshaw, S. A. Hasson, G. Yang and W. Elyaman (2020). "A novel Tmem119-tdTomato reporter mouse model for studying microglia in the central nervous system." *Brain Behav Immun* **83**: 180-191.

Sabatel, C., C. Radermecker, L. Fievez, G. Paulissen, S. Chakarov, C. Fernandes, S. Olivier, M. Toussaint, D. Pirottin, X. Xiao, P. Quatresooz, J. C. Sirard, D. Cataldo, L. Gillet, H. Bouabe, C. J. Desmet, F. Ginhoux, T. Marichal and F. Bureau (2017). "Exposure to Bacterial CpG DNA Protects from Airway Allergic Inflammation by Expanding Regulatory Lung Interstitial Macrophages." *Immunity* **46**(3): 457-473.

Saederup, N., A. E. Cardona, K. Croft, M. Mizutani, A. C. Cotleur, C. L. Tsou, R. M. Ransohoff and I. F. Charo (2010). "Selective chemokine receptor usage by central nervous system myeloid cells in CCR2-red fluorescent protein knock-in mice." *PLoS One* **5**(10): e13693.

Saijo, S., N. Fujikado, T. Furuta, S.-H. Chung, H. Kotaki, K. Seki, K. Sudo, S. Akira, Y. Adachi, N. Ohno, T. Kinjo, K. Nakamura, K. Kawakami and Y. Iwakura (2007). "Dectin-1 is required for host defense against *Pneumocystis carinii* but not against *Candida albicans*." *Nature Immunology* **8**(1): 39-46.

Saijo, S., S. Ikeda, K. Yamabe, S. Kakuta, H. Ishigame, A. Akitsu, N. Fujikado, T. Kusaka, S. Kubo, S.-H. Chung, R. Komatsu, N. Miura, Y. Adachi, N. Ohno, K. Shibuya, N. Yamamoto, K. Kawakami, S. Yamasaki, T. Saito, S. Akira and Y. Iwakura (2010). "Dectin-2 Recognition of α -Mannans and Induction of Th17 Cell Differentiation Is Essential for Host Defense against *Candida albicans*." *Immunity* **32**(5): 681-691.

Salek-Ardakani, S., T. Bell, C. P. Jagger, R. J. Snelgrove and T. Hussell (2019). "CD200R1 regulates eosinophilia during pulmonary fungal infection in mice." *Eur J Immunol* **49**(9): 1380-1390.

Santangelo, R., H. Zoellner, T. Sorrell, C. Wilson, C. Donald, J. Djordjevic, Y. Shounan and L. Wright (2004). "Role of extracellular phospholipases and mononuclear phagocytes in dissemination of cryptococcosis in a murine model." *Infection and immunity* **72**(4): 2229-2239.

Santiago-Tirado, F. H., M. D. Onken, J. A. Cooper, R. S. Klein and T. L. Doering (2017). "Trojan Horse Transit Contributes to Blood-Brain Barrier Crossing of a Eukaryotic Pathogen." *mBio* **8**(1): e02183-02116.

Scheiber, I. F., J. F. Mercer and R. Dringen (2014). "Metabolism and functions of copper in brain." *Prog Neurobiol* **116**: 33-57.

Schulze, B., D. Piehler, M. Eschke, H. von Buttlar, G. Köhler, T. Sparwasser and G. Alber (2014). "CD4(+) FoxP3(+) regulatory T cells suppress fatal T helper 2 cell immunity during pulmonary fungal infection." *Eur J Immunol* **44**(12): 3596-3604.

Schwerk, C., T. Tenenbaum, K. S. Kim and H. Schroten (2015). "The choroid plexus-a multi-role player during infectious diseases of the CNS." *Frontiers in cellular neuroscience* **9**: 80-80.

Schyns, J., Q. Bai, C. Ruscitti, C. Radermecker, S. De Schepper, S. Chakarov, F. Farnir, D. Pirottin, F. Ginhoux, G. Boeckstaens, F. Bureau and T. Marichal (2019). "Non-classical tissue monocytes and two functionally distinct populations of interstitial macrophages populate the mouse lung." *Nature Communications* **10**(1): 3964.

Scriven, J. E., L. M. Graham, C. Schutz, T. J. Scriba, K. A. Wilkinson, R. J. Wilkinson, D. R. Boulware, B. C. Urban, D. G. Lalloo and G. Meintjes (2016). "A Glucuronoxylomannan-Associated Immune Signature, Characterized by Monocyte Deactivation and an Increased Interleukin 10 Level, Is a Predictor of Death in Cryptococcal Meningitis." *J Infect Dis* **213**(11): 1725-1734.

Setianingrum, F., R. Rautemaa-Richardson and D. W. Denning (2018). "Pulmonary cryptococcosis: A review of pathobiology and clinical aspects." *Medical Mycology* **57**(2): 133-150.

Setianingrum, F., R. Rautemaa-Richardson and D. W. Denning (2019). "Pulmonary cryptococcosis: A review of pathobiology and clinical aspects." *Med Mycol* **57**(2): 133-150.

Sharma, A., V. Lal, M. Modi, D. Khurana, S. Bal and S. Prabhakar (2010). "Idiopathic CD4 lymphocytopenia presenting as refractory cryptococcal meningitis." *Ann Indian Acad Neurol* **13**(2): 136-138.

Shelburne, S. A., 3rd, J. Darcourt, A. C. White, Jr., S. B. Greenberg, R. J. Hamill, R. L. Atmar and F. Visnegarwala (2005). "The role of immune reconstitution inflammatory syndrome in AIDS-related *Cryptococcus neoformans* disease in the era of highly active antiretroviral therapy." *Clin Infect Dis* **40**(7): 1049-1052.

Shen, Q., M. J. Beucler, S. C. Ray and C. A. Rappleye (2018). "Macrophage activation by IFN- γ triggers restriction of phagosomal copper from intracellular pathogens." *PLOS Pathogens* **14**(11): e1007444.

Shi, M., S. S. Li, C. Zheng, G. J. Jones, K. S. Kim, H. Zhou, P. Kuberski and C. H. Mody (2010). "Real-time imaging of trapping and urease-dependent transmigration of *Cryptococcus neoformans* in mouse brain." *J Neurosci* **30**(15): 1683-1693.

Shiri, T., A. Loyse, L. Mwenge, T. Chen, S. Lakhi, D. Chanda, P. Mwaba, S. F. Molloy, R. S. Heyderman, C. Kanyama, M. C. Hosseinipour, C. Kouanfack, E. Temfack, S. Mfinanga, S. Kivuyo, A. K. Chan, J. N. Jarvis, O. Lortholary, S. Jaffar, L. W. Niessen and T. S. Harrison (2019). "Addition of Flucytosine to Fluconazole for the Treatment of Cryptococcal Meningitis in Africa: A Multicountry Cost-effectiveness Analysis." *Clinical Infectious Diseases*.

Shourian, M. and S. T. Qureshi (2019). "Resistance and Tolerance to Cryptococcal Infection: An Intricate Balance That Controls the Development of Disease." *Frontiers in Immunology* **10**(66).

Sifri, C. D., H. Y. Sun, T. V. Cacciarelli, B. Wispelwey, T. L. Pruett and N. Singh (2010). "Pretransplant cryptococcosis and outcome after liver transplantation." *Liver Transpl* **16**(4): 499-502.

Silva, M. G., A. Schrank, E. F. Bailão, A. M. Bailão, C. L. Borges, C. C. Staats, J. A. Parente, M. Pereira, S. M. Salem-Izacc, M. J. Mendes-Giannini, R. M. Oliveira, L. K. Silva, J. D. Nosanchuk, M. H. Vainstein and C. M. de Almeida Soares (2011). "The homeostasis of iron, copper, and zinc in *paracoccidioides brasiliensis*, *cryptococcus neoformans* var. *Grubii*, and *cryptococcus gattii*: a comparative analysis." *Front Microbiol* **2**: 49.

Singh, N. and H. Y. Sun (2008). "Iron overload and unique susceptibility of liver transplant recipients to disseminated disease due to opportunistic pathogens." *Liver Transpl* **14**(9): 1249-1255.

Smith, L. M., E. F. Dixon and R. C. May (2015). "The fungal pathogen *Cryptococcus neoformans* manipulates macrophage phagosome maturation." *Cell Microbiol* **17**(5): 702-713.

Smolders, J., E. B. M. Remmerswaal, K. G. Schuurman, J. Melief, C. G. van Eden, R. A. W. van Lier, I. Huitinga and J. Hamann (2013). "Characteristics of differentiated CD8+ and CD4+ T cells present in the human brain." *Acta Neuropathologica* **126**(4): 525-535.

Song, X. (2004). "Fc receptor signaling in primary human microglia: differential roles of PI-3K and Ras/ERK MAPK pathways in phagocytosis and chemokine induction." **75**(6): 1147-1155.

Spangenberg, E., P. L. Severson, L. A. Hohsfield, J. Crapser, J. Zhang, E. A. Burton, Y. Zhang, W. Spevak, J. Lin, N. Y. Phan, G. Habets, A. Rymar, G. Tsang, J. Walters, M. Nespi, P. Singh, S. Broome, P. Ibrahim, C. Zhang, G. Bollag, B. L. West and K. N. Green (2019). "Sustained microglial depletion with CSF1R inhibitor impairs parenchymal plaque development in an Alzheimer's disease model." *Nat Commun* **10**(1): 3758.

Spangenberg, E., P. L. Severson, L. A. Hohsfield, J. Crapser, J. Zhang, E. A. Burton, Y. Zhang, W. Spevak, J. Lin, N. Y. Phan, G. Habets, A. Rymar, G. Tsang, J. Walters, M. Nespi, P. Singh, S. Broome, P. Ibrahim, C. Zhang, G. Bollag, B. L. West and K. N. Green (2019). "Sustained microglial depletion with CSF1R inhibitor impairs parenchymal plaque development in an Alzheimer's disease model." *Nature Communications* **10**(1): 3758.

Spangenberg, E., P. L. Severson, L. A. Hohsfield, J. Crapser, J. Zhang, E. A. Burton, Y. Zhang, W. Spevak, J. Lin, N. Y. Phan, G. Habets, A. Rymar, G. Tsang, J. Walters, M. Nespi, P. Singh, S. Broome, P. Ibrahim, C. Zhang, G. Bollag, B. L. West and K. N. Green (2019). "Sustained microglial depletion with CSF1R inhibitor impairs parenchymal plaque development in an Alzheimer's disease model." *Nature Communications* **10**(1).

Spiteri, A. G., D. Ni, Z. L. Ling, L. Macia, I. L. Campbell, M. J. Hofer and N. J. C. King (2022). "PLX5622 Reduces Disease Severity in Lethal CNS Infection by Off-Target Inhibition of Peripheral Inflammatory Monocyte Production." *Frontiers in Immunology* **13**.

Spiteri, A. G., C. L. Wishart, R. Pamphlett, G. Locatelli and N. J. C. King (2022). "Microglia and monocytes in inflammatory CNS disease: integrating phenotype and function." *Acta Neuropathol* **143**(2): 179-224.

Srinivasan, M. (2004). "Fungal keratitis." *Curr Opin Ophthalmol* **15**(4): 321-327.

Steel, C. D., W.-K. Kim, L. D. Sanford, L. L. Wellman, S. Burnett, N. Van Rooijen and R. P. Ciavarra (2010). "Distinct macrophage subpopulations regulate viral encephalitis but not viral clearance in the CNS." *Journal of neuroimmunology* **226**(1-2): 81-92.

Subbarayal, P., K. Karunakaran, A.-C. Winkler, M. Rother, E. Gonzalez, T. F. Meyer and T. Rudel (2015). "EphrinA2 Receptor (EphA2) Is an Invasion and Intracellular Signaling Receptor for *Chlamydia trachomatis*." **11**(4): e1004846.

Subramaniam, K., B. Metzger, L. H. Hanau, A. Guh, L. Rucker, S. Badri and L.-A. Pirofski (2009). "IgM(+) memory B cell expression predicts HIV-associated cryptococcosis status." *The Journal of infectious diseases* **200**(2): 244-251.

Sun, D., M. Zhang, P. Sun, G. Liu, A. B. Strickland, Y. Chen, Y. Fu, M. Yosri and M. Shi (2020). "VCAM1/VLA4 interaction mediates Ly6Clow monocyte recruitment to the brain in a TNFR signaling dependent manner during fungal infection." *PLoS Pathog* **16**(2): e1008361.

Sun, H., X.-Y. Xu, H.-T. Shao, X. Su, X.-D. Wu, Q. Wang and Y. Shi (2013). "Dectin-2 is predominately macrophage restricted and exhibits conspicuous expression during *Aspergillus fumigatus* invasion in human lung." **284**(1-2): 60-67.

Sun, T.-S., X. Ju, H.-L. Gao, T. Wang, D. J. Thiele, J.-Y. Li, Z.-Y. Wang and C. Ding (2014). "Reciprocal functions of *Cryptococcus neoformans* copper homeostasis machinery during pulmonary infection and meningoencephalitis." *Nature Communications* **5**(1): 5550.

Sun, T. S., X. Ju, H. L. Gao, T. Wang, D. J. Thiele, J. Y. Li, Z. Y. Wang and C. Ding (2014). "Reciprocal functions of *Cryptococcus neoformans* copper homeostasis machinery during pulmonary infection and meningoencephalitis." *Nat Commun* **5**: 5550.

Szymczak, W. A., M. J. Davis, S. K. Lundy, C. Dufaud, M. Olszewski and L. A. Pirofski (2013). "X-linked immunodeficient mice exhibit enhanced susceptibility to *Cryptococcus neoformans* Infection." *mBio* **4**(4).

Ta, T. T., H. O. Dikmen, S. Schilling, B. Chausse, A. Lewen, J. O. Hollnagel and O. Kann (2019). "Priming of microglia with IFN- γ slows neuronal gamma oscillations in situ." *Proc Natl Acad Sci U S A* **116**(10): 4637-4642.

Tajima, K., D. Yamanaka, K.-I. Ishibashi, Y. Adachi and N. Ohno (2019). "Solubilized melanin suppresses macrophage function." *FEBS open bio* **9**(4): 791-800.

Takasato, M., K. Osafune, Y. Matsumoto, Y. Kataoka, N. Yoshida, H. Meguro, H. Aburatani, M. Asashima and R. Nishinakamura (2004). "Identification of kidney mesenchymal genes by a combination of microarray analysis and Sall1-GFP knockin mice." *Mech Dev* **121**(6): 547-557.

Taniwaki, M., M. Yamasaki, N. Ishikawa, K. Kawamoto and N. Hattori (2019). "Pulmonary cryptococcosis mimicking lung cancer." *The Lancet Infectious Diseases* **19**(9): 1033.

Taylor, P. R., S. V. Tsoni, J. A. Willment, K. M. Dennehy, M. Rosas, H. Findon, K. Haynes, C. Steele, M. Botto, S. Gordon and G. D. Brown (2007). "Dectin-1 is required for β -glucan recognition and control of fungal infection." *8*(1): 31-38.

Thomas, G., R. Tacke, C. C. Hedrick and R. N. Hanna (2015). "Nonclassical patrolling monocyte function in the vasculature." *Arterioscler Thromb Vasc Biol* **35**(6): 1306-1316.

Thornton, C. S., O. Larios, J. Grossman, T. P. Griener and S. Vaughan (2019). "Pulmonary *Cryptococcus* infections as a manifestation of idiopathic CD4 lymphocytopenia: case report and literature review." *BMC Infectious Diseases* **19**(1).

Toffaletti, D. L., T. H. Rude, S. A. Johnston, D. T. Durack and J. R. Perfect (1993). "Gene transfer in *Cryptococcus neoformans* by use of biolistic delivery of DNA." *J Bacteriol* **175**(5): 1405-1411.

Traynor, T. R., W. A. Kuziel, G. B. Toews and G. B. Huffnagle (2000). "CCR2 expression determines T1 versus T2 polarization during pulmonary *Cryptococcus neoformans* infection." *J Immunol* **164**(4): 2021-2027.

Trevijano-Contador, N., H. C. de Oliveira, R. García-Rodas, S. A. Rossi, I. Llorente, Á. Zaballos, G. Janbon, J. Ariño and Ó. Zaragoza (2018). "*Cryptococcus neoformans* can form titan-like cells in vitro in response to multiple signals." *PLoS pathogens* **14**(5): e1007007-e1007007.

Tümer, Z. and L. B. Møller (2010). "Menkes disease." *Eur J Hum Genet* **18**(5): 511-518.

Ural, B. B., S. T. Yeung, P. Damani-Yokota, J. C. Devlin, M. de Vries, P. Vera-Licona, T. Samji, C. M. Sawai, G. Jang, O. A. Perez, Q. Pham, L. Maher, P. Loke, M. Dittmann, B. Reizis and K. M. Khanna (2020). "Identification of a nerve-associated, lung-resident interstitial macrophage subset with distinct localization and immunoregulatory properties." *Sci Immunol* **5**(45).

Ural, B. B., S. T. Yeung, P. Damani-Yokota, J. C. Devlin, M. de Vries, P. Vera-Licona, T. Samji, C. M. Sawai, G. Jang, O. A. Perez, Q. Pham, L. Maher, P. Loke, ng, M. Dittmann, B. Reizis and K. M. Khanna (2020). "Identification of a nerve-associated, lung-resident interstitial macrophage subset with distinct localization and immunoregulatory properties." *Science Immunology* **5**(45): eaax8756.

Valentine, J. C., C. O. Morrissey, M. A. Tacey, D. Liew, S. Patil, A. Y. Peleg and M. R. Ananda-Rajah (2019). "A population-based analysis of invasive fungal disease in haematology-oncology patients using data linkage of state-wide registries and administrative databases: 2005 - 2016." *BMC Infectious Diseases* **19**(1).

Van Dyken, S. J., A. Mohapatra, J. C. Nussbaum, A. B. Molofsky, E. E. Thornton, S. F. Ziegler, A. N. McKenzie, M. F. Krummel, H. E. Liang and R. M. Locksley (2014). "Chitin activates parallel immune modules that direct distinct inflammatory responses via innate lymphoid type 2 and $\gamma\delta$ T cells." *Immunity* **40**(3): 414-424.

Vanherp, L., A. Ristani, J. Poelmans, A. Hillen, K. Lagrou, G. Janbon, M. Brock, U. Himmelreich and G. Vande Velde (2019). "Sensitive bioluminescence imaging of fungal dissemination to the brain in mouse models of cryptococcosis." *Dis Model Mech* **12**(6).

Vartivarian, S. E., G. H. Reyes, E. S. Jacobson, P. G. James, R. Cherniak, V. R. Mumaw and M. J. Tingler (1989). "Localization of mannoprotein in *Cryptococcus neoformans*." *Journal of bacteriology* **171**(12): 6850-6852.

Vecchiarelli, A., D. Pietrella, P. Lupo, F. Bistoni, D. C. McFadden and A. Casadevall (2003). "The polysaccharide capsule of *Cryptococcus neoformans* interferes with human dendritic cell maturation and activation." *J Leukoc Biol* **74**(3): 370-378.

Vecchiarelli, A., C. Retini, D. Pietrella, C. Monari and T. R. Kozel (2000). "T lymphocyte and monocyte interaction by CD40/CD40 ligand facilitates a lymphoproliferative response and killing of *Cryptococcus neoformans* in vitro." *Eur J Immunol* **30**(5): 1385-1393.

Vidal, J. E. and D. R. Boulware (2015). "LATERAL FLOW ASSAY FOR CRYPTOCOCCAL ANTIGEN: AN IMPORTANT ADVANCE TO IMPROVE THE CONTINUUM OF HIV CARE AND REDUCE CRYPTOCOCCAL MENINGITIS-RELATED MORTALITY." *Revista do Instituto de Medicina Tropical de Sao Paulo* **57 Suppl 19**(Suppl 19): 38-45.

Vu, K., R. Tham, J. P. Uhrig, G. R. Thompson, S. Na Pombejra, M. Jamklang, J. M. Bautos and A. Gelli (2014). "Invasion of the Central Nervous System by *Cryptococcus neoformans*." *J Neurosci* **34**(12): 4143-4151.

id="named-content-1">Cryptococcus neoformans Requires a Secreted Fungal Metalloprotease." *mBio* **5**(3): e01101-01114.

Walenkamp, A. M., P. Ellerbroek, J. Scharringa, E. Rijkers, A. I. Hoepelman and F. E. Coenjaerts (2003). "Interference of *Cryptococcus neoformans* with human neutrophil migration." *Adv Exp Med Biol* **531**: 315-339.

Walsh, N. M., M. R. Botts, A. J. McDermott, S. C. Ortiz, M. Wüthrich, B. Klein and C. M. Hull (2019). "Infectious particle identity determines dissemination and disease outcome for the inhaled human fungal pathogen *Cryptococcus*." *PLOS Pathogens* **15**(6): e1007777.

Walsh, N. M., M. Wuthrich, H. Wang, B. Klein and C. M. Hull (2017). "Characterization of C-type lectins reveals an unexpectedly limited interaction between *Cryptococcus neoformans* spores and Dectin-1." *PLoS One* **12**(3): e0173866.

Walton, F. J., A. Idnurm and J. Heitman (2005). "Novel gene functions required for melanization of the human pathogen *Cryptococcus neoformans*." *Mol Microbiol* **57**(5): 1381-1396.

Wang, Y., P. Aisen and A. Casadevall (1995). "Cryptococcus neoformans melanin and virulence: mechanism of action." *Infection and immunity* **63**(8): 3131-3136.

Ward, R. J., F. A. Zucca, J. H. Duyn, R. R. Crichton and L. Zecca (2014). "The role of iron in brain ageing and neurodegenerative disorders." *Lancet Neurol* **13**(10): 1045-1060.

Warnock, D. W. (1999). "Cryptococcus neoformans." **44**(1): 139-139.

Warrier, S. A. and S. Sathivasubramanian (2015). "Human immunodeficiency virus induced oral candidiasis." *Journal of pharmacy & bioallied sciences* **7**(Suppl 2): S812-S814.

Waterman, S. R., M. Hacham, G. Hu, X. Zhu, Y. D. Park, S. Shin, J. Panepinto, T. Valyi-Nagy, C. Beam, S. Husain, N. Singh and P. R. Williamson (2007). "Role of a CUF1/CTR4 copper regulatory axis in the virulence of *Cryptococcus neoformans*." *J Clin Invest* **117**(3): 794-802.

Waterman, S. R., Y. D. Park, M. Raja, J. Qiu, D. A. Hammoud, T. V. O'Halloran and P. R. Williamson (2012). "Role of CTR4 in the Virulence of *Cryptococcus neoformans*." *mBio* **3**(5).

Watkins, R. A., J. S. King and S. A. Johnston (2017). "Nutritional Requirements and Their Importance for Virulence of Pathogenic *Cryptococcus* Species." *Microorganisms* **5**(4).

Weinberg, P. B., S. Becker, D. L. Granger and H. S. Koren (1987). "Growth inhibition of *Cryptococcus neoformans* by human alveolar macrophages." *Am Rev Respir Dis* **136**(5): 1242-1247.

Weller, R. O., M. M. Sharp, M. Christodoulides, R. O. Carare and K. Møllgård (2018). "The meninges as barriers and facilitators for the movement of fluid, cells and pathogens related to the rodent and human CNS." *Acta Neuropathologica* **135**(3): 363-385.

Wheeler, D. L., A. Sariol, D. K. Meyerholz and S. Perlman (2018). "Microglia are required for protection against lethal coronavirus encephalitis in mice." *J Clin Invest* **128**(3): 931-943.

Wiesner, D. L., C. A. Specht, C. K. Lee, K. D. Smith, L. Mukaremera, S. T. Lee, C. G. Lee, J. A. Elias, J. N. Nielsen, D. R. Boulware, P. R. Bohjanen, M. K. Jenkins, S. M. Levitz and K. Nielsen (2015). "Chitin Recognition via Chitotriosidase Promotes Pathologic Type-2 Helper T Cell Responses to Cryptococcal Infection." *PLOS Pathogens* **11**(3): e1004701.

Williams, K. C., S. Corey, S. V. Westmoreland, D. Pauley, H. Knight, C. deBakker, X. Alvarez and A. A. Lackner (2001). "Perivascular macrophages are the primary cell type productively infected by simian immunodeficiency virus in the brains of macaques: implications for the neuropathogenesis of AIDS." *The Journal of experimental medicine* **193**(8): 905-915.

Williamson, P. R., J. N. Jarvis, A. A. Panackal, M. C. Fisher, S. F. Molloy, A. Loyse and T. S. Harrison (2016). "Cryptococcal meningitis: epidemiology, immunology, diagnosis and therapy." **13**(1): 13-24.

Williamson, P. R., J. N. Jarvis, A. A. Panackal, M. C. Fisher, S. F. Molloy, A. Loyse and T. S. Harrison (2017). "Cryptococcal meningitis: epidemiology, immunology, diagnosis and therapy." *Nat Rev Neurol* **13**(1): 13-24.

Wolf, Y., S. Yona, K. W. Kim and S. Jung (2013). "Microglia, seen from the CX3CR1 angle." *Front Cell Neurosci* **7**: 26.

Wormley, F. L., Jr., J. R. Perfect, C. Steele and G. M. Cox (2007). "Protection against cryptococcosis by using a murine gamma interferon-producing *Cryptococcus neoformans* strain." *Infect Immun* **75**(3): 1453-1462.

Wozniak, K. L., J. M. Vyas and S. M. Levitz (2006). "In vivo role of dendritic cells in a murine model of pulmonary cryptococcosis." *Infect Immun* **74**(7): 3817-3824.

Wynn, T. A. and K. M. Vannella (2016). "Macrophages in Tissue Repair, Regeneration, and Fibrosis." *Immunity* **44**(3): 450-462.

Xu, J., A. J. Eastman, A. Flaczyk, L. M. Neal, G. Zhao, J. Carolan, A. N. Malachowski, V. R. Stolberg, M. Yosri, S. W. Chensue, J. L. Curtis, J. J. Osterholzer and M. A. Olszewski (2016). "Disruption of Early Tumor Necrosis Factor Alpha Signaling Prevents Classical Activation of Dendritic Cells in Lung-Associated Lymph Nodes and Development of Protective Immunity against Cryptococcal Infection." *mBio* **7**(4): e00510-00516.

Xu, J., A. Ganguly, J. Zhao, M. Ivey, R. Lopez, J. J. Osterholzer, C. S. Cho and M. A. Olszewski (2021). "CCR2 Signaling Promotes Brain Infiltration of Inflammatory Monocytes and Contributes to Neuropathology during Cryptococcal Meningoencephalitis." *mBio* **12**(4): e0107621.

Xu, J., L. M. Neal, A. Ganguly, J. L. Kolbe, J. C. Hargarten, W. Elsegeiny, C. Hollingsworth, X. He, M. Ivey, R. Lopez, J. Zhao, B. Segal, P. R. Williamson and M. A. Olszewski (2020). "Chemokine receptor CXCR3 is required for lethal brain pathology but not pathogen clearance during cryptococcal meningoencephalitis." *Sci Adv* **6**(25): eaba2502.

Yang, J., L. Zhang, C. Yu, X. F. Yang and H. Wang (2014). "Monocyte and macrophage differentiation: circulation inflammatory monocyte as biomarker for inflammatory diseases." *Biomark Res* **2**(1): 1.

Yang, X., H. Wang, F. Hu, X. Chen and M. Zhang (2019). "Nonlytic exocytosis of *Cryptococcus neoformans* from neutrophils in the brain vasculature." *Cell Communication and Signaling* **17**(1).

Yokoyama, T., M. Kadowaki, M. Yoshida, K. Suzuki, M. Komori and T. Iwanaga (2018). "Disseminated Cryptococcosis with Marked Eosinophilia in a Postpartum Woman." *Intern Med* **57**(1): 135-139.

Yona, S., K. W. Kim, Y. Wolf, A. Mildner, D. Varol, M. Breker, D. Strauss-Ayali, S. Viukov, M. Guillemins, A. Misharin, D. A. Hume, H. Perlman, B. Malissen, E. Zelzer and S. Jung (2013). "Fate mapping reveals origins and dynamics of monocytes and tissue macrophages under homeostasis." *Immunity* **38**(1): 79-91.

Yuanjie, Z., C. Jianghan, X. Nan, W. Xiaojun, W. Hai, L. Wanqing and G. Julin (2012). "Cryptococcal meningitis in immunocompetent children." *Mycoses* **55**(2): 168-171.

Zaragoza, O., M. Alvarez, A. Telzak, J. Rivera and A. Casadevall (2007). "The relative susceptibility of mouse strains to pulmonary *Cryptococcus neoformans* infection is associated with pleiotropic differences in the immune response." *Infect Immun* **75**(6): 2729-2739.

Zaragoza, O., C. J. Chrisman, M. V. Castelli, S. Frases, M. Cuenca-Estrella, J. L. Rodriguez-Tudela and A. Casadevall (2008). "Capsule enlargement in *Cryptococcus neoformans* confers resistance to oxidative stress suggesting a mechanism for intracellular survival." *Cell Microbiol* **10**(10): 2043-2057.

Zhao, X.-F., M. M. Alam, Y. Liao, T. Huang, R. Mathur, X. Zhu and Y. Huang (2019). "Targeting Microglia Using Cx3cr1-Cre Lines: Revisiting the Specificity." *eNeuro* **6**(4): ENEURO.0114-0119.2019.

Zheng, C. F., L. L. Ma, G. J. Jones, M. J. Gill, A. M. Krensky, P. Kubes and C. H. Mody (2007). "Cytotoxic CD4+ T cells use granulysin to kill *Cryptococcus neoformans*, and activation of this pathway is defective in HIV patients." *Blood* **109**(5): 2049-2057.

Zheng, Z., C. White, J. Lee, T. S. Peterson, A. I. Bush, G. Y. Sun, G. A. Weisman and M. J. Petris (2010). "Altered microglial copper homeostasis in a mouse model of Alzheimer's disease." *J Neurochem* **114**(6): 1630-1638.

Zhou, Q., R. A. Gault, T. R. Kozel and W. J. Murphy (2006). "Immunomodulation with CD40 Stimulation and Interleukin-2 Protects Mice from Disseminated Cryptococcosis." *Infection and Immunity* **74**(4): 2161.

Zhou, Q., R. A. Gault, T. R. Kozel and W. J. Murphy (2007). "Protection from Direct Cerebral *Cryptococcus* Infection by Interferon- γ -Dependent Activation of Microglial Cells." *The Journal of Immunology* **178**(9): 5753-5761.

Zhou, X. and E. R. Ballou (2018). "The *Cryptococcus neoformans* Titan Cell: From In Vivo Phenomenon to In Vitro Model." *Current Clinical Microbiology Reports* **5**(4): 252-260.